DISSERTATION

THE PREDICTION OF CADMIUM, COPPER, LEAD, AND ZINC PARTITIONING IN CONTAMINATED SOILS

Submitted by

Geoffrey L. Upson

Department of Soil and Crop Sciences

In partial fulfillment of the requirements

for the Degree of Doctor of Philosophy

Colorado State University

Fort Collins, Colorado

Spring 2005

COLORADO STATE UNIVERSITY

March 11, 2005

WE HEREBY RECOMMEND THAT THE DISSERTATION PREPARED UNDER OUR SUPERVISION BY GEOFFREY LANSON UPSON ENTITLED **"THE PREDICTION OF CADMIUM, COPPER, LEAD, AND ZINC PARTITIONING IN CONTAMINATED SOILS"** BE ACCEPTED AS FULFILLING IN PART REQUIREMENTS FOR THE DEGREE OF DOCTOR OF PHILOSOPHY

Committee on Graduate Work

Sally J. Sutton (Sally J. Sutton)

(Grant Cardon)

K. A. Ba (Ken Barbarick)
Co-Adviser

Greg Butters (Greg Butters)
Adviser

Gary A. Peterson
Department Head

ABSTRACT OF DISSERTATION

THE PREDICTION OF CADMIUM, COPPER, LEAD, AND ZINC PARTITIONING IN CONTAMINATED SOILS

Determination of metal partitioning in contaminated soils can provide critical data in support of environmental risk assessments This research focused on the development of a general modeling approach that can predict metal partitioning in a variety of soils.

A competitive modeling approach (CMA) and a non-competitive modeling approach (NCMA) were developed to predict the partitioning of cadmium, copper, lead, and zinc in contaminated soils near Leadville, CO. The modeling approaches consisted of surrogate soils comprised of five specimen materials; kaolinite, illite, montmorillonite, iron oxide (FeOOH) and soil organic matter (SOM). Surrogate soil compositions were adjusted to approximate natural soils by applying a unique set of clay, FeOOH, and SOM weighting factors. The weighting factors were calculated from XRD and total aluminum, iron, and soil organic carbon (SOC) data. The Vanselow selectivity coefficient and four surface complexation models (Constant Capacitance Model, Generalized Two-Layer Model, Stockholm Humic Model, and a non-electrostatic surface complexation model) were applied to the surrogate soils to describe the sorption of the four metals to individual specimen materials.

Predicted concentrations of exchangeable, sorbed, and complexed metals were compared to experimental metals data generated from the selective extraction of four contaminated soils. The NCMA and CMA were tested across a range of pHs, soil textures, SOC levels, concentrations of soluble cadmium, copper, lead, and zinc, and total aluminum and iron.

Both modeling approaches were successful in estimating the experimental data within a range of one order of magnitude. Qualitatively, the CMA was a better predictor of sorbed and complexed metals data, while the NCMA was a slightly better predictor of exchangeable metals data. Careful evaluation of the data used to calculate weighting factors is recommended since errors in weighting factor values can cause significant changes in predicted metal partitioning.

Compared to the high concentrations of total metals reported in these soils, low concentrations of soluble, exchangeable, sorbed, and complexed metals were extracted by the selective extraction process or predicted by the NCMA and CMA. The results suggest that environmental assessments based primarily on total metals data may not describe accurately the potential a contaminated site poses to the environment.

Geoffrey L. Upson
Department of Soil and Crop Sciences
Colorado State University
Fort Collins, CO 80523
Spring 2005

ACKNOWLEDGEMENTS

I would like to thank Dr. Greg Butters who assumed the advisor role for this research program long after the dye had been cast. His expert guidance, assistance, enthusiasm, and patience (!) is much appreciated. I would also like to thank the rest of the committee, Drs. Ken Barbarick, Grant Cardon, and Sally Sutton, for their interest, advice, and reviews of the drafts. The final product would not be nearly as good without the participation of these four individuals.

Many thanks to Dr. Jim Self and his fine staff at the Colorado State University Soil Testing Laboratory who provided me with the facilities and the equipment to conduct my analyses and for the many interesting discussions on a variety of topics.

To my good friend and motorcycling companion, Dr. Mark Brick, who was a constant source of encouragement and advice through the years, many thanks for the friendship and camaraderie, it is greatly appreciated. To Bill Gangloff, Dave Gilbert, Jim Ippolito, Lucretia Sherrod-Tooley, Tim Shaver, Randy Poteet, and numerous other graduate students past and present, thanks for being part of the journey, for without you all it would have been far less enjoyable and memorable. Much appreciation is also extended to the Boston Red Sox, 2004 World Champions, for finally breaking 'The Curse' and providing a much needed boost to my spirits during the most difficult part of this research program, the writing of the dissertation.

Finally, to my wife, Sonce de Vries, your unwavering support, encouragement, advice, and love was the glue that held it all together over the past eight years. The successful completion of this program would not have happened without you.

TABLE OF CONTENTS

LIST OF TABLES

LIST OF FIGURES

APPENDICES

1.0 INTRODUCTION

Elevated concentrations of metals, rare earth elements, radionuclides, and anions in the environment pose a persistent and chronic risk to humans and plant and animal communities. Metals such as cadmium and lead, which are considered non-essential to plant and animal communities (Pais and Jones, Jr., 1997; Alloway, 1993), can be toxic even at low concentrations (Rida and Bouche, 1997; Gough et al., 1979). High concentrations of copper and zinc, classified as micronutrients, can interfere with biological functions by preventing the uptake of other essential elements (Pais and Jones, Jr., 1997; Alloway, 1993; Levy, 1990). Sources of metal contamination are primarily anthropogenic in nature and relate to past and present mining and smelting activities, coal power generation, and the improper disposal of hazardous waste. In the past 60 years, long-term contamination of some soils and water bodies by radionuclides has resulted from nuclear weapons production and testing and industrial accidents associated with nuclear power generation.

One source of contamination in the Rocky Mountain region is the mining and smelting of metal rich ores. Over the past 150 years, significant areas of soil and water have been subjected to the deposition of waste products containing high concentrations of metals. Cadmium, copper, lead, and zinc have migrated to adjacent soils and water bodies through a variety of processes such as uncontrolled acid mine drainage (AMD), wind and water erosion of abandoned mine tailings and smelter waste piles, and atmospheric deposition from smelter emissions.

The mining and smelting activities that led to the majority of contamination have largely ceased over the past 50-100 years. However, large amounts of waste containing high concentrations of metals are still providing an on-going and continuous source of contamination. The U. S. Environmental Protection Agency (USEPA) estimates approximately 220,000 abandoned mine land (AML) sites exist in the 11 western states (U. S. Geological Survey, 1997). The Mineral Policy Center (Lyon et al., 1993) has catalogued over 550,000 AML sites in 32 states, while Trout Unlimited (Schnitzer and Roberts, 2004) reported 40% (approximately 25,750 km) of headwater streams in the western United States are impacted by AMD. In Colorado, Hartman (2004) reported in addition to the existence of 7,000 AML sites, approximately 2,500 km of waterways are receiving AMD. Due to the increased awareness of health problems associated with environmental contamination caused by historic and current industrial activities, the number of sites classified as contaminated and requiring some form of mitigation increases each year. Clearly, the magnitude of this problem in the western United States defies any quick fix.

The U. S. Geological Survey (1997) estimates the majority of AML sites are located on or border federal lands administered by the U. S. Forest Service, Bureau of Land Management, and National Park Service. The fact that the majority of mine and tailings sites causing environmental problems are abandoned (i.e. the owners can not be located or the companies that operated the sites no longer exist) means the funding necessary to address these orphan sites comes from available federal and state funds.

Unless a particular mine, mine tailing, smelter site, or mining district is causing extensive environmental damage and is declared a superfund site under the Comprehensive Emergency Response, Compensation, and Liability Act (CERCLA) by USEPA (e.g. California Gulch in Leadville, CO), the funding for AML remediation must compete for limited federal and state funding with any number of other current environmental issues.

When funding is available, a significant portion of the budget can be spent prior to the implementation of any remediation. Prioritization of abandoned mines, mine tailings, or smelter sites according to their actual or potential impacts to the environment; identification of ownership; development and implementation of appropriate sampling and analyses plans; identification of justifiable and achievable cleanup criteria; and successful negotiation with all stakeholders as to the appropriate course of action can consume a great deal of time and money. The resolution of these numerous intertwined and complex scientific and political issues can result in long delays and very little progress. As a consequence, most of the mines and smelters operated more than a century ago continue to adversely impact regional Rocky Mountain streams, lakes, forests, pasture soils, and when AMD-contaminated water is used for crop irrigation purposes, agricultural soils further afield.

In an effort to streamline data acquisition, reduce the amount of data required for each step of the process described above, and predict the potential impacts to the environment from metals in contaminated soils and water bodies, research has been conducted to identify novel approaches in the areas of sampling, sample extraction and analyses, and the prediction of metal partitioning.

This research program combined experimental measurements with data from the literature to develop a robust computer-based modeling approach capable of predicting cadmium, copper, lead, and zinc partitioning in contaminated soils near Leadville, CO.

2.0 GOAL AND OBJECTIVES

The overall goal of this research was to develop a robust modeling approach capable of predicting cadmium, copper, lead, and zinc partitioning in metal-contaminated soils. The specific objectives were:

1. identify extractant solutions and analytical methods, and compare the performance of different extractant solutions and analytical methods in quantifying cadmium, copper, lead, and zinc partitioning in contaminated soils;
2. identify appropriate specimen materials to represent the clay, oxide, and organic fractions in the soils studied and construct a series of surrogate soils;
3. calculate cation exchange, specific sorption, and complexation constants for the specimen materials based on metal adsorption/desorption experiments;
4. conduct an extensive literature review to obtain additional binding constants and surface chemistry data for use in developing the modeling approach;
5. calculate and apply a set of unique weighting factors to proportion the clay, oxide, and soil organic matter fractions in the surrogate soils to more closely approximate natural soils; and
6. compare predicted metal partitioning with metal partitioning data derived from selective extraction procedures.

3.0 LITERATURE REVIEW

3.1 Background

Federal regulators limit concentrations of metals in the environment through various federal laws and regulations such as CERCLA and the Resource Conservation and Recovery Act (RCRA). State and county regulators can apply additional local environmental and solid waste regulations to address contamination issues within their jurisdictions. Safe concentrations of metals in soils, sediments, and water bodies are generally specified or derived from guidance incorporated in the various regulations. When safe concentrations of metals are exceeded, some form of mitigation or remediation may be required.

Soil criteria are generally based on total metals data because the data are obtained readily and easy to understand. The data represent the sum of a particular metal from all solid phases present in the system sampled and present the worst case scenario of potential contaminant levels in the system. No distinction is made between metals that are weakly or tightly bound to various soil components nor metals incorporated into the crystal structure of clays and oxide minerals. The use of such data does not quantify the true impact of the site on the environment nor predict the fate and transport of metals in the system. Total metals analysis does not describe 1. the potential over time for metals to sorb and desorb from various solid phases such as oxides, clay minerals, or soil organic matter (SOM); 2. the subsequent resorption of metals to other solid phases; 3. the migration of metals through the soil profile to adjacent receptors; nor 4. the dissolution/precipitation of minerals containing metals. Any of these processes individually or in combination could significantly impact solution phase metals concentrations (e.g. Cd^{+2}, Pb^{+2}, etc.), which are considered the bioavailable fraction (McBride et al., 1997; Sauve, 1999).

A remediation program based on total metals data increases the potential for reducing concentrations of metals to levels significantly lower than concentrations recommended by an environmental risk assessment based on metal partitioning (e.g. soluble or bioavailable metals concentrations, exchangeable metals, etc.) data. The collection of site-specific data that describes the partitioning and bioavailability potential of metals can provide the risk assessor with a more realistic picture of the environmental risks posed by a contaminated system. In the case of abandoned mines and tailing sites and limited state and federal funds, the extra expense of remediating sites to contaminant levels lower than necessary results in fewer sites being successfully remediated.

Based on the need of risk assessors and regulators to reduce data requirements and streamline the collection of site-specific data, the study of metal partitioning in contaminated systems has been approached from three separate paths. First, with the advent of more powerful computer systems, researchers have combined large environmental datasets with empirical equations and mechanistic models to predict the partitioning and potential bioavailability of metals under a variety of conditions (Kent et al., 1988; Loux et al., 1989; Paulson and Balistrieri, 1999; Gustafsson, 2001). Most of the datasets used in available chemical equilibrium/speciation programs (e.g. ECOSAT, MINEQL+, Visual MINTEQ, MINTEQA2, etc.) are based on sorption experiments using specimen (pure) or synthetic materials for oxides (Dzombak and Morel, 1990), humic substances (Bunzl et al., 1976), and clays (Ziper et al., 1988). Second, other researchers have developed sequential extraction procedures that delineate a soil or sediment system into discrete subsystems representing individual soil components (Tessier et al., 1979; Levy, 1990). Quantifying metals concentrations associated with each solid phase generates an overall picture of metal partitioning in a system and the potential impacts a particular site poses to the environment. A third approach has been the analyses of environmental datasets by linear and non-linear regression methods to identify a few key components of a system that allow the formulation of empirical equations for predicting a metal's bioavailability potential (McBride et al., 1997; Kalbitz and Wennrich, 1998; Radovanovic and Koelmans, 1998; Sauve, 1999; Voegelin et al., 2001). Each of these approaches has the potential of reducing the amount of physical and chemical data required (while generating better data) to predict the potential environmental impacts of a site.

Regardless of the approach, sample extraction and analytical methods that had been primarily associated with agricultural issues were modified for use in environmental studies. Thus, over the past 50 years, the focus of these agricultural methods changed from measuring the excess or deficiency of macronutrients and micronutrients with regards to crop and animal production to measuring trace concentrations of macronutrients, micronutrients, and nonessential elements associated with environmental health or contamination issues. Development and refinement of analytical technologies, such as inductively coupled plasma–atomic emission spectroscopy (ICP-AES) and graphite furnace atomic absorption spectroscopy (GFAAS) systems, that were capable of measuring metals at concentrations in the range of low parts per billion to low parts per trillion became necessary to address health and environmental problems caused by trace concentrations of metals.

The data generated by these modified sample extraction procedures and refined analytical methods have been used in conjunction with empirical equations and mechanistic models to describe metal sorption processes and predict metal partitioning in numerous media under a variety of conditions. Researchers have used these results to determine future impacts on the environment, identify appropriate cleanup levels, aid in identifying suitable remediation technology, and provide assurance that remediation has been accomplished.

Ultimately, the two primary goals of researchers, risk assessors, and regulators are to identify a streamlined process that can provide quality data from a select number of sample extraction and analytical methods and develop a robust, computer-based, multi-site model that can incorporate the data and provide accurate predictions as to a contaminated site's potential environmental impact.

In summary, advancements in our understanding of metal sorption and desorption processes in soils and sediments have come in four distinct areas of research; selection of specimen materials to mimic individual soil components, evaluation of extractant solutions and methodologies, development of spectroscopic and microscopic technologies, and development and refinement of empirical equations and mechanistic predictive models. Although the four areas of research are distinct, they are also extensively intertwined. A thorough review of the literature indicates that over the past 40 years, a majority of sorption experiments involving metals have incorporated the previous findings from one or more of these four areas of research to advance the understanding of metal chemistry at the solid-solution interface. The following sections describe the general advancement of each area of research.

3.2 Metal Sorption Research

3.2.1 Identification and Selection of Specimen and Synthetic Materials

The two primary benefits of using specimen or synthetic (specimen) in metal sorption experiments are to provide a well-characterized homogeneous surface for sorption reactions and reduce the number of variables present in the experiment. Specimen materials are generally characterized by one or two classes of reactive sites (e.g. exchange, specific sorption, and complexation sites). Using specimen materials to represent specific soil components in conjunction with controlled experimental conditions (e.g. manipulation of pH, ionic strength, temperature, atmosphere, solid/solution ratio, etc.) allows the researcher to study the impact of individual variables on sorption processes by selectively changing one variable at a time. As a result, sorption reactions can be quantitatively described. Based on a review of approximately 300 articles involving metal sorption experiments, over 80% incorporated one or more specimen materials. Research into metal sorption processes did not really start until the

1970s as evidenced by the fact that only 5 of the approximately 240 studies incorporating metals and specimen materials pre-dated 1970.

The most commonly used specimen materials over the past 40 years have been kaolinite (KGa-1, KGa-2), illite (Silver Hill, MT; Morris, IL; and Fithian, IL), and montmorillonite (SWy-1, SWy-2, Camp Berteau) clay minerals, synthetic iron oxides (ferrihydrite, goethite, hematite), and humic substances consisting of various types of peat, humic acid, and fulvic acid.

Clay Minerals

Kaolinite, a 1:1 clay, and illite, a non-expanding 2:1 clay, consist primarily of permanent negative charge sites located on external planar surfaces. The permanent negative charge is the result of isomorphic substitution in the octahedral and tetrahedral layers during the formation of primary and secondary clay minerals. There are also variable charge sites located on the broken edges of clay particles associated with silica or aluminum (i.e. Si-OH and Al-OH). Variable charge sites are generally positive in low pH environments and negative in high pH environments. The change in charge at these sites is due to protonation at low pH values and deprotonation at high pH values. However, the majority of the surface charge associated with these two particular clay minerals comes from permanent negative charge sites.

Smectites are a family of expanding 2:1 clay minerals that include the bentonites, chlorites, and montmorillonites and consist of permanent and variable charge sites. In smectites, the variable charge sites constitute a greater fraction of the overall charge. The permanent negative charge sites are located on both the interlayer and exterior planar surfaces, while the variable charge sites are located at the broken edges of the clay particle. Montmorillonites have been used extensively in metal sorption studies because they provide an opportunity to study both ion exchange and specific sorption processes on one material unlike kaolinite, illite, and the oxide minerals.

The permanent negative charge sites, described commonly as siloxane cavities, are roughly hexagonal consisting of six corner-sharing silica tetrahedra (Sposito, 1989). The amount of negative charge associated with these sites is dependent on the amount of substitution in the clay structure. If very little substitution has occurred as is the case for kaolinites and illites, the siloxane cavity will not present a strong attraction for cations in the surrounding solution. Cation sorption at these weaker sites involve mostly electrostatic forces and the formation of readily exchangeable outer-sphere surface complexes. If significant isomorphic substitution has occurred as is normally the case for smectites, the siloxane cavity will present a stronger attraction for soluble cations. Cation sorption at these stronger sites involves in addition to electrostatic forces, ionic and covalent bonding with the formation of inner-sphere complexes that are not readily exchangeable.

Researchers have used these three clay mineral types (sometimes in combination with fulvic and humic acids) to investigate ion exchange between metals and sorbed cations (e.g. Ca, K, Na, etc.) and specific sorption reactions between metals and protons. The data have been used to generate selectivity sequences or affinity orders (Farrah and Pickering, 1978; Hatton and Pickering, 1980; Slavek and Pickering, 1981) and calculate selectivity coefficients and thermodynamic equilibrium constants (Krishnamoorthy and Overstreet, 1950; Bittell and Miller, 1974; Stuanes, 1976; Farrah et al., 1980; Van Bladel et al., 1993; Helios-Rybicka et al., 1995; Auboiroux et al., 1998). Additional research has investigated the effects of pH, ionic strength, competing cations, sorbent/sorbate ratios, metals concentrations, different background electrolytes, and organic acids on the sorption of metal cations by clays (Bingham et al., 1964; Wold and Pickering, 1981; Puls et al., 1991; Arnfalk et al., 1996), the selectivity and efficiency of various extractant solutions to recover sorbed metals from clays (Farrah and Pickering, 1978), and the adsorption/desorption kinetics of metal cations (Bereket et al, 1997).

Adsorption data have been modeled using empirical adsorption isotherms such as the Freundlich equation (Heydemann, 1959; Helios-Rybicka, 1983; Altin et al., 1998; Echeverria et al., 2002), the single-site, two-site, and competitive Langmuir equations (Farrah et al., 1980; Morley and Gadd, 1995; Echeverria et al., 2002), the linear adsorption (K_d) and general adsorption equations (Garcia-Miragaya et al., 1983; Puls et al., 1991), electrostatic surface complexation models (Stadler and Schindler, 1993; Holm and Zhou, 1994; Bradbury and Baeyens, 1997a,b; Barbier et al., 2000), and non-electrostatic surface complexation models (Cowan et al., 1992; Lothenbach et al., 1997). Several researchers have developed multi-site models to describe metal sorption data associated with kaolinite and montmorillonite (Schindler et al., 1987; Zachara et al., 1992; Auboiroux et al., 1998; Ikshan et al., 1999) by combining selectivity coefficients or adsorption isotherms with surface complexation models.

Oxide Minerals

A second class of specimen materials, oxide minerals, has found widespread use in metal sorption studies. These minerals contain only variable charge sites which are generally described as SOH functional groups. The S represents a cation (e.g. Si, Al, Fe, Mn, etc.) that is part of the mineral's crystal structure. Similar to variable charge sites present at clay mineral edges, reactive SOH groups lose H^+ ions as the pH of the system goes from an acid to an alkaline environment (i.e. $SOH_2^+ \rightarrow SOH \rightarrow SO^-$). Depending on the metal cation and the sorption model used to describe the sorption process, binding sites can be divided into two classes, low affinity and high affinity sites, and two configurations, monodentate and bidentate (Dzombak and Morel, 1986, 1990).

Although the majority of metal sorption studies conducted in the past 35 years have used some form of an iron oxide as the specimen material, some studies have used silica gels (Dugger et al., 1964), silica and alumina (Benyahya and Garnier, 1999), gibbsite or aluminum oxides and hydroxides (Kinniburgh et al., 1976; Paulson and Balistrieri, 1999), aluminum-coated silica (Lutzenkirchen and Behra, 1997) to describe surface complexation reactions and calculate thermodynamic parameters (e.g. ΔG, ΔH). Additional specimen materials have included manganese oxide (Matocha et al., 2002; Tonkin et al., 2004), zinc sulphide (Ronngren et al., 1991), iron oxide coated sand (Stahl and James, 1991a), and manganese oxide coated sand (Stahl and James, 1991b).

The selection of iron oxides to investigate the chemical binding of metals to oxide fractions was due to the fact that iron oxides are the most common oxide minerals in soils and sediments. Iron oxides represent a major reactive surface in the environment because they can exist either as fine particles or coatings on clays and other minerals.

Although sorption data generated from experiments using iron oxides have been described using selectivity sequences (Kinniburgh et al., 1976), selectivity coefficients (Zachara et al., 1993), and adsorption isotherms such as the Freundlich, Langmuir, and linear adsorption equations (Kinniburgh et al., 1976; Dzombak and Morel, 1986), most of the sorption research conducted with iron oxides has been concentrated on the development and refinement of surface complexation models. The models are described in more detail in section 3.2.4. Amorphous and crystalline iron oxides have been used in developing the Diffuse or Double Layer Model (Huang and Stumm, 1973; Davis and Leckie, 1978; Paulson and Balistrieri, 1999), the Constant Capacitance Model (Schindler et al., 1976; Ronngren et al., 1991), the Generalized Two-Layer Model (Dzombak and Morel, 1986, 1990), the Triple Layer Model (Hayes and Leckie, 1987; Jung et al., 1998; Robertson and Leckie, 1998), and several non-electrostatic models (Cowan et al., 1991, 1992; Zachara et al., 1992). Additional research has investigated desorption kinetics (Backes et al., 1995; Glover et al., 2002), effects of time, pH, ionic strength, metals concentrations, and sorbent/sorbate ratios (Swallow et al., 1980; Ford et al., 1997), and the calculation of thermodynamic parameters (Dugger et al., 1964).

Humic Substances

Since 1990, metal sorption studies involving humic substances (peats, humic acids, and fulvic acids) increased significantly due to the application of new spectroscopic techniques and powerful chemical equilibrium/speciation computer programs. Research into metal sorption processes associated with humic substances focused primarily on the investigation of adsorption/desorption kinetics (Bunzl et al., 1976), calculation of distribution and selectivity coefficients (Bunzl, 1974a,b; Crist et al., 1996; Evangelou et al., 1999), application of adsorption isotherm equations (Sanders and McGrath, 1988), and the effects of pH, competing cations, ionic strength, metals concentrations, and humic substances concentrations on sorption processes (Kerndorff and Schnitzer, 1980; Davis, 1984; and Nakhone, 1997). Using Electron Spin Resonance (ESR) technology, McBride (1978) and Bloom and McBride (1979) determined Cu^{+2} and VO^{+2} formed rigid inner-sphere complexes with oxygen ligands of reactive groups, while other transition metals retained their hydration spheres and were weakly bound by electrostatic interactions.

Research into the development of predictive humic models built upon the earlier development of surface complexation models associated with oxide specimen materials (Huang and Stumm, 1973; Schindler et al., 1976). In the past 15 years, complex humic models incorporating large environmental datasets were developed for use with available chemical equilibrium/speciation computer programs (e.g. ECOSAT, MINTEQA2, Visual MINTEQ, etc.). The most common humic models are the Non-Ideal Competitive Adsorption-Donnan Model (Marinsky et al., 1980; Benedetti et al., 1995; Kinniburgh et al., 1996), Humic Ion-Binding Model V (Tipping and Hurley, 1992; Tipping, 1993) and Model VI (Tipping, 1998), Windermere Humic Aqueous Model (Tipping, 1994; Dwayne and Tipping, 1998), and the Stockholm Humic Model (Gustafsson, 2001, Gustafsson et al., 2003a,b). The models are described in more detail in section 3.2.4.

Limitations of Surrogate Materials

The major limitation in using specimen materials for metal sorption studies is the potential that the specimen materials will have significantly different surface chemistry attributes than the soil fractions they represent. Soil particles in the clay mineral and oxide fractions are more likely to be mixtures of two or more minerals or coated with oxide minerals or humic substances. Thus, individual soil particles will exhibit a heterogeneous surface rather than a homogeneous surface. Substitution within the crystal structure and other surface imperfections can modify the surface chemistry significantly, resulting in additional changes in binding capacity and types of sorption processes. As a consequence, the sorption of metal cations on individual soil fractions can be significantly different than the sorption of metals on specimen materials.

However, the use of specimen materials in laboratory sorption studies has provided important insights into ion exchange, specific sorption, and complexation reactions under a variety of controlled environments. The data generated have provided the foundation for conducting research into metal sorption processes in more complex systems.

3.2.2 Identification and Evaluation of Extractant Solutions and Procedures

In tandem with metal sorption studies involving specimen materials was the identification and evaluation of extractant solutions and the development of sequential and selective extraction procedures. Many of the extractants used for the recovery of metal cations in environmental studies were adapted from agricultural procedures. Determination of the selectivity and efficiency of various extractant solutions to recover metal cations from different solid surfaces or reactive sites was accomplished using specimen materials. The assumption was the selectivity and efficiency of a particular extractant solution in a controlled surrogate system was qualitatively similar to its selectivity and efficiency in a complex natural system. Although the same basic extractants (e.g. deionized water, 0.01M $Ca(NO_3)_2$, etc.) were used to recover soluble and exchangeable metals from specimen materials and soils, the selection of extractants for the more tightly bound metals was based on the ability of an extractant to recover metals from specific types of sorption sites (e.g. cation exchange, specific sorption, and complexation sites) or soil fractions (e.g. clay minerals, oxide minerals, humic substances).

Deionized water (DIW) or a weak solution (i.e. 0.005M to 0.05M) consisting of either Ca^{+2} or Mg^{+2} with Cl^- or NO_3^- as a counterion have been used to recover soluble metals (Levy, 1990; Sauve, 1999). The weak electrolyte solution is the extractant of choice due to the potential of DIW to solubilize humic substances during the extraction procedure and thus recover metals associated with weakly sorbed or complexed sites (Gerritse and van Driel, 1984; Sauve, 1999).

Extractant solutions used in the recovery of exchangeable metals are more varied. Extractants in the range of 0.1M-1.0M consisting of Na^+, K^+, NH_4^+, Ca^{+2}, or Mg^{+2} with NO_3^-, Cl^-, SO_4^{-2}, or ClO_4^- as a counterion have been used on a wide range of specimen clay minerals and in the sequential extraction of soils (Krishnamoorthy and Overstreet, 1950; El-Sayed et al., 1970; McBride, 1979, 1980; Tessier et al., 1979; Sposito et al., 1981, 1983; Jarvis, 1986: Levy, 1990; Dijkstra et al., 2004). Generally, NO_3^- is used as the counterion because it complexes the least with metal cations in solution and minimizes interferences.

Selection of extractants for the recovery of specifically sorbed and complexed metals has been more difficult. The selection of such extractants has been based on such considerations as electronegativity, ionic radius, and valence of the exchanger cation, plus the pH, temperature, and ionic strength of the system (Dugger et al., 1964; Andersson, 1977; Soon and Bates, 1982; Miller et al., 1986; Keizer and Bruggenwert, 1991).

Other researchers have attempted to recover metals from specific soil fractions by using extractants such as H_2O_2, $Na_4P_2O_7$, $K_4P_2O_7$, NaOCl, NaOH, or HNO_3 to recover complexed metal cations from organic materials (Miller and McFee, 1983; Li and Shuman, 1996) and NH_2OH-HCl, $(NH_4)_2C_2O_4$, EDTA, CH_3COOH, or NaOAc to recover exchangeable and specifically sorbed metal cations from carbonates and amorphous/crystalline Fe-, Mn-, Al-oxides (Miller and McFee, 1983; Levy, 1990; Krishnamurti et al., 1995, 1997). Metal cations were recovered from the residual soil fraction using some combination of strong acids like HF, HNO_3, $HClO_4$, HCl, or H_2O_2 (Tessier et al., 1979; Li and Shuman , 1996).

Researchers have incorporated the results of extractant studies involving a single component to develop sequential extraction procedures for determining metal partitioning in complex natural systems. The procedures were based on the theory that by combining different extractant solutions in a particular sequence, metals could be selectively recovered from specific operationally defined fractions. It was assumed that the sequence of the different extractant solutions would not recover metals from more than one fraction or prevent the recovery of metals from other fractions later in the extraction sequence (Stover et al., 1976; Tessier et al., 1979; Miller et al., 1986). The general approach has been to first extract the soil with the least aggressive extractant (e.g. DIW, $CaCl_2$, etc.) to recover the soluble and exchangeable fractions and then proceed to successively harsher extractants (i.e. acids and bases) to recover the tightly bound oxide and organic complexes or occluded fractions (Miller et al., 1986). Although all extraction procedures recover soluble and exchangeable metals, the real variation in the different sequences is the recovery of metals from the different oxide and organic fractions present in soils.

From the 1950s to the 1970s, experiments incorporating some form of sequential extraction procedures studied primarily the partitioning of macronutrients and micronutrients (e.g. Cu, Zn) in soils at native or background concentrations (Le Riche and Weir, 1963; McLaren and Crawford, 1973a,b; Shuman, 1979; Tessier et al., 1979) Beginning in the mid-1970s, a number of sequential extraction procedures were developed for the recovery of trace metals from soils and sediments amended with sewage sludge (Stover et al., 1976), soil amendments (Li and Shuman, 1996), fertilizers (Gray et al., 1999; Krishnamurti et al., 1997), or impacted by aerial depositions from smelters (Hickey and Kittrick, 1984) and mining activities (Levy, 1990). Most studies delineated the system into four or five fractions consisting of Fe-oxide, organic matter, and sand, silt, and clay mineral fractions (Le Riche and Weir, 1963; Shuman, 1979); sorbed, organic, carbonate, and sulfide fractions (Stover et al., 1976; Sposito et al., 1982); carbonate, Fe- and Mn-oxide, organic, and residual fractions (Tessier et al., 1979); organic and oxide/carbonate fractions (Soon and Bates, 1982); amorphous Fe-oxide, crystalline Fe-oxide and organic matter fractions (Kuo et al., 1983); crystalline Fe-oxide occluded, sulfide, and residual fractions (Miller and McFee, 1983); organic, clay, Fe- and Mn-oxide fractions, and fixed irreversibly (Fic and Isenbeck-Schroter, 1989); and organic and Fe- and Mn-oxide fractions, and total metals (Levy, 1990).

Later studies of metal contaminated soils delineated the soil into seven or more fractions based on an ever increasing complex suite of extractants or extraction steps. Miller et al. (1986) and Li and Shuman (1996) delineated the soil into specifically sorbed, organically bound, Mn-oxide occluded, amorphous Fe-oxide occluded, crystalline Fe-oxide occluded, and acid soluble or residual fractions. Krishnamurti et al. (1997) fractionated Saskatchewan agricultural soils into carbonate bound, metal-organic complex bound, easily reducible metal-oxide bound, organic bound, amorphous mineral colloid bound, crystalline Fe-oxide bound, and residual fractions.

Limitations of Extractant Solutions and Sequential Extraction Procedures

The major questions associated with the use of selective extractant solutions and sequential extraction procedures on complex systems are 1. what percentage of metal cations sorbed onto a specific soil component are recovered, and 2. are the metals recovered only from the targeted component or several components. The efficiency of an extractant solution is generally unknown since the overall sum of metals recovered from the individual components is usually less than the total metals concentration reported. The potential of metals from one or more soil components to desorb and resorb onto different soil components including the targeted component during the extraction procedure has not been quantified. Although conclusions about metal partitioning in soils based solely on the results of selective extractants and sequential extraction procedures is probably not warranted, advancements in this area of research in conjunction with specimen materials research and the development of spectroscopic methods have provided critical data in describing the locations of sorbed metals in complex systems and the possible sorption reactions involved.

3.2.3 Development and Application of Spectroscopic and Microscopic Techniques

The development of spectroscopic and microscopic techniques over the past 35 years has provided critical support in the understanding of metal sorption on solid surfaces at the solid-solution interface and the subsequent development of surface complexation models. Although X-ray diffraction (XRD) has been the primary technique used in the analysis of clay mineral structures for the past 75 years (Moore and Reynolds, 1997), it wasn't until the late 1960s and early 1970s that XRD analysis was used in conjunction with other spectroscopic techniques such as infrared (IR), electron spin resonance (ESR), and electron paramagnetic resonance (EPR) spectroscopies to aid in identifying the structures and locations of sorbed metals.

One of the earliest studies reviewed was Hildebrand and Blum (1974), who were able to discriminate the locations of lead complexes on kaolinite, illite, and montmorillonite based on shifts in XRD peaks and IR spectra. Clementz et al. (1973) and McBride and Mortland (1974) combined XRD and ESR techniques to study copper and manganese sorption on montmorillonite, while McBride (1976) used the same techniques to determine the sorption of Cu^{+2} as $Cu(H_2O)_4^{+2}$ at acidic pHs was on the exterior planar surface of kaolinite and not at proton saturated edge sites.

Beginning in the early 1990s, research into the sorption of metals on solid surfaces in natural complex systems experienced a significant increase due to the development of more sophisticated spectroscopic and microscopic techniques. Technologies such as atomic force microscopy (AFM), transmission electron microscopy (TEM), scanning electron microscopy (SEM), Fourier transform-infrared (FT-IR) spectroscopy, X-ray absorption spectroscopy (XAS) and its derivatives X-ray absorption fine structure (XAFS), extended X-ray absorption fine structure (EXAFS), X-ray absorption near-edge structure (XANES), and reflection X-ray absorption fine structure spectroscopy (REFLEXAFS); electron microprobe (EM), electron probe microanalysis (EPMA), X-ray microfluorescence (uXRF), X-ray microdiffraction (uXRD), and secondary ion mass spectrometry (SIMS) have resulted in the discrimination of solid surfaces at sub-micron dimensions and the enhanced description of sorbed metal structures based on detailed images.

Tingle et al. (1993) used XRF, XPS, and surface analysis by laser ionization in conjunction with nonresonant photoionization and time-of-flight spectroscopy to conclude the majority of lead in mine tailings and soils from the Leadville, CO area were as coatings and films. O'Day et al. (1998) used XAS, XAFS, SEM, and XANES along with XRD, EM, and SIMS analysis to obtain detailed images of cadmium, lead, and zinc complexes on and in particles of contaminated sediments. Ostergren et al. (1999) quantified lead partitioning in Leadville, CO mine tailings and soils and Arkansas River sediments using XAFS and EPMA.

Strawn and Sparks (1999) used XAFS and XANES to describe the conditions necessary for inner-sphere and outer-sphere complexation of lead on specimen montmorillonite, while Gier and Johns (2000) used XPS to study the adsorption and structure of cesium, barium, copper, lead, and zinc on the outer and interlayer surfaces of well-characterized micas and illites. Using EPR, Hyun et al. (2000) showed copper exhibited a free tumbling motion at acidic pHs indicative of non-sorbed or ion-exchanged cations, while at higher pHs, free tumbling motion decreased indicating the formation of a more rigid structure associated with surface complexation.

Otto et al. (2001a,b) used NMR to show that cadmium bound to oxygen containing functional groups on fulvic acid exhibited a rapid exchange between free and complexed cadmium species.

Morton et al. (2003) used XAS technology to show that copper sorbed to permanent charge sites (i.e. cation exchange) were outer-sphere complexes, while those sorbed to edge sites (i.e. specific sorption) were a mixture of monodentate and bidentate inner-sphere complexes. Manceau et al. (2003) used uXRF, uXRD, and EXAFS to delineate the structure of manganese and zinc complexes on and in ferromanganese nodules found in loess soils of the Mississippi Basin. Based on EXAFS, Sarrett et al. (2004) concluded the partitioning of sorbed zinc in the organic horizon of a contaminated soil was 45% zinc-organic matter complexes, 20% outer-sphere zinc complexes, 10% zinc-phosphates, and 10% zinc-iron oxides.

Limitations of Spectroscopic and Microscopic Techniques

The major limitations of this technology are the sample size required and changes in the surface of the sample during sample preparation and analyses. The amount of sample required for spectroscopic and microscopic analyses is extremely small and the question becomes one of whether the sample analyzed accurately represents the system being studied. The solid surface of the sample is exposed to high vacuums, application of various coatings, and bombardment by high energy rays. The combined effect of these changes can alter the structure of the surface and existing surface complexes.

Although, the adverse impact of these two issues on the data is unclear, the development and increase in sophistication of spectroscopic and microscopic technologies over the past 25 years has allowed scientists to analyze at an ever increasing spatial resolution the in-situ, heavy metal sorption processes on a variety of surfaces under a range of conditions. Application of TEM and EM techniques have provided images of solid surfaces at the sub-micron scale and data on the distribution of elements on those surfaces. The data obtained from the application of these technologies on a variety of materials have confirmed or refined previously developed theories regarding sorption locations and types of surface complexes formed. Soils and sediments rather than individual specimen or synthetic materials can be analyzed directly.

3.2.4 Development and Application of Empirical and Mechanistic Models

Empirical equations (i.e. linear and non-linear regression equations, selectivity coefficients, adsorption isotherms, etc.) and mechanistic models (i.e. surface complexation models) have been used to describe experimental data from a large number of metal sorption studies. The studies have investigated ion exchange and sorption reactions on a variety of inorganic and organic surrogate materials, soils, and sediments.

Basically, empirical equations or models are mathematical descriptions of the experimental data. Most empirical approaches require less than three or four adjustable parameters to characterize the experimental data. Surface complexation models (SCMs) describe data obtained from complex multi-component systems and can be used for the prediction of metal partitioning or the characterization of other datasets (Dzombak and Morel, 1990). One class of SCMs incorporates the electrostatic effects of surface complexation reactions, while a second class of SCMs, described as non-electrostatic models (NEM), assume the electrostatic effects of surface complexation reactions have little impact on the overall system and can be ignored. Both classes of SCMs incorporate multiple reactive surface functional groups to describe surface complexation reactions at the solid-solution interface.

Ion exchange reactions are generally described as reactions involving the exchange of a cation or anion on a charged surface with a similarly charged ion in the surrounding solution. Ion exchange reactions, which involve only electrostatic forces, are diffusion-controlled, rapid, reversible, and stoichiometric reactions (Sparks, 1995).

Sorption reactions involve the interaction of a surface functional group with an ion or molecule in the surrounding solution that results in a stable surface complex. Sposito (1989) described a surface functional group as " a chemically reactive molecular unit bound into the structure of a solid at its periphery such that the reactive components of the unit can be bathed by a fluid". Inorganic surface functional groups are located primarily at sites associated with clay edges (i.e. Al-OH, Si-OH) and metal oxides/ hydroxides (i.e. FeOOH, MnO, etc.). Carboxyl, carbonyl, and phenolic are the primary organic functional groups. To some degree, the charge associated with surface functional groups are pH dependent and as such become more negative via deprotonation (i.e. $Si-O^-$, $Fe-O^-$, etc.) at high pHs or more positive by protonation ($Si-OH_2^+$, $Fe-OH_2^+$, etc.) at low pHs.

Metal complexes can be bound to the surface in either a monodentate or bidentate configuration and as inner-sphere or outer-sphere surface complexes (Sposito, 1989; Dzombak and Morel, 1990; Sparks, 1995). The outer-sphere metal complex retains its hydration sphere between the solid surface and the electrostatically bound cation, while the inner-sphere metal complex contains no hydration sphere and is bound strongly to the solid surface by covalent or ionic bonding (Sposito, 1989). The outer-sphere complex is considered weakly bound compared to the inner-sphere complex and the sorption reaction is rapid, reversible, and affected by the ionic strength of the surrounding aqueous solution (Sparks, 1995). In contrast, the inner-sphere surface complexation process is slow, partly reversible, and not affected by the ionic strength of the surrounding solution (Sparks, 1995). The outer-sphere surface complexation process is analogous to ion exchange reactions in that electrostatic forces are involved and the reactions are rapid and reversible.

Empirical Equations

Selectivity Coefficients

Selectivity coefficients, which are used primarily to describe ion exchange reactions in soils and specimen materials, were developed in the late 1920s, early 1930s, and 1950s. The Kerr, Vanselow, Gapon, Krishnamoorthy and Overstreet, and Gaines and Thomas equations were proposed in 1928, 1932, 1933, 1949, and 1953, respectively (Sparks, 1995). The Kerr, Gapon, and Krishnamoorthy and Overstreet equations describe the solid and solution phases in concentration terms. However, the differences in the three equations are related to the concentration units used in the equations and the description of heterovalent ion exchange. Kerr used molar concentrations to describe the solid-solution system, while Gapon and Krishnamoorthy and Overstreet used equivalent concentrations (Sparks, 1995). Krishnamoorthy and Overstreet also added a factor to compensate for differences in the valence of the exchanging ions (Sparks, 1995). The Vanselow and Gaines-Thomas equations describe the system using activities (Sparks, 1995), but the two equations differ in their treatment of the solid exchanger phase. For exchanges involving similarly charged cations, all selectivity equations reduce to the Kerr equation (Sparks, 1995).

Although there are numerous variants of these selectivity coefficient equations available, the most commonly used equations in environmental soil chemistry have been the Vanselow, Kerr, and Gapon equations. Krishnamoorthy and Overstreet (1950) compared the ability of the Kerr, Gapon, Vanselow, and Guggenheim equations to describe Cu^{+2} and Pb^{+2} exchange on bentonite, while Bittell and Miller (1974) used the basic Kerr equation to study divalent metal cation exchange on kaolinite, montmorillonite and illite. The Vanselow equation has been applied to clays (Sposito and Mattigod, 1979; Schindler et al., 1987; Auboiroux et al., 1998) and soils (Zachara et al., 1992, 1993). The Gapon is used primarily in agriculture related to saline-sodic issues and the exchange of macronutrients.

Adsorption Isotherm Equations

Adsorption isotherm equations have been used to describe the adsorption of metal cations to a variety of specimen materials and soils. The most commonly used adsorption isotherm equations are the Langmuir, Freundlich, and linear adsorption isotherm. The popularity of these equations is due primarily to the ease of fitting data and quantifying parameters.

A review of the literature indicates the Freundlich (Helios-Rybicka, 1983; Buchter et al., 1989; Jopony and Young, 1994; Elzinga et al., 1999) and linear adsorption equations (Gerritse and Van Driel, 1984; Merrington and Alloway, 1994; Gomes et al., 2001; Sauve et al., 2003) are applied more frequently than the Langmuir equation (Harter and Baker, 1977; Selim et al., 1992; Basta et al., 1993; Altin et al., 1998; Shukla et al., 1998) in adsorption studies involving soils. The Langmuir equation is used more in adsorption studies involving specimen materials (Farrah et al., 1980; Sanders and McGrath, 1988; Ikshan et al., 1999; Shukla, 2000). The Langmuir equation is more limited in its application than the Freundlich or linear adsorption equations due to the assumptions used to develop the Langmuir equation. Basically, those assumptions include 1. reactive sites, which are located only on planar surfaces, are limited, identical, and sorb one ion or molecule; 2. the energy of adsorption, which is the same for all sites, is independent of the extent of surface coverage; 3. the sorbed ions or molecules are treated as point charges and there is no interaction between adjacent sorption sites; and 4. the maximum adsorption capacity is achieved when all surface sites are occupied, which translates into a monolayer of sorbed ions or molecules (Dzombak and Morel, 1990; Sparks, 1995).

The general good fit of sorption data achieved with the Freundlich equation is a combination of function robustness and the insensitivity of the log – log plots commonly used to plot experimental data. Because the Freundlich equation allows multiple layers of adsorption, there is no maximum adsorption capacity. Thus, at high solute concentrations, the Freundlich equation will continue to describe adsorption processes when surface precipitation is a more distinct possibility (Dzombak and Morel, 1990). However, the Freundlich equation is used frequently to describe pesticide or metals behavior in soils because the concentrations of pesticides and metals are generally low and the subsequent loading of solid surfaces is below the point where surface precipitation would be expected (Sparks, 1995).

The linear adsorption equation is restricted to a narrow range of low solute concentrations due to the assumption that the adsorption of ions or molecules is a linear response phenomenon. At high solute concentrations, adsorption has been shown to be non-linear (Davis and Kent, 1990; Dzombak and Morel, 1990; Sparks, 1995; Stumm and Morgan, 1996).

One additional adsorption isotherm equation is the Brunauer-Emmett-Teller (BET) equation proposed by Brunauer et al. (1938). The BET equation, which assumed adsorption could occur in multiple layers (contrary to the Langmuir equation), is not used in metal sorption studies other than to determine the surface area of solids via nitrogen gas adsorption measurements.

Linear/Non-Linear Regression Equations

A third class of empirical equations used in fate and transport metal studies is the linear/non-linear regression equation, which is used to quantify concentrations of free cations (e.g. M^{+2}) in the soil solution. The development of this class of equations has been the result of studies investigating the bioavailability and phytoavailability of metals in soils. Based on correlation analysis of large environmental datasets, linear/non-linear regression equations were developed to predict free metal cation concentrations in a wide range of soil types and environments (McBride et al., 1997; Sauve, 1999; Sauve et al., 1997, 1998a,b,c, 2000a,b; Wu et al., 2000; Lofts et al., 2004). Generally, the only data contained in these equations are pH, concentrations of total metals, and soil organic matter. However, this class of equations is limited to the prediction of free metal cation concentrations in the soil solution and not metal partitioning in natural soils.

Surface Complexation Models (SCMs)

The application of SCMs to the prediction of metal partitioning in natural soils has been limited by the complexity of the soil environment, the availability of surface chemistry and environmental data, and the inherent limitations of existing models to extrapolate data from sorption studies involving simple, single-component systems to the more complex natural systems. However, a great deal of research has been conducted in the past 20 years in the area of SCM development and its application to complex multi-component systems.

All SCMs are based on electric double-layer (EDL) theory first proposed by Gouy and Chapman in 1910 and 1913, respectively. Simply stated, Gouy and Chapman derived an equation for describing the distribution of ionic species at a charged solid-solution interface. The two layers envisioned in EDL theory consist of an infinite plane of charge surrounded by a diffuse layer of countercharge or the combination of a compact layer of bound countercharge and a diffuse layer of additional countercharge (Sparks, 1995). Because Gouy and Chapman treated the countercharges in the diffuse and bound layers as points of charge instead of considering ionic diameters, at high potential values and thin diffuse layer thickness the concentration of charged species at the surface became unrealistically high (Dzombak and Morel, 1986, 1990).

In 1924, Stern modified the EDL by dividing the solid-solution interface into two planes of charge and taking into account the ionic radius of the counterions. These two modifications limited the concentration of sorbed ions at each plane. The first layer, called the Stern layer, was the location of a finite number of adsorbed H^+ and OH^-, and other specifically adsorbed ions (i.e. inner-sphere surface complexes)(Sparks, 1995). The second plane, called the diffuse layer, was the location of non-specifically bound (i.e. outer-sphere) complexes and disassociated charged solutes. In 1947, Grahame expanded the Stern layer into two planes, the inner Helmholtz plane where inner-sphere surface complexes were located and the outer Helmholtz plane where outer-sphere surface complexes were located (Sparks, 1995). Grahame included also an electrostatic correction factor for describing the relationship of surface charge and electric potential associated with the adsorption of ions and molecules at specific sorption sites (Sparks, 1995). Stern and Grahame's refinements to EDL theory formed the basis for surface complexation theory and led to its application in the area of colloid chemistry and the subsequent development of electrostatic SCMs (Dzombak and Morel, 1990; Stumm and Morgan, 1996).

All electrostatic SCMs are based on the following parameters: 1. sorption reactions occur at specific surface sites; 2. sorption reactions are described by mass law and material balance equations; 3. surface charge is the result of surface complexation reactions; and 4. the effect of surface charge on the extent of surface complexation is addressed by applying a electrostatic (coulombic) correction factor to the mass law constants (Dzombak and Morel, 1990).

A second type of SCM, which predated development of electrostatic SCMs, was the non-electrostatic SCM (NSCM). The NSCMs were first proposed in the 1950s and 1960s by Kurbatov (1951), Ahrland (1961), Stanton and Maatman (1963) (Dzombak and Morel, 1990), and Dugger et al. (1964) who concluded chemical interactions involved in surface complexation reactions were much stronger than electrostatic interactions and as a consequence, the coulombic correction factor could be excluded from mass law equations. Cowan et al (1991, 1992) developed a NSCM for predicting the sorption of Cd^{+2} to specimen and soil silicates, while Van Benschoten et al. (1998) developed a NSCM for predicting metal desorption during remediation of heavily contaminated soils.

The majority of all SCM research conducted to date has involved specimen materials that contain specific sorption sites (i.e. Fe-, Mn-, Al-, Ti-, Si-oxides and humic materials, etc.). The most common electrostatic SCMs used currently in metal sorption studies are the Constant Capacitance Model (CCM), Diffuse or Double Layer Model (DLM), Generalized Two-Layer Model (GTLM), Triple Layer Model (TLM), Non-Ideal Competitive Adsorption (NICA)-Donnan Model, Humic-Ion Binding Model V/VI, Stockholm Humic Model (SHM), and the Windermere Humic Aqueous Model (WHAM).

The CCM, DLM, GTLM, and TLM are used with clays and oxides, while the NICA-Donnan, Model V/VI, SHM, and WHAM are used primarily with humic materials. The differences between the various SCMs used with clay and oxide minerals are the delineation of planes of charge and the location of inner-sphere and outer-sphere surface complexes at the solid-solution interface.

SCMs – Oxide Minerals

Provided in this section are descriptions of critical components and assumptions incorporated into the two SCMs (i.e., CCM and GTLM) used in this research program for clay and oxide surfaces.

Constant Capacitance Model

The CCM was proposed by Schindler, Stumm, and their co-workers (Goldberg, 1995 and references quoted therein) in the mid-1970s to describe adsorption reactions at oxide-solution interfaces. In developing this SCM, the researchers assumed: 1. all surface complexes [i.e. H^+, OH^-, metal (M^{m+}) and non-metal (C^{c+}) cations, and anions (A^{a-})] were inner-sphere complexes; 2. no surface complexes were formed with ions from the background electrolyte; 3. one plane of charge represented the solid surface and was the location of all inner-sphere complexes; and 4. there was a linear relationship between surface charge density and surface potential (i.e. parallel plate capacitor configuration) (Davis and Kent, 1990; Dzombak and Morel, 1990; Stumm and Morgan, 1996) described by the equation

$$\sigma_o = (CSa/F)\,\psi_o \qquad (1)$$

where C is capacitance density (F m^{-2}), S is the surface area (m^2 g^{-1}), a is the suspension density (g L^{-1}), F is the Faraday constant (C mol_c^{-1}), σ has units of mol_c L^{-1}, and ψ_o has units of volts (V) (Goldberg, 1995). Amphoteric surface hydroxyl groups (i.e. S-OH) form all ionized surface sorption sites (i.e. SOH_2^+ and SO^-) and monodentate and bidentate surface complexes (e.g. $SO\text{-}M^+$, $(SO)_2\text{-}M$) are allowed. The most appropriate application of the CCM is in strong ionic strength systems (i.e. high solute/sorbent ratio).

Diffuse Double Layer/ Generalized Two-Layer Model

The diffuse double layer (DDL) model was proposed by Stumm and co-workers (Goldberg, 1995 and references quoted therein) in the mid-1970s to describe adsorption processes at oxide-solution interfaces. The DDL was modified by Dzombak and Morel (1990), who included a multi-site model proposed by Benjamin and Leckie (1981) and a surface precipitation model proposed by Farley et al. (1985). The modified model, known as the Generalized Two-Layer Model (GTLM), described adsorption reactions at the hydrous ferric oxide (HFO)-solution interface.

Application of the DDL is limited to low ionic strength systems, while the GTLM can operate in any ionic strength system. The ability of the GTLM to function in a range of ionic environments was due to the inclusion of two types of sorption sites; a large population of low affinity sites and a small population of high affinity sites. The inclusion of these two types of sorption sites in the GTLM allowed the description of adsorption and surface precipitation of cations and anions at medium to high solute concentrations (Dzombak and Morel, 1990). However, the GTLM is limited to monodentate surface complexes, while the DDL can describe both monodentate and bidentate surface complexes.

In the GTLM, the first plane of charge at the surface (i.e. σ_o) is the location of all inner-sphere surface complexes (e.g. H^+, OH^-, M^{m+}, A^{a-}), while the second plane of charge (i.e. σ_d) represents the closest distance of approach for all counterions in the diffuse layer (Davis and Kent, 1990; Dzombak and Morel, 1990; Stumm and Morgan, 1996). Although the two planes of charge are equal (i.e. $\sigma_o = \sigma_d$), there is a non-linear relationship between the surface charge of the second plane and the surface potential of the diffuse layer described by the equation

$$\sigma_d = -Sa / F\,(8\varepsilon_o DRTI)^{1/2} \sinh(F\psi_d / 2RT) \qquad (2)$$

where ε_o is the permittivity of vacuum, D is the dielectric constant of water, I is the ionic strength, $\mathrm{sgn}\psi_d = 1$ if $\psi_d > 0$ and $\mathrm{sgn}\ \psi_d = -1$ if $\psi_d < 0$ (d represents the diffuse plane), and c_i and z_i are the concentration and charge of solution species i (Davis and Kent, 1990; Stumm and Morgan, 1996).

SCMs – Humic Models

The development of SCMs for describing the exchange and complexation of metals with humic substances (HS) paralleled development of SCMs associated with oxide minerals. The parallel development of SCMs was due to the recognition that HS had potentially the largest impact on the fate and transport of metals in soils, sediments, and water systems and contained variable charge sorption sites (i.e. carboxylic and phenolic groups) similar to those located on clays and oxide minerals.

The development of several humic models in the past 20 years was based on the number, distribution, and strengths (i.e. pK_as) of carboxylic and phenolic functional groups associated with different HS (Gustafsson, 2001). Models such as the NICA-Donnan and the Gaussian DOM used a continuous distribution of pK_a values to describe the acid-base and metal complexation properties of various HS, while Model V, Model VI, WHAM, and SHM used a discrete-site pK_a value distribution system. Some models used an impermeable sphere geometry to describe the HS structure, while other models used a permeable sphere-like gel structure (Gustafsson, 2001).

The impermeable sphere structure, which assumed an interface environment similar to oxide minerals, corrected for ion binding electrostatics using empirical equations relating charge and potential (Tipping and Hurley, 1992), a SCM such as the DLM, or the Basic Stern Model (BSM) (Gustafsson, 2001). In permeable gel-like systems (e.g. SHM), charge associated with interior and exterior gel surfaces were neutralized by the inclusion of charge screening counterions (Gustafsson, 2001). The SHM was selected to model metal partitioning on humic materials in this research program and is described in the following section.

Stockholm Humic Model

The SHM was developed by Gustafsson in the late 1990s to describe the exchange and complexation of metals and protons with dissolved, suspended, and solid phase humic and fulvic acids (Gustafsson, 2001, 2004; Gustafsson et al., 2003a,b). The SHM was based on Models V/VI and WHAM (Tipping, 1994, 1998; Benedetti et al., 1995). The acid-base properties of humic and fulvic acids, which are assumed to have a permeable gel-like structure, are described by a discrete-site pK_a distribution (Gustafsson, 2003a).

The SHM, which has undergone continuous modification over the past five years, can describe the exchange and complexation of inorganic and organic compounds in solid and liquid systems containing dissolved and solid phase fulvic and humic acids. Generic surface chemistry data, binding constants, and other humic chemistry data have been acquired from a number of large environmental soil and water datasets. The datasets were generated from studies investigating the transport and fate of metals in humic rich environments. The SHM, which is an integral part of the Visual MINTEQ chemical speciation/equilibrium software program was developed by Gustafsson. The freeware Windows program is based on USEPA's MINTEQA2 chemical speciation/equilibrium program.

Limitations of Empirical Equations and Models

The application of an empirical equation or SCM to data generated from metal sorption studies includes the assumptions that the system being studied is at equilibrium and hysteresis or sorption irreversibility is not present in the system. Determination of system equilibrium is fairly straightforward and basically requires the monitoring of metals and exchange cation concentrations. Whether the study is an ion exchange or adsorption experiment, the point where the concentrations of metals and cations in solution do not change any further generally indicates system equilibrium. The amount of time required to achieve equilibrium will depend significantly on the material being studied and other system conditions.

Hysteresis is more difficult to quantify due to the fact that most studies conducted over the past 50 years have studied only the sorption of metals on specimen materials, soils, and sediments and not the desorption process. The assumption has been the desorption reaction is the exact opposite of the sorption reaction. However, hysteresis has been well documented in several adsorption/desorption studies involving clays (Farrah and Pickering, 1978; Sposito and Mattigod, 1979; Verburg and Baveye, 1994), iron oxide (Ford et al., 1997), and soils and sediments (McLaren et al., 1983; Nakhone, 1997; Gao et al., 2003). Researchers have concluded some cases of hysteresis were the result of experimental conditions such as sorbent type, non-attainment of system equilibrium, and physical, chemical and microbiological transformations that inhibited the desorption process during the experiment. As a consequence, the adsorption isotherm equations and SCMs discussed above have not been validated for predicting the desorption of metals from specimen materials and soils.

The application of one empirical equation or SCM to a large number of varied systems has been inhibited by the development of empirical equations and SCMs containing significantly different surface chemistry data and binding constant values. The lack of consistency in binding constant values and surface chemistry data prevents the application of one equation or SCM to other systems (Davis and Kent, 1990; Dzombak and Morel, 1990; Stumm and Morgan, 1996).

Despite the limitations described above, a great deal of progress has been made in the application of these models to more complex systems. Much of this progress has been the result of findings in the area of spectroscopic and microscopic research and the increasing availability of comprehensive surface chemistry and binding constant datasets. Inclusion of data from these two areas of research into existing equation and models has expanded their application to more complex systems.

3.3 Research Program

The primary focus of this research was to develop a robust modeling approach which can predict cadmium, copper, lead, and zinc partitioning in contaminated soils. The modeling approach included surrogate soils comprised of five specimen materials. Metal sorption modeling was accomplished using the Vanselow selectivity coefficient and four SCMs in combination with two Windows-based chemical equilibrium/speciation software programs; MINEQL$^+$, Version 4.5 (Schecher and McAvoy, 2001) and Visual MINTEQ, Version 2.30 (Gustafsson, 2004). MINEQL$^+$ was used to model specimen clays and oxides while Visual MINTEQ was used to model soil organic matter. Model inputs were based on experimental data generated from basic physical and chemical analyses and the selective extraction of metals from contaminated soils, plus data from the literature. The modeling approach was tested over a range of pHs, soil textures, soil organic carbon levels, and concentrations of soluble cadmium, copper, lead, and zinc and total aluminum and iron. Ideally, the modeling approach developed is not limited to predicting only cadmium, copper, lead, and zinc partitioning, but can predict, with some modifications, the partitioning of other transition and heavy metals under similar soil conditions.

4.0 MATERIALS AND METHODS

4.1 Sampling and Preparation Methods

Fourteen soil samples were collected in 1998 from three locations in an irrigated pasture on the Bernie Smith Ranch, which is located approximately 11 km southwest of Leadville, CO. Seven soil samples were collected in 1999 from two additional locations. The 1998 samples were collected in 5-cm intervals beginning at the surface, while the 1999 samples were collected at varied intervals based on horizonation. All locations were sampled to different total depths. These pasture soils have been described previously as Typic Cryaquolls consisting of an organic surface horizon underlain by one or more C horizons containing metal-contaminated sandy material (Levy, 1990). The sandy material was transported by water to this pasture as a result of regional surface mining activities during the late 1800s and early 1900s (Levy, 1990).

After the removal of macro-size pieces of undecomposed organic material, pebbles, and other debris, the samples were air-dried, homogenized, and passed through a 2-mm sieve. Approximately 20 g of the sieved samples were gently crushed with a mortar and pestle prior to chemical analyses.

4.2 Chemical and Physical Analyses – All Leadville, CO Soils

4.2.1 Total Metals Analysis

One g of each sample was digested with HNO_3, $HClO_4$, and HF over a 24 hour period according to the method described by Hossner (1996). In addition to a set of QA/QC samples consisting of blanks, duplicates and NIST standards, sample extracts were analyzed for total elemental content by ICP-AES using a Jarrell Ash 61E system.

4.2.2 Texture, pH, and Carbon Analyses

Particle size analysis for texture classification was conducted using the hydrometer method described by Gee and Bauder (1996). The pH was measured in a 1:1 soil paste consisting of 10 g of soil and 10 ml of 0.01M $CaCl_2$.

Total carbon content was measured using a LECO Model 1200 CHN analyzer, while inorganic carbon content was determined by the gravimetric method as described by Loeppert and Suarez (1996). Organic carbon content was calculated by subtracting the inorganic carbon value from the total carbon value.

4.3 Additional Chemical and Physical Analyses for Selected Samples

Based on total metals analysis, particle size (texture) determination, pH, and carbon speciation; two samples from one 1998 soil profile and two samples from one 1999 soil profile were selected for further chemical analyses. The two 1998 samples were from the third location sampled (i.e. 98-3) and represented the depths of 5-10 cm (i.e. 98-3-5-10) and 20-25 cm (i.e. 98-3-20-25). The two 1999 samples were from the first location sampled (i.e. 99-1) and represented consecutive intervals 0-7 cm (i.e. 99-1-0-7) and 7-12 cm (i.e. 99-1-7-12). The selected samples provided a range of pHs, textures, concentrations of metals, and carbon content with which to test a predictive modeling approach.

4.3.1 XRD Analysis

The XRD analysis of the <2 mm fraction of samples 99-1-0-7 and 99-1-7-12 were conducted by the University of Wyoming, Materials Characterization Laboratory, Laramie, WY. The XRD data reported by Al-Farranj (2002) were used for samples 98-3-5-10 and 98-3-20-25.

4.3.2 Cation Exchange Capacity

Cation exchange capacity (CEC) was measured at 'field pH' using a method described by Sumner and Miller (1996). The method was modified as described below for use with a vacuum extraction system. The procedure included the following steps:

1a. 5 g of sample were added to an extractor tube;

1b. 50 mL of 0.2M NH_4Cl were filtered through the tube and collected;

1c. Step 1b was repeated two times, generating an additional 100 mL of filtrate;

1d. The 150 mL of filtrate were combined and brought to a total volume of 250 mL with fresh 0.2M NH_4Cl;

2a. 50 mL of de-ionized water (DIW) were filtered through the tube and collected;

2b. Step 2a was repeated two times, generating an additional 100 mL of filtrate;

2c. The 150 mL of filtrate were combined and brought to a total volume of 250 mL with fresh DIW;

3a. 50 mL of 0.2M KNO_3 were filtered through the tube and collected;

3b. Step 3a was repeated two times, generating an additional 100 mL of filtrate;

3c. The 150 mL of filtrate were combined and brought to a total volume of 250 mL with fresh 0.2M KNO_3;

4. The three filtrates from each sample were analyzed for Ca, Mg, Na, P, Al, Fe, Mn, Ti, Cu, Zn, Ni, Mo, Cd, Cr, Sr, B, Ba, Pb, Si, V, and NH_4 by ICP-AES using a Thermo Jarrell Ash IRIS Advantage System.

Cations extracted with NH_4Cl-DIW-KNO_3 were initially reported in units of mg L^{-1}. The results were then converted to mg kg^{-1} and finally to $cmol_c$ kg^{-1}. Normally, CEC is based solely on the amount of NH_4^+ recovered during the 0.2M KNO_3 extraction step and is calculated using the equation (Sumner and Miller, 1996):

$$CEC = [(NH_4^+ \text{ x } 3) / 18] \qquad (3)$$

However, CEC can also be calculated by summing the concentrations of all extracted cations in the three filtrates. The advantages of this approach are the contribution of each cation to the overall CEC can be determined and the total concentrations of extracted cadmium, copper, lead, and zinc can be compared to the exchangeable metals concentrations reported for the 0.5M $Ca(NO_3)_2$ procedure described in section 4.3.5. If the procedure is accurate, the CECs based on NH_4^+ and on the sum of all extracted cations except NH_4^+ should be very similar.

4.3.3 Soluble Metals [DIW Extractable]

Soluble metals [DIW extractable metals] were recovered using DIW at a 40:1 dilution. Each extraction sequence consisted of placing 2.5 g of soil with 100 mL of DIW in a 250 mL centrifuge bottle on a horizontal shaker for two hours. After two hours, the samples were centrifuged at approximately 12,000 rpm for 15–20 minutes. One 10 mL aliquot was collected and acidified to pH <2 for metals analysis by ICP-AES, while a second aliquot was collected for pH measurement. The remaining solution was decanted and discarded. One hundred mL of fresh DIW were added and the sample placed back on the shaker for two hours. The procedure was repeated until four extractions had been completed. All soil samples were treated in triplicate. The acidified extracts were analyzed for Cd, Cu, Pb, Zn, Ca, Mg, Na, K, P, Al, Fe, Mn, Ti, Ni, Mo, Cr, Sr, B, Ba, Si, and V by ICP-AES using a Jarrell Ash 61E system.

4.3.4 Soluble Metals [0.01 M $Ca(NO_3)_2$ Extractable]

A second set of soluble metals [0.01M $Ca(NO_3)_2$ extractable metals] were recovered using a solution of 0.01M $Ca(NO_3)_2$ at a 40:1 dilution. The procedure was designed to mirror the water soluble extraction procedure described in section 4.3.3, except a vacuum extraction system was used instead of the horizontal shaker system. To each vacuum extractor tube, 2.5 g of sample were added and then 100 mL of 0.01M

$Ca(NO_3)_2$ filtered through the tube at a rate of 50 mL per hour. Each 100 mL of filtrate was collected separately representing one two-hour extraction period. A total of 400 mL of extractant solution were filtered through each sample tube over an 8 hour period. The preparation and analysis of the 0.01M $CaCl_2$ extracts were identical to the methods described in section 4.3.3, except a Thermo Jarrell Ash IRIS Advantage system was used instead of the Jarrell Ash 61E system.

4.3.5 Exchangeable Metals [0.5M $Ca(NO_3)_2$ Extractable]

Exchangeable metals [0.5M $Ca(NO_3)_2$ extractable metals] were recovered with a horizontal shaker system using a solution of 0.5M $Ca(NO_3)_2$ at a 40:1 dilution. The extraction of each sample and subsequent analysis of the $Ca(NO_3)_2$ extracts were identical to the methods described in section 4.3.3.

4.3.6 Exchangeable Metals [NH_4Cl-DIW-KNO_3 Extractable]

A second set of exchangeable metals concentrations [NH_4Cl-DIW-KNO_3 extractable metals] were calculated from data generated by the CEC procedure described in section 4.3.2.

4.3.7 Specifically Sorbed and Complexed Metals [0.03M $La(NO_3)_3$ or 0.05M $Pb(NO_3)_2$ Extractable with Horizontal Shaker System]

Specifically sorbed and complexed metals [0.03M $La(NO_3)_3$ or 0.05M $Pb(NO_3)_2$ extractable metals] were recovered with a horizontal shaker system using either a solution containing 0.03M $La(NO_3)_3$ and 0.1M $Ca(NO_3)_2$ or 0.05M $Pb(NO_3)_2$ and 0.1M $Ca(NO_3)_2$ at a 40:1 dilution. One set of samples was treated with the 0.03M $La(NO_3)_3$ solution, while a second set of samples was treated with the 0.05M $Pb(NO_3)_2$ solution. The extraction of each sample and subsequent analysis of the 0.03M $La(NO_3)_3$ and 0.05M $Pb(NO_3)_2$ extracts were identical to the methods described in section 4.3.3.

4.3.8 Specifically Sorbed and Complexed Metals [0.03M $La(NO_3)_3$ or 0.05M $Pb(NO_3)_2$ Extractable with Vacuum Extraction System]

A second set of specifically sorbed and complexed metals [0.03M $La(NO_3)_3$ or 0.05M $Pb(NO_3)_2$ extractable metals] were recovered with a vacuum extraction system using either a solution containing 0.03M $La(NO_3)_3$ and 0.1M $Ca(NO_3)_2$ or 0.05M $Pb(NO_3)_2$ and 0.1M $Ca(NO_3)_2$ at a 40:1 dilution. The procedure was designed to mirror the specifically sorbed and complexed cations procedure described in section 4.3.7 except samples were extracted using the vacuum system rather than the shaker system. To each extractor tube, 2.5 g of sample were added and then 100 mL of either the 0.03M $La(NO_3)_3$ or the 0.05M $Pb(NO_3)_2$ solution filtered through the tube at a rate of 50 mL per hour. Each 100 mL of filtrate was collected separately representing one two-hour extraction period. A total of 400 mL of extractant solution were filtered through each sample tube over an 8 hour period. The extraction of each sample and subsequent analysis of the 0.03M $La(NO_3)_3$ and 0.05M $Pb(NO_3)_2$ extracts were identical to the methods described in sections 4.3.3 and 4.3.4.

4.4. Laboratory Methods – Specimen Materials

Construction of surrogate soils to approximate the four Leadville soils required the selection of appropriate specimen materials. Initially, kaolinite, goethite, and Pahokee peat were selected to represent the clay mineral, iron oxide, and soil organic matter (SOM) fractions of the Leadville soils. However, XRD data obtained for soil profiles 99-1 and 98-3 after the completion of laboratory experiments identified the significant presence of illite and smectite clay minerals. As a result, the number of specimen materials were increased to five. The model inputs used for kaolinite, goethite, and peat were a combination of experimental data and data obtained from the literature, while model inputs for illite and smectite were based solely on data obtained from the literature.

4.4.1. Preparation of Specimen Materials

Kaolinite

Georgia kaolinite (KGa-1b) was obtained from the Clay Minerals Society's (CMS) Source Clays Repository (West Lafayette, IN). The KGa-1b sample was treated with $CaCl_2$ using the following procedure. In a 50 mL centrifuge tube containing 1.003 g of kaolinite [equal to 1.000 g of oven-dried (OD) KGa-1b], 130 mL of 0.01M $CaCl_2$ solution adjusted to a pH of 5.50 were added in four separate treatments (i.e., 40 mL, 30 mL, 30 mL, and 30 mL). The clay suspension was placed on a horizontal shaker for 48 hours (each) during the first three treatments and 24 hours during the fourth and final treatment. After each treatment, the tubes were centrifuged at 12,000 rpm for 20 minutes.

The solution was decanted and the pH measured. Fresh $CaCl_2$ solution was added and the tubes placed back on the shaker. The saturation procedure was complete when the pH remained stable, which occurred between the third and fourth treatments. The calcium-treated kaolinite was oven dried at 105^0C for 24 hours and stored in centrifuge tubes until needed.

Pahokee Peat

Pahokee peat was obtained from the International Humic Substances Society (St. Paul, MN) and treated with $CaCl_2$ using the following procedure. In a 250 mL bottle containing 3.0 g of peat, 100 mL of 0.01M $CaCl_2$ adjusted to a pH of 5.50 were added. The suspension was shaken for 24 hours, after which the suspension was centrifuged at 12,000 rpm for up to one hour and the pH measured. One hundred mL of fresh 0.01M $CaCl_2$ at pH 5.50 were added and the suspension shaken for an additional 18 hours. After the second treatment, the pH of the suspension was 5.09. To raise the pH of the suspension, 240 uL of 1.30M NaOH were added over three days of continuous agitation until the pH stabilized at 5.50. The suspensions were then centrifuged at 12,000 rpm for up to one hour. The $CaCl_2$ solution was decanted and the peat oven dried at 105^0C for 24 hours. The calcium-treated peat was stored in 250 mL bottles until needed.

Goethite

The procedure described by Atkinson et al. (1968) was used to synthesize goethite. To each of the four 1-L bottles, 170 mL (202.3 g) of 0.45M $Fe(NO_3)_3 \cdot 9\,H_2O$

and 30 mL (33.24 g) of 2.5 M NaOH were added. A brown precipitate formed immediately and the suspensions were shaken intermittently for 25 minutes until the precipitate had dissolved. After suspension pHs were measured, the loosely covered bottles were left undisturbed for 50 hours at room temperature. At the end of the 50 hour aging process, varying amounts of 1.30M NaOH and 2.50M NaOH solution were added over a short a period of time to raise the suspension pH to 11.6–12.0. When the desired pH range had been achieved, the loosely capped bottles were placed in an oven at 62^0C ± 2^0C for four days. The suspensions were stirred briefly every 12 hours during this time. After removing the bottles from the oven and allowing them to cool, the suspensions were centrifuged until the precipitate had settled. The solution was decanted and DIW added to the precipitate. The bottles were shaken for one hour, centrifuged, and pH and conductivity measurements collected. The rinsing procedure was repeated until conductivity measurements approached the conductivity of DIW.

The synthetic goethite was air-dried and gently crushed to a fine powder before storing in a 1-L HDPE bottle. The Materials Characterization Laboratory at the University of Wyoming, Laramie, WY conducted XRD and SEM analyses and collected BET measurements on the synthetic material.

The synthetic goethite was treated with $CaCl_2$ by adding 30 mL of 0.01M $CaCl_2$ to 1.013 g [equal to 1.000 g OD] of synthetic goethite in a 50 mL centrifuge tube. The suspension was shaken for 24 hours and the pH measured. The process was repeated until the pH remained steady at 5.50 ± 0.2. The calcium-treated goethite was stored in 50 mL centrifuge tubes until needed.

4.4.2 Metal Sorption / Desorption Experiments [Kaolinite, Peat, and Goethite]

Prior to spiking the treated specimen materials with cadmium, copper, lead, or zinc, all specimen materials were treated with 0.01M $CaCl_2$. Based on moisture content measurements, 1.003 g of kaolinite, 1.157 g of peat, or 1.013 g of goethite [all equal to 1.000 g of OD specimen] were added to 50 mL centrifuge tubes along with 30 mL of 0.01M $CaCl_2$ adjusted to pH 5.50. The tubes were then placed on a horizontal shaker for 24 hours. The samples were centrifuged at approximately 12,000 rpm for up to one hour. The solutions were decanted and pH measurements collected. This procedure was repeated until suspension pHs stabilized at 5.50 ± 0.2.

Thirty mL of spike solution containing either cadmium, copper, lead, or zinc or all four metals were added to the samples. Although the molar concentrations of the different metals in the 30 mL of spike solution varied, the concentration of each metal was calculated so that 4.83 umol of metal were added to 1.000 g of OD specimen material (e.g. 1 mg of lead per 1 g OD specimen material). The pHs of solutions (i.e. spike and extractant) were adjusted to 5.50 ± 0.1. The system was open to the atmosphere and the pH was allowed to drift during the experiments. All procedures were run in triplicate.

The suspensions were shaken for approximately 24 hours and then centrifuged for up to one hour. One 10 mL aliquot for metal analysis was collected from each sample and acidified to pH <2 with HNO_3. After a second aliquot had been collected for pH measurement, the remaining solution was decanted and discarded. Thirty mL of 1.0M KNO_3 were then added and the samples returned to the shaker for approximately one hour. The samples were centrifuged at approximately 12,000 rpm for up to 30 minutes. Two 10 mL aliquots were collected from each sample for metal analysis and pH measurement.

After decanting and discarding the excess KNO_3 solution, 30 mL of a solution containing 0.03M $La(NO_3)_3$ and 0.1M $Ca(NO_3)_2$ were added to each sample. The suspensions were returned to the shaker for various periods of time (i.e., 4, 24, and 48 hours). The samples were centrifuged at approximately 12,000 rpm for up to 30 minutes. Two 10 mL aliquots were collected from each sample for metal analysis and pH measurement.

In addition to the full suite of QA/QC samples, the acidified aliquots were analyzed for cadmium, copper, lead, and zinc by ICP-AES using a Thermo Jarrell Ash IRIS Advantage system. Results were reported in mg L^{-1} and converted to mg kg^{-1} of oven-dried specimen material.

4.4.3 Calculation of Vanselow Selectivity Coefficients, Specific Sorption Constants, and Complexation Constants

Vanselow selectivity coefficients were calculated for the exchange of cadmium, copper, lead, and zinc with calcium-treated kaolinite. The two cation exchange reactions and associated Vanselow selectivity coefficient equations used were:

Cation Exchange Reactions

$$\text{X2-Ca} + \text{MC}^{2+} \Leftrightarrow \text{X2-MC} + \text{Ca}^{2+} \qquad (4)$$

$$\text{X2-Ca} + \text{MCCl}^{+} \Leftrightarrow \text{2X-MCCl} + \text{Ca}^{2+} \qquad (5)$$

where X2-Ca represents calcium associated with two cation exchange (X^-) sites on the kaolinite surface and MC^{2+} and $MCCl^+$ represent soluble metal cations (MC) (i.e. Cd, Cu, Pb, Zn) species and complexes, respectively.

Vanselow Selectivity Coefficients

$$K_{V1} = [X2\text{-}MC]\{Ca^{2+}\} / [X2\text{-}Ca]\{MC^{2+}\} \qquad (6)$$

$$K_{V2} = [X\text{-}MCCl]^2\{Ca^{2+}\} / [X2\text{-}Ca]\{MCCl^+\}^2 \qquad (7)$$

where brackets [ ] represent the concentrations of bound cations on the solid phase, which is expressed in mol kg^{-1}; braces { } represent the activity of cations in solution. K_{V1} and K_{V2} represent cation exchange reactions (4) and (5), respectively.

Specific sorption (sorption) constants (K_M) were also calculated based on the two following reactions:

Sorption Reactions

$$[SOH][MC^{2+}]_s \Leftrightarrow [SO\text{-}MC^+][H^+]_s \qquad (8)$$

$$[SOH]^2[MC^{2+}]_s \Leftrightarrow [(SO)_2\text{-}MC][H^+]_s^2 \qquad (9)$$

where [SOH], [$SO\text{-}MC^+$], and [$(SO)_2$-MC] represent the concentrations of sorbed protons and metal cations at specific sorption sites on the kaolinite surface, which is expressed in mol kg^{-1}; $[MC^{2+}]_s$ and $[H^+]_s$ represent the concentrations of metal cations and protons adjacent to the kaolinite surface in mol L^{-1}.

The concentrations of metal cations ($MC^{2+}{}_s$) and protons ($H^+{}_s$) adjacent to the kaolinite surface were calculated from the concentrations of metal cations ($MC^{2+}{}_b$) and protons ($H^+{}_b$) in the bulk solution using the Boltzmann equation (i.e. electrostatic correction factor). The two equations used were:

Boltzmann Equations

$$[MC^{2+}]_s = [MC^{2+}]_b \exp(-z_iF\psi_s / RT) \qquad (10)$$

$$[H^+]_s = [H^+]_b \exp(-z_iF\psi_s / RT) \qquad (11)$$

where brackets $[\ ]_s$ and $[\ ]_b$ are in mol L^{-1} and z_i, ψ_s, R, F, and T represent cation valence, surface potential, molar gas constant, Faraday constant, and temperature (K^0), respectively. The sorption constant equations used were:

Sorption Equations

$$K_{M1} = [SO\text{-}MC^+][H^+]_s / [SOH][MC^{2+}]_s \qquad (12)$$

$$K_{M2} = [(SO)_2\text{-}MC][H^+]_s^2 / [SOH]^2[MC^{2+}]_s \qquad (13)$$

where K_{M1} and K_{M2} represent specific sorption reactions (8) and (9), respectively and log K_{V1}, K_{V2}, K_{M1}, and K_{M2} values are reported in Tables 2 and 3.

Constants for sorption reactions involving SOH sites and soluble $MCCl^+$ complexes were not calculated because predicted concentrations of sorbed MCCl complexes [SO-MCCl] were negligible (i.e. <1E-6M). Sorption constants for iron oxide and cation exchange and complexation constants for peat were not calculated. Cation exchange, sorption and complexation binding data for iron oxide, peat, illite, and montmorillonite were obtained from the literature.

4.5 Modeling

4.5.1 Model Selection

The selection of an empirical equation and/or mechanistic model to describe cadmium, copper, lead, and zinc partitioning associated with the five specimen materials (i.e. kaolinite, illite, montmorillonite, FeOOH, and SOM) was based on the following criteria: 1. simplicity of the equation or model (i.e. number of parameters); 2. inclusion of datasets providing binding constants, surface chemistry data, and equation or model parameters; and 3. the availability of the equation or model in one of the existing chemical equilibrium/speciation software programs. A final consideration was the ability to enter the appropriate equations or model parameters into existing software programs in the event neither was included.

The Generalized Two-Layer Model (GTLM) was selected to describe metal sorption associated with oxide minerals because it is one of the simplest models available. The GTLM includes extensive databases of binding constants, surface chemistry data, and model parameters for a variety of oxides. The GTLM and its databases have been extensively tested and have found wide acceptance in the area of metal sorption research. The GTLM is incorporated into several chemical equilibrium/speciation programs such as MINEQL$^+$ (Schecher and McAvoy, 1994), MINEQL$^+$, Version 4.5 for Windows (Schecher and McAvoy, 2001), MINTEQA2 (HydroGeoLogic, Inc. and Allison Geoscience Consultants, Inc., 1999), and Visual MINTEQ, Version 2.30 (Gustafsson, 2004).

The choice for describing the exchange and complexation of metals associated with humic substances was the Stockholm Humic Model (SHM). The SHM, which also contains extensive databases containing surface chemistry data, model parameters, and exchange and complexation constants, has been extensively tested and is incorporated into Visual MINTEQ.

The Vanselow selectivity coefficient equation was selected for describing metal cation exchange reactions on clay surfaces. The exchange reactions can be easily written and incorporated into the MINEQL$^+$ problem input files. The Constant Capacitance Model (CCM) was selected to describe the metal sorption reactions associated with kaolinite because of its simplicity and the fact that the CCM is one of four surface complexation models (SCM) included in MINEQL$^+$. Metal sorption reactions associated with montmorillonite surfaces were described using a non-electrostatic SCM format, which was incorporated into MINEQL$^+$. The rationale for using a non-electrostatic modeling approach for metal sorption reactions associated with montmorillonite versus an electrostatic modeling approach was the absence of electrostatic modeling data for montmorillonite in the literature. Since the majority of this clay's exposed surface is controlled by cation exchange reactions, the assumption was that the impact of ignoring electrostatic interactions associated with the montmorillonite surface would be minimal to the overall surrogate system.

4.5.2 Modeling Software

MINEQL$^+$, Version 4.5 for Windows (Schecher and McAvoy, 2001) was selected to model the sorption of metals to kaolinite, illite, montmorillonite, and goethite specimen materials. Visual MINTEQ, Version 2.30 (Gustafsson, 2004) was selected to model the sorption of metals to specimen organic materials.

4.5.3 Modeling Data from the Literature

Model input data for the five specimen materials were obtained primarily from the literature. For kaolinite, goethite, and peat, the data from the literature supplemented or replaced experimental data generated during the adsorption/desorption experiments. For illite and montmorillonite, data from the literature were the only data available for modeling these components.

Initially, a search of the literature produced a large body of data regarding sorption reactions, chemical composition, and the structure of the five specimen materials. The data were reduced to studies that involved at least one of the four metals of interest, were conducted in the general range of pHs measured in the Leadville soils, and used $CaCl_2$ as the background electrolyte.

Whereas sufficient modeling data were available for kaolinite, montmorillonite, and goethite, the data were insufficient for illite and specimen organic materials. Excluding copper, cation exchange constants for cadmium, lead, and zinc were available for illite from the literature. A cation exchange constant for copper was calculated based on a metal cation-illite affinity sequence and a lead cation exchange constant. Farrah et al. (1980) reported a metal cation-illite affinity sequence of Pb (1.9), Cu (1.4), Zn (1.3), and Cd (1.0), while Khan and Khan (1985) calculated a lead-illite exchange constant of (K) 2.7. The following equation was developed to calculate a cation exchange constant for copper (K_{Cu}):

$$K_{Cu} = (2.7/1.9) \times 1.4 = 2.0; \log K_{Cu} = 0.300 \tag{14}$$

The log K cation exchange constant values for the four metals are reported in Table 5.

To avoid using potentially incompatible reactions and constants for the modeling of specimen organic materials, the existing databases in the Visual MINTEQ program were selected. However, the Visual MINTEQ databases describe reactions associated with humic acids (HA) and fulvic acids (FA) and not peat or SOM. Therefore, data from several literature sources and the Pahokee peat sorption/desorption experiments were combined with carbon data from the Leadville soils and converted to HA and FA model inputs. After converting to HA and FA, the existing Visual MINTEQ databases could be used. The conversion of peat model inputs to HA and FA model inputs and back to SOM model outputs are described in section 4.5.6.

4.5.4 Model Input Files

Once all physical, chemical, and surface reaction data had been collected for the five specimen materials; model input files were generated in the specific formats required by the MINEQL$^+$ and Visual MINTEQ programs. Tables 1-3 list chemical, physical, and surface reaction data used to describe the kaolinite system, while Tables 4-5 and 6-7 list data used to describe the illite and montmorillonite systems, respectively. Tables 8-9 and 10-11 list critical data used to describe the FeOOH and SOM systems.

Simulations were conducted using a non-competitive modeling approach (NCMA) and a competitive modeling approach (CMA). A NCMA simulation was conducted for each pH value (i.e. 4.15, 5.56, and 6.21), each metal (i.e. cadmium, copper, lead, and zinc) and each specimen material (i.e. kaolinite, illite, montmorillonite, FeOOH, and soil organic matter). An example of one NCMA simulation is the modeling of copper sorption onto montmorillonite at pH 5.56. CMA simulations were identical to NCMA simulations with respect to pH values and specimen materials. However, CMA simulations were conducted with all four metals instead of one metal like the NCMA simulations. An example of one CMA simulation is the modeling of cadmium, copper, lead, and zinc sorption onto montmorillonite at pH 5.56.

The input concentrations of metals used to model montmorillonite, kaolinite, illite, and FeOOH were 1,000, 500, 100, 50, 10, 5, 1, 0.5, 0.1, 0.05, and 0.01 mg L^{-1}. Due to the very large sorptive capacity of humic substances, the input concentrations of metals included 10,000, 5,000, and 2,500 mg L^{-1} in addition to the range used for clay minerals and FeOOH.

4.5.5 Model Output Files

The output files for the five specimen materials listed the concentrations of all species in mol L^{-1}. The output files for soluble species such as Cd^{+2}, Cu^{+2}, Pb^{+2}, Zn^{+2}, and their complexes (e.g., $CdCl^{+}$, $CdNO_3^{+}$, etc.) were converted from mol L^{-1} to mg L^{-1}, while the sorbed species (e.g., X2-Cd, 2X-CdCl, SO-Cd^{+}, (SO)2-Cd, etc.) were converted to mg kg^{-1} oven-dried (OD) specimen material. If more than one metal cation complex existed for a particular sorption reaction, the complexes were combined and reported as total exchangeable (e.g. X2-Cd + 2X-CdCl), total sorbed (e.g. SO-Cd^{+} + (SO)2-Cd), or total complexed metals. This was particularly necessary for the SOM output files where a minimum of five complexed metal complexes were generally listed (e.g. FA-Cu^{+}, (FA)2-Cu, (FA)2-CuOH, HA-Cu^{+}, (HA)2-Cu, (HA)2-CuOH, etc.).

After converting output data to the appropriate units (i.e. mg L^{-1} and mg kg^{-1}) and combining similar metal cation complexes, tables of sorption curves were generated using the predicted soluble species (mg L^{-1}) as the x-axis and the predicted exchangeable, sorbed, or complexed concentrations (mg kg^{-1}) as the y-axes.

To calculate predicted concentrations of exchangeable, sorbed, and complexed metals that corresponded to experimentally derived soluble metals data, two values from the x-axis (i.e. predicted concentration of soluble metals) were selected to bracket the experimental value. Then two values from the y-axes (i.e. predicted concentrations of exchangeable, sorbed, or complexed metals) were selected that corresponded to the two values from the x-axis. These four values were used to generate a linear regression equation (i.e. $y = mx + b$). Using the experimental value as the x value, a predicted exchangeable, sorbed, or complexed metals value was calculated, which corresponded to the experimental soluble metals value. The predicted concentrations of exchangeable, sorbed, and complexed metals were then compared to experimental metals data generated from the selective extraction of the Leadville soils.

Each sorption table containing one metal and one specimen material was combined into a master table. Therefore, each master table contains one metal and five specimen materials (e.g. Cu-kaolinite modeling output + Cu-illite modeling output + Cu-montmorillonite modeling output + Cu-FeOOH modeling output + Cu-SOM modeling output). An additional master table was generated from the modeling of all four metal cations and the five specimen materials (e.g., Cd,Cu,Pb,Zn-kaolinite modeling output +

Cd,Cu,Pb,Zn-illite modeling output + Cd,Cu,Pb,Zn-montmorillonite modeling output + Cd,Cu,Pb,Zn-FeOOH modeling output + Cd,Cu,Pb,Zn-SOM modeling output).

Weighting factors were then applied to each specimen material in the master table. Application of weighting factors proportioned the composition (i.e., percent kaolinite, percent illite, percent montmorillonite, percent FeOOH, and percent SOM) of the surrogate soil. Each of the four surrogate soils was used to approximate one of the four Leadville soils. The procedure for calculating the various weighting factors is described in Section 4.5.6.

The final step was to sum the predicted concentrations of exchangeable, sorbed, and complexed metals calculated from the experimental soluble metals data [e.g. total exchangeable (kaolinite) + total exchangeable (illite) + total exchangeable (montmorillonite) + total exchangeable (SOM)] across all five specimen materials. The total predicted exchangeable, total predicted sorbed, and total predicted complexed metals concentrations for each surrogate soil were then compared with experimental metals data generated from the selective extraction of a corresponding Leadville soil. An example of a master table (sample 99-1-0-7 zinc) is provided in Appendix C (Table 1).

4.5.6 Weighting Factors, Conversions, and Multipliers

Weighting factors were calculated for three clay minerals, FeOOH, and SOM. As mentioned previously, the weighting factors were used to proportion the composition of each surrogate soil to more closely approximate one of the Leadville soils. These adjustments were necessary to calculate realistic modeling outputs for comparison with the experimental metals data. The factors, which are described in the following sections, are the summation of a variety of data sources. For illustrative purposes, data from sample 99-1-0-7 were selected to demonstrate the process used to calculate weighting factors for the five specimen materials. Table 12 lists the equations and weighting factor values for the three clay minerals, while Table 13 lists the equations and weighting factor values for FeOOH and SOM.

Calculation of Clay Weighting Factors

Estimating the clay composition in sample 99-1-0-7 was accomplished using a method described by Klages and Hopper (1980). From 99-1-0-7 XRD data, the areas under the curves of particular signature peaks [i.e. 17.0 Angstrom (Å) peak for smectite, 10 Å peak for illite, and 7.2 Å peak for kaolinite] were calculated and then multiplied by specified adjustment values. The qualitative result for 99-1-0-7 was a clay composition consisting of 20% kaolinite, 70% illite, and 10% smectite.

Next, the mole weight of each clay mineral was calculated based on structural formulas listed in the CMS datasheets. The percent by weight for Al^{3+} in each clay was calculated and equaled 21% for kaolinite, 13% for illite, and 11% for montmorillonite.

The total Al^{3+} concentration reported in sample 99-1-0-7, 42.9g/kg-soil, was obtained from total metal analysis described earlier and used in calculating the clay weighting factors in this particular surrogate soil. The use of total Al^{3+} in calculating the clay weighting factors was based on a review of 99-1-0-7 XRD data. Although feldspars, micas, and amorphous/crystalline aluminum oxides could be present, the assumption used in this approach was the impact of any Al^{3+} tied up in non-clay minerals on the overall sorptive capacity of the soil was minimal. Therefore, the total Al^{3+} concentration reported for sample 99-1-0-7 was assumed to be structurally bound to clay minerals. The calculations of each clay weighting factor for surrogate soil 99-1-0-7 are described below and included in Table 12:

<u>Kaolinite (K) Modeling Output Data (MOD)</u>

MOD (mg-metal cation (MC)/kg-K) x (kg-K/1000g-K) x (1g-K/0.21g-Al^{3+}) x (42.9g-Al^{3+}/kg-soil) x 0.20 = 0.04 x (mg-MC/kg-soil) (15)

<u>Illite (I) MOD</u>

MOD (mg-MC/kg-I) x (kg-I/1000g-I) x (1g-I/0.13g-Al^{3+}) x (42.9g-Al^{3+}/kg-soil) x 0.70 = 0.23 x (mg-MC/kg-soil) (16)

<u>Montmorillonite (M) MOD</u>

MOD (mg-MC/kg-M) x (kg-M/1000g-M) x (1g-M/0.11g-Al^{3+}) x (42.9g-Al^{3+}/kg-soil) x 0.10 = 0.04 x (mg-MC/kg-soil) (17)

Calculation of FeOOH Weighting Factors

Al-Farranj (2002) reported the concentrations of crystalline and non-crystalline FeOOH ranged from 50% to 73% of the total Fe^{3+} content in soil profile 98-3. The 50% value was selected for calculating the FeOOH weighting factor in surrogate soil 99-1-0-7. The percent by weight of Fe^{3+} in FeOOH was calculated and equaled 63%. Based on a total Fe^{3+} concentration of 60.9g/kg-soil, the calculation of the 99-1-0-7 FeOOH weighting factor was:

FeOOH MOD

MOD (mg-MC/kg-FeOOH) x (kg-FeOOH/1000g-FeOOH) x (1g-FeOOH/0.63g-Fe^{3+}) x (60.9g-Fe^{3+}/kg-soil) x 0.50 = 0.05 x (mg-MC/kg-soil) (18)

Calculation of Soil Organic Matter Conversions, Multipliers, and Weighting Factors

As stated previously, Visual MINTEQ software does not include peat or SOM databases. This limitation required the conversion of peat model inputs to HA and FA model inputs by first converting peat model inputs to SOM model inputs and then converting SOM model inputs to HA and FA model inputs. After converting model input data to g-HA L^{-1} and g-FA L^{-1}, the HA and FA databases were used to model the organic fraction in surrogate soils. Data used to calculate the numerous conversions came from a variety of data sources and are described below and included in Table 10:

Conversion of peat (g L^{-1}) to SOM (g L^{-1}) to 'active' humic substances [HS] (g L^{-1})

(g-Peat/L) [experimental setup] x (0.457g-C/g-peat) [IHSS data sheet for Pahokee peat] x (1.90g-SOM/g-C) [Nelson and Sommers, 1996; Broadbent, 1953] x (0.54g-humic substances (HS)/g-SOM) [Stevenson, 1995] x

(0.525g-'active' HS /g-HS)[Gustafsson and Pechova, 2003]

= 0.25 x g-'active' HS L^{-1} (19)

Conversion of 'active' HS (g L^{-1}) to humic acid and fulvic acid (g L^{-1})

(g-'active' HS/L) x 0.62 [Gustafsson, 2004] = g-HA L^{-1} (20a)

(g-'active' HS/L) x 0.38 [Gustafsson, 2004] = g-FA L^{-1} (20b)

Visual MINTEQ model output data were reported initially as mol-metal cation (MC) L^{-1}. After combining similarly sorbed metals complexes (e.g., HA-Cu, (HA)2-Cu, (HA)2-CuOH, FA-Cu, (FA)2-Cu, and (FA)2-CuOH, etc.), concentrations were converted to mg-MC kg^{-1}-SOM using equations 21 and 22. Although peat was used as a specimen material for the organic fraction in the Leadville soils, peat is not a likely component of these soils. Therefore, model output data for HA and FA, which was based originally on peat model inputs, were converted to SOM model output data. Copper is used as an example of converting mol-Cu L^{-1} to mg-Cu kg^{-1}-SOM:

Copper MOD

MOD (mol-Cu/L) x (63,546mg-Cu/mol-Cu) x $(L/28.9g\text{-}SOM)^*$ x (1000g-SOM/kg-SOM) = 2,195,534 x mg-Cu kg^{-1}-SOM => 2.2E6 x mg-Cu kg^{-1}-SOM (21)

*(33.3g-peat/L) [experimental setup] x (0.457g-C/1g-peat) x (1.90g-SOM/1g-C) = 28.9g-SOM L^{-1} (22)

The value of 2.2E6 is described as a multiplier for converting mol-Cu L^{-1} in the Visual MINTEQ output to mg-Cu kg^{-1}-SOM. The calculated multipliers for Cd^{+2}, Pb^{+2}, and Zn^{+2} were 3.9E6, 7.2E6, and 2.3E6, respectively.

The final calculation required was the conversion of mg-MC kg^{-1}-SOM to mg-MC kg^{-1}-soil (i.e. SOM weighting factor). Thus, the equation for the 99-1-0-7 SOM weighting factor is described below and included in Table 13:

SOM MOD

MOD (mg-MC/kg-SOM) x (kg-SOM/1000 g-SOM) x (1 g-SOM/0.53 g-C) x (18.0 g-C /kg-soil) = 0.03 x (mg-MC/kg-soil) (23)

The same procedures were used for converting cadmium, lead, and zinc from mol-MC L^{-1} to mg-MC kg^{-1}-soil in the other three Leadville soils. The results of those calculations are also included in Tables 10 and 13.

To determine the impact of errors in weighting factor values on the prediction of metal partitioning in surrogate soils, a sensitivity analysis was conducted. The results are described in Section 6.0.

Table 1

Kaolinite System Modeling Parameters

Chemical Speciation Software Used: Mineql$^+$, Version 4.5

Specimen Modeling Parameters	
Cation Exchange Capacity (cmol$_c$ kg^{-1})	2.0[1]
Surface Area (m^2 g^{-1})	10.05[1]
Binding Site Concentration (sites m^{-2})	2.31E18[2]
Solids Concentration (g L^{-1})	33.3[3]
X2-Ca Sites Concentration (mol L^{-1})	3.33E-04[4]
SOH Sites Concentration (mol L^{-1})	1.28E-03[5]
CO_2 (Log P)	-3.48
Precipitation of Solids Allowed ?	No
Background Electrolyte	0.01M $CaCl_2$[3]
pHs	4.15; 5.56; 6.21[6]
Metal(s) Input Concentrations (mg L^{-1})	1,000; 500; 100; 50; 10; 5; 1; 0.5; 0.1; 0.05; 0.01

1 Van Olphen and Fripiat, 1979.
2 Davis and Kent, 1990.
3 Experimental setup.
4 X2-Ca equation (includes data from footnotes 1 and 3):
X2-Ca (mol L^{-1}) = (33.3g-K/L) x (kg-K/1000g-K) x (2 cmol$_c$/kg-K) x (1 mol$_c$/100 cmol$_c$) x (1 mol X2-Ca/2 mol$_c$) = 3.33E-4
5 SOH equation (includes data from footnotes 1, 2, and 3):
SOH (mol L^{-1}) = (33.3g-K/L) x (10.05 m^2/g-K) x (2.31E18 SOH sites/m^2) x (1 mol SOH sites/6.023E23 SOH sites) = 1.28E-3
6 pH of 99-1-7-12, 99-1-0-7, and both 98-3 soil samples, respectively.

Table 2

Kaolinite System #1: Modeling Inputs for Reactions and Constants
[Kaolinite + Cadmium or Copper or Lead or Zinc][NCMA]

Primary Reactions Modeled	Experimental Data[1] [Log K_V and Log K_M]	Literature Data[2] [Log K_V and Log K_M]
$SOH + H^+ \Leftrightarrow SOH_2^+$		4.37
$SOH \Leftrightarrow SO^- + H^+$		-9.18
Metal Cation Complex: $CdCl_2$ Background Electrolyte: 0.01M $CaCl_2$		
$X2\text{-}Ca + Cd^{+2} \Leftrightarrow X2\text{-}Cd + Ca^{+2}$	0.335	
$X2\text{-}Ca + CdCl^+ \Leftrightarrow 2X\text{-}CdCl + Ca^{+2}$	2.53	
$SO\text{-}Ca^+ + Cd^{+2} \Leftrightarrow SO\text{-}Cd^+ + Ca^{+2}$	-4.43	
$(SO)2\text{-}Ca + Cd^{+2} \Leftrightarrow (SO)2\text{-}Cd + Ca^{+2}$	-8.65	
Metal Cation Complex: $Cu(NO_3)_2$ Background Electrolyte: 0.01M $CaCl_2$		
$X2\text{-}Ca + Cu^{+2} \Leftrightarrow X2\text{-}Cu + Ca^{+2}$	0.715	
$X2\text{-}Ca + CuCl^+ \Leftrightarrow 2X\text{-}CuCl + Ca^{+2}$	6.84	
$SO\text{-}Ca^+ + Cu^{+2} \Leftrightarrow SO\text{-}Cu^+ + Ca^{+2}$	-3.28	
$(SO)2\text{-}Ca + Cu^{+2} \Leftrightarrow (SO)2\text{-}Cu + Ca^{+2}$	-7.47	
Metal Cation Complex: $Pb(NO_3)_2$ Background Electrolyte: 0.01M $CaCl_2$		
$X2\text{-}Ca + Pb^{+2} \Leftrightarrow X2\text{-}Pb + Ca^{+2}$	0.853	
$X2\text{-}Ca + PbCl^+ \Leftrightarrow 2X\text{-}PbCl + Ca^{+2}$	4.41	
$SO\text{-}Ca^+ + Pb^{+2} \Leftrightarrow SO\text{-}Pb^+ + Ca^{+2}$	-2.82	
$(SO)2\text{-}Ca + Pb^{+2} \Leftrightarrow (SO)2\text{-}Pb + Ca^{+2}$	-6.80	
Metal Cation Complex: $Zn(NO_3)_2$ Background Electrolyte: 0.01M $CaCl_2$		
$X2\text{-}Ca + Zn^{+2} \Leftrightarrow X2\text{-}Zn + Ca^{+2}$	0.188	
$X2\text{-}Ca + ZnCl^+ \Leftrightarrow 2X\text{-}ZnCl + Ca^{+2}$	5.40	
$SO\text{-}Ca^+ + Zn^{+2} \Leftrightarrow SO\text{-}Zn^+ + Ca^{+2}$	-1.66	
$(SO)2\text{-}Ca + Zn^{+2} \Leftrightarrow (SO)2\text{-}Zn + Ca^{+2}$	-8.53	

[1] Log K_V and log K_M calculated from experimental data.
[2] Schindler et al., 1987.

Table 3

Kaolinite System #2: Modeling Inputs for Reactions and Constants [Kaolinite + Cadmium and Copper and Lead and Zinc][CMA]

Primary Reactions Modeled	Experimental Data[1] [Log K_V and Log K_M]	Literature Data[2] [Log K_V and Log K_M]
$SOH + H^{+} \Leftrightarrow SOH_2^{+}$		4.37
$SOH \Leftrightarrow SO^{-} + H^{+}$		-9.18
Metal Cation Complex: $CdCl_2$ Background Electrolyte: 0.01M $CaCl_2$		
$X2\text{-}Ca + Cd^{+2} \Leftrightarrow X2\text{-}Cd + Ca^{+2}$	0.314	
$X2\text{-}Ca + CdCl^{+} \Leftrightarrow 2X\text{-}CdCl + Ca^{+2}$	2.49	
$SO\text{-}Ca^{+} + Cd^{+2} \Leftrightarrow SO\text{-}Cd^{+} + Ca^{+2}$	-4.49	
$(SO)2\text{-}Ca + Cd^{+2} \Leftrightarrow (SO)2\text{-}Cd + Ca^{+2}$	-8.50	
Metal Cation Complex: $Cu(NO_3)_2$ Background Electrolyte: 0.01M $CaCl_2$		
$X2\text{-}Ca + Cu^{+2} \Leftrightarrow X2\text{-}Cu + Ca^{+2}$	0.363	
$X2\text{-}Ca + CuCl^{+} \Leftrightarrow 2X\text{-}CuCl + Ca^{+2}$	6.14	
$SO\text{-}Ca^{+} + Cu^{+2} \Leftrightarrow SO\text{-}Cu^{+} + Ca^{+2}$	-3.34	
$(SO)2\text{-}Ca + Cu^{+2} \Leftrightarrow (SO)2\text{-}Cu + Ca^{+2}$	-7.34	
Metal Cation Complex: $Pb(NO_3)_2$ Background Electrolyte: 0.01M $CaCl_2$		
$X2\text{-}Ca + Pb^{+2} \Leftrightarrow X2\text{-}Pb + Ca^{+2}$	0.792	
$X2\text{-}Ca + PbCl^{+} \Leftrightarrow 2X\text{-}PbCl + Ca^{+2}$	4.29	
$SO\text{-}Ca^{+} + Pb^{+2} \Leftrightarrow SO\text{-}Pb^{+} + Ca^{+2}$	-2.87	
$(SO)2\text{-}Ca + Pb^{+2} \Leftrightarrow (SO)2\text{-}Pb + Ca^{+2}$	-6.87	
Metal Complex: $Zn(NO_3)_2$ Background Electrolyte: 0.01M $CaCl_2$		
$X2\text{-}Ca + Zn^{+2} \Leftrightarrow X2\text{-}Zn + Ca^{+2}$	0.264	
$X2\text{-}Ca + ZnCl^{+} \Leftrightarrow 2X\text{-}ZnCl + Ca^{+2}$	5.55	
$SO\text{-}Ca^{+} + Zn^{+2} \Leftrightarrow SO\text{-}Zn^{+} + Ca^{+2}$	-4.93	
$(SO)2\text{-}Ca + Zn^{+2} \Leftrightarrow (SO)2\text{-}Zn + Ca^{+2}$	-8.94	

1 Log K_V and log K_M calculated from experimental data.
2 Schindler et al., 1987.

Table 4

Illite System Modeling Parameters

Chemical Speciation Software Used: Mineql$^+$, Version 4.5

Specimen Modeling Parameters

Cation Exchange Capacity (cmol$_c$ kg^{-1})	37.4[1]
Surface Area (m^2 g^{-1})	97.6[1]
Binding Site Concentration (sites m^{-2})	2.31E18[2]
Solids Concentration (g L^{-1})	33.3[3]
X2-Ca Sites Concentration (mol L^{-1})	6.24E-03[4]
SOH Sites Concentration (mol L^{-1})	NA
CO_2 (Log P)	-3.48
Precipitation of Solids Allowed ?	No
Background Electrolyte	0.01M $CaCl_2$[3]
pHs	4.15; 5.56; 6.21[5]
Metal(s) Input Concentrations (mg L^{-1})	1,000; 500; 100; 50; 10; 5; 1; 0.5; 0.1; 0.05; 0.01

[1] Calculated from Van Olphen and Fripiat (1979) and Davis and Kent (1990).
[2] Davis and Kent, 1990.
[3] Experimental setup.
[4] X2-Ca equation (includes data from footnotes 1, 2, and 3):
X2-Ca (mol L^{-1}) = (33.3g-I/L) x (1kg-I/1000g-I) x (37.4 cmol$_c$/kg-I) x (1 mol$_c$/100 cmol$_c$) x (1 mol X2-Ca/2 mol$_c$) = 6.24E-3
[5] pH of 99-1-7-12, 99-1-0-7, and both 98-3 soil samples, respectively.

Table 5

Illite Systems #1 and #2: Modeling Inputs for Reactions and Constants [Illite + Cadmium or Copper or Lead or Zinc][NCMA] and [Illite + Cadmium and Copper and Lead and Zinc][CMA]

Primary Reactions Modeled	Experimental Data [Log K_V]	Literature Data [Log K_V]
Metal Cation Complex: $CdCl_2$		
$X2\text{-}Ca + Cd^{+2} \Leftrightarrow X2\text{-}Cd + Ca^{+2}$		0.116[1]
Metal Cation Complex: $Cu(NO_3)_2$		
$X2\text{-}Ca + Cu^{+2} \Leftrightarrow X2\text{-}Cu + Ca^{+2}$		0.300[2]
Metal Cation Complex: $Pb(NO_3)_2$		
$X2\text{-}Ca + Pb^{+2} \Leftrightarrow X2\text{-}Pb + Ca^{+2}$		0.433[3]
Metal Cation Complex: $Zn(NO_3)_2$		
$X2\text{-}Ca + Zn^{+2} \Leftrightarrow X2\text{-}Zn + Ca^{+2}$		0.167[1]

1 Van Bladel et al., 1993.

2 Based on a metal cation-illite affinity sequence of Pb (1.9), Cu (1.4), Zn (1.3), and Cd (1.0) (Farrah et al., 1980) and a lead constant of $K_{Pb} = 2.71$ (Khan and Khan, 1985), the calculated K_{Cu} for illite was: $K_{Cu} = (2.71/1.9) \times 1.4 = 2.00$; log $K_{Cu} = 0.300$

3 Khan and Khan, 1985

Table 6

Montmorillonite System Modeling Parameters

Chemical Speciation Software Used: Mineql$^+$, Version 4.5

Specimen Modeling Parameters

Cation Exchange Capacity [median] ($\text{cmol}_c\ \text{kg}^{-1}$)	86.0[1]
Surface Area [median] ($\text{m}^2\ \text{g}^{-1}$)	662. (EGME)[2,3] 23.9 (BET)[4,5]
Binding Site Concentration (sites m^{-2})	2.31E18[6]
Solids Concentration (g L^{-1})	33.3[7]
X2-Ca Sites Concentration [median] (mol L^{-1})	1.43E-02[8]
SOH Sites Concentration [median] (mol L^{-1})	3.06E-03[9]
CO_2 (Log P)	-3.48
Precipitation of Solids Allowed ?	No
Background Electrolyte	0.01M $CaCl_2$[7]
pHs	4.15; 5.56; 6.21[9]
Metal(s) Input Concentrations (mg L^{-1})	1,000; 500; 100; 50; 10; 5; 1; 0.5; 0.1; 0.05; 0.01

1 Median of 37 values obtained from the literature (Appendix A).
2 Median of 3 values obtained from the literature (Appendix A).
3 Ethylene glycol mono-ether (EGME) or glycerol method measures both internal (X sites) and external (SOH sites) surface areas.
4 Median of 7 values obtained from the literature (Appendix A).
5 Brunauer-Emmett-Teller (BET) or N_2 method measures external (SOH sites) surface areas.
6 Davis and Kent, 1990.
7 Experimental setup.
8 X2-Ca equation (includes data from footnotes 1 and 7):
X2-Ca (mol L^{-1}) = (33.3g-M/L) x (1kg-M/1000g-M) x (86.0 cmol_c/kg-M) x (1 mol_c/100 mol_c) x (1 mol X2-Ca/2 mol_c) = 1.43E-2

Table 6 (cont.)

9 SOH equation (includes data from footnotes 1, 4, 5, 6, and 7): SOH (mol L^{-1}) = (33.3g-M/L) x (23.9 m^2/g-M) x (2.31E18 SOH sites/m^2) x (1 mol SOH/6.023E23 SOH sites) = 3.06E-3

10 pH of 99-1-7-12, 99-1-0-7, and both 98-3 soil samples, respectively

Table 7

Montmorillonite Systems #1 and #2: Modeling Inputs for Reaction and Constants
[Montmorillonite + Cadmium or Copper or Lead or Zinc][NCMA]
and
[Montmorillonite + Cadmium and Copper and Lead and Zinc][CMA]

Primary Reactions Modeled	Experimental Data [Log K_V and Log K_M]	Literature Data [Log K_V and Log K_M]
$SOH + H^+ \Leftrightarrow SOH_2^+$		4.60[1]
$SOH \Leftrightarrow SO^- + H^+$		-7.90[1]
Metal Cation Complex: $CdCl_2$		
$X2\text{-}Ca + Cd^{+2} \Leftrightarrow X2\text{-}Cd + Ca^{+2}$		0.305[2]
$SO\text{-}Ca^+ + Cd^{+2} \Leftrightarrow SO\text{-}Cd^+ + Ca^{+2}$		-3.80[1]
Metal Cation Complex: $Cu(NO_3)_2$		
$X2\text{-}Ca + Cu^{+2} \Leftrightarrow X2\text{-}Cu + Ca^{+2}$		0.378[2]
$SO\text{-}Ca^+ + Cu^{+2} \Leftrightarrow SO\text{-}Cu^+ + Ca^{+2}$		-1.90[1]
Metal Cation Complex: $Pb(NO_3)_2$		
$X2\text{-}Ca + Pb^{+2} \Leftrightarrow X2\text{-}Pb + Ca^{+2}$		0.488[2]
$SO\text{-}Ca^+ + Pb^{+2} \Leftrightarrow SO\text{-}Pb^+ + Ca^{+2}$		-2.10[1]
Metal Cation Complex: $Zn(NO_3)_2$		
$X2\text{-}Ca + Zn^{+2} \Leftrightarrow X2\text{-}Zn + Ca^{+2}$		0.241[2]
$SO\text{-}Ca^+ + Zn^{+2} \Leftrightarrow SO\text{-}Zn^+ + Ca^{+2}$		-3.20[1]

1 Lothenbach et al., 1997.
2 Auboiroux et al., 1998.

Table 8

FeOOH System Modeling Parameters

Chemical Speciation Software Used: Mineql$^+$, Version 4.5

Specimen Modeling Parameters	
Cation Exchange Capacity (cmol$_c$ kg^{-1})	NA[1]
Surface Area (m^2 g^{-1})	600[2]
Binding Site Concentration (sites m^{-2})	2.31E18[3]
Solids Concentration (g L^{-1})	33.3[4]
X2-Ca Sites Concentration (mol L^{-1})	NA[1]
S(wk)OH Sites Concentration (mol L^{-1})	7.49E-02[5]
S(st)OH Sites Concentration (mol L^{-1})	1.87E-03[6]
CO_2 (Log P)	-3.48
Precipitation of Solids Allowed ?	No
Background Electrolyte	0.01M $CaCl_2$[4]
pHs	4.15; 5.56; 6.21[7]
Metal(s) Input Concentrations (mg L^{-1})	1,000; 500; 100; 50; 10; 5; 1; 0.5; 0.1; 0.05; 0.01

1 Not applicable for FeOOH, SOH sites only.
2 Dzombak and Morel, 1990.
3 Davis and Kent, 1990.
4 Experimental setup.
5 S(wk)OH equation (includes 0.2 mol S(wk)OH/mol Fe^{3+} (Dzombak and Morel, 1990) and data from footnote 4): S(wk)OH (mol L^{-1}) = (0.2 mol S(wk)OH/1 mol Fe^{3+}) x (1 mol Fe^{3+}/1 mol FeOOH) x (1 mol FeOOH/89g FeOOH) x (33.3g FeOOH/L) = 7.49E-2
6 S(st)OH equation (includes 0.005 mol S(st)OH/mol Fe^{3+} (Dzombak and Morel, 1990) and data from footnote 4): S(st)OH (mol L^{-1}) = (0.005 mol S(st)OH/1 mol Fe^{3+}) x (1 mol Fe^{3+}/1 mol FeOOH) x (1 mol FeOOH/89g FeOOH) x (33.3g FeOOH/L) = 1.87E-3
7 pH of 99-1-7-12, 99-1-0-7, and both 98-3 soil samples, respectively.

Table 9

FeOOH Systems #1and #2: Modeling Inputs for Reactions and Constants
[FeOOH + Cadmium or Copper or Lead or Zinc][NCMA]
and
[FeOOH + Cadmium and Copper and Lead and Zinc][CMA]

Primary Reactions Modeled	Experimental Data [Log K_M]	Literature Data[1] [Log K_M]
$S(wk)OH + H^+ \Leftrightarrow S(wk)OH_2^+$		7.29
$S(st)OH + H^+ \Leftrightarrow S(st)OH_2^+$		7.29
$S(wk)OH \Leftrightarrow S(wk)O^- + H^+$		-8.93
$S(st)OH \Leftrightarrow S(st)O^- + H^+$		-8.93
$S(wk)OH + Ca^{+2} \Leftrightarrow S(wk)O\text{-}Ca^+ + H^+$		-5.85
$S(st)OH + Ca^{+2} \Leftrightarrow S(st)OH\text{-}Ca^{+2}$		4.97
Metal Cation Complex: $CdCl_2$		
$S(wk)OH + Cd^{+2} \Leftrightarrow S(wk)O\text{-}Cd^+ + H^+$		-2.90
$S(st)OH + Cd^{+2} \Leftrightarrow S(st)O\text{-}Cd^+ + H^+$		0.470
Metal Cation Complex: $Cu(NO_3)_2$		
$S(wk)OH + Cu^{+2} \Leftrightarrow S(wk)O\text{-}Cu^+ + H^+$		0.600
$S(st)OH + Cu^{+2} \Leftrightarrow S(st)O\text{-}Cu^+ + H^+$		2.89
Metal Cation Complex: $Pb(NO_3)_2$		
$S(wk)OH + Pb^{+2} \Leftrightarrow S(wk)O\text{-}Pb^+ + H^+$		0.300
$S(st)OH + Pb^{+2} \Leftrightarrow S(st)O\text{-}Pb^+ + H^+$		4.65
Metal Cation Complex: $Zn(NO_3)_2$		
$S(wk)OH + Zn^{+2} \Leftrightarrow S(wk)O\text{-}Zn^+ + H^+$		-1.99
$S(st)OH + Zn^{+2} \Leftrightarrow S(st)O\text{-}Zn^+ + H^+$		0.990

[1] Dzombak and Morel (1990) and updated databases incorporated in Mineql$^+$, Version 4.5 for Windows (Schecher and McAvoy, 2001).

Table 10

Soil Organic Matter (SOM) System Modeling Parameters

Chemical Speciation Software Used: Visual MINTEQ, Version 2.30

Default Settings:

Main thermodynamic database: thermo.mdb
Solids database: type6.mdb
Component database: comp.mdb
Dissolved organic matter (DOM) complexes database: gaussian.mdb

Visual MINTEQ – Stockholm Humic Model (SHM) parameters

Fulvic acid: typicalFA.MPF.TXT
Humic acid: soilha.MPF.TXT
SHM site setting file: Default.MSI.TXT (same file for humic and fulvic acids)

SHM Input File

Select suspension

DOC parameters: ratio of 'active' DOM to DOC = 2; dissolved FA = 100% of 'active' DOM

Pahokee Peat Concentration (g L^{-1})	33.3[1]

Conversion of peat to SOM to 'active' humic substances (HS) (g L^{-1})

(33.3g-peat/L)[1] x (0.457g-C/g-peat)[2] x (1.90g-SOM/g-C)[3] x (0.54g-HS/g-SOM)[4] x (0.525g-'active' HS/g-HS)[5] = 8.2 g-'active' HS/L

Conversion of 'active' HS to humic acid (HA) and fulvic acid (FA) (g L^{-1})

(8.2 g-'active' HS/L) x 0.62[6] = 5.1 g-HA L^{-1}; (8.2 g-'active' HS/L) x 0.38[6] = 3.1 g-FA L^{-1}

Calculation of dissolved FA (DFA) (mg L^{-1}) from FA (g L^{-1}) and conversion of DFA to dissolved organic carbon (DOC) (mg L^{-1})

3.1 g-FA L^{-1} x 0.075[7] = 235 mg DFA L^{-1} x 0.50[6] = 117 mg DOC L^{-1}

Surface Area – FA, HA (m^2 g^{-1})[8]	approximately 3,500; 2,700

Table 10 (cont.)

Soil Organic Matter (SOM) System Modeling Parameters

Site Concentration – FA, HA (mmol L^{-1})[8]	21.9; 27.1
Visual Minteq Databases Used for Exchange and Complexation Reactions and Constants	
FA – shmgeneric.MDB ; HA – shmgeneric.MDB and gthumic.CDB	
CO_2 (Log P)	-3.48
Precipitation of Solids Allowed ?	No
Background Electrolyte	0.01M $CaCl_2$[1]
pHs	4.15; 5.56; 6.21[9]
Metal(s) Input Concentrations (mg L^{-1})	10,000; 5,000; 2,500; 1,000; 500; 100; 50; 10; 5; 1; 0.5; 0.1; 0.05; 0.01

1 Experimental setup.
2 International Humic Substances Society Pahokee peat data sheet.
3 Nelson and Sommers, 1996; Broadbent, 1953.
4 Stevenson, 1995.
5 Gustafsson and Pechova, 2003.
6 Gustafsson, 2004.
7 Sauve et al., 2000b.
8 Calculated by Visual MINTEQ based on model inputs.
9 pH of 99-1-7-12, 99-1-0-7, and both 98-3 soil samples.

Table 11

SOM Systems #1 and #2: Modeling Inputs for Reactions and Constants
[SOM + Cadmium or Copper or Lead or Zinc][NCMA]
and
[SOM + Cadmium and Copper and Lead and Zinc][CMA]

Primary Reactions Modeled	Literature Data[1] [Log K]
Solid and Dissolved Humic Acid (HA) and Fulvic Acid (FA) Complexes	
$HFA\text{-}H$[2] $\Leftrightarrow HFA\text{-} + H^{+1}$	0.00
$HFA\text{-}H + Ca^{+2} \Leftrightarrow HFA\text{-}Ca^{+} + H^{+1}$	-2.5
$2HFA\text{-}H + Ca^{+2} \Leftrightarrow (HFA)_2\text{-}Ca + 2H^{+1}$	-11.3
$HFA\text{-}H + Cd^{+2} \Leftrightarrow HFA\text{-}Cd^{+} + H^{+1}$	-1.65
$2HFA\text{-}H + Cd^{+2} \Leftrightarrow (HFA)_2\text{-}Cd + 2H^{+1}$	-9.3
$HFA\text{-}H + Cu^{+2} \Leftrightarrow HFA\text{-}Cu^{+} + H^{+1}$	-0.6
$2HFA\text{-}H + Cu^{+2} \Leftrightarrow (HFA)_2\text{-}Cu + 2H^{+1}$	-5.8
$2HFA\text{-}H + CuOH^{+1} \Leftrightarrow (HFA)_2\text{-}CuOH^{-} + 2H^{+1}$	-13.3
$HFA\text{-}H + Pb^{+2} \Leftrightarrow HFA\text{-}Pb^{+} + H^{+1}$	-0.15
$2HFA\text{-}H + Pb^{+2} \Leftrightarrow (HFA)_2\text{-}Pb + 2H^{+1}$	-6.15
$HFA\text{-}H + Zn^{+2} \Leftrightarrow HFA\text{-}Zn^{+} + H^{+1}$	-1.35
$2HFA\text{-}H + Zn^{+2} \Leftrightarrow (HFA)_2\text{-}Zn + 2H^{+1}$	-9.0
Primary Gel (G) Complexes[3]; dum = dummy component	
$2FA\text{-}dum + Ca^{+2} \Leftrightarrow FA\text{-}Ca^{+2}$ (G)	0.00
$2FA\text{-}dum + Cd^{+2} \Leftrightarrow FA\text{-}Cd^{+2}$ (G)	0.00
$2FA\text{-}dum + Cu^{+2} \Leftrightarrow FA\text{-}Cu^{+2}$ (G)	0.00
$FA\text{-}dum + H^{+} \Leftrightarrow FA\text{-}H^{+}$ (G)	0.00
$2FA\text{-}dum + Pb^{+2} \Leftrightarrow FA\text{-}Pb^{+2}$ (G)	0.00
$2FA\text{-}dum + Zn^{+2} \Leftrightarrow FA\text{-}Zn^{+2}$ (G)	0.00
$2HA\text{-}dum + Ca^{+2} \Leftrightarrow HA\text{-}Ca^{+2}$ (G)	0.00
$2HA\text{-}dum + Cd^{+2} \Leftrightarrow HA\text{-}Cd^{+2}$ (G)	0.00
$2HA\text{-}dum + Cu^{+2} \Leftrightarrow HA\text{-}Cu^{+2}$ (G)	0.00
$HA\text{-}dum + H^{+} \Leftrightarrow HA\text{-}H^{+}$ (G)	0.00
$2HA\text{-}dum + Pb^{+2} \Leftrightarrow HA\text{-}Pb^{+2}$ (G)	0.00
$2HA\text{-}dum + Zn^{+2} \Leftrightarrow HA\text{-}Zn^{+2}$ (G)	0.00

Table 11 (cont.)

SOM System #1 and #2: Modeling Inputs for Reactions and Constants
[SOM + Cadmium or Copper or Lead or Zinc][NCMA]
and
[SOM + Cadmium and Copper and Lead and Zinc][CMA]

Primary Reactions Modeled	Literature Data[1] [Log K]
Primary Diffuse Layer (D) Complexes[4]	
$2H^{+1}$ (D) + Ca^{+2} ⇔ Ca^{+2} (D) + $2H^{+1}$	0.00
$2H^{+1}$ (D) + Cd^{+2} ⇔ Cd^{+2} (D) + $2H^{+1}$	0.00
$2H^{+1}$ (D) + Cu^{+2} ⇔ Cu^{+2} (D) + $2H^{+1}$	0.00
$2H^{+1}$ (D) + Pb^{+2} ⇔ Pb^{+2} (D) + $2H^{+1}$	0.00
$2H^{+1}$ (D) + Zn^{+2} ⇔ Zn^{+2} (D) + $2H^{+1}$	0.00

1 All reactions and associated constants for either solid or dissolved phase humic acid or fulvic acid from the database, shmgeneric.MDB, in Visual MINTEQ.

2 HFA-H is a composite surface that represents either solid or dissolved humic acid (HA-H) and fulvic acid (FA-H).

3 All reactions and associated constants are from the SHM gel parameters database in Visual MINTEQ and represent cations weakly complexed to the interior of the gel-like organic particle.

4 All reactions and associated constants are from the database, gthumic.cdb, in Visual MINTEQ and represent cations weakly held in the diffuse layer surrounding the organic particle.

Table 12: Clay Weighting Factors

	Weighting Factors (WF)[1]
Sample Location: 98-3-5-10	
Kaolinite (K): (mg-MC^2/kg-K)(kg-K/1000g-K)(1g-K/0.21g-Al^{+3})(45.9g-Al^{+3}/kg-soil)(0.20) =	**0.04**
Illite (I): (mg-MC/kg-I)(kg-I/1000g-I)(1g-I/0.13g-Al^{+3})(45.9g-Al^{+3}/kg-soil)(0.70) =	**0.25**
Montmorillonite (M): (mg-MC/kg-M)(kg-M/1000g-M)(1g-M/0.11g-Al^{+3})(45.9g-Al^{+3}/kg-soil)(0.10)=	**0.04**
Sample Location: 98-3-20-25	
Kaolinite (K): (mg-MC/kg-K)(kg-K/1000g-K)(1g-K/0.21g-Al^{+3})(50.9g-Al^{+3}/kg-soil)(0.10) =	**0.02**
Illite (I): (mg-MC/kg-I)(kg-I/1000g-I)(1g-I/0.13g-Al^{+3})(50.9g-Al^{+3}/kg-soil)(0.80) =	**0.31**
Montmorillonite (M): (mg-MC/kg-M)(kg-M/1000g-M)(1g-M/0.11g-Al^{+3})(50.9g-Al^{+3}/kg-soil)(0.10)=	**0.05**
Sample Location: 99-1-0-7	
Kaolinite (K): (mg-MC/kg-K)(kg-K/1000g-K)(1g-K/0.21g-Al^{+3})(42.9g-Al^{+3}/kg-soil)(0.20) =	**0.04**
Illite (I): (mg-MC/kg-I)(kg-I/1000g-I)(1g-I/0.13g-Al^{+3})(42.9g-Al^{+3}/kg-soil)(0.70) =	**0.23**
Montmorillonite (M): (mg-MC/kg-M)(kg-M/1000g-M)(1g-M/0.11g-Al^{+3})(42.9g-Al^{+3}/kg-soil)(0.10)=	**0.04**

Table 12: Clay Weighting Factors (cont.)

Sample Location: 99-1-7-12	WF x (mg-MC[1]/kg-soil)
Kaolinite (K): (mg-MC/kg-K)(kg-K/1000g-K)(1g-K/0.21g-Al^{+3})(38.9g-Al^{+3}/kg-soil)(0.10) =	**0.02**
Illite (I): (mg-MC/kg-I)(kg-I/1000g-I)(1g-I/0.13g-Al^{+3})(38.9g-Al^{+3}/kg-soil)(0.60) =	**0.18**
Montmorillonite (M): (mg-MC/kg-M)(kg-M/1,000g-M)(1g-M/0.11g-Al^{+3})(38.9g-Al^{+3}/kg-soil)(0.30)=	**0.11**

1 WF x (mg-MC/kg-clay mineral) = mg-MC/kg-soil.
2 MC – metal cation (i.e. cadmium, copper, lead, and zinc).

Table 13: FeOOH and Soil Organic Matter Weighting Factors

FeOOH	**Weighting Factors (WF)**[1]
Sample Location: 98-3-5-10 Total Fe^{+3} (g kg^{-1} soil) 61.9	
(mg-MC^{2}/kg-FeOOH)(kg-FeOOH/1000g-FeOOH)(1g-FeOOH/0.63g-Fe^{+3})(61.9g-Fe^{+3}/kg-soil)(0.50) =	**0.05**
Sample Location: 98-3-20-25 Total Fe^{+3} (g kg^{-1} soil) 118	
(mg-MC/kg-FeOOH)(kg-FeOOH/1000g-FeOOH)(1g-FeOOH/0.63g-Fe^{+3})(118g-Fe^{+3}/kg-soil)(0.50) =	**0.09**
Sample Location: 99-1-0-7 Total Fe^{+3} (g kg^{-1} soil) 61.0	
(mg-MC/kg-FeOOH)(kg-FeOOH/1000g-FeOOH)(1g-FeOOH/0.63g-Fe^{+3})(61.0g-Fe^{+3}/kg-soil)(0.50) =	**0.05**
Sample Location: 99-1-7-12 Total Fe^{+3} (g kg^{-1} soil) 55.0	
(mg-MC/kg-FeOOH)(kg-FeOOH/1000g-FeOOH)(1g-FeOOH/0.63g-Fe^{+3})(55.0g-Fe^{+3}/kg-soil)(0.50) =	**0.04**

Soil Organic Matter [SOM]	**Weighting Factors (WF)**[3]
Sample Location: 98-3-5-10 Total Organic Carbon (OC) (g kg^{-1} soil) 36.4	
(mg-MC/kg-SOM)(kg-SOM/1000g-SOM)(1g-SOM/0.53g-OC)(36.4g-OC/kg-soil) =	**0.07**
Sample Location: 98-3-20-25 Total Organic Carbon (OC) (g kg^{-1} soil) 20.1	
(mg-MC/kg-SOM)(kg-SOM/1000g-SOM)(1g-SOM/0.53g-OC)(20.1g-OC/kg-soil) =	**0.04**

Table 13: FeOOH and Soil Organic Matter Weighting Factors (cont.)

FeOOH	**Weighting Factors (WF)^{3}**
Sample Location: 99-1-0-7 Total Organic Carbon (OC) (g kg^{-1} soil) 18.0	
(mg-MC/kg-SOM)(kg-SOM/1000g-SOM)(1g-SOM/0.53g-OC)(18.0g-OC/kg-soil) =	**0.03**
Sample Location: 99-1-7-12 Total Organic Carbon (OC) (g kg^{-1} soil) 16.0	
(mg-MC/kg-SOM)(kg-SOM/1000g-SOM)(1g-SOM/0.53g-OC)(16.0g-OC/kg-soil) =	**0.03**

1 WF x (mg-MC/kg-FeOOH) = mg-MC/kg-soil.

2 MC – metal cation (i.e. cadmium, copper, lead, and zinc).

3 WF x (mg-MC/kg-SOM) = mg-MC/kg-soil.

5.0 RESULTS AND DISCUSSION

Of the 21 soil samples collected in 1998 and 1999, four were selected for additional chemical analyses and inclusion in the modeling portion of this research. The four samples selected; 98-3-5-10, 98-3-20-25, 99-1-0-7, and 99-1-7-12, provided a range of pHs, soil textures, organic carbon, and concentrations of soluble cadmium, copper, lead, and zinc and total aluminum and iron.

5.1 Laboratory Methods – Leadville, CO Soils

5.1.1 Total Metals

The concentrations of total cadmium, copper, lead, and zinc in soil samples 98-3-5-10, 98-3-20-25, 99-1-0-7, and 99-1-7-12 are listed in Table 14. The four soil samples contain concentrations of cadmium, copper, lead and zinc that exceed both the range and average concentrations of metal cations in soils reported by Lindsay (2001). The Lindsay data are included in Table 14 for comparison. In sample 98-3-5-10, total cadmium, copper, lead, and zinc are 98.0, 435, 18,640, and 18,020 mg kg^{-1}, respectively, while in 98-3-20-25, total cadmium, copper, lead, and zinc are 146, 213, 14,440, and 14,120 mg kg^{-1}, respectively. In sample 99-1-0-7, total cadmium, copper, lead, and zinc are 43.2, 633, 4,435, and 7,760 mg kg^{-1}, respectively. Total cadmium, copper, lead, and zinc in sample 99-1-7-12 are 11.2, 336, 3,233, and 1,822 mg kg^{-1}, respectively. The concentrations of cations reported for all 1998 and 1999 sample locations are included in

Appendix B, Tables B1–B5. The data show the soils in this particular pasture still exhibit the impacts from past mining, smelting, and surface irrigation activities.

5.1.2 pH, Carbon Speciation, and Texture

Table 15 lists pH, carbon speciation, and soil texture for the four selected soils, while soil texture and carbon profiles for all 1998 and 1999 sample locations are reported in Appendix B, Figures B1-B10. The pH for the two 98-3 samples is 6.2, while the pHs for samples 99-1-0-7 and 99-1-7-12 are 5.6 and 4.1, respectively. Organic carbon constitutes 100 % of the total carbon reported in the two 99-1 samples and sample 98-3-20-25. In sample 98-3-5-10, organic carbon is approximately 95% with 5% inorganic carbon. Soil textures for samples 98-3-5-10 and 98-3-20-25 are loam and silty clay loam, respectively. The soil texture for the 99-1 samples is sandy loam.

The abrupt changes detected in texture, carbon content, major cation concentrations, and metals concentrations in the 1998 and 1999 soil profiles (Appendix B) are indicative of buried horizons described by Levy (1990). The data support the previous conclusions by Levy (1990) that these pasture soils have been inundated over the past century with contaminated materials from upgradient sources. The barren surface at location 99-1 and the changes noted in pH and concentrations of major cations and metals as depth increased are reflective of the intermittent inflow of metal-contaminated materials from upgradient sources.

Table 14. Leadville, CO soils - total metals concentrations

Sample Location	Total Aluminum	Total Cadmium	Total Copper	Total Iron	Total Lead	Total Manganese	Total Zinc
	mg kg^{-1}	mg kg^{-1}	mg kg^{-1}	mg kg^{-1}	mg kg^{-1}	mg kg^{-1}	mg kg^{-1}
98-3-5-10	45,860	98.0	435	61,876	18,640	3,375	18,020
98-3-20-25	50,880	146	213	117,520	14,440	8,741	14,120
99-1-0-7	42,860	43.2	633	60,949	4,435	3,770	7,760
99-1-7-12	38,870	11.2	336	55,026	3,233	1,410	1,822
Range[1]	10,000-300,000	0.01-0.7	2-100	7,000-550,000	2-200	20-3,000	10-300
Average[1]	71,000	0.06	30	38,000	10	600	50

1 Lindsay, 1979

Table 15. Leadville, CO soils - pH, carbon speciation, and texture

Sample Location	pH	Total Carbon	Total Organic Carbon	Total Inorganic Carbon	Sand	Silt	Clay
		mg kg^{-1}	mg kg^{-1}	mg kg^{-1}	%	%	%
98-3-5-10	6.21	38,240	36,390	1,850	47.8	44.0	8.2
98-3-20-25	6.21	20,100	20,100	0	16.8	46.8	36.4
99-1-0-7	5.56	18,000	18,000	0	66.4	23.4	10.2
99-1-7-12	4.15	16,050	16,050	0	58.1	33.7	8.2

5.1.3 X-Ray Diffraction Results

The Materials Characterization Laboratory at the University of Wyoming, Laramie, WY conducted X-ray diffraction (XRD) and scanning electron microscopy (SEM) analyses of samples from the 99-1 location (Figures 1 and 2). The XRD data from Al-Farraj (2002) were used for the 98-3 location. The XRD data from both the University of Wyoming and Al-Farraj show a mixture of smectites, illites, and kaolinite as the primary clay minerals in these soils. The University of Wyoming data indicate also the presence of jarosite [$KFe_3(SO_4)(OH)_6$], an iron sulfate mineral, and small round amorphous particles in the 2-5μ range. The particles detected are most likely pyrite (FeS_2). The SEM data confirm the presence of significant quantities of iron, sulfur, and zinc in the 99-1 samples.

5.1.4 Changes in Extraction Methodology

Preliminary comparisons of predicted metal partitioning with experimental data generated in 2000 were poor. Initially, it was assumed the poor fit of predicted values to experimental data was due to the assumptions, conversions, multipliers, weighting factors, or binding constants used in developing the surrogate soils and the predictive modeling approach. Based on an extensive review of surrogate soil parameters and model inputs, the conclusion was the source of poor correlation was not the general modeling approach. Selective extraction procedures used in 2000 were evaluated and at least two potential problems identified.

Figure 1. XRD data for sample 99-1-0-7

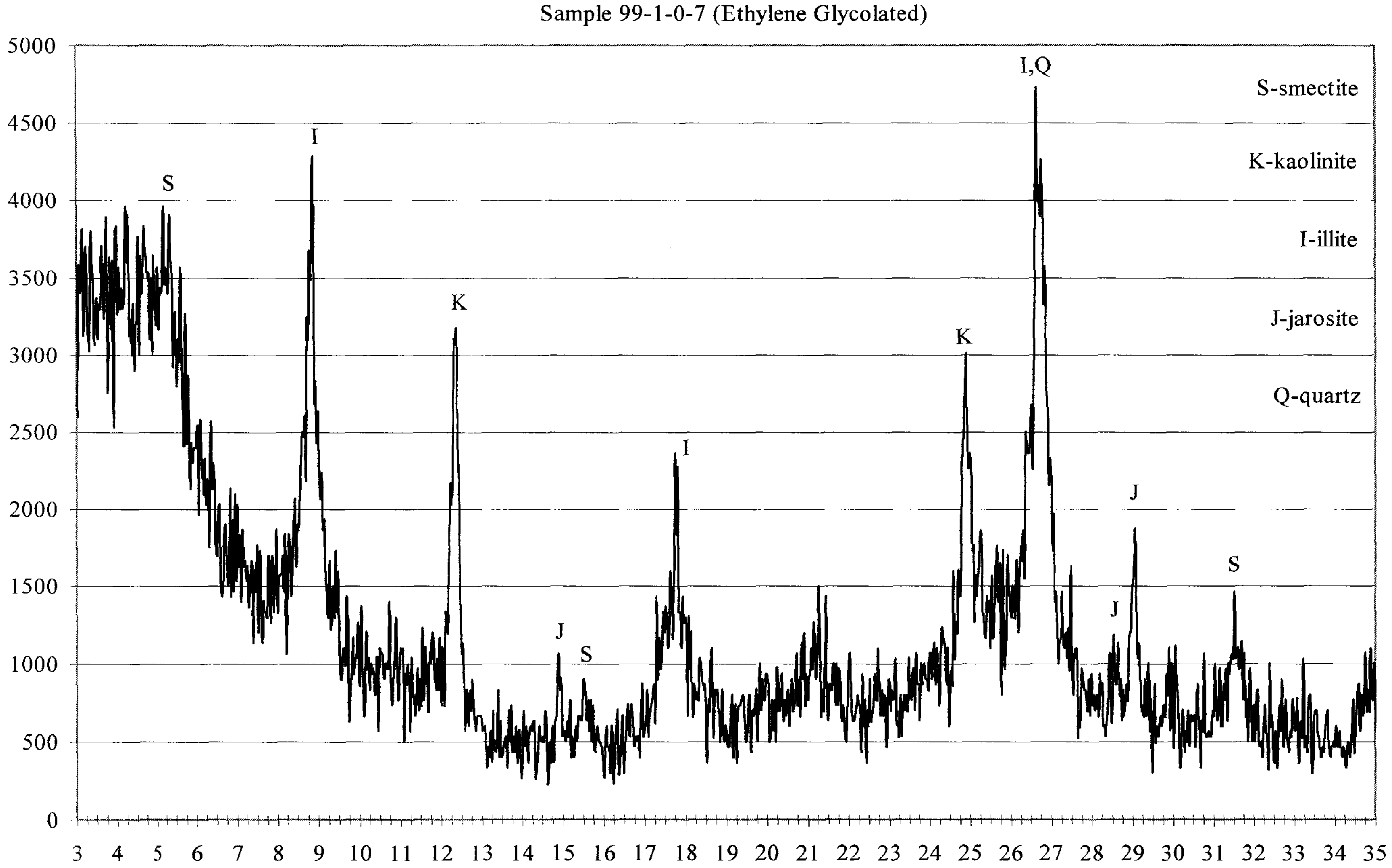

Figure 2. XRD data for sample 99-1-7-12

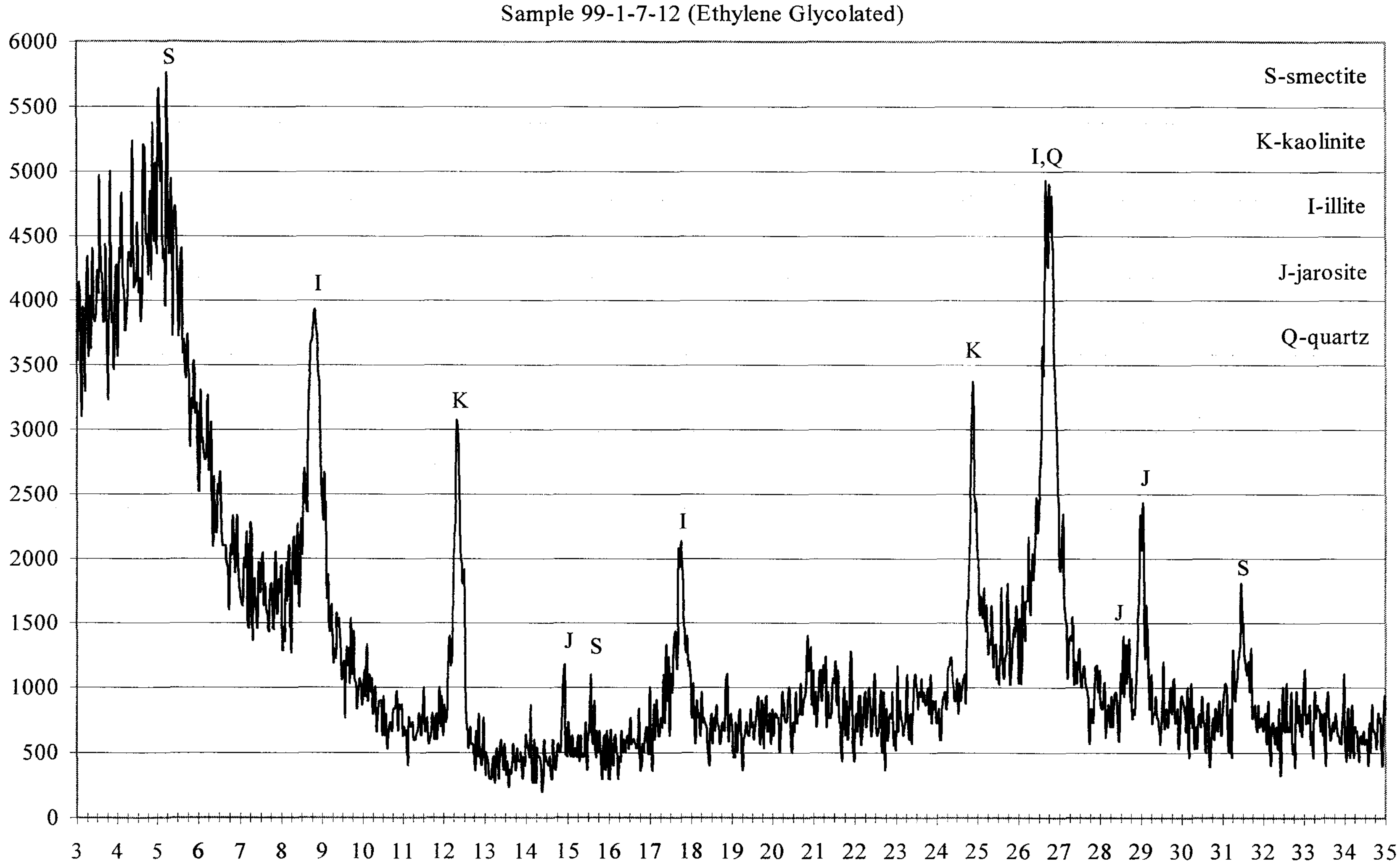

The first issue evaluated was the use of the horizontal shaker system (HSS) during the selective extraction process. Use of the HSS causes significant disruption of the soil structure and maximizes the recovery of metals. Concentrations of metals recovered by this method are greater than the concentrations of metals expected under less aggressive techniques such as the filtration of extractant solutions through columns. Since the goal of this modeling approach is to predict metal partitioning in relatively undisturbed contaminated soils and not the partitioning of metals in soil suspensions subjected to intensive agitation similar to the HSS, the conclusion is the selective extraction procedures should incorporate a less aggressive physical extraction procedure. Therefore, to determine whether a less aggressive extraction procedure would generate data that correlated better with predicted values, cation exchange capacity (CEC) was measured in 2003 using a vacuum extraction system (VES).

The second issue evaluated was the use of DIW to recover soluble metals. As previously described in section 4.5.5, soluble metals concentrations are the most critical model inputs because the data are used in conjunction with regression equations to calculate predicted concentrations of metals. The problems identified with the DIW extraction procedure were; 1. no measurable concentrations of soluble cadmium were obtained for any soil sample, 2. in sample 99-1-0-7, more copper was recovered with DIW than with 0.5M $Ca(NO_3)_2$, and 3. very high zinc concentrations (i.e. 2.63-16.5 mg L^{-1}) and very low copper (<0.5 mg L^{-1}) and lead (<2 mg L^{-1}) were recovered with DIW. The inconsistent soluble metals data resulted in wide variations in the predicted concentrations of exchangeable, sorbed, and complexed metals.

Although, the DIW extraction procedure did recover small quantities of cadmium, higher concentrations of cadmium were detected in the DIW blanks. The cause of cadmium contamination in the blanks is unknown, but the subtraction of blank cadmium concentrations from sample cadmium concentrations resulted in values of less than the method detection limit (<MDL). To generate useable model inputs for soluble cadmium, empirical equations proposed by Sauve (1999, 2000a) were used in place of experimental data. Sauve's empirical equations are based on total metals, pH, and carbon data from large sets of environmental data. The use of cadmium concentrations calculated from empirical equations versus experimental soluble metals data probably had a significant impact on the poor fit of predicted concentrations of exchangeable, sorbed, and complexed cadmium to experimental data.

The recovery of more copper with DIW than 0.5M $Ca(NO_3)_2$ in 99-1-0-7 and the recovery of high levels of zinc with DIW are most likely related to the twin increase in colloidal particles in solution and the solubilization of humic materials during the aggressive extraction process. Preliminary modeling of copper complexation with soil organic matter using Visual MINTEQ's Stockholm Humic Model (SHM) predicted copper, which preferentially binds to humic acids (HA) and fulvic acids (FA), would be transferred to the solution phase as complexed copper during the solubilization of HA and FA.

The SHM predicted also that a significant percent of the total zinc present in these soils would be located in the diffuse layer surrounding HA and FA particles or as charge screening ions. Diffuse layer (i.e. D complexes) and charge screening (i.e. G complexes) metals such as zinc, are weakly held and easily extracted with DIW.

The preliminary SHM predictions support earlier conclusions by Gerritse and Van Driel (1984), McBride et al. (1997), and Sauve et al. (1999, 2000b) that the extraction of soils with DIW could solubilize metal-HA, -FA complexes resulting in the recovery of complexed metals in addition to water soluble metals.

As a result of the problems associated with DIW extraction of these soils, soluble metals concentrations were measured in 2003 using 0.01M $Ca(NO_3)_2$ as recommended by McBride et al. (1997) and Sauve et al. (1999, 2000b). Use of 0.01M $Ca(NO_3)_2$ as an extractant for soluble metals minimized the solubilization of metal-HA, -FA complexes. Based on the results of CEC measurements and the subsequent re-analyses of these four soils for soluble metals; the extraction of metals with 0.03M $La(NO_3)_3$ and 0.05M $Pb(NO_3)_2$ were conducted a second time in 2004 using the VES. Comparison of the 2000 and 2003-2004 datasets are discussed in section 5.1.6.

Based on the previous discussions regarding selective extraction procedures, operational definitions are provided below regarding the types of bound metal cations recovered by the different extractant solutions tested. The term "soluble metals" describes soluble metal ions and complexes which are not bound to any charged solid or act as charge neutralizing cations. The term "exchangeable metals" includes solvated metal ions and complexes that are bound by electrostatic forces (i.e. non-specific adsorption) to the charged surface of a solid as an outer-sphere complex or located in the diffuse layer surrounding a charged particle as charge neutralizing cations. The terms "sorbed metals", which are associated with clay minerals and oxides, and "complexed metals", which are associated with SOM, include metal ions and complexes bound by ionic or covalent bonding (i.e. specific adsorption) to the charged surface of solids as inner-sphere complexes.

5.1.5 Cation Exchange Capacity (CEC)

The Soil Testing Laboratory at Colorado State University, Fort Collins, CO measured CEC using a VES in conjunction with the method described by Sumner and Miller (1996). The method is described in detail in section 4.3.2. The CEC was calculated two different ways, the first was based on the amount of NH_4^+ recovered by 0.2M KNO_3 and the second was based on the sum of all cations recovered by the three solutions (i.e. 0.2M NH_4Cl, DIW, and 0.2M KNO_3). Tables 16-19 list the results of both CEC calculations for the four soil samples. As depth increases, the CEC at location 98-3 increases from 17.5 to 18.4 $cmol_c\ kg^{-1}$ while at location 99-1, the CEC decreases slightly from 10.6 to 10.1 $cmol_c\ kg^{-1}$. The lower CEC in the more acidic 99-1 soil profile is due to the smaller concentrations of available exchange sites caused by the combination of lower organic carbon, lower clay content, and higher sand content.

Comparison of CECs calculated by both methods for each soil sample show that analyzing for and summing each individual cation is approximately as accurate as the CEC based on the concentration of NH_4^+ reported. The result is somewhat surprising since the calculation of CEC by summing individual cations includes soluble cations

Table 16. Sample 98-3-5-10 cation exchange capacity

Sample 98-3-5-10 Cations	NH_4Cl Extraction mg kg^{-1}	DIW Extraction mg kg^{-1}	KNO_3 Extraction mg kg^{-1}	Total Cations Extracted mg kg^{-1}	Total Cations Extracted $cmol_c\ kg^{-1}$	Cation/ Total CEC %
Ca	658	171	236	1065	5.31	30.8
Mg	401	106	78.3	585	4.82	27.9
Na	301	116	42.5	460	2.00	11.6
K	64.6	22.4	0.000	87.0	0.223	1.29
P	0.280	0.360	0.010	0.650	0.010	0.06
Al	5.20	0.010	0.390	5.60	0.062	0.36
Fe	46.4	0.440	0.380	47.2	0.254	1.47
Mn	8.20	2.97	4.80	16.0	0.058	0.34
Ti	13.3	1.20	2.40	16.9	0.141	0.82
Cu	1.12	0.440	0.180	1.74	0.005	0.03
Zn	301	127	218	646	1.98	11.4
Ni	0.290	0.070	0.050	0.410	0.001	0.01
Mo	0.490	0.180	0.370	1.04	0.007	0.04
Cd	23.1	5.80	3.37	32.3	0.057	0.33
Cr	0.010	0.010	0.010	0.030	0.000	0.00
Sr	0.990	0.320	1.11	2.42	0.006	0.03
B	0.220	0.090	0.110	0.420	0.012	0.07
Ba	1.90	0.360	15.6	17.9	0.026	0.15
Pb	77.1	1.17	9.50	87.8	0.085	0.49
Si	13.2	13.7	8.10	35.0	0.498	2.89
V	1.60	0.600	0.670	2.87	0.020	0.11
Total Acidity					1.70	9.84
Total CEC ($cmol_c/kg$)					17.3	
NH_4^+ CEC (cmolc/kg)					17.5	
Total CEC / NH_4^+ CEC (%)					98.7	

Table 17. Sample 98-3-20-25 cation exchange capacity

Sample 98-3-20-25 Cations	NH_4Cl Extraction mg kg^{-1}	DIW Extraction mg kg^{-1}	KNO_3 Extraction mg kg^{-1}	Total Cations Extracted mg kg^{-1}	Total Cations Extracted $cmol_c$ kg^{-1}	Cation/ Total CEC %
Ca	1033	92.3	111	1236	6.17	36.8
Mg	440	40.9	32.2	513	4.22	25.2
Na	59.8	4.60	33.0	97.4	0.424	2.53
K	98.2	18.7	0.000	117	0.299	1.79
P	0.010	0.100	0.010	0.120	0.002	0.01
Al	9.10	3.00	1.40	13.5	0.150	0.90
Fe	49.0	1.50	0.400	50.9	0.273	1.63
Mn	13.9	7.25	4.40	25.6	0.093	0.56
Ti	12.9	2.40	3.50	18.8	0.157	0.94
Cu	0.820	0.300	0.190	1.31	0.004	0.02
Zn	329	146	163	638	1.95	11.6
Ni	0.410	0.040	0.030	0.480	0.002	0.01
Mo	0.550	0.220	0.250	1.02	0.006	0.04
Cd	41.1	5.80	3.16	50.1	0.089	0.53
Cr	0.120	0.010	0.010	0.140	0.001	0.00
Sr	1.95	0.190	0.520	2.66	0.006	0.04
B	0.190	0.030	0.100	0.320	0.009	0.05
Ba	8.00	0.880	18.9	27.8	0.040	0.24
Pb	58.3	19.0	22.2	99.5	0.096	0.57
Si	20.6	17.7	7.00	45.3	0.645	3.85
V	0.900	0.400	0.270	1.57	0.011	0.06
Total Acidity					2.10	12.5
Total CEC ($cmol_c$/kg)					16.8	
NH_4^+ CEC (cmolc/kg)					18.4	
Total CEC / NH_4^+ CEC (%)					91.0	

Table 18. Sample 99-1-0-7 cation exchange capacity

Sample 99-1-0-7 Cations	NH_4Cl Extraction mg kg^{-1}	DIW Extraction mg kg^{-1}	KNO_3 Extraction mg kg^{-1}	Total Cations Extracted mg kg^{-1}	Total Cations Extracted $cmol_c$ kg^{-1}	Cation/ Total CEC %
Ca	460	74.9	130	665	3.32	37.3
Mg	157	28.1	34.5	220	1.81	20.3
Na	36.6	4.30	37.2	78.1	0.340	3.82
K	74.8	19.9	0.000	94.7	0.242	2.72
P	0.010	0.010	0.020	0.040	0.001	0.01
Al	2.20	0.190	0.010	2.40	0.027	0.30
Fe	8.30	1.11	0.140	9.55	0.051	0.58
Mn	66.9	14.2	25.1	106	0.387	4.34
Ti	9.50	1.30	4.10	14.9	0.125	1.40
Cu	1.43	0.180	0.220	1.83	0.006	0.06
Zn	196	53.8	113	363	1.11	12.5
Ni	0.330	0.020	0.070	0.420	0.001	0.02
Mo	0.330	0.080	0.160	0.570	0.004	0.04
Cd	6.00	0.900	0.970	7.87	0.014	0.16
Cr	0.010	0.010	0.010	0.030	0.000	0.00
Sr	0.370	0.120	0.300	0.790	0.002	0.02
B	0.130	0.050	0.160	0.340	0.009	0.11
Ba	1.50	0.200	2.20	3.90	0.006	0.06
Pb	7.10	1.42	3.80	12.3	0.012	0.13
Si	9.30	8.80	4.90	23.0	0.328	3.68
V	0.300	0.740	0.870	1.91	0.013	0.15
Total Acidity					1.10	12.4
Total CEC ($cmol_c$/kg)					8.90	
NH_4^+ CEC (cmolc/kg)					10.6	
Total CEC / NH_4^+ CEC (%)					84.0	

Table 19. Sample 99-1-7-12 cation exchange capacity

Sample 99-1-7-12 Cations	NH_4Cl Extraction mg kg^{-1}	DIW Extraction mg kg^{-1}	KNO_3 Extraction mg kg^{-1}	Total Cations Extracted mg kg^{-1}	Total Cations Extracted $cmol_c$ kg^{-1}	Cation // Total CEC %
Ca	521	36.9	82.5	640	3.20	33.5
Mg	200	12.9	19.0	232	1.91	20.0
Na	49.6	2.00	35.9	87.5	0.381	3.99
K	111	6.50	0.000	118	0.301	3.15
P	0.010	0.010	0.010	0.030	0.000	0.01
Al	16.2	0.010	22.1	38.3	0.426	4.47
Fe	66.1	2.27	2.40	70.8	0.380	3.99
Mn	81.5	12.1	23.3	117	0.426	4.46
Ti	8.90	1.10	2.90	12.9	0.108	1.13
Cu	6.61	1.29	3.33	11.2	0.035	0.37
Zn	187	38.9	93.8	320	0.978	10.3
Ni	0.540	0.050	0.140	0.730	0.002	0.03
Mo	0.290	0.030	0.160	0.480	0.003	0.03
Cd	3.40	0.470	0.740	4.61	0.008	0.09
Cr	1.00	0.010	0.010	1.02	0.004	0.04
Sr	0.340	0.100	0.350	0.790	0.002	0.02
B	0.160	0.030	0.120	0.310	0.009	0.09
Ba	2.80	0.530	12.0	15.3	0.022	0.23
Pb	54.4	7.28	35.9	97.6	0.094	0.99
Si	7.20	11.6	5.20	24.0	0.342	3.59
V	0.400	0.010	0.740	1.15	0.008	0.08
Total Acidity					0.900	9.44
Total CEC ($cmol_c$/kg)					9.53	
NH_4^+ CEC (cmolc/kg)					10.1	
Total CEC / NH_4^+ CEC (%)					94.4	

recovered during the treatment of the soil with NH_4Cl-DIW-KNO_3. The NH_4^+ method excludes the recovery and reporting of soluble cations.

The advantages of summing each cation recovered are the determination of each cation's impact on the overall CEC and as a check on the relative efficiencies of the various extractant solutions. The CECs calculated by summing each cation's concentration are 99% (98-3-5-10), 91% (98-3-20-25), 84% (99-1-0-7), and 94% (99-1-7-12) of the reported CECs based on NH_4^+recovery.

The percent of total CEC occupied by calcium, magnesium, sodium, and potassium ranges from 61 to 72% with the lowest percentages found in the more acidic 99-1 soil profile. Of interest is the percent of total CEC occupied by cadmium, copper, lead, and zinc. Exchangeable zinc concentrations range from 10 to 13% of the total CEC, while the concentrations of exchangeable cadmium, copper, and lead are all less than 1%. The results can be partially explained based on the location of sorption, binding strength of the four metals, and their total concentrations in the four soils. Based on reported metal cation affinity sequences for clay minerals (Farrah et al., 1980), FeOOH (Dzombak and Morel, 1990), and humic substances (Gustafsson, 2004), zinc is less strongly bound to these materials than lead and copper. As a consequence, lead and copper can compete more successfully than zinc for available strong binding sites associated with the clay, FeOOH and SOM fractions. Thus, the very high concentrations of lead and zinc in these four soils means a higher percent of the zinc than lead will associate with exchangeable and weak binding sites in these soils.

5.1.6 Comparison of Data from 2000 and 2003-2004 Extraction Methods

As discussed in section 5.1.4, the poor comparison between predicted concentrations of metals and experimental data was potentially caused by problems in the extraction methods used in 2000. The two modifications made in the 2003-2004 extraction methods were the replacement of DIW with 0.01M $Ca(NO_3)_2$ to extract soluble metals and the replacement of the HSS with the VES. Table 20 lists the concentrations of metals recovered with the different extractant solutions and physical extraction systems in 2000 and 2003-2004. Although soluble metals concentrations are normally reported in units of mg L^{-1}, soluble metals concentrations have been converted to mg kg^{-1} in Table 20 to simplify comparisons between methods and extractant solutions.

Comparison of Metals Recovered by DIW and 0.01M $Ca(NO_3)_2$ Extractant Solutions

The reported cadmium values using DIW are less than the method detection limit in all soils. The 0.01M $Ca(NO_3)_2$ procedure recovered 3.20 (0-7 cm) and 9.08 (7-12 cm) mg kg^{-1} from the 99-1 soil profile and 33.4 (5-10 cm) and 37.6 (20-25 cm) mg kg^{-1} from the 98-3 soil profile. The concentrations of cadmium reported for the 0.01M $Ca(NO_3)_2$ extraction procedure are 20-33% of the total cadmium measured in these soils.

Excluding sample 99-1-0-7, DIW and 0.01M $Ca(NO_3)_2$ recovered approximately the same amount of copper (i.e. 0.200-1.56 mg kg^{-1}) from these soils. The copper concentrations reported are <1% of the total copper measured. In 99-1-0-7, DIW recovered 16.4 mg kg^{-1} and 0.01M $Ca(NO_3)_2$ recovered 0.320 mg kg^{-1}, representing 2.6% and <1% of the total copper measured, respectively.

Table 20. Comparison of experimental data from the 2000 and 2003-2004 selective extraction procedures

Sample	Metal	(2000) Total Metals[1]	(2000) Water Soluble Metals[2]	(2000) Exchangeable Metals[3]	(2000) Lanthanum Extractable Metals[4]	(2000) Lead Extractable Metals[5]	(2003) Calcium Soluble Metals[6]	(2003) Exchangeable Metals[7]	(2004) Lanthanum Extractable Metals[8]	(2004) Lead Extractable Metals[9]
		mg kg^{-1}	mg kg^{-1}	mg kg^{-1}	mg kg^{-1}	mg kg^{-1}	mg kg^{-1}	mg kg^{-1}	mg kg^{-1}	mg kg^{-1}
98-3-5-10	Cd	98.0	0.120*	49.7	48.9	59.8	33.4	32.3	45.6	106
	Cu	435	1.20	5.19	6.14	64.8	0.720	1.74	1.24	67.4
	Pb	18,640	74.0	1,490	3,358	NA	9.40	87.8	91.2	NA
	Zn	18,020	472	2,490	3,162	5,789	163	646	152	794
98-3-20-25	Cd	146	0.120*	68.4	68.7	88.0	37.6	50.1	72.5	97.3
	Cu	213	0.200*	0.520	0.540	12.2	0.240	1.31	0.344	3.10
	Pb	14,440	1.00*	218	689	NA	1.24	99.5	31.7	NA
	Zn	14,120	184	2,249	3,000	4,740	133	638	131	443
99-1-0-7	Cd	43.2	0.120*	12.7	12.8	18.1	9.08	7.87	15.6	29.0
	Cu	633	16.4	9.24	19.8	119	0.320	1.83	0.596	103
	Pb	4,435	4.48	39.2	121	NA	0.320	12.3	12.1	NA
	Zn	7,760	660	1,226	1,666	2,903	65.2	363	91.6	296
99-1-7-12	Cd	11.2	0.120*	2.23	0.590	0.800	3.20	4.61	4.76	5.35
	Cu	336	1.56	26.3	33.7	49.6	1.04	11.2	10.1	54.1
	Pb	3,233	5.32	279	328	NA	3.48	97.6	120	NA
	Zn	1,822	105	328	385	412	32.1	320	38.5	49.2

1- HNO_3-$HClO_4$-HF

2- DIW with shaker system

3- 0.5M $Ca(NO_3)_2$ with shaker system

4- 0.03M $La(NO_3)_3$-0.1M $Ca(NO_3)_2$ with shaker system

5- 0.05M $Pb(NO_3)_2$-0.1M $Ca(NO_3)_2$ with shaker system

6- 0.01M $Ca(NO_3)_2$ with vacuum extraction system

7- NH_4Cl-DIW-KNO_3 with vacuum extraction system

8- 0.03M $La(NO_3)_3$-0.1M $Ca(NO_3)_2$ with vacuum extraction system

9- 0.05M $Pb(NO_3)_2$-0.1M $Ca(NO_3)_2$ with vacuum extraction system

*- One-half of method detection limit

At the 99-1 location, DIW recovered 4.48 (0-7 cm) and 5.32 (7-12 cm) mg kg^{-1} of lead, while 0.01M $Ca(NO_3)_2$ recovered 0.320 (0-7 cm) and 3.48 (7-12 cm) mg kg^{-1} of lead. At the 98-3 location, DIW recovered significantly more lead from the 98-3-5-10 sample (i.e. 74.0 mg kg^{-1}) than 0.01M $Ca(NO_3)_2$ (i.e. 9.40 mg kg^{-1}). For the 98-3-20-25 sample, DIW and 0.01M $Ca(NO_3)_2$ recovered the same amount of lead, 1.00 and 1.24 mg kg^{-1}, respectively. The reported lead concentrations for all samples are <0.4% of the total lead measured.

Excluding sample 98-3-20-25, DIW recovered approximately 3-10X more zinc than 0.01M $Ca(NO_3)_2$ in all samples. In 98-3-20-25, DIW recovered 184 mg $kg^{-1}$of zinc, while 0.01M $Ca(NO_3)_2$ recovered 133 mg kg^{-1} of zinc. The reported concentrations of zinc are <8.5% of the total zinc measured.

The data indicate that on a percent basis, a significant fraction of the total cadmium (i.e. 20-33%) present in these soils is potentially bioavailable (i.e. soluble) versus <1% for copper, <0.4% for lead, and <8.5% for zinc. However, the very high concentrations of lead and zinc in the Leadville soils translate into significant concentrations of potentially bioavailable lead and zinc being measured.

Comparison of Metals Recovered by Calcium, NH_4Cl-DIW-KNO_3, Lanthanum, and Lead Extractant Solutions

In the following subsections, the total amount of each metal recovered by the various extractant solutions tested are compared. Based on a comparison of recoveries, conclusions are made as to a solution's relative selectivity and extraction efficiency.

Cadmium

For cadmium, two of the four extractants used in 2000, 0.5M $Ca(NO_3)_2$ and 0.03M $La(NO_3)_3$, and three of the four extractants used in 2003-2004, 0.01M $Ca(NO_3)_2$, NH_4Cl-DIW-KNO_3, and 0.03M $La(NO_3)_3$, recovered approximately the same amounts of cadmium. Lead nitrate, which was used in 2000 and 2004, extracted approximately 1.5-2.0X the amount of cadmium recovered by the other extractants. On a percent basis, the fraction of total cadmium recovered by the first five extractants ranges from 20-50%, while 0.05M $Pb(NO_3)_2$ recovered 48-108% in 2004 and 7.1-61% in 2000. The data indicate up to 50% of the total cadmium reported for these soils was located in the soil solution, adsorbed to exchange sites, or weakly complexed by HA and FA. The remaining 50% appears to be bound to sorption sites on oxide minerals or strongly complexed by HA and FA. Based on the data, cadmium exhibits a higher potential than the other three metals to leach through the soil profile.

The slight differences in exchangeable (i.e. 0.5M $Ca(NO_3)_2$ and NH_4Cl-DIW-KNO_3) and lanthanum-extractable cadmium concentrations between 2000 and 2003-2004 appear to show the use of the HSS may have increased the recovery of cadmium over the VES. However, the VES appears to significantly increase lead-extractable cadmium. The reason for this distinct difference between the two systems is unknown.

Copper

Excluding sample 99-1-7-12, the three extractants, DIW, 0.5M $Ca(NO_3)_2$, and 0.03M $La(NO_3)_3$, used in 2000 recovered approximately the same amount of copper. A similar trend is noted for the three extractants, 0.01M $Ca(NO_3)_2$, NH_4Cl-DIW-KNO_3, and 0.03M $La(NO_3)_3$, used in 2003-2004, except the range of concentrations reported for copper in 2003-2004 are lower than the range of concentrations reported for 2000. The data indicate the HSS had a greater impact on the recovery of copper in these soils than the VES. The data suggest also that 0.03M $La(NO_3)_3$ is not any more efficient with regards to copper extraction than the other extractants tested. The finding is contrary to the conclusions of Miller et al (1986), who determined $La(NO_3)_3$ was capable of extracting strongly sorbed copper. Excluding sample 99-1-7-12, the extraction of copper by the extractant solutions listed above account for <3% of the total copper present in these soils.

Approximately the same amount of copper was recovered by 0.05M $Pb(NO_3)_2$ in both 2000 and 2004, indicating there is no impact on the recovery of lead-extractable copper using either physical extraction system. On a percent basis, 0.05M $Pb(NO_3)_2$ recovered significantly more copper (i.e. 5.7-19% of total copper) than the other extractants.

In sample 99-1-7-12, DIW and 0.01M $Ca(NO_3)_2$ recovered approximately the same amount of copper (i.e. <0.3% of total copper), while 0.5M $Ca(NO_3)_2$, 0.03M $La(NO_3)_3$, and NH_4Cl-DIW-KNO_3 extracted significantly higher concentrations of copper. The amounts of copper recovered by 0.05M $Pb(NO_3)_2$ in both years are similar and the concentrations reported are 1.5-5.0X higher than the concentrations of copper recovered by the weaker extractant solutions.

None of the extractants recovered more than 20% of the total copper present in these soils suggesting either the solutions selected for copper recovery are unable to extract sorbed or complexed copper or the majority of copper is unrecoverable for other reasons. Considering these soils have been receiving metals for more than 100 years, it is possible that a significant percent of the copper exists as a precipitate on solid surfaces or is partly occluded in the crystal structure of secondary minerals.

Lead

Comparison of lead data from both years indicates a significant impact on the recovery of lead between the two physical extraction systems used. The HSS extracted 2-36X more lead than the VES and increased the effectiveness of 0.03M $La(NO_3)_3$ to extract lead as evidenced by the recovery of 1.5-4.0X more lead than 0.5M $Ca(NO_3)_2$. In 2004, the extraction efficiency of 0.03M $La(NO_3)_3$ was much less distinct with $La(NO_3)_3$ and NH_4Cl-DIW-KNO_3 extracting similar quantities of lead from the two surface samples, 98-3-5-10 and 99-1-0-7. The NH_4Cl-DIW-KNO_3 sequence recovered 3X more lead than 0.03M $La(NO_3)_3$ from sample 98-3-20-25 and 0.03M $La(NO_3)_3$ recovered 33% more lead than NH_4Cl-DIW-KNO_3 in sample 99-1-7-12.

Since no comparison between the lanthanum and lead extractant solutions was possible, the selectivity and extraction efficiency of 0.03M $La(NO_3)_3$ for recovering lead can not be determined. On a percent basis, approximately 90% of the total lead reported in these soils was unrecovered. The data indicate the possibility that lead, similar to copper, exists as a precipitate on solid surfaces or is partly occluded in the crystal structure of secondary minerals. Based on these findings and data from sorption-desorption experiments conducted using specimen materials (section 5.2.4), it appears 0.03M $La(NO_3)_3$ is unable to extract sorbed or complexed lead and has no greater selectivity for lead than NH_4Cl-DIW-KNO_3.

Zinc

Trends in the recovery of zinc are very similar to those described for the extraction of lead. There is a significant impact on the recovery of zinc using the HSS versus the VES. The HSS recovered 4-23X more zinc than the VES. In 2000, 0.05M $Pb(NO_3)_2$ recovered significantly more zinc than 0.03M $La(NO_3)_3$ and 0.03M $La(NO_3)_3$ recovered significantly more zinc than 0.5M $Ca(NO_3)_2$ in all soils. On a percent basis, zinc recoveries for the different extractants range from 21-37% for 0.05M $Pb(NO_3)_2$, 18-31% for 0.03M $La(NO_3)_3$, and 14-18% for 0.5M $Ca(NO_3)_2$.

Excluding sample 98-3-5-10, 2004 data show completely different results in that NH_4Cl-DIW-KNO_3 recovered more zinc than either 0.03M $La(NO_3)_3$ or 0.05M $Pb(NO_3)_2$. Of the three extractant solutions, $La(NO_3)_3$ extracted the least amount of zinc. In sample 98-3-5-10, 0.05M $Pb(NO_3)_2$ extracted 23% more zinc than NH_4Cl-DIW-KNO_3. On a percent basis, zinc recoveries range from 3.6-18% for NH_4Cl-DIW-KNO_3, 2.7-4.4% for 0.05M $Pb(NO_3)_2$, and <2.1% for 0.03M $La(NO_3)_3$. The reason for the higher zinc recoveries using NH_4Cl-DIW-KNO_3 rather than 0.05M $Pb(NO_3)_2$ is uncertain, but may be associated with the use of DIW during the analyses of cation exchange capacity. The DIW may have increased total zinc recoveries by extracting some additional complexed zinc. However, even subtracting out the zinc recovered during the DIW step in the CEC procedure (Tables 16-19), NH_4Cl-DIW-KNO_3 is as effective as 0.05M $Pb(NO_3)_2$ in three soils and significantly more effective in the fourth soil. The reason for the significant decrease in zinc recovery using 0.03M $La(NO_3)_3$ compared to NH_4Cl-DIW-KNO_3 is unknown.

Summary

The experimental data indicate the physical component of these selective extraction procedures can have a very significant impact on the extraction of certain metals like lead and zinc and essentially no impact on the recoveries of other metals, such as cadmium and copper. The extraction efficiency of 0.03M $La(NO_3)_3$ and 0.05M $Pb(NO_3)_2$ with regards to lead and zinc increased using the HSS.

Based on earlier work by Miller et al (1986), 0.03M $La(NO_3)_3$ was originally selected to recover sorbed and complexed metals in these soils. However, the data show 0.03M $La(NO_3)_3$ acts more like a weak electrolyte solution [i.e. 0.01M $Ca(NO_3)_2$] or as an extractant used in the recovery of exchangeable metals (i.e. NH_4Cl-DIW-KNO_3). This result supports previous conclusions reported by Jarvis (1986), Brookins (1989), and Janssen et al (2003a,b).

The data show also, particularly in the case of lead and zinc, that despite very high total concentrations, only low lead and zinc concentrations are recovered during the selective extraction process. The same general trend is noted for cadmium and copper, which were present in these soils at much lower concentrations than lead and zinc. The cause for this particular result is uncertain, but it may be related to a combination of the inability of the various solutions to fully extract these metals from targeted sorption sites and their existence in these soils as precipitates.

Based on the comparison of 2000 and 2003-2004 data and the reasons stated in the introduction of this section, the VES was selected as the physical extraction component for these procedures. Soluble metal cations were recovered with 0.01M $Ca(NO_3)_2$, while 0.05M $Pb(NO_3)_2$ was used to recover sorbed and complexed cadmium, copper, and zinc. No comparison of predicted sorbed and complexed lead with experimental lead data can be made due to the fact that 0.03M $La(NO_3)_3$ was unable to extract sorbed and complexed lead from these soils. Due to the unexpected high zinc recoveries using NH_4Cl-DIW-KNO_3 in 2004, 0.03M $La(NO_3)_3$ was selected to recover exchangeable metals in these soils.

5.2 Laboratory Methods – Specimen Materials

The objective of the adsorption/desorption experiments conducted on specimen materials (kaolinite, Pahokee peat, and synthetic iron oxide) was to calculate selectivity coefficients and sorption and complexation constants. The specimen materials and their associated binding constants were to be used to predict the partitioning of cadmium, copper, lead, and zinc in various soil solid fractions. One set of adsorption/desorption experiments were conducted in a single-metal system which involved the addition of one metal (i.e., cadmium, copper, lead, or zinc) at a concentration of approximately 4.8 umol g^{-1} of oven-dried specimen material. The second set of experiments were conducted in a multi-metal system which involved the addition of all four metals under the same experimental conditions as the single-metal experiments.

Values for Vanselow selectivity coefficients [Eq. 6 and 7] and sorption constants [Eq. 12 and 13] were calculated for both metal systems involving kaolinite. However, constant values could not be calculated for peat or FeOOH specimen materials. The sorptive capacities of peat and FeOOH exceeded the amount of each metal added individually or in combination thus, preventing the ability to calculate constant values.

As a result, the selectivity coefficients and sorption constants calculated for kaolinite (Tables 2 and 3) were used in the modeling portion of this research, while the sorption constants listed for FeOOH (Table 9) and the complexation constants listed for organic materials (Table 11) were obtained from the literature. The selectivity coefficients and sorption constants listed for illite (Table 5) and montmorillonite (Table 7) were also obtained from the literature. The one benefit of the adsorption/desorption experiments was the qualitative determination of the selectivity and extraction efficiency of the two solutions used, 1.0M KNO_3 and 0.03M $La(NO_3)_3$-0.01M $Ca(NO_3)_2$.

5.2.1 Kaolinite

The amount of each metal bound to kaolinite is reported as a percent of the total amount of each metal added. Sorption percentages ranged from 3.4 to 3.1% for cadmium (Figures 3 and 4), 13 to 11% for copper (Figures 5 and 6), 27 to 17% for lead (Figures 7 and 8), and 5.6 to 5.7% for zinc (Figures 9 and 10). The low sorption percentages reported indicate the amount of metals added exceed the sorptive capacity of kaolinite.

Figure 3. Kaolinite system with cadmium [cadmium sorption/desorption]

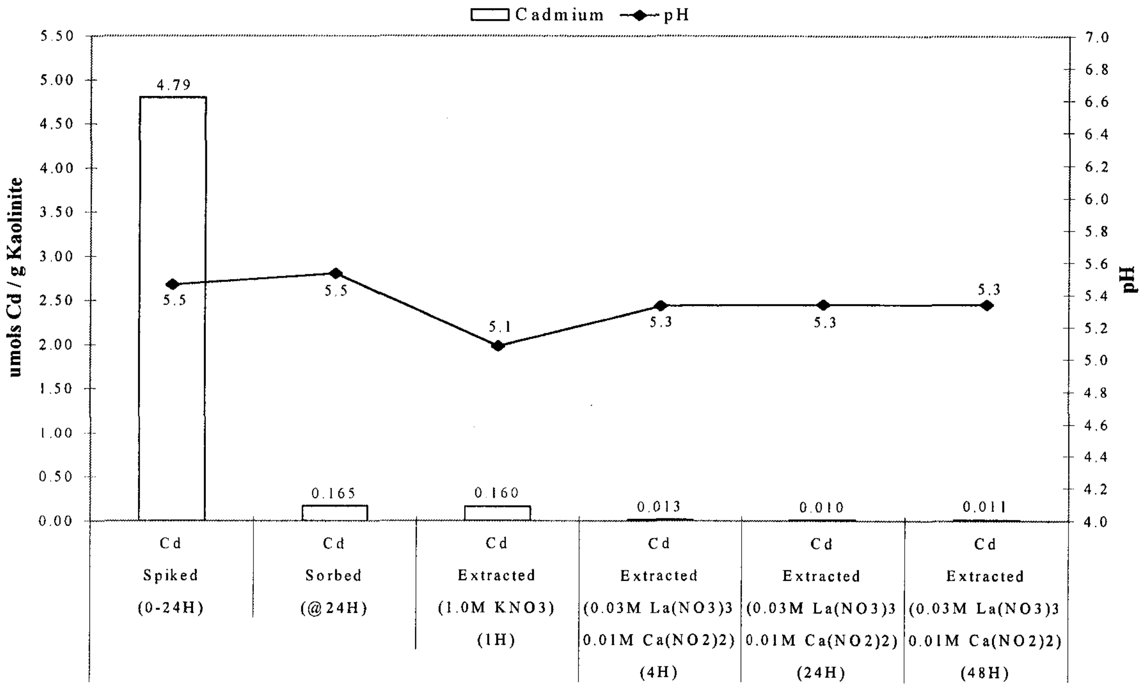

Figure 4. Kaolinite system with cadmium, copper, lead, and zinc [cadmium sorption/desorption]

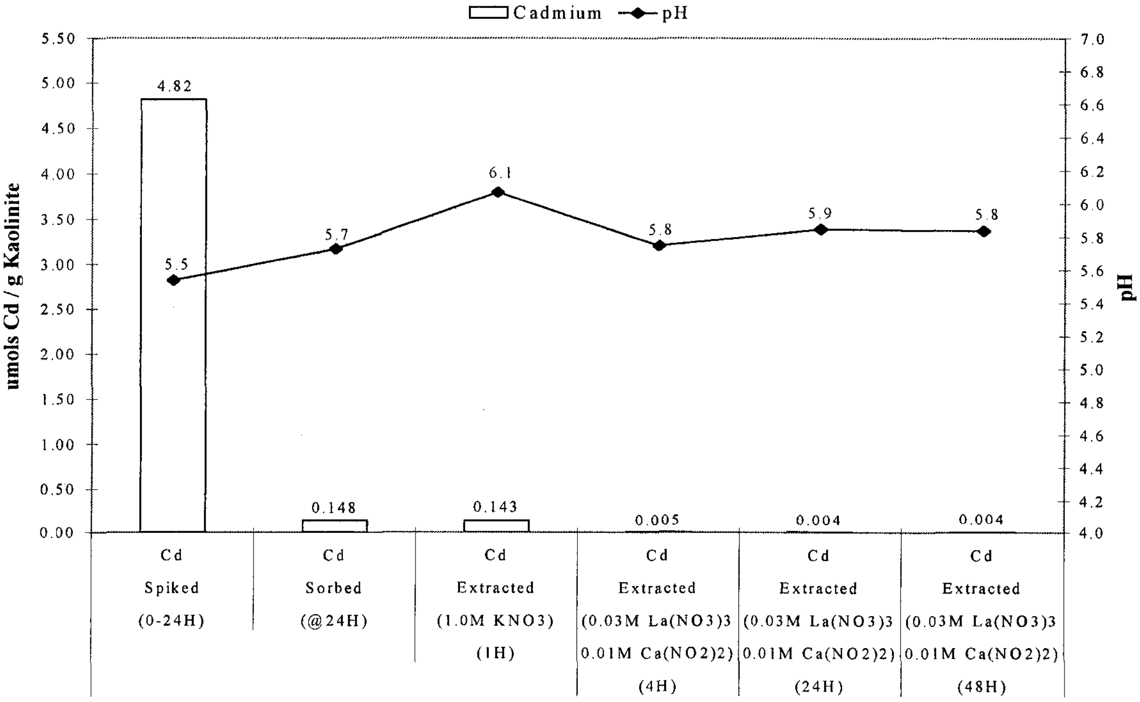

Figure 5. Kaolinite system with copper [copper sorption/desorption]

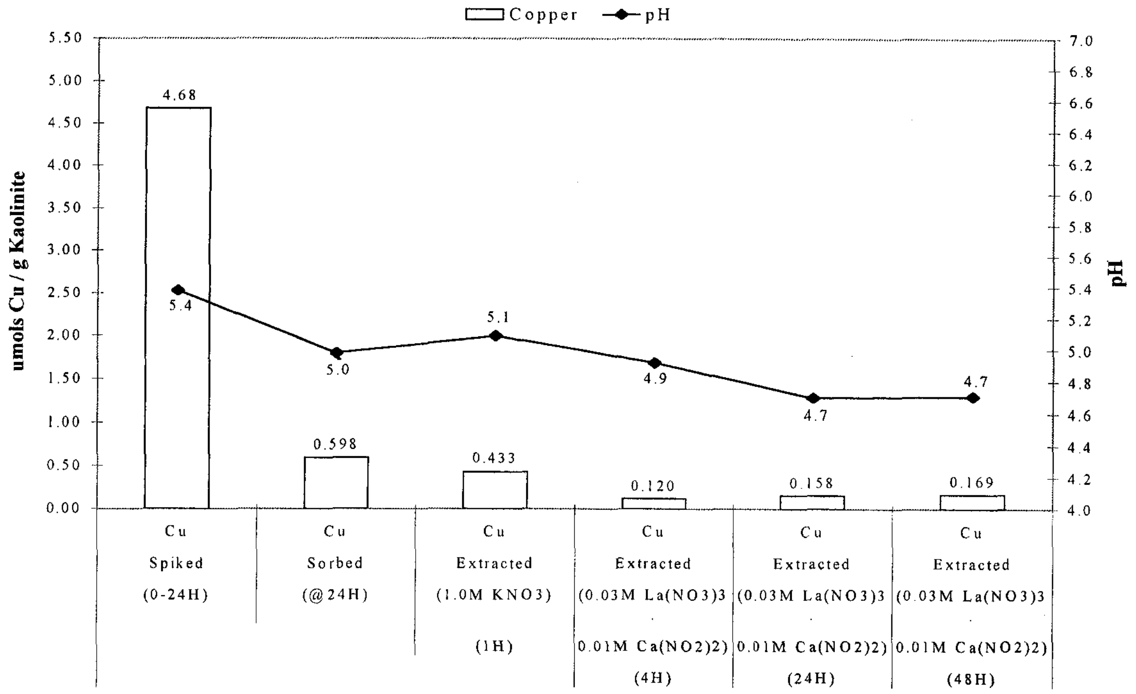

Figure 6. Kaolinite system with cadmium, copper, lead, and zinc [copper sorption/desorption]

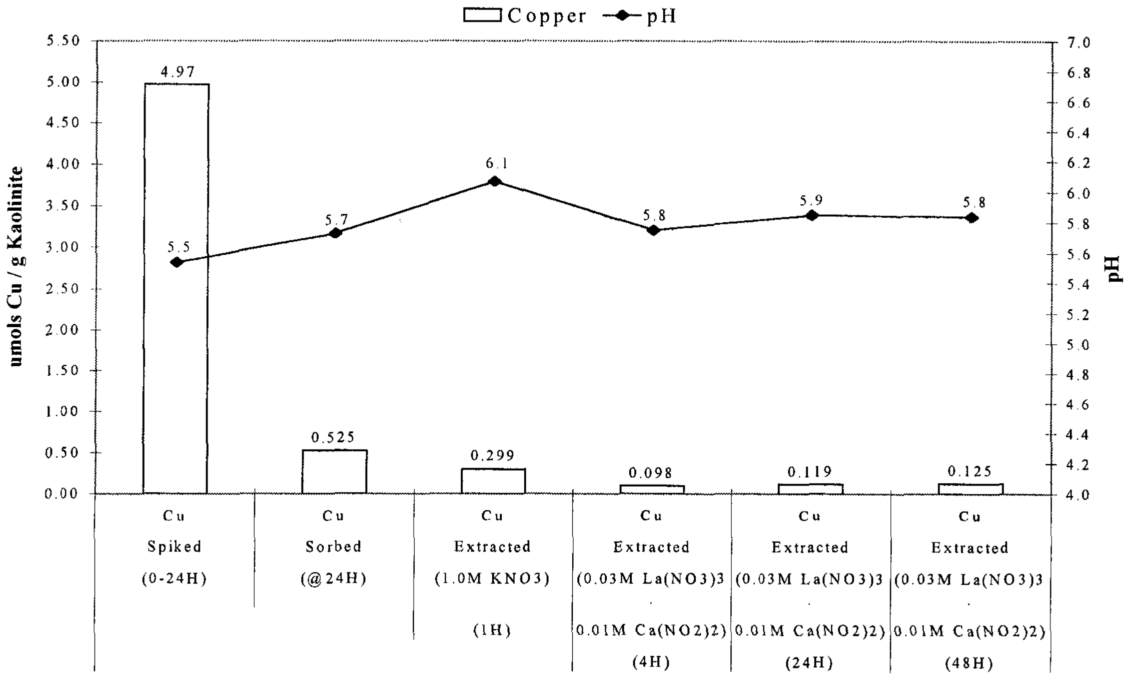

Figure 7. Kaolinite system with lead [lead sorption/desorption]

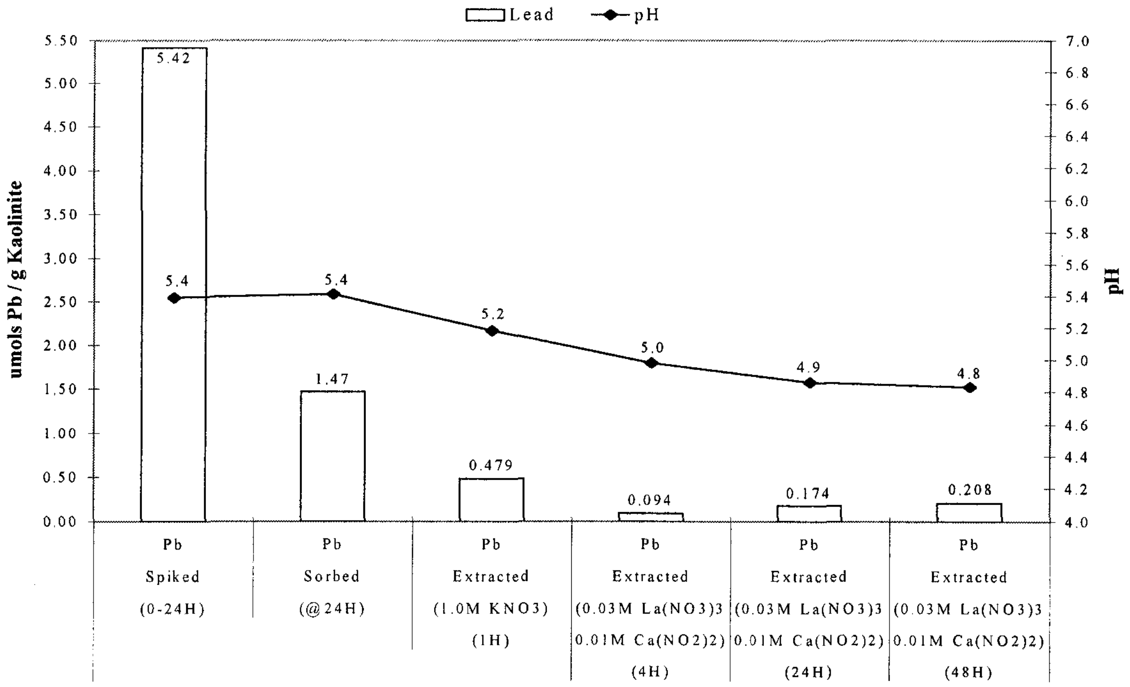

Figure 8. Kaolinite system with cadmium, copper, lead, and zinc [lead sorption/desorption]

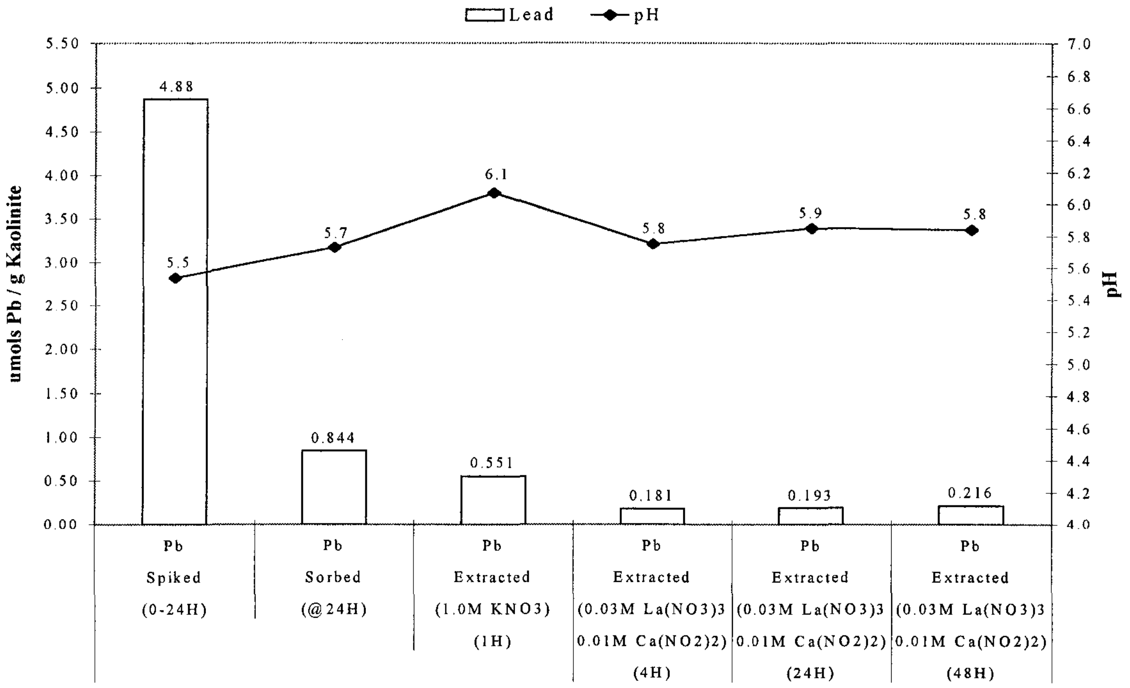

Figure 9. Kaolinite system with zinc [zinc sorption/desorption]

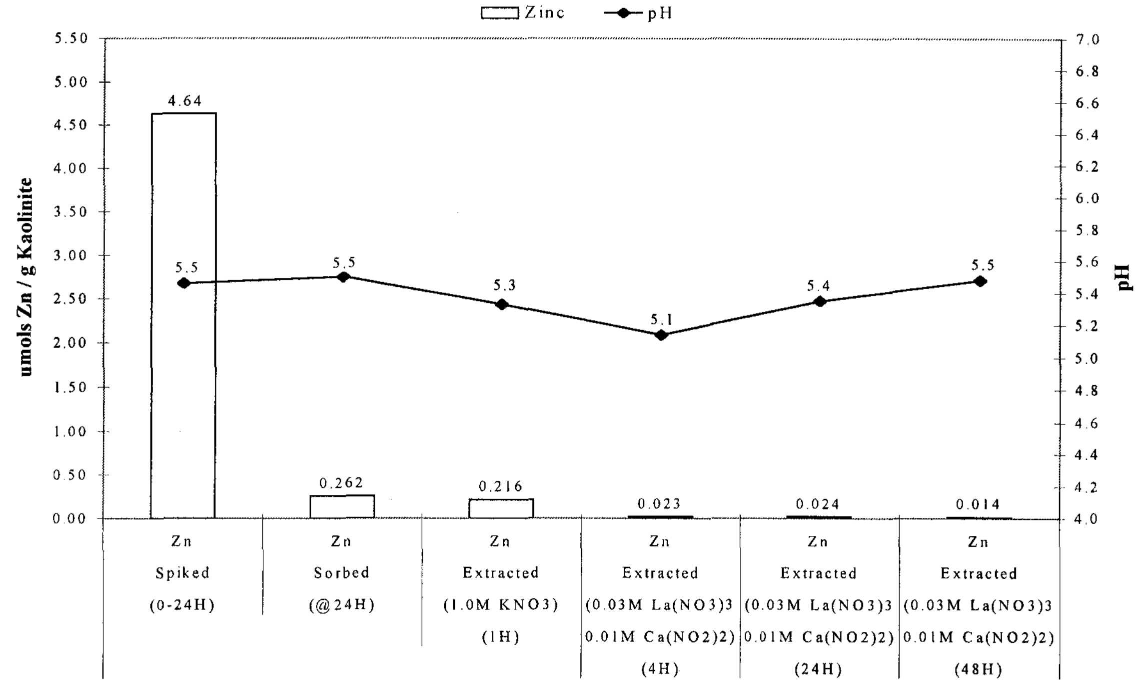

Figure 10. Kaolinite system with cadmium, copper, lead, and zinc [zinc sorption/desorption]

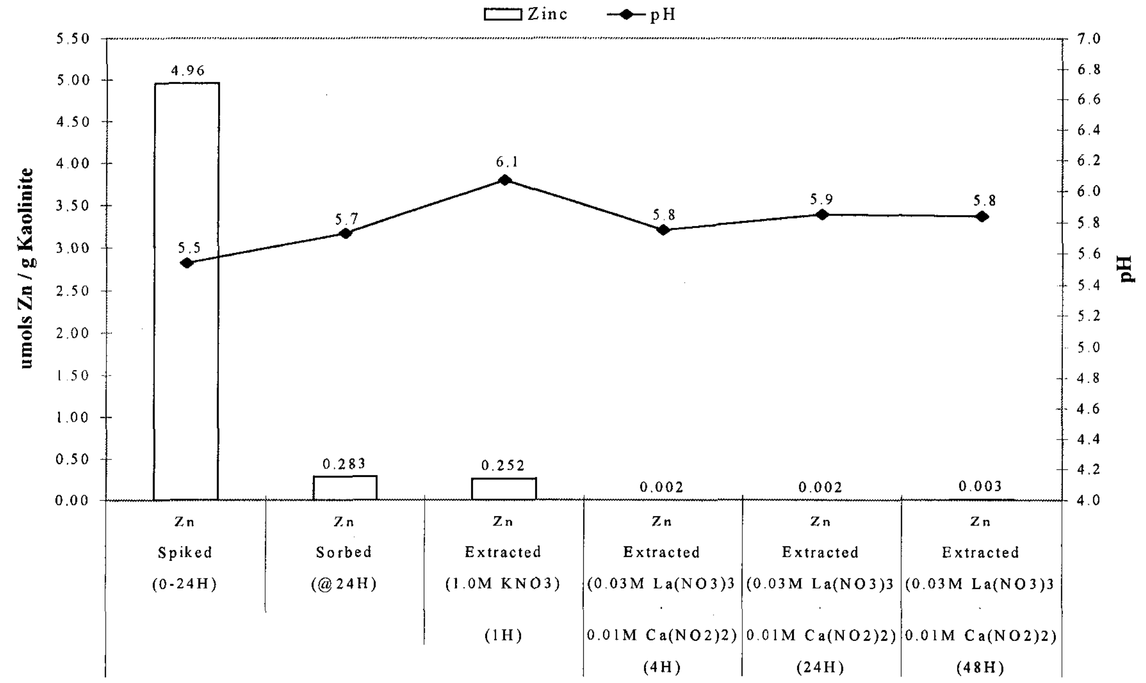

Of interest is the finding that the amount of lead bound to kaolinite decreased 43% between the two systems, while copper decreased 12%, cadmium decreased 10%, and zinc increased 17%. Some portion of the cadmium decrease and zinc increase was the influence of measurement variation at the low metals concentrations reported. The result is unexpected because lead is more strongly bound to kaolinite than the other three metals. A smaller decrease in bound lead and larger decreases in bound cadmium, copper, and zinc would have been expected in the multi-metal system. Based on total lead recoveries reported for the single-metal (47%) and multi-metal (91%) systems, it is possible the reported amount of lead bound to kaolinite in the single-metal system included the formation of inner-sphere complexes or surface precipitates, which were not recoverable. The competitive sorption of four metals in the multi-metal system may have inhibited the formation of lead complexes or surface precipitates.

The extraction of metals by 1.0M KNO_3, which includes soluble and exchangeable metals (i.e. exchangeable metals), is reported as a percent of the total amount of each metal bound to kaolinite. The percent recovery of exchangeable metals in the single-metal system versus the multi-metal system remained the same for cadmium (97%), decreased for copper (72 to 57%), increased for lead (33 to 65%), and increased slightly for zinc (82 to 89%). The 32% increase in exchangeable lead is a combination of the 43% decrease in the total amount of lead bound to kaolinite and a 15% increase in exchangeable lead. The percentages reported for the other three metals are also a combination of decreases in the total amount of metal bound to kaolinite, measurement variation, and decreases/increases in exchangeable metals. However, the data show that lead is a better competitor for available exchange sites than the other three metals in the multi-metals system.

The extraction of metals with 0.03M $La(NO_3)_3$-0.01M $Ca(NO_3)_2$, defined as sorbed metals, is reported as a percent of the total amount of each metal bound to kaolinite. The percent recovery of sorbed metals in the single-metal system versus the multi-metal system decreased for cadmium from 7.9 to 3.4%, decreased for copper from 28 to 24%, increased for lead from 14 to 26%, and decreased for zinc from 9.2 to 1.1%. The 12% increase in sorbed lead is a combination of the 43% decrease in the total amount of lead bound to kaolinite, a 7.7% increase in sorbed lead, and measurement variation at low concentrations. The data show lead is a better competitor than the other three metals in the multi-metal system for available binding sites.

Based on the combined amount of metals extracted by KNO_3 and $La(NO_3)_3$, total recoveries in both systems were calculated. Total recoveries are reported as a percent of the total amount of each metal bound to kaolinite in the single-metal system and the multi-metal system. The recoveries ranged from 105 to 100% for cadmium, 101 to 80.8% for copper, 46.7 to 90.9% for lead, and 91.6 to 90.1% for zinc. Cadmium, which has the lowest affinity of the four metals for kaolinite, shows the smallest amount sorbed and the highest total recovery in both systems. Zinc, which has a stronger affinity for kaolinite than cadmium but less than copper or lead, shows the second smallest amount sorbed and the second highest total recovery in both systems. Copper, which is more strongly bound to kaolinite than cadmium and zinc but less than lead, shows the second highest amount sorbed and the third highest total recovery in both systems. Lead exhibits the greatest affinity for kaolinite based on comparison of sorption and recovery percentages reported for the other three metals. The increase in total lead recovery reported for the multi-metal system is skewed by the 43% decrease in total lead bound to kaolinite.

In the single- and multi-metal systems, the pHs of the kaolinite-cadmium and kaolinite-zinc experiments remained approximately constant during the sorption and extraction phases of the experiment. The absence of any pH change and the almost complete recovery of all cadmium and zinc by KNO_3 in both metal systems confirm the conclusion that cadmium and zinc are present either in the diffuse layer as charge screening cations or bound as easily extractable outer-sphere complexes. For the kaolinite–copper and kaolinite–lead experiments associated with the single-metal system, the pHs remained essentially constant during the KNO_3 extraction step, but decreased approximately 0.7 pH units during the $La(NO_3)_3$ extraction step. The decreases in pH indicate protons were being released during the extraction step and may have been the result of lanthanum cations binding to sites containing protons (e.g. $SOH + La^{+3} \rightarrow SO\text{-}La^{+2} + H^{+}$). For unknown reasons, no decrease in pH was detected during the $La(NO_3)_3$ extraction step in the multi-metals system.

The increase in copper and lead recovery over 48 hours by $La(NO_3)_3$ indicates $La(NO_3)_3$ is able to partially extract the more tightly bound metals. Given enough time, it is unknown if $La(NO_3)_3$ would have been able to recover all remaining bound lead and copper. This is contrary to section 5.1.6 conclusions which indicated $La(NO_3)_3$ acts more like a weak electrolyte.

5.2.2 Iron Oxide (FeOOH)

Except for zinc, the sorptive capacity of synthetic FeOOH exceeded the amount of each metal added in the single-metal system which resulted in the complete sorption of cadmium, copper, and lead (Figures 11, 13, and 15). Zinc sorption was approximately 91% of the total amount of zinc added (Figure 17). In the multi-metal system, cadmium sorption decreased to 46% (Figure 12), copper decreased to 56% (Figure 14), and zinc decreased to 48% (Figure 18). Essentially all lead added to the multi-metal system was bound to FeOOH (Figure 16). The data suggest lead, which has the strongest affinity for FeOOH of the four metals, depresses the sorption of cadmium, copper, and zinc.

The extraction of bound cadmium, copper, lead, and zinc by 1.0M KNO_3 in both systems ranged from 2.41 to 22.7% for cadmium, 0.0 to 0.15% for copper, 0.0 to 0.13% for lead, and 0.55 to 1.33% for zinc with the higher recoveries reported for the multi-metal system. With the exception of cadmium, KNO_3 is unable to extract or exchange with bound copper, lead, and zinc. The data show cadmium, which is the least tightly bound of the four metals, is associated primarily with weak sorption sites as previously described by Dzombak and Morel (1990).

The reason for the significant increase in pH by 0.6 to 1.3 pH units during the 1.0M KNO_3 extraction step is uncertain, but is related to the addition of 1.0M KNO_3. The increase in ionic strength during the 1.0M KNO_3 step decreased the diffuse layer thickness surrounding the colloidal FeOOH particles, which resulted in the closer approach of soluble cations to the FeOOH surface. Protons, which bind more strongly to FeOOH than the other soluble cations present, may have been able to overcome

Figure 11. FeOOH system with cadmium [cadmium sorption/desorption]

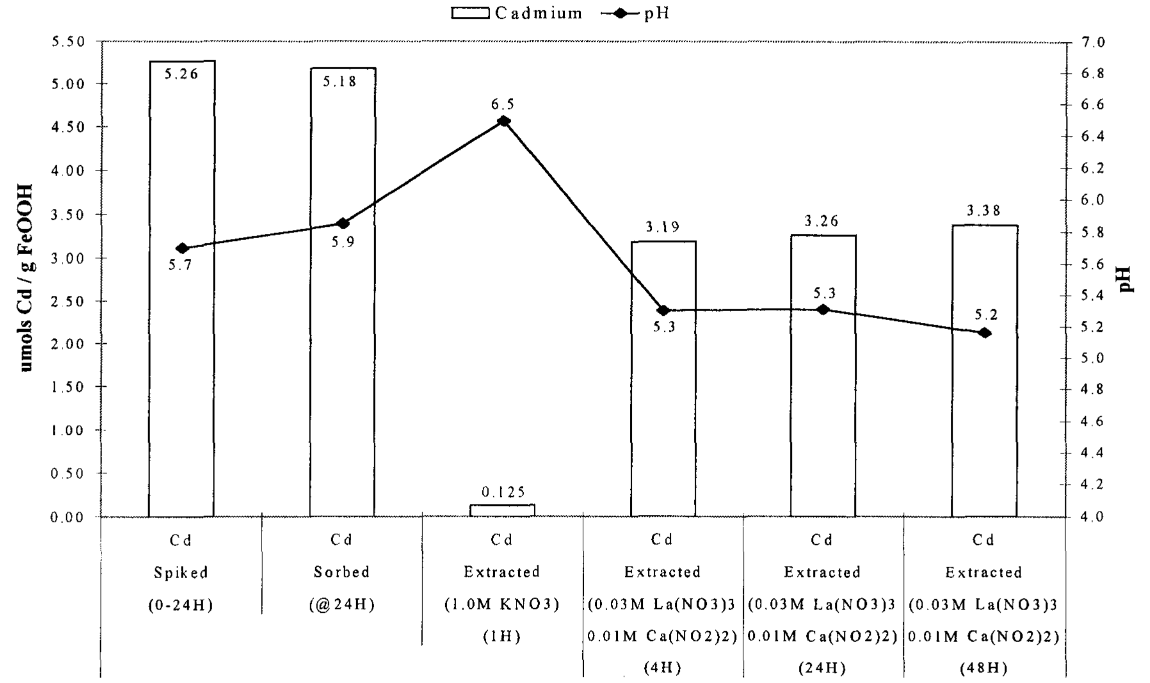

Figure 12. FeOOH system with cadmium, copper, lead, and zinc [cadmium sorption/desorption]

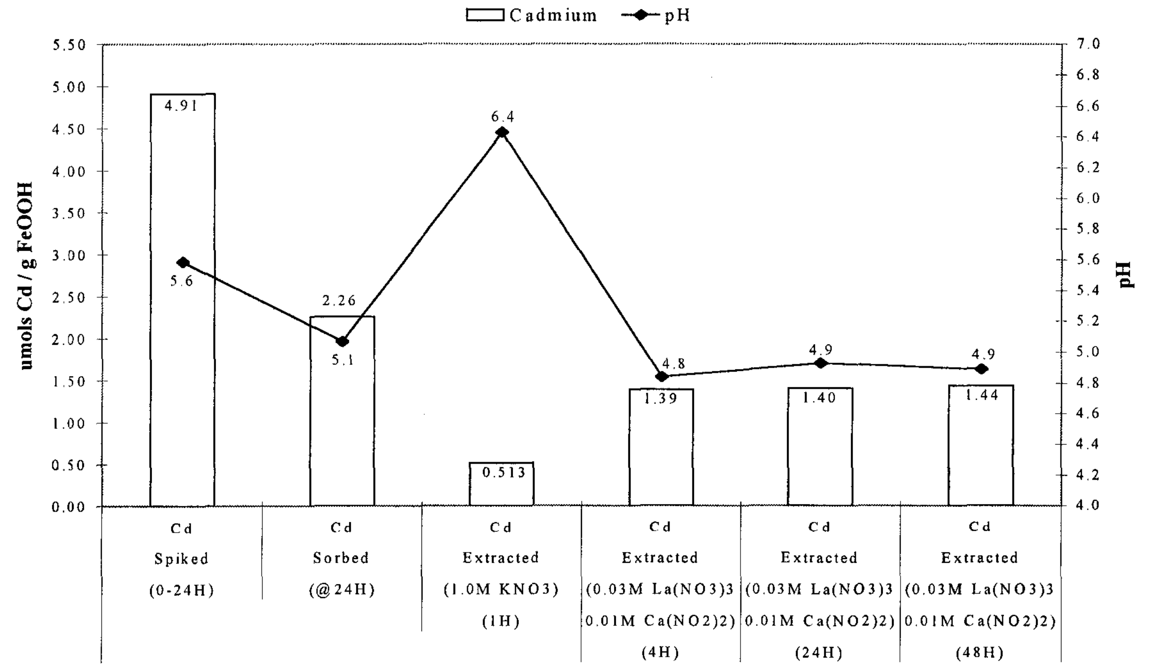

Figure 13. FeOOH system with copper [copper sorption/desorption]

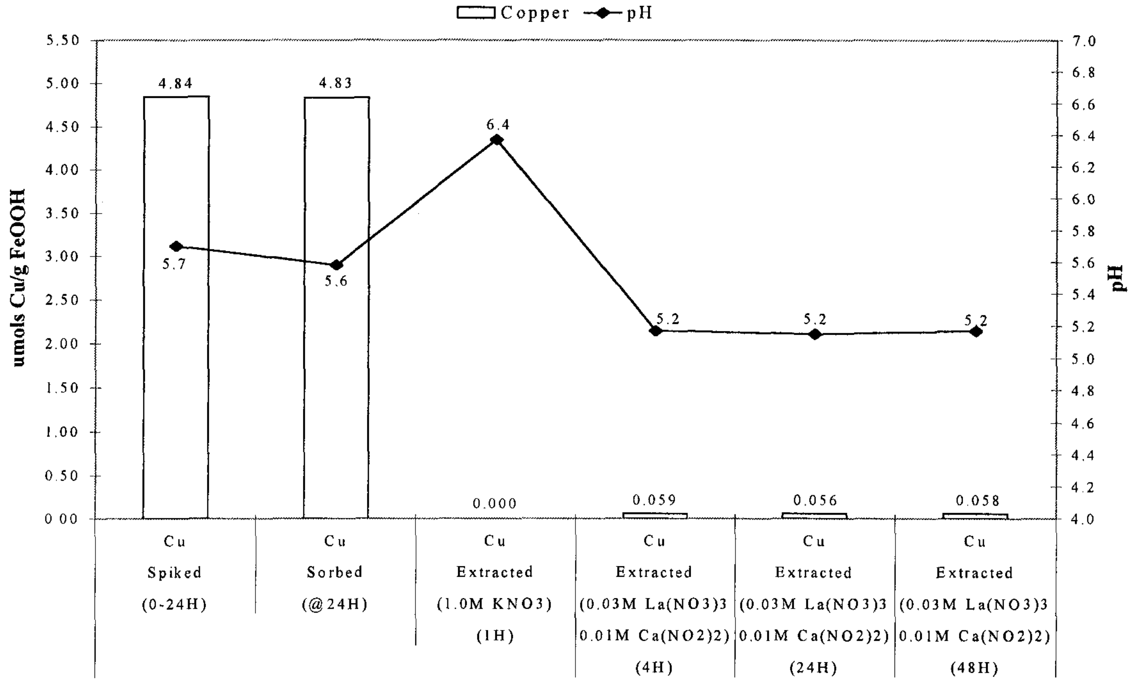

Figure 14. FeOOH system with cadmium, copper, lead, and zinc [copper sorption/desorption]

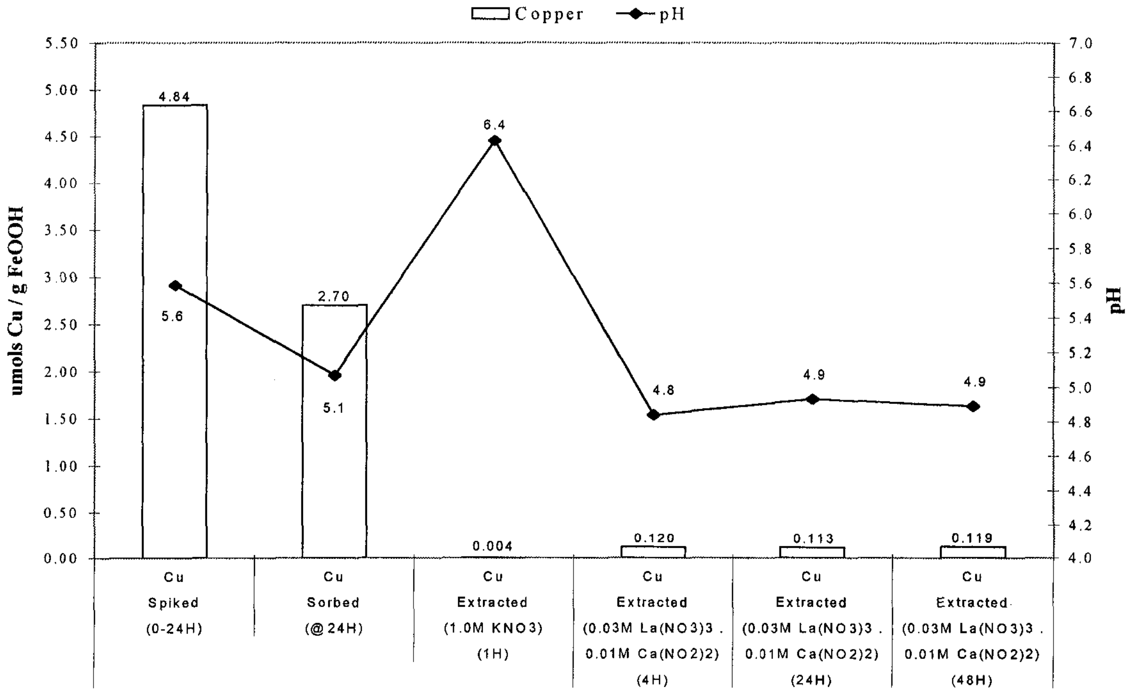

Figure 15. FeOOH system with lead [lead sorption/desorption]

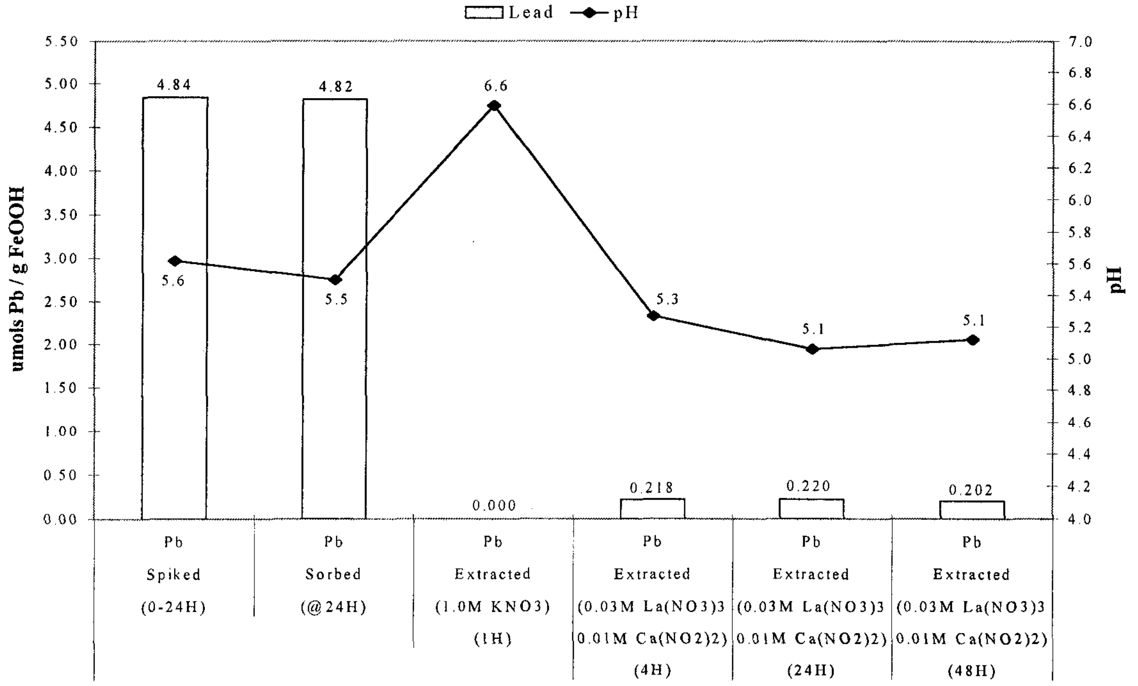

Figure 16. FeOOH system with cadmium, copper, lead, and zinc [lead sorption/desorption]

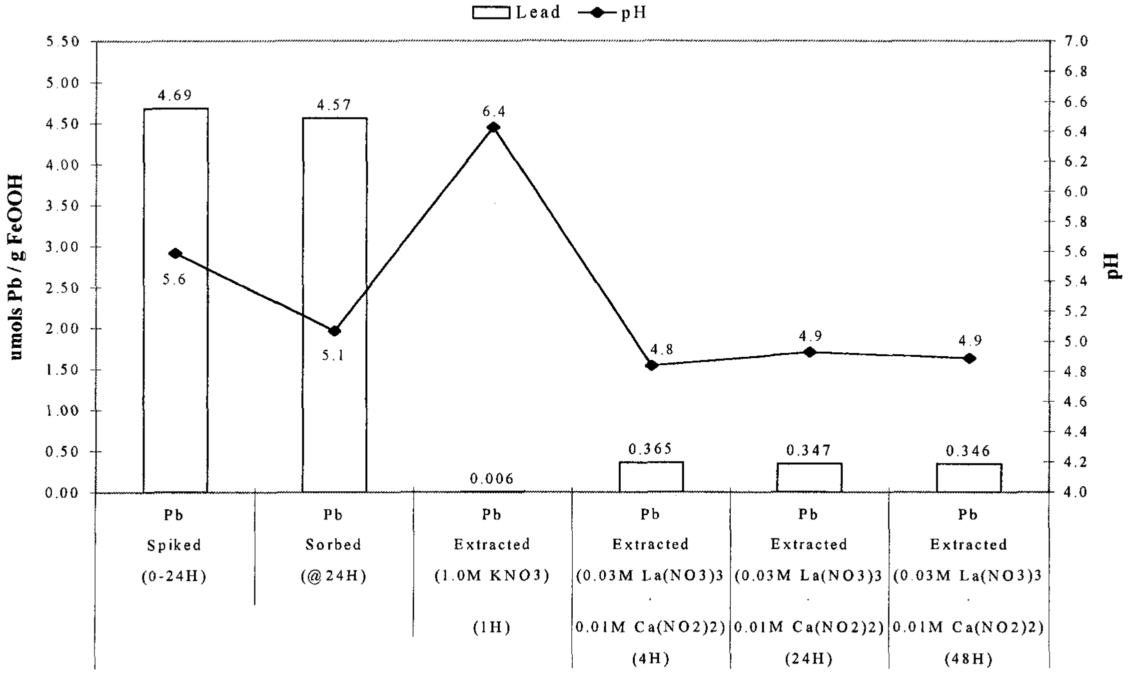

Figure 17. FeOOH system with zinc [zinc sorption/desorption]

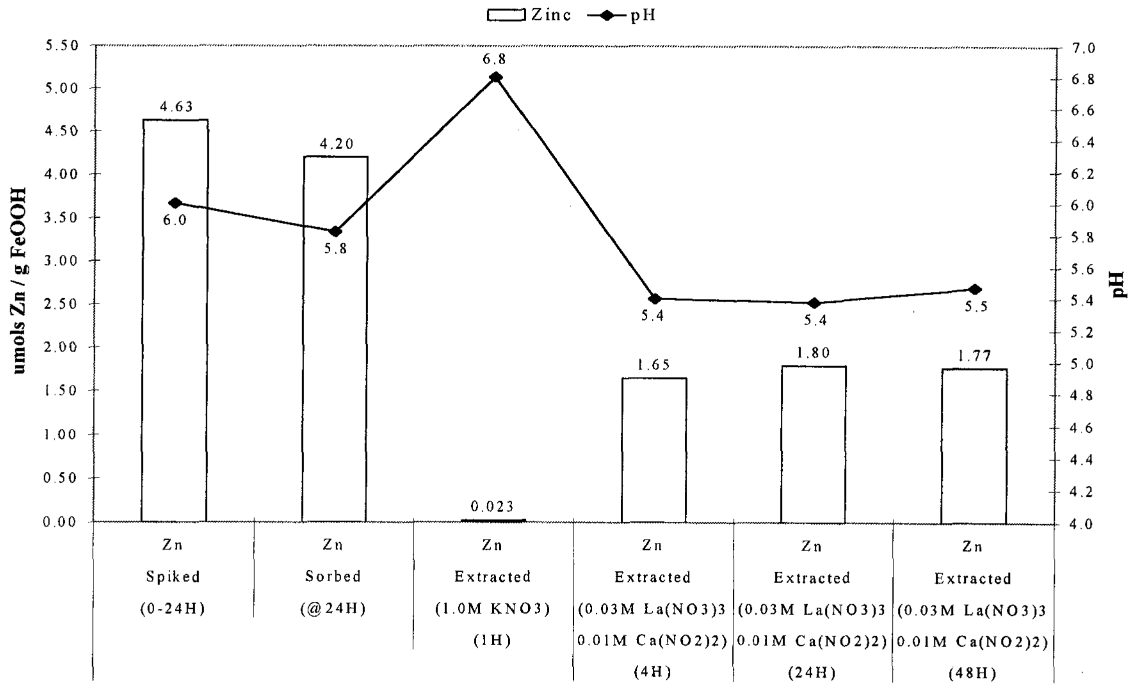

Figure 18. FeOOH system with cadmium, copper, lead, and zinc [zinc sorption/desorption]

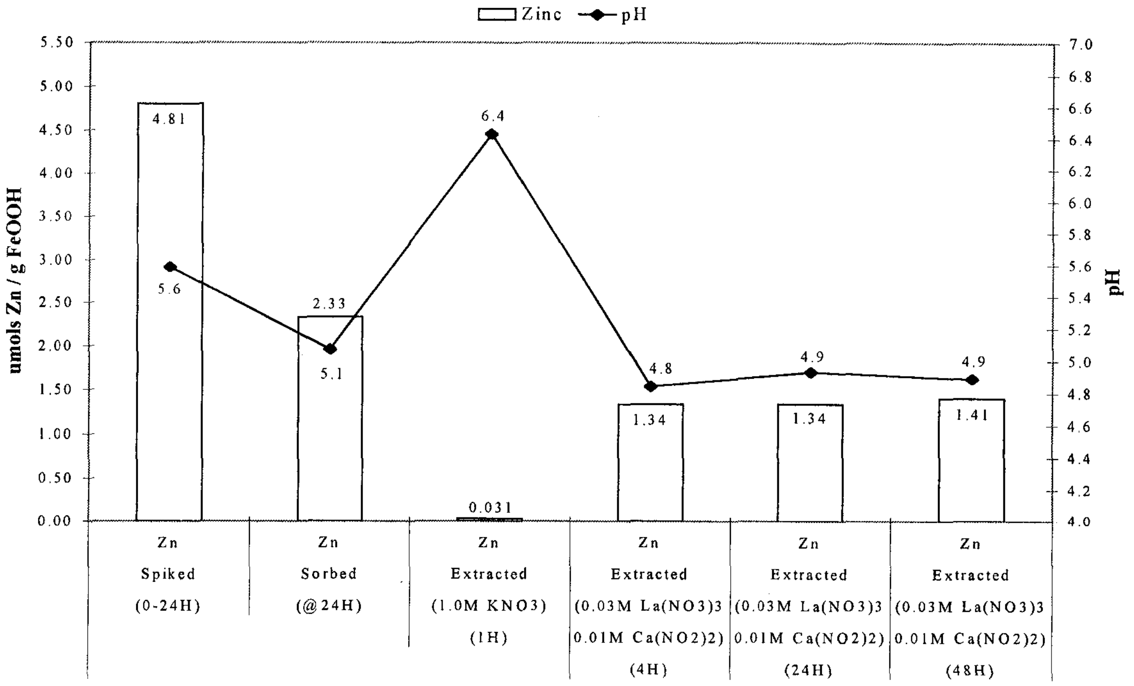

electrostatic repulsion from the mostly positive surface and bind to available SO- and SOH sites (e.g. SO- + H^+ → SOH; SOH + H^+ → SOH_2^+). The increased sorption of protons decreased the concentration of protons in solution, which resulted in a higher pH.

Extraction of metals by 0.03M $La(NO_3)_3$ in the single-metal system versus the multi-metal system ranged from 65 to 64% for cadmium, 1.2 to 1.4% for copper, 4.6 to 8.0% for lead, and 43 to 61% for zinc. The similarity in the reported recoveries between the two systems for cadmium and copper are the result of the decrease in percent of the total amount of cadmium and copper sorbed matching the decrease in percent of lanthanum-extractable cadmium and copper. The increase in recovery reported for zinc in the multi-metal system is the result of the decrease in percent of the total amount of zinc sorbed being greater than the decrease in percent of lanthanum-extractable zinc. The slight increase in the reported lead recovery for the multi-metal system is the result of a slight increase in the amount of lanthanum-extractable lead.

During the $La(NO_3)_3$ extraction step, the pHs of the single-metal systems decreased by 0.4 to 0.6 pH units, while in the multi-metal system the pH decreased 0.7 pH units. The decrease in pHs of both systems may be indicative of proton release during the sorption of lanthanum cations to available SOH sites.

The total percent recovery of each metal in the single-metal system versus the multi-metal system ranged from 68 to 86% for cadmium, 1.2 to 4.6% for copper, 4.6 to 8.1% for lead, and 44 to 62% for zinc. The increase in reported recoveries for the multi-metal system is related to the percent decreases in the total amount of metals sorbed being greater than the percent decreases reported for lanthanum-extractable metals.

The experimental data generally confirm FeOOH-metal affinity sequences reported by Dzombak and Morel (1990). Those affinity sequences, which are based on surface complexation constants, are $Pb^{+2} > Cu^{+2} > Zn^{+2} > Cd^{+2}$ for strong sites and $Cu^{+2} > Pb^{+2} > Zn^{+2} > Cd^{+2}$ for weak sites (Dzombak and Morel, 1990).

5.2.3 Pahokee Peat

Because the sorptive capacity of Pahokee peat exceeded the amount of any metal added in either the single-metal or multi-metal systems (Figures 19-26), complexation constants could not be calculated.

Regardless of which system or metal, less than 1.5% of any metal complexed by peat was recovered by 1.0M KNO_3. Based on the very low recovery of metals and the absence of any pH change during the KNO_3 extraction step, potassium was not able to extract or exchange with complexed cadmium, copper, hydrogen, lead, or zinc.

The 0.03M $La(NO_3)_3$ solution extracted significantly more cadmium (42%) and zinc (56%) than copper (0.5%) or lead (0%) in the single-metal system. The percent recovery of all four metals by 0.03M $La(NO_3)_3$ in the multi-metal system increased to 46% for cadmium, 0.8% for copper, 2.8% for lead, and 66% for zinc. The data show that with respect to the use of $La(NO_3)_3$ as an extractant solution, copper and lead are more strongly complexed to peat than cadmium or zinc and copper has a slightly greater affinity for peat than lead in the multi-metal system.

Figure 19. Peat system with cadmium [cadmium sorption/desorption]

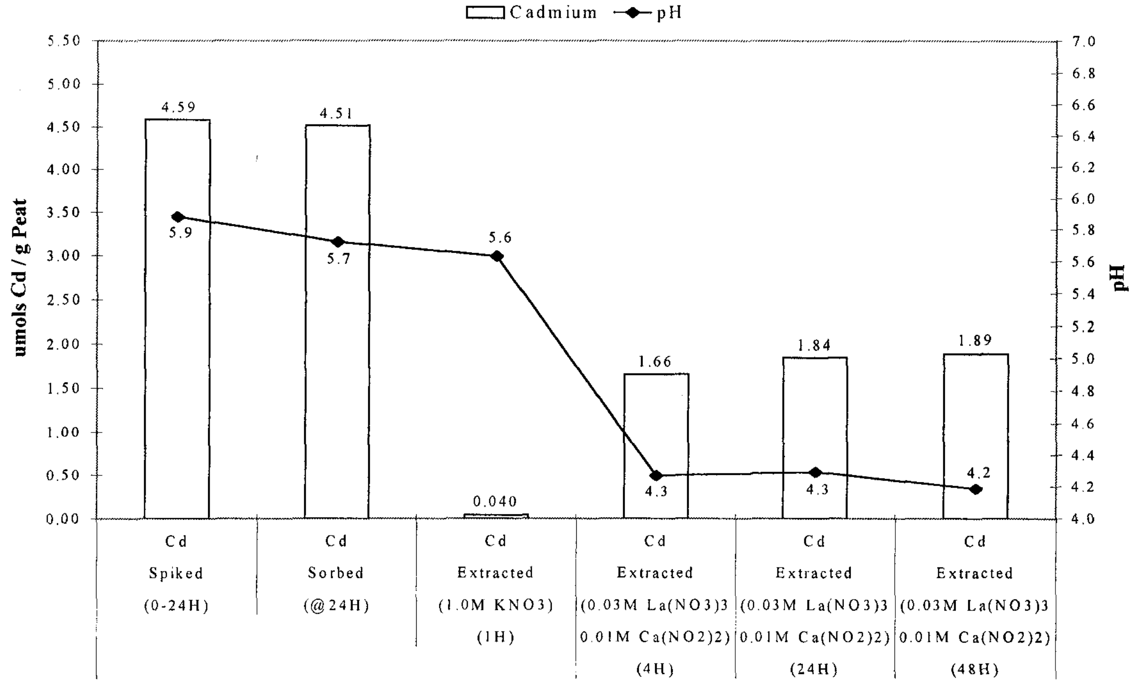

Figure 20. Peat system with cadmium, copper, lead, and zinc [cadmium sorption/desorption]

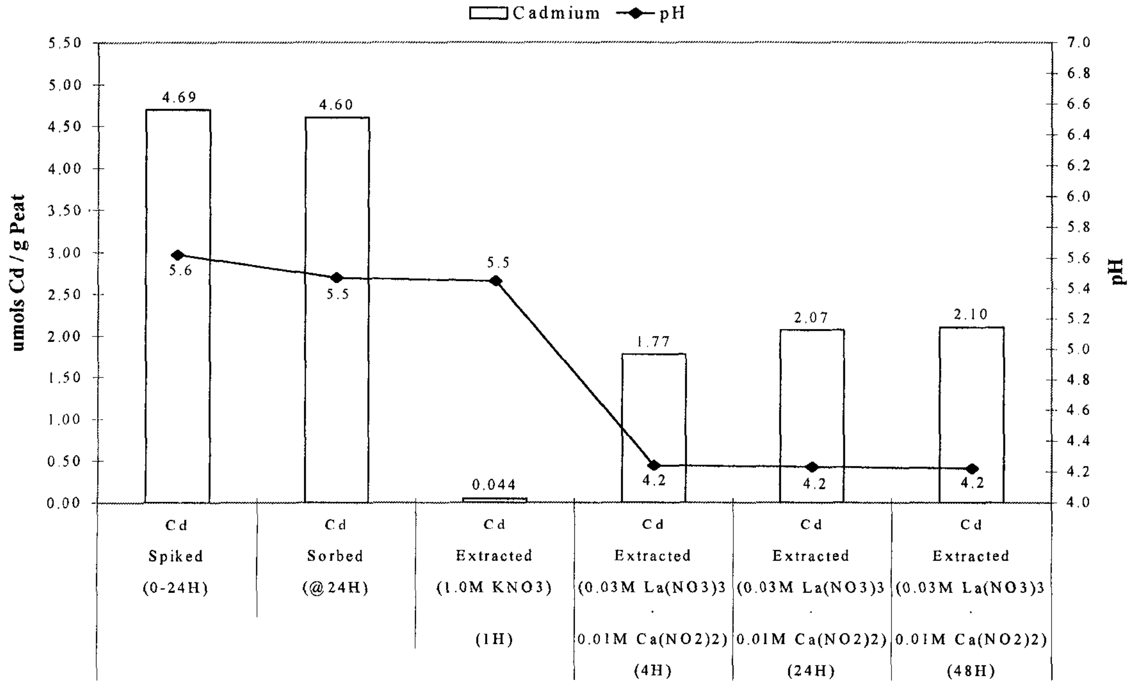

Figure 21. Peat system with copper [copper sorption/desorption]

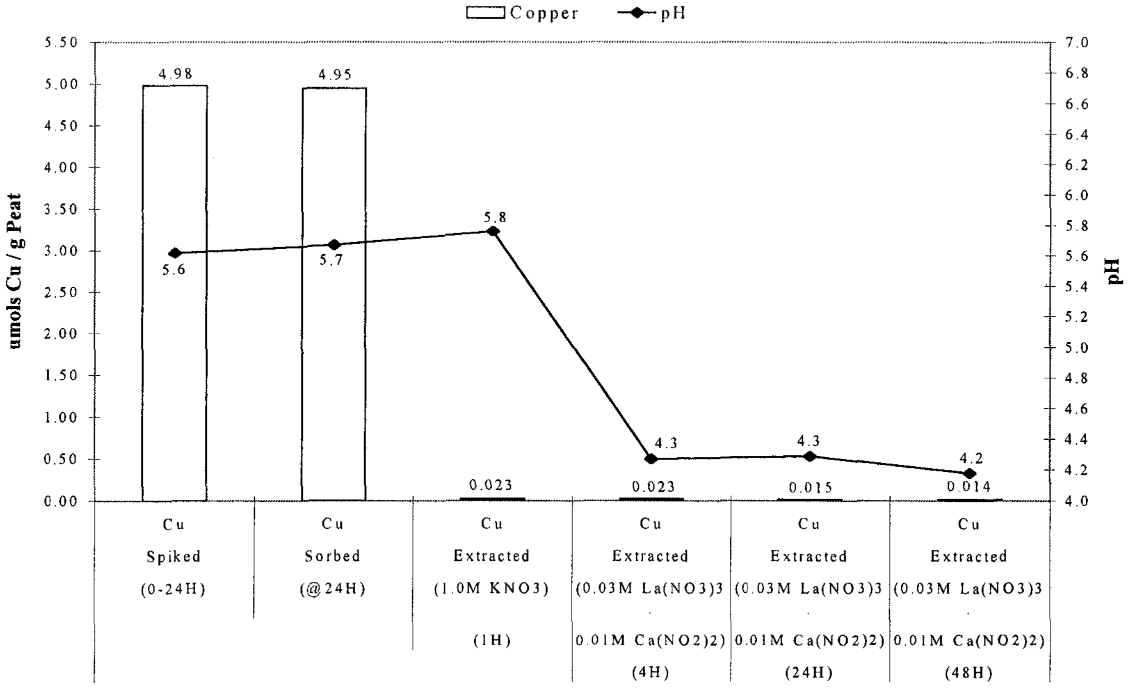

Figure 22. Peat system with cadmium, copper, lead, and zinc [copper sorption/desorption]

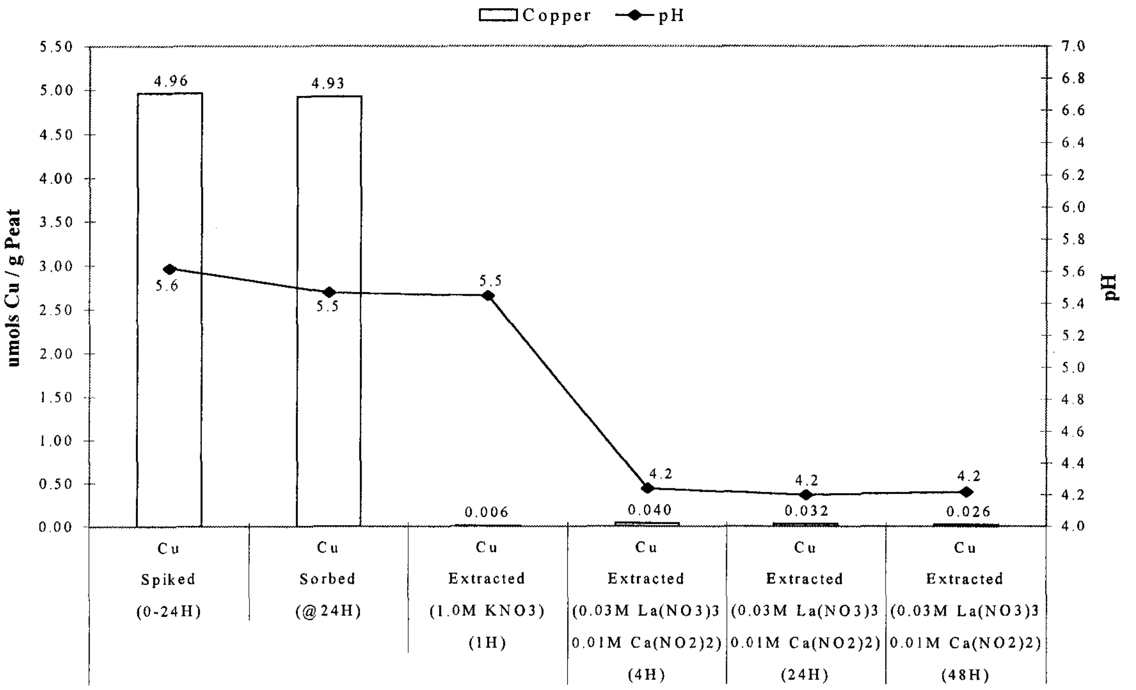

Figure 23. Peat system with lead [lead sorption/desorption]

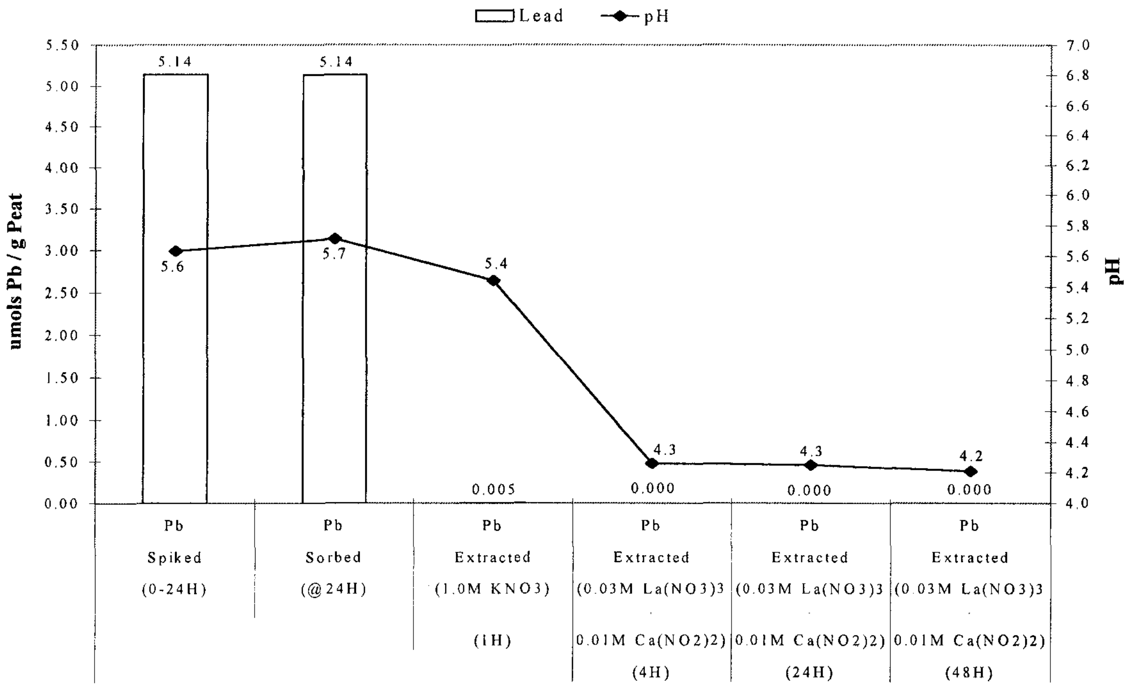

Figure 24. Peat system with cadmium, copper, lead, and zinc [lead sorption/desorption]

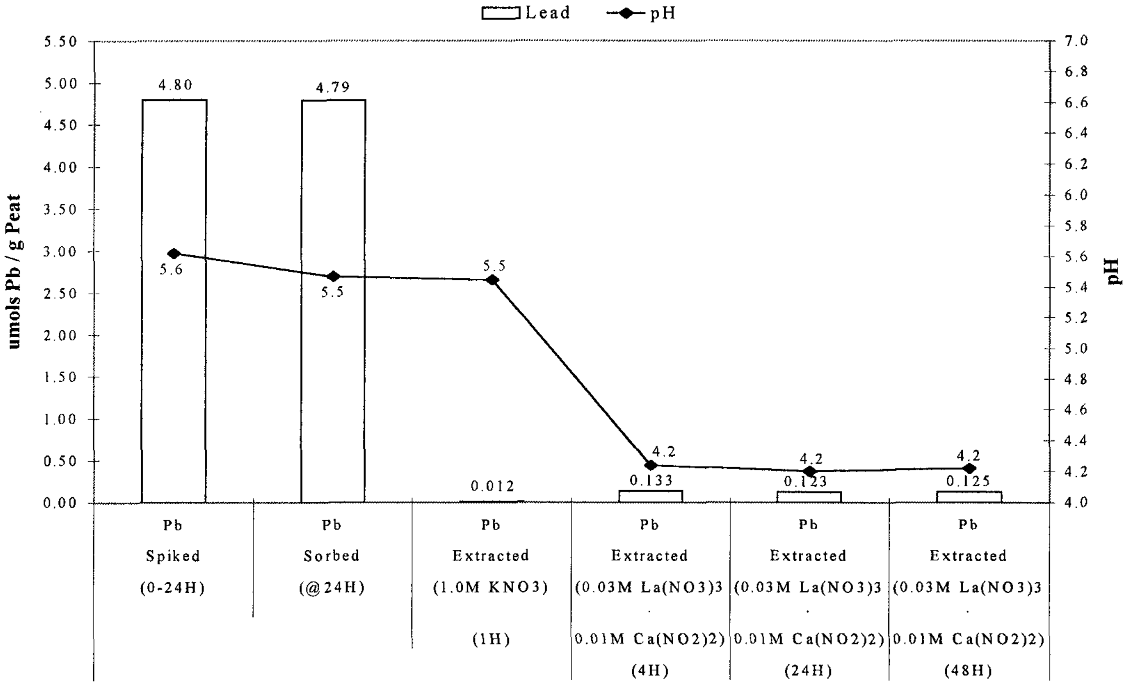

Figure 25. Peat system with zinc [zinc sorption/desorption]

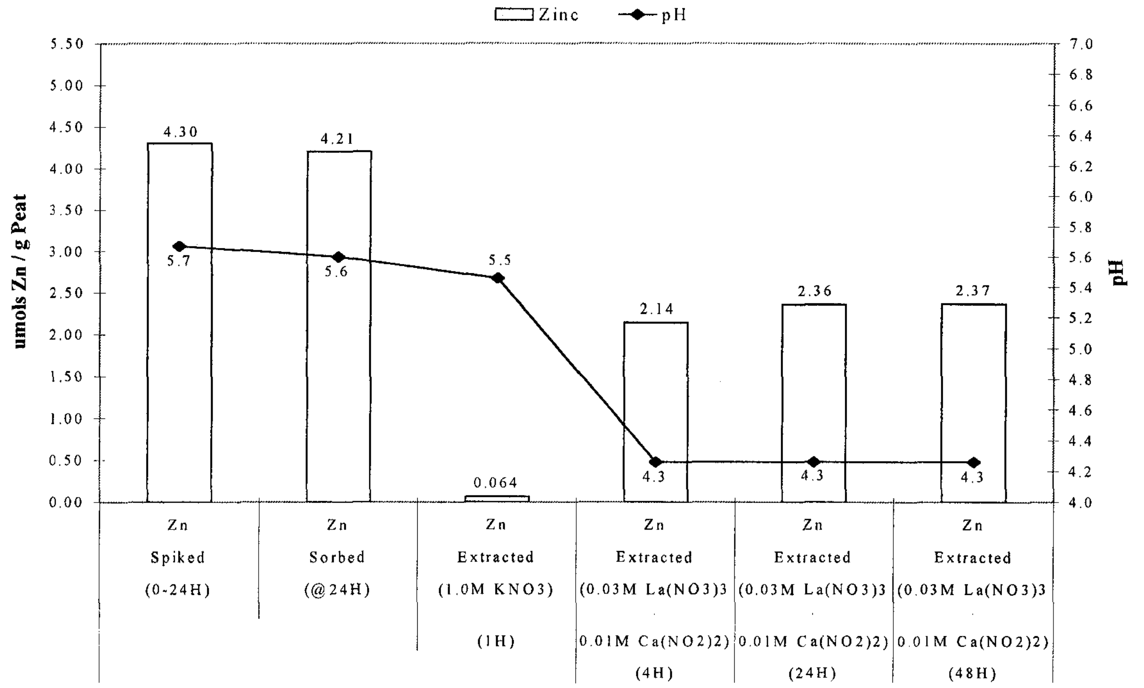

Figure 26. Peat system with cadmium, copper, lead, and zinc [zinc sorption/desorption]

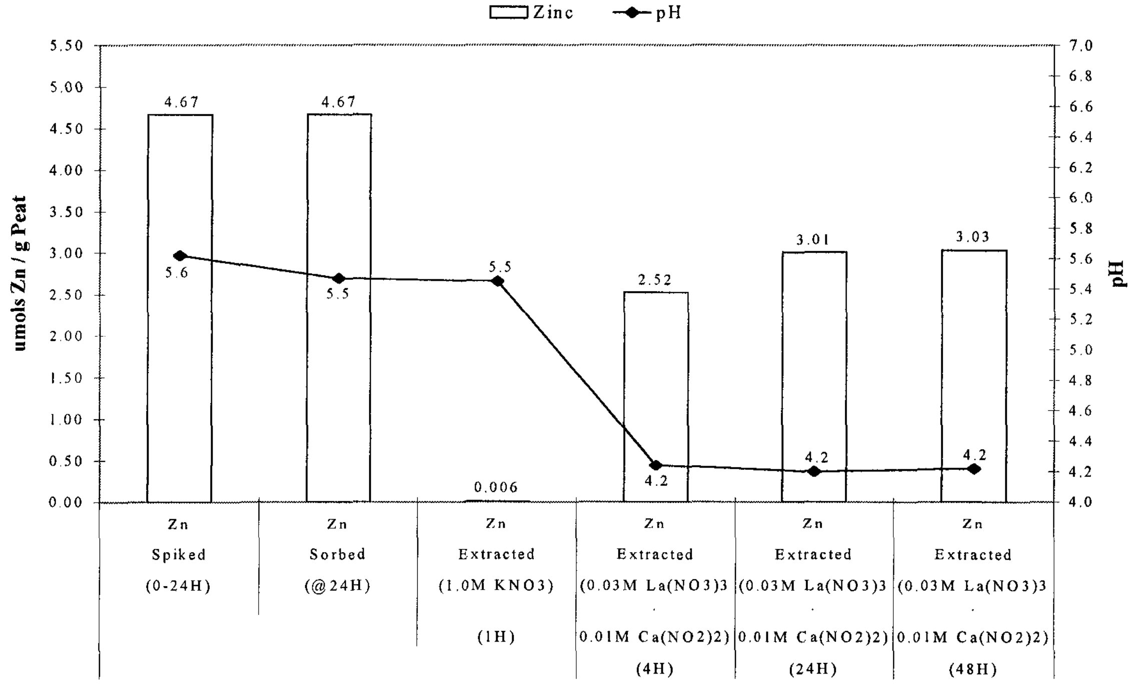

The significant reduction in pHs by 1.1 to 1.5 pH units in both systems during the 0.03M $La(NO_3)_3$ extraction step suggests protons are being released from carboxyl and phenolic groups during the complexation of lanthanum cations. The reported low recovery of complexed copper and lead may be due to a combination of three factors; 1. the sorption capacity of the peat exceeds the total amount of cadmium, calcium, copper, lanthanum, lead, and zinc added, 2. lanthanum cations are not able to extract the more tightly complexed lead and copper, and 3. the complexation of lanthanum may reduce the quantity of lanthanum cations available for exchange with the four metals.

The total recovery of each metal by KNO_3 and $La(NO_3)_3$ in the single-metal system versus the multi-metal system ranged from 43 to 47% for cadmium, 0.9% for copper, 0.1 to 3.0% for lead, and 58 to 65% for zinc. Based on the data, the relative affinity of the four metals for peat is Cu>Pb>Cd>Zn, an affinity sequence similar to the one reported by Farrah and Pickering (1978), but slightly different than the affinity sequence of Pb>Cu>Zn>Cd reported by Gustafsson (2004).

5.2.4 Conclusions

The simple systems used in these experiments (i.e. one type of specimen material plus one or four metals) allowed the calculation of Vanselow selectivity coefficients [Eq. 6 and 7] and sorption constants [Eq. 12 and 13] for kaolinite as well as, the qualitative determination of the ability of $La(NO_3)_3$ to extract adsorbed metals. With regards to lead and copper bound to peat and FeOOH, $La(NO_3)_3$ was unable to extract these two metals. The $La(NO_3)_3$ solution was able to extract 42-46% of the cadmium and 56-65% of the zinc complexed by peat and approximately 65% of the cadmium and 43-61% of the zinc bound to FeOOH. It is unknown if the extraction efficiency of $La(NO_3)_3$ for these four metals bound to FeOOH and peat would improve in situations where the amount of metals added exceeded the sorptive capacity of these materials. However, the data indicate that $La(NO_3)_3$ can partly extract metals, such as cadmium and zinc, which are weakly complexed by peat or sorbed to weak sites located on FeOOH.

In the kaolinite systems, the majority of bound cadmium, copper, lead, and zinc was recovered using 1.0M KNO_3. The data show that cadmium and zinc are associated predominately with the soluble and exchangeable fractions, while lead and copper are bound primarily to both the exchangeable and specifically sorbed fractions. Assuming no precipitation of lead or copper complexes occurred, $La(NO_3)_3$ was able to extract only a portion of these bound metals during the time period of these experiments. Additional recoveries may have been achieved if the extractions were conducted over a longer period of time.

The ability of $La(NO_3)_3$ to extract metals in these experiments is similar to the extraction of metals in the Leadville soils by $La(NO_3)_3$. The experimental data support the previous conclusion that the use of $La(NO_3)_3$ is more appropriate for the recovery of exchangeable metals. The ability of 1.0M KNO_3 to recover metals from exchange sites is very similar to 0.5M $Ca(NO_3)_2$.

5.3 Modeling Results

5.3.1 Modeling Approach

As discussed in sections 5.1.4, 5.1.6, and 5.2, selective extraction procedures were re-evaluated in 2004 due to the poor comparison of predicted concentrations of metals to the 2000 experimental data. The finding that the physical component of the selective extraction process had a significant impact on the recovery of zinc in all samples and lead in one sample led to the incorporation of a less aggressive physical component, i.e. the VES.

The problems identified with the use of DIW to extract soluble metals resulted in the selection of 0.01M $Ca(NO_3)_2$. Three extractant solutions were evaluated for use in recovering exchangeable metals from the Leadville soils. Based on CEC results, the NH_4-DIW-KNO_3 procedure was initially selected to replace 0.5M $Ca(NO_3)_2$ data from 2000. However, in reviewing the performance of $La(NO_3)_3$ and the results of the sorption/desorption experiments, it appeared the selectivity and extraction efficiency of $La(NO_3)_3$ was comparable to the NH_4-DIW-KNO_3 procedure. The data showed NH_4-DIW-KNO_3 and $La(NO_3)_3$ extracted very similar concentrations of cadmium, copper, and lead. However, the NH_4-DIW-KNO_3 procedure extracted unexpectedly high concentrations of zinc that significantly exceeded the quantities of zinc extracted by $La(NO_3)_3$ and $Pb(NO_3)_2$. Therefore, 0.03M $La(NO_3)_3$ was selected to recover exchangeable metals even though data from the adsorption/desorption experiments showed $La(NO_3)_3$ was also able to extract sorbed metals in the kaolinite system. The potential that $La(NO_3)_3$ would recover significant amounts of sorbed metals in addition to exchangeable metals from these soils was considered minimal, because the kaolinite fraction comprised only a small fraction of the overall CEC and available binding sites.

Lead nitrate was selected to extract sorbed and complexed metals from the Leadville soils. The selection of $Pb(NO_3)_2$ precluded the comparison of predicted concentrations of sorbed and complexed lead to experimental data.

To quantify specific fractions of metal cations recovered from these soils for comparison to predicted metal partitioning, the concentrations of metal cations recovered by the weaker extractants were subtracted from the concentrations of metal cations recovered by the stronger extractants. For example, the concentrations of soluble metals recovered by 0.01M $Ca(NO_3)_2$ were subtracted from the concentrations of soluble and exchangeable metals recovered by 0.03M $La(NO_3)_3$. The concentrations of soluble and exchangeable metals recovered by 0.03M $La(NO_3)_3$ were subtracted from the concentrations of soluble, exchangeable, and sorbed/complexed metals recovered by 0.05M $Pb(NO_3)_2$. It was assumed the partitioning of metals calculated using this approach would be the same as if the soils had been sequentially extracted with the three extractants described above.

Model performance tables which compare predicted concentrations of cadmium, copper, lead, and zinc to experimental data are included in sections 5.3.2-5.3.5. Two model performance tables are provided for each metal and each surrogate soil. One table represents predicted metal partitioning based on the non-competitive modeling approach (NCMA), while the second table represents predicted metal partitioning based on the competitive modeling approach (CMA).

5.3.2 Cadmium

99-1-0-7 Cadmium (Tables 21 and 22)

The total cadmium concentration reported for sample 99-1-0-7 is 43.2 mg kg^{-1}. The soluble, exchangeable, and sorbed/complexed cadmium concentrations are 9.08, 6.52, and 13.4 mg kg^{-1}, respectively. The NCMA predicted exchangeable, sorbed, and complexed cadmium concentrations of 4.71, 0.992, and 118 mg kg^{-1}, respectively. The CMA predicted exchangeable, sorbed, and complexed cadmium concentrations of 3.12, 0.977, and 57.8 mg kg^{-1}, respectively. Both modeling approaches predicted exchangeable cadmium concentrations that are relatively close to the reported values for this soil. Although the CMA is a better predictor of cadmium partitioning than the NCMA, both modeling approaches overpredicted the concentration of sorbed/complexed cadmium. Both the CMA and NCMA predicted a total cadmium concentration greater than the experimental data.

99-1-7-12 Cadmium (Tables 23 and 24)

The total cadmium concentration reported for sample 99-1-7-12 is 11.2 mg kg^{-1}. The soluble, exchangeable, and sorbed/complexed cadmium concentrations are 3.20, 1.56, and 0.590 mg kg^{-1}, respectively. The NCMA predicted exchangeable, sorbed, and complexed cadmium concentrations of 0.563, 0.001, and 2.06 mg kg^{-1}, respectively. The CMA predicted exchangeable, sorbed, and complexed cadmium concentrations of 0.557, 0.001, and 1.71 mg kg^{-1}, respectively.

Table 21. Comparison of modeling output data to experimental data for cadmium in sample 99-1-0-7 [non-competitive modeling approach – cadmium only]

Modeling Data: [99-1-0-7] [Input and Predicted Concentrations]	Input Soluble Cadmium[1]	Predicted Exchangeable Cadmium[2]	Predicted Sorbed and Complexed Cadmium[2]	Total Predicted E, S, and C[3] Cadmium
	mg L^{-1}	mg kg^{-1}	mg kg^{-1}	mg kg^{-1}
	0.227	4.71	0.992 [S]; 118 [C]	124
Experimental Data: [99-1-0-7] [Cd^{+2}_{Total}] = 43.2 mg kg^{-1}	**Soluble Cadmium[1]**	**Exchangeable Cadmium[4]**	**Sorbed and Complexed Cadmium[5]**	**Total E, S, and C[3] Cadmium**
Vacuum Extraction Method	mg kg^{-1}	mg kg^{-1}	mg kg^{-1}	mg kg^{-1}
0.01M $Ca(NO_3)_2$ Extractable	9.08	-	-	-
0.03M $La(NO_3)_3$ Extractable	[9.08]	6.52	-	-
0.05M $Pb(NO_3)_2$ Extractable	[9.08]	[6.52]	13.4	19.9

1 Soluble cadmium concentration based on extraction with 0.01M calcium nitrate.

2 Predicted value obtained from the sum of all component desorption curves at reported soluble cadmium concentration.

3 [E] Exchangeable; [S] Sorbed; [C] Complexed.

4 Exchangeable cadmium equals 0.03M lanthanum nitrate extractable cadmium minus 0.01M calcium nitrate extractable cadmium (i.e., 15.6-9.08).

5 Sorbed and complexed cadmium equals 0.05M lead nitrate extractable cadmium minus the sum of 0.03M lanthanum nitrate extractable cadmium and 0.01M calcium nitrate extractable cadmium (i.e., 29.0-(6.52+9.08)).

Table 22. Comparison of modeling output data to experimental data for cadmium in sample 99-1-0-7 [competitive modeling approach – cadmium with copper, lead, and zinc]

Modeling Data: [99-1-0-7] [Input and Predicted Concentrations]	Input Soluble Cadmium[1]	Predicted Exchangeable Cadmium[2]	Predicted Sorbed and Complexed Cadmium[2]	Total Predicted E, S, and C[3] Cadmium
	mg L^{-1}	mg kg^{-1}	mg kg^{-1}	mg kg^{-1}
	0.227	3.12	0.977 [S]; 57.8 [C]	61.9
Experimental Data: [99-1-0-7] [Cd^{+2}_{Total}] = 43.2 mg kg^{-1}	Soluble Cadmium[1]	Exchangeable Cadmium[4]	Sorbed and Complexed Cadmium[5]	Total E, S, and C[3] Cadmium
Vacuum Extraction Method	mg kg^{-1}	mg kg^{-1}	mg kg^{-1}	mg kg^{-1}
0.01M $Ca(NO_3)_2$ Extractable	9.08	-	-	-
0.03M $La(NO_3)_3$ Extractable	[9.08]	6.52	-	-
0.05M $Pb(NO_3)_2$ Extractable	[9.08]	[6.52]	13.4	19.9

1 Soluble cadmium concentration based on extraction with 0.01M calcium nitrate.

2 Predicted value obtained from the sum of all component desorption curves at reported soluble cadmium concentration.

3 [E] Exchangeable; [S] Sorbed; [C] Complexed.

4 Exchangeable cadmium equals 0.03M lanthanum nitrate extractable cadmium minus 0.01M calcium nitrate extractable cadmium (i.e., 15.6-9.08).

5 Sorbed and complexed cadmium equals 0.05M lead nitrate extractable cadmium minus the sum of 0.03M lanthanum nitrate extractable cadmium and 0.01M calcium nitrate extractable cadmium (i.e., 29.0-(6.52+9.08)).

Table 23. Comparison of modeling output data to experimental data for cadmium in sample 99-1-7-12 [non-competitive modeling approach – cadmium only]

Modeling Data: [99-1-7-12] [Input and Predicted Concentrations]	Input Soluble Cadmium[1]	Predicted Exchangeable Cadmium[2]	Predicted Sorbed and Complexed Cadmium[2]	Total Predicted E, S, and C[3] Cadmium
	$mg\ L^{-1}$	$mg\ kg^{-1}$	$mg\ kg^{-1}$	$mg\ kg^{-1}$
	0.080	0.563	0.001 [S]; 2.06 [C]	2.62
Experimental Data: [99-1-7-12] $[Cd^{+2}_{Total}] = 11.2\ mg\ kg^{-1}$	**Soluble Cadmium[1]**	**Exchangeable Cadmium[4]**	**Sorbed and Complexed Cadmium[5]**	**Total E, S, and C[3] Cadmium**
Vacuum Extraction Method	$mg\ kg^{-1}$	$mg\ kg^{-1}$	$mg\ kg^{-1}$	$mg\ kg^{-1}$
0.01M $Ca(NO_3)_2$ Extractable	3.20	-	-	-
0.03M $La(NO_3)_3$ Extractable	[3.20]	1.56	-	-
0.05M $Pb(NO_3)_2$ Extractable	[3.20]	[1.56]	0.590	2.15

[1] Soluble cadmium concentration based on extraction with 0.01M calcium nitrate.

[2] Predicted value obtained from the sum of all component desorption curves at reported soluble cadmium concentration.

[3] [E] Exchangeable; [S] Sorbed; [C] Complexed.

[4] Exchangeable cadmium equals 0.03M lanthanum nitrate extractable cadmium minus 0.01M calcium nitrate extractable cadmium (i.e., 4.76-3.20).

[5] Sorbed and complexed cadmium equals 0.05M lead nitrate extractable cadmium minus the sum of 0.03M lanthanum nitrate extractable cadmium and 0.01M calcium nitrate extractable cadmium (i.e., 5.35-(1.56+3.20)).

Table 24. Comparison of modeling output data to experimental data for cadmium in sample 99-1-7-12 [competitive modeling approach – cadmium with copper, lead, and zinc]

Modeling Data: [99-1-7-12] [Input and Predicted Concentrations]	Input Soluble Cadmium[1]	Predicted Exchangeable Cadmium[2]	Predicted Sorbed and Complexed Cadmium[2]	Total Predicted E, S, and C[3] Cadmium
	mg L^{-1}	mg kg^{-1}	mg kg^{-1}	mg kg^{-1}
	0.080	0.557	0.001 [S]; 1.71 [C]	2.27
Experimental Data: [99-1-7-12] $[Cd^{+2}_{Total}]$ = 11.2 mg kg^{-1}	Soluble Cadmium[1]	Exchangeable Cadmium[4]	Sorbed and Complexed Cadmium[5]	Total E, S, and C[3] Cadmium
Vacuum Extraction Method	mg kg^{-1}	mg kg^{-1}	mg kg^{-1}	mg kg^{-1}
0.01M $Ca(NO_3)_2$ Extractable	3.20	-	-	-
0.03M $La(NO_3)_3$ Extractable	[3.20]	1.56	-	-
0.05M $Pb(NO_3)_2$ Extractable	[3.20]	[1.56]	0.590	2.15

1 Soluble cadmium concentration based on extraction with 0.01M calcium nitrate.

2 Predicted value obtained from the sum of all component desorption curves at reported soluble cadmium concentration.

3 [E] Exchangeable; [S] Sorbed; [C] Complexed.

4 Exchangeable cadmium equals 0.03M lanthanum nitrate extractable cadmium minus 0.01M calcium nitrate extractable cadmium (i.e., 4.76-3.20).

5 Sorbed and complexed cadmium equals 0.05M lead nitrate extractable cadmium minus the sum of 0.03M lanthanum nitrate extractable cadmium and 0.01M calcium nitrate extractable cadmium (i.e., 5.35-(1.56+3.20)).

Under the specified surrogate soil conditions of pH 4.15 and above average total cadmium content, both modeling approaches accurately predicted the very low concentrations of exchangeable, sorbed, and complexed cadmium reported for this soil.

98-3-5-10 Cadmium (Tables 25 and 26)

The total cadmium concentration reported for sample 98-3-5-10 is 98.0 mg kg^{-1}. The soluble, exchangeable, and sorbed/complexed cadmium concentrations are 33.4, 12.2, and 60.4 mg kg^{-1}, respectively. The experimentally derived partitioning of cadmium reported for this soil exceeds the reported total cadmium concentration of 98.0 mg kg^{-1}. However, the two results are within the measurement variation of the analytical method. The NCMA predicted exchangeable, sorbed, and complexed cadmium concentrations of 35.0, 34.1, and 733 mg kg^{-1}, respectively. The CMA predicted exchangeable, sorbed, and complexed cadmium concentrations of 15.0, 18.4, and 228 mg kg^{-1}, respectively.

The CMA provides a closer fit of the experimental data and accurately predicts the exchangeable cadmium concentration reported for this soil. However, both modeling approaches overpredict the reported concentration of sorbed/complexed cadmium. The total amount of cadmium predicted for this soil significantly exceeds the reported total cadmium concentration.

Table 25. Comparison of modeling output data to experimental data for cadmium in sample 98-3-5-10 [non-competitive modeling approach – cadmium only]

Modeling Data: [98-3-5-10] [Input and Predicted Concentrations]	Input Soluble Cadmium[1]	Predicted Exchangeable Cadmium[2]	Predicted Sorbed and Complexed Cadmium[2]	Total Predicted E, S, and C[3] Cadmium
	mg L^{-1}	mg kg^{-1}	mg kg^{-1}	mg kg^{-1}
	0.836	35.0	34.1 [S]; 733 [C]	802
Experimental Data: [98-3-5-10] $[Cd^{+2}_{Total}] = 98.0$ mg kg^{-1}	**Soluble Cadmium[1]**	**Exchangeable Cadmium[4]**	**Sorbed and Complexed Cadmium[5]**	**Total E, S, and C[3] Cadmium**
Vacuum Extraction Method	mg kg^{-1}	mg kg^{-1}	mg kg^{-1}	mg kg^{-1}
0.01M $Ca(NO_3)_2$ Extractable	33.4	-	-	-
0.03M $La(NO_3)_3$ Extractable	[33.4]	12.2	-	-
0.05M $Pb(NO_3)_2$ Extractable	[33.4]	[12.2]	60.4	72.6

1 Soluble cadmium concentration based on extraction with 0.01M calcium nitrate.

2 Predicted value obtained from the sum of all component desorption curves at reported soluble cadmium concentration.

3 [E] Exchangeable; [S] Sorbed; [C] Complexed.

4 Exchangeable cadmium equals 0.03M lanthanum nitrate extractable cadmium minus 0.01M calcium nitrate extractable cadmium (i.e., 45.6-33.4).

5 Sorbed and complexed cadmium equals 0.05M lead nitrate extractable cadmium minus the sum of 0.03M lanthanum nitrate extractable cadmium and 0.01M calcium nitrate extractable cadmium (i.e., 106-(12.2+33.4)).

Table 26. Comparison of modeling output data to experimental data for cadmium in sample 98-3-5-10 [competitive modeling approach – cadmium with copper, lead, and zinc]

Modeling Data: [98-3-5-10] [Input and Predicted Concentrations]	Input Soluble Cadmium[1]	Predicted Exchangeable Cadmium[2]	Predicted Sorbed and Complexed Cadmium[2]	Total Predicted E, S, and C[3] Cadmium
	mg L^{-1}	mg kg^{-1}	mg kg^{-1}	mg kg^{-1}
	0.836	15.0	18.4 [S]; 228 [C]	261

Experimental Data: [98-3-5-10] $[Cd^{+2}_{Total}] = 98.0\ \text{mg kg}^{-1}$	Soluble Cadmium[1]	Exchangeable Cadmium[4]	Sorbed and Complexed Cadmium[5]	Total E, S, and C[3] Cadmium
Vacuum extraction Method	mg kg^{-1}	mg kg^{-1}	mg kg^{-1}	mg kg^{-1}
0.01M $Ca(NO_3)_2$ Extractable	33.4	-	-	-
0.03M $La(NO_3)_3$ Extractable	[33.4]	12.2	-	-
0.05M $Pb(NO_3)_2$ Extractable	[33.4]	[12.2]	60.4	72.6

1 Soluble cadmium concentration based on extraction with 0.01M calcium nitrate.

2 Predicted value obtained from the sum of all component desorption curves at reported soluble cadmium concentration.

3 [E] Exchangeable; [S] Sorbed; [C] Complexed.

4 Exchangeable cadmium equals 0.03M lanthanum nitrate extractable cadmium minus 0.01M calcium nitrate extractable cadmium (i.e., 45.6-33.4).

5 Sorbed and complexed cadmium equals 0.05M lead nitrate extractable cadmium minus the sum of 0.03M lanthanum nitrate extractable cadmium and 0.01M calcium nitrate extractable cadmium (i.e., 106-(12.2+33.4)).

98-3-20-25 Cadmium (Tables 27 and 28)

The total cadmium content reported for sample 98-3-20-25 is 146 mg kg^{-1}. The soluble, exchangeable, and sorbed/complexed cadmium concentrations are 37.6, 34.9, and 24.8 mg kg^{-1}, respectively. The NCMA predicts exchangeable, sorbed, and complexed cadmium concentrations of 23.0, 71.6, and 440 mg kg^{-1}, respectively, while the CMA predicts exchangeable, sorbed, and complexed cadmium concentrations of 10.7, 36.3, and 126 mg kg^{-1}, respectively.

The CMA and NCMA predict exchangeable cadmium concentrations within a reasonable range of the experimental data. However, both modeling approaches overpredict the concentration of sorbed/complexed cadmium reported for this soil and predict more total cadmium than the reported total cadmium concentration. The CMA provides a better fit of the experimental data than the NCMA.

Summary of Cadmium Modeling

In the four soils tested, the CMA and NCMA predict within a narrow range the exchangeable cadmium concentrations reported for these soils. Both modeling approaches overpredict concentrations of sorbed/complexed cadmium in three out of four soils. The results indicate that at higher pHs and soluble cadmium concentrations, the ability of both modeling approaches to predict sorbed/complexed cadmium decrease. From the tables, the problem appears to reside in the prediction of cadmium complexed to SOM. An extensive review of model parameters, conversions, multipliers, weighting factors, and modeling performance related to the other three metals complexed to SOM

Table 27. Comparison of modeling output data to experimental data for cadmium in sample 98-3-20-25 [non-competitive modeling approach – cadmium only]

Modeling Data: [98-3-20-25] [Input and Predicted Concentrations]	Input Soluble Cadmium[1]	Predicted Exchangeable Cadmium[2]	Predicted Sorbed and Complexed Cadmium[2]	Total Predicted E, S, and C[3] Cadmium
	$mg\ L^{-1}$	$mg\ kg^{-1}$	$mg\ kg^{-1}$	$mg\ kg^{-1}$
	0.940	23.0	71.6 [S]; 440 [C]	535
Experimental Data: [98-3-20-25] $[Cd^{+2}_{Total}] = 146\ mg\ kg^{-1}$	Soluble Cadmium[1]	Exchangeable Cadmium[4]	Sorbed and Complexed Cadmium[5]	Total E, S, and C[3] Cadmium
Vacuum Extraction Method	$mg\ kg^{-1}$	$mg\ kg^{-1}$	$mg\ kg^{-1}$	$mg\ kg^{-1}$
0.01M $Ca(NO_3)_2$ Extractable	37.6	-	-	-
0.03M $La(NO_3)_3$ Extractable	[37.6]	34.9	-	-
0.05M $Pb(NO_3)_2$ Extractable	[37.6]	[34.9]	24.8	59.7

[1] Soluble cadmium concentration based on extraction with 0.01M calcium nitrate.

[2] Predicted value obtained from the sum of all component desorption curves at reported soluble cadmium concentration.

[3] [E] Exchangeable; [S] Sorbed; [C] Complexed.

[4] Exchangeable cadmium equals 0.03M lanthanum nitrate extractable cadmium minus 0.01M calcium nitrate extractable cadmium (i.e., 72.5-37.6).

[5] Sorbed and complexed cadmium equals 0.05M lead nitrate extractable cadmium minus the sum of 0.03M lanthanum nitrate extractable cadmium and 0.01M calcium nitrate extractable cadmium (i.e., 97.3-(34.9+37.6)).

Table 28. Comparison of modeling output data to experimental data for cadmium in sample 98-3-20-25 [competitive modeling approach – cadmium with copper, lead, and zinc]

Modeling Data: [98-3-20-25] [Input and Predicted Concentrations]	Input Soluble Cadmium[1]	Predicted Exchangeable Cadmium[2]	Predicted Sorbed and Complexed Cadmium[2]	Total Predicted E, S, and C[3] Cadmium
	mg L^{-1}	mg kg^{-1}	mg kg^{-1}	mg kg^{-1}
	0.940	10.7	36.3 [S]; 126 [C]	173
Experimental Data: [98-3-20-25] [Cd^{+2}_{Total}] = 146 mg kg^{-1}	**Soluble Cadmium[1]**	**Exchangeable Cadmium[4]**	**Sorbed and Complexed Cadmium[5]**	**Total E, S, and C[3] Cadmium**
Vacuum Extraction Method	mg kg^{-1}	mg kg^{-1}	mg kg^{-1}	mg kg^{-1}
0.01M $Ca(NO_3)_2$ Extractable	37.6	-	-	-
0.03M $La(NO_3)_3$ Extractable	[37.6]	34.9	-	-
0.05M $Pb(NO_3)_2$ Extractable	[37.6]	[34.9]	24.8	59.7

[1] Soluble cadmium concentration based on extraction with 0.01M calcium nitrate.

[2] Predicted value obtained from the sum of all component desorption curves at reported soluble cadmium concentration.

[3] [E] Exchangeable; [S] Sorbed; [C] Complexed.

[4] Exchangeable cadmium equals 0.03M lanthanum nitrate extractable cadmium minus 0.01M calcium nitrate extractable cadmium (i.e., 72.5-37.6).

[5] Sorbed and complexed cadmium equals 0.05M lead nitrate extractable cadmium minus the sum of 0.03M lanthanum nitrate extractable cadmium and 0.01M calcium nitrate extractable cadmium (i.e., 97.3-(34.9+37.6)).

indicate the overprediction of complexed cadmium may be associated with the binding constants listed for cadmium in the Visual MINTEQ databases. Nevertheless, the CMA proves to be a better predictor of cadmium partitioning than the NCMA. Overprediction of sorbed/complexed cadmium in the CMA is within reasonable variation of the experimental data.

5.3.3 Copper

99-1-0-7 Copper (Tables 29 and 30)

The total copper concentration reported for sample 99-1-0-7 is 633 mg kg^{-1}. The soluble, exchangeable, and sorbed/complexed copper concentrations are 0.320, 0.276, and 102 mg kg^{-1}, respectively. The NCMA predicts exchangeable, sorbed, and complexed copper concentrations of 1.65, 8.40, and 73.2 mg kg^{-1}, respectively. The CMA predicts exchangeable, sorbed, and complexed copper concentrations of 2.12, 16.2, and 76.4 mg kg^{-1}, respectively. Both modeling approaches accurately predict the reported concentrations of exchangeable and sorbed/complexed copper in this soil.

99-1-7-12 Copper (Tables 31 and 32)

The total copper concentration reported for sample 99-1-7-12 is 336 mg kg^{-1}. The soluble, exchangeable, and sorbed/complexed copper concentrations are 1.04, 9.06, and 44.0 mg kg^{-1}, respectively. The NCMA predicts exchangeable, sorbed, and complexed copper concentrations of 0.976, 0.222, and 21.0 mg kg^{-1}, respectively, while the CMA predicts exchangeable, sorbed, and complexed copper concentrations of 0.876, 0.222, and

Table 29. Comparison of modeling output data to experimental data for copper in sample 99-1-0-7 [non-competitive modeling approach – copper only]

Modeling Data: [99-1-0-7] [Input and Predicted Concentrations]	Input Soluble Copper[1]	Predicted Exchangeable Copper[2]	Predicted Sorbed and Complexed Copper[2]	Total Predicted E, S, and C[3] Copper
	mg L^{-1}	mg kg^{-1}	mg kg^{-1}	mg kg^{-1}
	0.008	1.65	8.40 [S]; 73.2 [C]	83.2

Experimental Data: [99-1-0-7] $[Cu^{+2}_{Total}] = 633$ mg kg^{-1}	Soluble Copper[1]	Exchangeable Copper[4]	Sorbed and Complexed Copper[5]	Total E, S, and C[3] Copper
Vacuum extraction Method	mg kg^{-1}	mg kg^{-1}	mg kg^{-1}	mg kg^{-1}
0.01M $Ca(NO_3)_2$ Extractable	0.320	-	-	-
0.03M $La(NO_3)_3$ Extractable	[0.320]	0.276	-	-
0.05M $Pb(NO_3)_2$ Extractable	[0.320]	[0.276]	102	103

1 Soluble copper concentration based on extraction with 0.01M calcium nitrate.

2 Predicted value obtained from the sum of all component desorption curves at reported soluble copper concentration.

3 [E] Exchangeable; [S] Sorbed; [C] Complexed.

4 Exchangeable copper equals 0.03M lanthanum nitrate extractable copper minus 0.01M calcium nitrate extractable copper (i.e., 0.596-0.320).

5 Sorbed and complexed copper equals 0.05M lead nitrate extractable copper minus the sum of 0.03M lanthanum nitrate extractable copper and 0.01M calcium nitrate extractable copper (i.e., 103-(0.276+0.320)).

Table 30. Comparison of modeling output data to experimental data for copper in sample 99-1-0-7 [competitive modeling approach – copper with cadmium, lead, and zinc]

Modeling Data: [99-1-0-7] [Input and Predicted Concentrations]	Input Soluble Copper[1]	Predicted Exchangeable Copper[2]	Predicted Sorbed and Complexed Copper[2]	Total Predicted E, S, and C[3] Copper
	mg L^{-1}	mg kg^{-1}	mg kg^{-1}	mg kg^{-1}
	0.008	2.12	16.2 [S]; 76.4 [C]	94.7
Experimental Data: [99-1-0-7] [Cu^{+2}_{Total}] = 633 mg kg^{-1}	Soluble Copper[1]	Exchangeable Copper[4]	Sorbed and Complexed Copper[5]	Total E, S, and C[3] Copper
Vacuum Extraction Method	mg kg^{-1}	mg kg^{-1}	mg kg^{-1}	mg kg^{-1}
0.01M $Ca(NO_3)_2$ Extractable	0.320	-	-	-
0.03M $La(NO_3)_3$ Extractable	[0.320]	0.276	-	-
0.05M $Pb(NO_3)_2$ Extractable	[0.320]	[0.276]	102	103

1 Soluble copper concentration based on extraction with 0.01M calcium nitrate.

2 Predicted value obtained from the sum of all component desorption curves at reported soluble copper concentration.

3 [E] Exchangeable; [S] Sorbed; [C] Complexed.

4 Exchangeable copper equals 0.03M lanthanum nitrate extractable copper minus 0.01M calcium nitrate extractable copper (i.e., 0.596-0.320).

5 Sorbed and complexed copper equals 0.05M lead nitrate extractable copper minus the sum of 0.03M lanthanum nitrate extractable copper and 0.01M calcium nitrate extractable copper (i.e., 103-(0.276+0.320)).

Table 31. Comparison of modeling output data to experimental data for copper in sample 99-1-7-12 [non-competitive modeling approach – copper only]

Modeling Data: [99-1-7-12] [Input and Predicted Concentrations]	Input Soluble Copper[1]	Predicted Exchangeable Copper[2]	Predicted Sorbed and Complexed Copper[2]	Total Predicted E, S, and C[3] Copper
	mg L^{-1}	mg kg^{-1}	mg kg^{-1}	mg kg^{-1}
	0.026	0.976	0.222 [S]; 21.0 [C]	22.2

Experimental Data: [99-1-7-12] [Cu^{+2}_{Total}] = 336 mg kg^{-1}	Soluble Copper[1]	Exchangeable Copper[4]	Sorbed and Complexed Copper[5]	Total E, S, and C[3] Copper
Vacuum Extraction Method	mg kg^{-1}	mg kg^{-1}	mg kg^{-1}	mg kg^{-1}
0.01M $Ca(NO_3)_2$ Extractable	1.04	-	-	-
0.03M $La(NO_3)_3$ Extractable	[1.04]	9.06	-	-
0.05M $Pb(NO_3)_2$ Extractable	[1.04]	[9.06]	44.0	53.1

[1] Soluble copper concentration based on extraction with 0.01M calcium nitrate.

[2] Predicted value obtained from the sum of all component desorption curves at reported soluble copper concentration.

[3] [E] Exhangeable; [S] Sorbed; [C] Complexed.

[4] Exchangeable copper equals 0.03M lanthanum nitrate extractable copper minus 0.01M calcium nitrate extractable copper (i.e., 10.1-1.04).

[5] Sorbed and complexed copper equals 0.05M lead nitrate extractable copper minus the sum of 0.03M lanthanum nitrate extractable copper and 0.01M calcium nitrate extractable copper (i.e., 54.1-(9.06+1.04)).

Table 32. Comparison of modeling output data to experimental data for copper in sample 99-1-7-12 [competitive modeling approach – copper with cadmium, lead, and zinc]

Modeling Data: [99-1-7-12] [Input and Predicted Concentrations]	Input Soluble Copper[1]	Predicted Exchangeable Copper[2]	Predicted Sorbed and Complexed Copper[2]	Total Predicted E, S, and C[3] Copper
	mg L^{-1}	mg kg^{-1}	mg kg^{-1}	mg kg^{-1}
	0.026	0.876	0.222 [S]; 15.6 [C]	16.7
Experimental Data: [99-1-7-12] $[Cu^{+2}_{Total}]$ = 336 mg kg^{-1}	**Soluble Copper[1]**	**Exchangeable Copper[4]**	**Sorbed and Complexed Copper[5]**	**Total E, S, and C[3] Copper**
Vacuum Extraction Method	mg kg^{-1}	mg kg^{-1}	mg kg^{-1}	mg kg^{-1}
0.01M $Ca(NO_3)_2$ Extractable	1.04	-	-	-
0.03M $La(NO_3)_3$ Extractable	[1.04]	9.06	-	-
0.05M $Pb(NO_3)_2$ Extractable	[1.04]	[9.06]	44.0	53.1

[1] Soluble copper concentration based on extraction with 0.01M calcium nitrate.

[2] Predicted value obtained from the sum of all component desorption curves at reported soluble copper concentration.

[3] [E] Exhangeable; [S] Sorbed; [C] Complexed.

[4] Exchangeable copper equals 0.03M lanthanum nitrate extractable copper minus 0.01M calcium nitrate extractable copper (i.e., 10.1-1.04).

[5] Sorbed and complexed copper equals 0.05M lead nitrate extractable copper minus the sum of 0.03M lanthanum nitrate extractable copper and 0.01M calcium nitrate extractable copper (i.e., 54.1-(9.06+1.04)).

15.6 mg kg^{-1}, respectively. Both modeling approaches underpredict the reported concentrations of exchangeable and soluble/complexed copper. The NCMA is a better predictor of copper partitioning than the CMA.

98-3-5-10 Copper (Tables 33 and 34)

The total copper concentration reported for sample 98-3-5-10 is 435 mg kg^{-1}. The soluble, exchangeable, and sorbed/complexed copper concentrations are 0.720, 0.520, and 66.2 mg kg^{-1}, respectively. The NCMA predicts exchangeable, sorbed, and complexed copper concentrations of 6.30, 13.2, and 293 mg kg^{-1}, respectively. The CMA predicts exchangeable, sorbed, and complexed copper concentrations of 5.93, 20.6, and 237 mg kg^{-1}, respectively. Both modeling approaches predict exchangeable copper, while overpredicting the concentration of sorbed/complexed copper reported for this soil. The CMA is a better predictor of copper partitioning in 98-3-5-10 than the NCMA.

98-3-20-25 Copper (Table 35 and 36)

The total copper content reported for sample 98-3-20-25 is 213 mg kg^{-1}. The soluble, exchangeable, and sorbed/complexed copper concentrations are 0.240, 0.104, and 2.76 mg kg^{-1}, respectively. The NCMA predicts exchangeable, sorbed, and complexed copper concentrations of 1.55, 14.7, and 78.4 mg kg^{-1}, respectively. The CMA predicts exchangeable, sorbed, and complexed copper concentrations of 3.18, 3.14, and 129 mg kg^{-1}, respectively. Both modeling approaches predict the concentration of exchangeable copper reported for this soil and overpredict the reported concentration of

Table 33. Comparison of modeling output data to experimental data for copper in sample 98-3-5-10 [non-competitive modeling approach – copper only]

Modeling Data: [98-3-5-10] [Input and Predicted Concentrations]	Input Soluble Copper[1]	Predicted Exchangeable Copper[2]	Predicted Sorbed and Complexed Copper[2]	Total Predicted E, S, and C[3] Copper
	mg L^{-1}	mg kg^{-1}	mg kg^{-1}	mg kg^{-1}
	0.018	6.30	13.2 [S]; 293 [C]	312
Experimental Data: [98-3-5-10] [Cu$^{+2}_{\text{Total}}$] = 435 mg kg^{-1}	**Soluble Copper[1]**	**Exchangeable Copper[4]**	**Sorbed and Complexed Copper[5]**	**Total E, S, and C[3] Copper**
Vacuum Extraction Method	mg kg^{-1}	mg kg^{-1}	mg kg^{-1}	mg kg^{-1}
0.01M $Ca(NO_3)_2$ Extractable	0.720	-	-	-
0.03M $La(NO_3)_3$ Extractable	[0.720]	0.520	-	-
0.05M $Pb(NO_3)_2$ Extractable	[0.720]	[0.520]	66.2	66.7

1 Soluble copper concentration based on extraction with 0.01M calcium nitrate.

2 Predicted value obtained from the sum of all component desorption curves at reported soluble copper concentration.

3 [E] Exhangeable; [S] Sorbed; [C] Complexed.

4 Exchangeable copper equals 0.03M lanthanum nitrate extractable copper minus 0.01M calcium nitrate extractable copper (i.e., 1.24-0.720).

5 Sorbed and complexed copper equals 0.05M lead nitrate extractable copper minus the sum of 0.03M lanthanum nitrate extractable copper and 0.01M calcium nitrate extractable copper (i.e., 67.4-(0.520+0.720)).

Table 34. Comparison of modeling output data to experimental data for copper in sample 98-3-5-10 [competitive modeling approach – copper with cadmium, lead, and zinc]

Modeling Data: [98-3-5-10] [Input and Predicted Concentrations]	Input Soluble Copper[1]	Predicted Exchangeable Copper[2]	Predicted Sorbed and Complexed Copper[2]	Total Predicted E, S, and C[3] Copper
	mg L^{-1}	mg kg^{-1}	mg kg^{-1}	mg kg^{-1}
	0.018	5.93	20.6 [S]; 237 [C]	264
Experimental Data: [98-3-5-10] $[Cu^{+2}_{Total}]$ = 435 mg kg^{-1}	Soluble Copper[1]	Exchangeable Copper[4]	Sorbed and Complexed Copper[5]	Total E, S, and C[3] Copper
Vacuum Extraction Method	mg kg^{-1}	mg kg^{-1}	mg kg^{-1}	mg kg^{-1}
0.01M $Ca(NO_3)_2$ Extractable	0.720	-	-	-
0.03M $La(NO_3)_3$ Extractable	[0.720]	0.520	-	-
0.05M $Pb(NO_3)_2$ Extractable	[0.720]	[0.520]	66.2	66.7

1 Soluble copper concentration based on extraction with 0.01M calcium nitrate.

2 Predicted value obtained from the sum of all component desorption curves at reported soluble copper concentration.

3 [E] Exhangeable; [S] Sorbed; [C] Complexed.

4 Exchangeable copper equals 0.03M lanthanum nitrate extractable copper minus 0.01M calcium nitrate extractable copper (i.e., 1.24-0.720).

5 Sorbed and complexed copper equals 0.05M lead nitrate extractable copper minus the sum of 0.03M lanthanum nitrate extractable copper and 0.01M calcium nitrate extractable copper (i.e., 67.4-(0.520+0.720)).

Table 35. Comparison of modeling output data to experimental data for copper in sample 98-3-20-25 [non-competitive modeling approach – copper only]

Modeling Data: [98-3-20-25] [Input and Predicted Concentrations]	Input Soluble Copper[1]	Predicted Exchangeable Copper[2]	Predicted Sorbed and Complexed Copper[2]	Total Predicted E, S, and C[3] Copper
	mg L^{-1}	mg kg^{-1}	mg kg^{-1}	mg kg^{-1}
	0.006	1.55	14.7 [S]; 78.4 [C]	94.7
Experimental Data: [98-3-20-25] $[Cu^{+2}_{Total}] = 213$ mg kg^{-1}	**Soluble Copper[1]**	**Exchangeable Copper[4]**	**Sorbed and Complexed Copper[5]**	**Total E, S, and C[3] Copper**
Vacuum Extraction Method	mg kg^{-1}	mg kg^{-1}	mg kg^{-1}	mg kg^{-1}
0.01M $Ca(NO_3)_2$ Extractable	0.240	-	-	-
0.03M $La(NO_3)_3$ Extractable	[0.240]	0.104	-	-
0.05M $Pb(NO_3)_2$ Extractable	[0.240]	[0.104]	2.76	2.86

1 Soluble copper concentration based on extraction with 0.01M calcium nitrate.

2 Predicted value obtained from the sum of all component desorption curves at reported soluble copper concentration.

3 [E] Exhangeable; [S] Sorbed; [C] Complexed.

4 Exchangeable copper equals 0.03M lanthanum nitrate extractable copper minus 0.01M calcium nitrate extractable copper (i.e., 0.344-0.240).

5 Sorbed and complexed copper equals 0.05M lead nitrate extractable copper minus the sum of 0.03M lanthanum nitrate extractable copper and 0.01M calcium nitrate extractable copper (i.e., 3.10-(0.104+0.240)).

Table 36. Comparison of modeling output data to experimental data for copper in sample 98-3-20-25 [competitive modeling approach – copper with cadmium, lead, and zinc]

Modeling Data: [98-3-20-25] [Input and Predicted Concentrations]	Input Soluble Copper[1]	Predicted Exchangeable Copper[2]	Predicted Sorbed and Complexed Copper[2]	Total Predicted E, S, and C[3] Copper
	mg L^{-1}	mg kg^{-1}	mg kg^{-1}	mg kg^{-1}
	0.006	3.18	3.14 [S]; 129 [C]	135
Experimental Data: [98-3-20-25] $[Cu^{+2}_{Total}]$ = 213 mg kg^{-1}	**Soluble Copper[1]**	**Exchangeable Copper[4]**	**Sorbed and Complexed Copper[5]**	**Total E, S, and C[3] Copper**
Vacuum Extraction Method	mg kg^{-1}	mg kg^{-1}	mg kg^{-1}	mg kg^{-1}
0.01M $Ca(NO_3)_2$ Extractable	0.240	-	-	-
0.03M $La(NO_3)_3$ Extractable	[0.240]	0.104	-	-
0.05M $Pb(NO_3)_2$ Extractable	[0.240]	[0.104]	2.76	2.86

[1] Soluble copper concentration based on extraction with 0.01M calcium nitrate.

[2] Predicted value obtained from the sum of all component desorption curves at reported soluble copper concentration.

[3] [E] Exhangeable; [S] Sorbed; [C] Complexed.

[4] Exchangeable copper equals 0.03M lanthanum nitrate extractable copper minus 0.01M calcium nitrate extractable copper (i.e., 0.344-0.240).

[5] Sorbed and complexed copper equals 0.05M lead nitrate extractable copper minus the sum of 0.03M lanthanum nitrate extractable copper and 0.01M calcium nitrate extractable copper (i.e., 3.10-(0.104+0.240)).

sorbed/complexed copper. The NCMA is a better predictor of copper partitioning in this soil.

Summary of Copper Modeling

The NCMA and CMA can predict within a narrow range the concentrations of exchangeable copper reported for the four Leadville soils. Both modeling approaches can predict sorbed and complexed copper in sample 99-1-7-12 at pH 4.15, although the NCMA is slightly more accurate. In sample 99-1-0-7 at pH 5.56, the CMA is a better predictor of copper partitioning than the NCMA. In samples 98-3-5-10 and 98-3-20-25 at pH 6.21, both modeling approaches overpredict sorbed/complexed copper. The CMA is a better predictor than the NCMA in 98-3-5-10, while the opposite is indicated for 98-3-20-25.

Of interest is the increase noted in CMA predicted concentrations of sorbed and complexed copper in samples 99-1-0-7 and 98-3-20-25. Normally, predicted values for sorbed and complexed metals would be less using the CMA than the NCMA, since there are more cations competing for a limited concentration of binding sites. However, in the case of copper and some of the lead and zinc results, the opposite occurred. The predicted increase was related primarily to SOM and FeOOH sorption processes, the rounding of numbers in the software program at low model input metals concentrations, and the non-linear nature of the SOM and FeOOH sorption curves.

In isolated instances at the low end of the range of model inputs used in these simulation exercises, the amount of metal complexed or sorbed was sometimes slightly greater than the amount of metal initially added ($<10^{-6}$ mol L^{-1}). As a consequence, a negative value was sometimes reported in the predicted soluble metals column of the model output. To avoid negative values in the model output and the sorption curves used to calculate predicted metals concentrations, the range of metals concentrations used in the model input was multiplied by a number just large enough to provide a positive value in the predicted soluble metals column of the model output (e.g. the number for copper in sample 98-3-5-10 was 1.0001).

In the model output file, the predicted soluble metals concentration (i.e. total metal input – total bound metal) was multiplied by the inverse of the number used in the model input (e.g. the number for copper in sample 98-3-5-10 was 0.99990001). The extra steps avoided the generation of negative values for the concentration of predicted soluble metals. However, these modifications slightly changed the regression equations generated from the FeOOH and SOM sorption curves which subsequently changed the predicted concentrations of sorbed and complexed metals. As a result, sometimes the predicted concentrations of complexed or sorbed metals in the CMA are larger than the predicted concentrations of complexed or sorbed metals in the NCMA. The impact to the overall performance of the CMA is minimal due to its isolated nature and the minor changes in predicted values. Overall, the CMA is a better predictor of copper partitioning in these soils than the NCMA. The predicted partitioning is within reasonable variation of the experimental data.

5.3.4 Lead

99-1-0-7 Lead (Tables 37 and 38)

The total lead concentration reported for sample 99-1-0-7 is 4,435 mg kg^{-1}. The soluble, exchangeable, and sorbed/complexed lead concentrations are 0.320 mg kg^{-1}, 11.8 mg kg^{-1}, and NA, respectively. The NCMA predicts exchangeable, sorbed, and complexed lead concentrations of 2.42, 149, and 166 mg kg^{-1}, respectively. The CMA predicts exchangeable, sorbed, and complexed lead concentrations of 1.04, 107, and 63.9 mg kg^{-1}, respectively. Both modeling approaches slightly underpredict the concentration of exchangeable lead reported for this soil. The predicted sorbed and complexed lead concentrations can not be compared to any experimental data. However, based on published metal cation affinity sequences for clays (Farrah et al., 1980), FeOOH (Dzombak and Morel, 1990), and humic substances (Gustafsson, 2004), and binding constants incorporated in the Visual MINTEQ and MINEQL$^+$ databases, the predicted partitioning between the FeOOH and SOM fractions appears reasonable.

99-1-7-12 Lead (Tables 39 and 40)

The total lead concentration reported for sample 99-1-7-12 is 3,233 mg kg^{-1}. The soluble, exchangeable, and sorbed/complexed lead concentrations are 3.48 mg kg^{-1}, 117 mg kg^{-1}, and NA, respectively. The NCMA predicts exchangeable, sorbed, and complexed lead concentrations of 2.33, 26.6, and 48.1 mg kg^{-1}, respectively, while the CMA predicts exchangeable, sorbed, and complexed lead concentrations of 1.87, 19.0, and 22.6 mg kg^{-1}, respectively. Both modeling approaches significantly underpredict the

Table 37. Comparison of modeling output data to experimental data for lead in sample 99-1-0-7 [non-competitive modeling approach – lead only]

Modeling Data: [99-1-0-7] [Input and Predicted Concentrations]	Input Soluble Lead[1]	Predicted Exchangeable Lead[2]	Predicted Sorbed and Complexed Lead[2]	Total Predicted E, S, and C[3] Lead
	mg L^{-1}	mg kg^{-1}	mg kg^{-1}	mg kg^{-1}
	0.008	2.42	149 [S]; 166 [C]	317
Experimental Data: [99-1-0-7] $[Pb^{+2}_{Total}]$ = 4,435 mg kg^{-1}	**Soluble Lead[1]**	**Exchangeable Lead[4]**	**Sorbed and Complexed Lead**	**Total E, S, and C[3] Lead**
Vacuum Extraction Method	mg kg^{-1}	mg kg^{-1}	mg kg^{-1}	mg kg^{-1}
0.01M $Ca(NO_3)_2$ Extractable	0.320	-	-	-
0.03M $La(NO_3)_3$ Extractable	[0.320]	11.8	-	-
0.05M $Pb(NO_3)_2$ Extractable	NA	NA	NA	NA

1 Soluble lead concentration based on extraction with 0.01M calcium nitrate.

2 Predicted value obtained from the sum of all component desorption curves at reported soluble lead concentration.

3 [E] Exhangeable; [S] Sorbed; [C] Complexed.

4 Exchangeable lead equals 0.03M lanthanum nitrate extractable lead minus 0.01M calcium nitrate extractable lead (i.e., 12.1-0.320).

NA - Not analyzed.

Table 38. Comparison of modeling output data to experimental data for lead in sample 99-1-0-7 [competitive modeling approach – lead with cadmium, copper, and zinc]

Modeling Data: [99-1-0-7] [Input and Predicted Concentrations]	Input Soluble Lead[1]	Predicted Exchangeable Lead[2]	Predicted Sorbed and Complexed Lead[2]	Total Predicted E, S, and C[3] Lead
	mg L^{-1}	mg kg^{-1}	mg kg^{-1}	mg kg^{-1}
	0.008	1.04	107 [S]; 63.9 [C]	172

Experimental Data: [99-1-0-7] $[Pb^{+2}_{Total}]$ = 4,435 mg kg^{-1}	Soluble Lead[1]	Exchangeable Lead[4]	Sorbed and Complexed Lead	Total E, S, and C[3] Lead
Vacuum Extraction Method	mg kg^{-1}	mg kg^{-1}	mg kg^{-1}	mg kg^{-1}
0.01M $Ca(NO_3)_2$ Extractable	0.320	-	-	-
0.03M $La(NO_3)_3$ Extractable	[0.320]	11.8	-	-
0.05M $Pb(NO_3)_2$ Extractable	NA	NA	NA	NA

[1] Soluble lead concentration based on extraction with 0.01M calcium nitrate.

[2] Predicted value obtained from the sum of all component desorption curves at reported soluble lead concentration.

[3] [E] Exhangeable; [S] Sorbed; [C] Complexed.

[4] Exchangeable lead equals 0.03M lanthanum nitrate extractable lead minus 0.01M calcium nitrate extractable lead (i.e., 12.1-0.320).

NA - Not analyzed.

Table 39. Comparison of modeling output data to experimental data for lead in sample 99-1-7-12 [non-competitive modeling approach – lead only]

Modeling Data: [99-1-7-12] [Input and Predicted Concentrations]	Input Soluble Lead[1]	Predicted Exchangeable Lead[2]	Predicted Sorbed and Complexed Lead[2]	Total Predicted E, S, and C[3] Lead
	mg L^{-1}	mg kg^{-1}	mg kg^{-1}	mg kg^{-1}
	0.087	2.32	26.6 [S]; 48.1 [C]	77.0

Experimental Data: [99-1-7-12] [Pb^{+2}_{Total}] = 3,233 mg kg^{-1}	Soluble Lead[1]	Exchangeable Lead[4]	Sorbed and Complexed Lead	Total E, S, and C[3] Lead
Vacuum Extraction Method	mg kg^{-1}	mg kg^{-1}	mg kg^{-1}	mg kg^{-1}
0.01M $Ca(NO_3)_2$ Extractable	3.48	-	-	-
0.03M $La(NO_3)_3$ Extractable	[3.48]	117	-	-
0.05M $Pb(NO_3)_2$ Extractable	NA	NA	NA	NA

1 Soluble lead concentration based on calcium nitrate vacuum extraction method.

2 Predicted value obtained from the sum of all component desorption curves at reported soluble lead concentration.

3 [E] Exhangeable; [S] Sorbed; [C] Complexed.

4 Exchangeable lead equals 0.03M lanthanum nitrate extractable lead minus 0.01M calcium nitrate extractable lead (i.e., 120-3.48).

NA - Not analyzed.

Table 40. Comparison of modeling output data to experimental data for lead in sample 99-1-7-12 [competitive modeling approach – lead with cadmium, copper, and zinc]

Modeling Data: [99-1-7-12] [Input and Predicted Concentrations]	Input Soluble Lead[1]	Predicted Exchangeable Lead[2]	Predicted Sorbed and Complexed Lead[2]	Total Predicted E, S, and C[3] Lead
	mg L^{-1}	mg kg^{-1}	mg kg^{-1}	mg kg^{-1}
	0.087	1.87	19.0 [S]; 22.6 [C]	43.5
Experimental Data: [99-1-7-12] $[Pb^{+2}_{Total}]$ = 3,233 mg kg^{-1}	Soluble Lead[1]	Exchangeable Lead[4]	Sorbed and Complexed Lead	Total E, S, and C[3] Lead
Vacuum Extraction Method	mg kg^{-1}	mg kg^{-1}	mg kg^{-1}	mg kg^{-1}
0.01M $Ca(NO_3)_2$ Extractable	3.48	-	-	-
0.03M $La(NO_3)_3$ Extractable	[3.48]	117	-	-
0.05M $Pb(NO_3)_2$ Extractable	NA	NA	NA	NA

1 Soluble lead concentration based on calcium nitrate vacuum extraction method.

2 Predicted value obtained from the sum of all component desorption curves at reported soluble lead concentration.

3 [E] Exhangeable; [S] Sorbed; [C] Complexed.

4 Exchangeable lead equals 0.03M lanthanum nitrate extractable lead minus 0.01M calcium nitrate extractable lead (i.e., 120-3.48).

NA - Not analyzed.

concentration of exchangeable lead reported for this soil. However, the predicted lead partitioning reported by the NCMA and CMA appear reasonable based on published data.

The recovery of 10X more soluble and exchangeable lead from 99-1-7-12, the lowest pH soil, than 99-1-0-7 is unexpected and may be the result of smaller concentrations of available FeOOH and SOM binding sites. Lower concentrations of sorbed and complexed lead are expected in strongly acid soils due to a less negative solid surface. The decrease in negatively charged solid surfaces is due to the increased sorption of protons, which bind more strongly to FeOOH and SOM than lead. Any conclusions regarding the ability of the two modeling approaches to predict exchangeable lead in this soil depends on the cause of the high concentrations of exchangeable lead.

98-3-5-10 Lead (Tables 41 and 42)

The total lead concentration reported for sample 98-3-5-10 is 18,640 mg kg^{-1}. The soluble, exchangeable, and sorbed/complexed lead concentrations are 9.40 mg kg^{-1}, 81.8 mg kg^{-1}, and NA, respectively. The NCMA predicts exchangeable, sorbed, and complexed lead concentrations of 41.8, 1,052, and 2,355 mg kg^{-1}, respectively. The CMA predicts exchangeable, sorbed, and complexed lead concentrations of 7.24, 149, and 261 mg kg^{-1}, respectively. In this case, the NCMA is a better predictor of exchangeable lead than the CMA.

The significant decrease in CMA predicted concentrations of sorbed/complexed lead may be the result of copper and zinc competition for available binding sites. Similar results were described for lead sorption in the kaolinite system (Section 5.2.1).

Table 41. Comparison of modeling output data to experimental data for lead in sample 98-3-5-10 [non-competitive modeling approach – lead only]

Modeling Data: [98-3-5-10] [Input and Predicted Concentrations]	Input Soluble Lead[1]	Predicted Exchangeable Lead[2]	Predicted Sorbed and Complexed Lead[2]	Total Predicted E, S, and C[3] Lead
	mg L^{-1}	mg kg^{-1}	mg kg^{-1}	mg kg^{-1}
	0.235	41.8	1,052 [S]; 2,355 [C]	3,449
Experimental Data: [98-3-5-10] [Pb^{+2}_{Total}] = 18,640 mg kg^{-1}	**Soluble Lead[1]**	**Exchangeable Lead[4]**	**Sorbed and Complexed Lead**	**Total E, S, and C[3] Lead**
Vacuum Extraction Method	mg kg^{-1}	mg kg^{-1}	mg kg^{-1}	mg kg^{-1}
0.01M $Ca(NO_3)_2$ Extractable	9.40	-	-	-
0.03M $La(NO_3)_3$ Extractable	[9.40]	81.8	-	-
0.05M $Pb(NO_3)_2$ Extractable	NA	NA	NA	NA

1 Soluble lead concentration based on extraction with 0.01M calcium nitrate.

2 Predicted value obtained from the sum of all component desorption curves at reported soluble lead concentration.

3 [E] Exhangeable; [S] Sorbed; [C] Complexed.

4 Exchangeable lead equals 0.03M lanthanum nitrate extractable lead minus 0.01M calcium nitrate extractable lead (i.e., 91.2-9.40).

NA - Not analyzed.

Table 42. Comparison of modeling output data to experimental data for lead in sample 98-3-5-10 [competitive modeling approach – lead with cadmium, copper, and zinc]

Modeling Data: [98-3-5-10] [Input and Predicted Concentrations]	Input Soluble Lead[1]	Predicted Exchangeable Lead[2]	Predicted Sorbed and Complexed Lead[2]	Total Predicted E, S, and C[3] Lead
	mg L^{-1}	mg kg^{-1}	mg kg^{-1}	mg kg^{-1}
	0.235	7.24	149 [S]; 261 [C]	417
Experimental Data: [98-3-5-10] $[Pb^{+2}_{Total}]$ = 18,640 mg kg^{-1}	**Soluble Lead[1]**	**Exchangeable Lead[4]**	**Sorbed and Complexed Lead**	**Total E, S, and C[3] Lead**
Vacuum Extraction Method	mg kg^{-1}	mg kg^{-1}	mg kg^{-1}	mg kg^{-1}
0.01M $Ca(NO_3)_2$ Extractable	9.40	-	-	-
0.03M $La(NO_3)_3$ Extractable	[9.40]	81.8	-	-
0.05M $Pb(NO_3)_2$ Extractable	NA	NA	NA	NA

1 Soluble lead concentration based on extraction with 0.01M calcium nitrate.

2 Predicted value obtained from the sum of all component desorption curves at reported soluble lead concentration.

3 [E] Exhangeable; [S] Sorbed; [C] Complexed.

4 Exchangeable lead equals 0.03M lanthanum nitrate extractable lead minus 0.01M calcium nitrate extractable lead (i.e., 91.2-9.40).

NA - Not analyzed.

98-3-20-25 Lead (Tables 43 and 44)

The total lead concentration reported for sample 98-3-20-25 is 14,440 mg kg^{-1}. The soluble, exchangeable, and sorbed/complexed lead concentrations are 1.24 mg kg^{-1}, 30.5 mg kg^{-1}, and NA, respectively. The NCMA predicts exchangeable, sorbed, and complexed lead concentrations of 16.8, 739, and 1,050 mg kg^{-1}, respectively. The CMA predicts exchangeable, sorbed, and complexed lead concentrations of 2.29, 25.7, and 132 mg kg^{-1}, respectively. The NCMA appears to be a better predictor of exchangeable lead in this soil. The CMA model results, which are similar to 98-3-5-10, indicate the competition of lead, zinc, and copper for available binding sites may play an important role in predicted lead partitioning.

Summary of Lead Modeling

Only limited comparisons between the modeling results and experimental data can be made due to the absence of any experimental sorbed/complexed lead data. Although both modeling approaches make reasonable predictions of exchangeable lead, the NCMA is a better predictor than the CMA. The predicted lead partitioning appears to be reasonable based on published metal cation affinity sequences.

5.3.5 Zinc

99-1-0-7 Zinc (Tables 45 and 46)

The total zinc concentration reported for sample 99-1-0-7 is 7,760 mg kg^{-1}. The soluble, exchangeable, and sorbed/complexed zinc concentrations are 65.2, 26.4, and 204

Table 43. Comparison of modeling output data to experimental data for lead in sample 98-3-20-25 [non-competitive modeling – lead only]

Modeling Data: [98-3-20-25] [Input and Predicted Concentrations]	Input Soluble Lead[1]	Predicted Exchangeable Lead[2]	Predicted Sorbed and Complexed Lead[2]	Total Predicted E, S, and C[3] Lead
	mg L^{-1}	mg kg^{-1}	mg kg^{-1}	mg kg^{-1}
	0.031	16.8	739 [S]; 1,050 [C]	1,806
Experimental Data: [98-3-20-25] [Pb^{+2}_{Total}] = 14,440 mg kg^{-1}	**Soluble Lead[1]**	**Exchangeable Lead[4]**	**Sorbed and Complexed Lead**	**Total E, S, and C[3] Lead**
Vacuum Extraction Method	mg kg^{-1}	mg kg^{-1}	mg kg^{-1}	mg kg^{-1}
0.01M $Ca(NO_3)_2$ Extractable	1.24	-	-	-
0.03M $La(NO_3)_3$ Extractable	[1.24]	30.5	-	-
0.05M $Pb(NO_3)_2$ Extractable	NA	NA	NA	NA

---

[1] Soluble lead concentration based on extraction with 0.01M calcium nitrate.

[2] Predicted value obtained from the sum of all component desorption curves at reported soluble lead concentration.

[3] [E] Exhangeable; [S] Sorbed; [C] Complexed.

[4] Exchangeable lead equals 0.03M lanthanum nitrate extractable lead minus 0.01M calcium nitrate extractable lead (i.e., 31.7-1.24).

NA - Not analyzed.

Table 44. Comparison of modeling output data to experimental data for lead in sample 98-3-20-25 [competitive modeling approach – lead with cadmium, copper, and zinc]

Modeling Data: [98-3-20-25] [Input and Predicted Concentrations]	Input Soluble Lead[1]	Predicted Exchangeable Lead[2]	Predicted Sorbed and Complexed Lead[2]	Total Predicted E, S, and C[3] Lead
	mg L^{-1}	mg kg^{-1}	mg kg^{-1}	mg kg^{-1}
	0.031	2.29	25.7 [S]; 132 [C]	160
Experimental Data: [98-3-20-25] [Pb^{+2}_{Total}] = 14,440 mg kg^{-1}	**Soluble Lead[1]**	**Exchangeable Lead[4]**	**Sorbed and Complexed Lead**	**Total E, S, and C[3] Lead**
Vacuum Extraction Method	mg kg^{-1}	mg kg^{-1}	mg kg^{-1}	mg kg^{-1}
0.01M $Ca(NO_3)_2$ Extractable	1.24	-	-	-
0.03M $La(NO_3)_3$ Extractable	[1.24]	30.5	-	-
0.05M $Pb(NO_3)_2$ Extractable	NA	NA	NA	NA

1 Soluble lead concentration based on extraction with 0.01M calcium nitrate.

2 Predicted value obtained from the sum of all component desorption curves at reported soluble lead concentration.

3 [E] Exhangeable; [S] Sorbed; [C] Complexed.

4 Exchangeable lead equals 0.03M lanthanum nitrate extractable lead minus 0.01M calcium nitrate extractable lead (i.e., 31.7-1.24).

NA - Not analyzed.

Table 45. Comparison of modeling output data to experimental data for zinc in sample 99-1-0-7 [non-competitive modeling approach – zinc only]

Modeling Data: [99-1-0-7] [Input and Predicted Concentrations]	Input Soluble Zinc[1]	Predicted Exchangeable Zinc[2]	Predicted Sorbed and Complexed Zinc[2]	Total Predicted E, S, and C[3] Zinc
	mg L^{-1}	mg kg^{-1}	mg kg^{-1}	mg kg^{-1}
	1.63	21.4	34.8 [S]; 183 [C]	239
Experimental Data: [99-1-0-7] $[Zn^{+2}_{Total}]$ = 7,760 mg kg^{-1}	Soluble Zinc[1]	Exchangeable Zinc[4]	Sorbed and Complexed Zinc[5]	Total E, S, and C[3] Zinc
Vacuum Extraction Method	mg kg^{-1}	mg kg^{-1}	mg kg^{-1}	mg kg^{-1}
0.01M $Ca(NO_3)_2$ Extractable	65.2	-	-	-
0.03M $La(NO_3)_3$ Extractable	[65.2]	26.4	-	-
0.05M $Pb(NO_3)_2$ Extractable	[65.2]	[26.4]	204	231

1 Soluble zinc concentration based on extraction with 0.01M calcium nitrate.

2 Predicted value obtained from the sum of all component desorption curves at reported soluble zinc concentration.

3 [E] Exhangeable; [S] Sorbed; [C] Complexed.

4 Exchangeable zinc equals 0.03M lanthanum nitrate extractable zinc minus 0.01M calcium nitrate extractable zinc (i.e., 91.6-65.2).

5 Sorbed and complexed zinc equals 0.05M lead nitrate extractable zinc minus the sum of 0.03M lanthanum nitrate extractable zinc and 0.01M calcium nitrate extractable zinc (i.e., 296-(26.4+65.2)).

Table 46. Comparison of modeling output data to experimental data for zinc in sample 99-1-0-7 [competitive modeling approach – zinc with cadmium, copper, and lead]

Modeling Data: [99-1-0-7] [Input and Predicted Concentrations]	Input Soluble Zinc[1]	Predicted Exchangeable Zinc[2]	Predicted Sorbed and Complexed Zinc[2]	Total Predicted E, S, and C[3] Zinc
	mg L^{-1}	mg kg^{-1}	mg kg^{-1}	mg kg^{-1}
	1.63	19.3	21.7 [S]; 117 [C]	158

Experimental Data: [99-1-0-7] [Zn^{+2}_{Total}] = 7,760 mg kg^{-1}	Soluble Zinc[1]	Exchangeable Zinc[4]	Sorbed and Complexed Zinc[5]	Total E, S, and C[3] Zinc
Vacuum Extraction Method	mg kg^{-1}	mg kg^{-1}	mg kg^{-1}	mg kg^{-1}
0.01M $Ca(NO_3)_2$ Extractable	65.2	-	-	-
0.03M $La(NO_3)_3$ Extractable	[65.2]	26.4	-	-
0.05M $Pb(NO_3)_2$ Extractable	[65.2]	[26.4]	204	231

1 Soluble zinc concentration based on extraction with 0.01M calcium nitrate.

2 Predicted value obtained from the sum of all component desorption curves at reported soluble zinc concentration.

3 [E] Exhangeable; [S] Sorbed; [C] Complexed.

4 Exchangeable zinc equals 0.03M lanthanum nitrate extractable zinc minus 0.01M calcium nitrate extractable zinc (i.e., 91.6-65.2).

5 Sorbed and complexed zinc equals 0.05M lead nitrate extractable zinc minus the sum of 0.03M lanthanum nitrate extractable zinc and 0.01M calcium nitrate extractable zinc (i.e., 296-(26.4+65.2)).

mg kg^{-1}, respectively. The NCMA predicts exchangeable, sorbed, and complexed zinc concentrations of 21.4, 34.8, and 183 mg kg^{-1}, respectively. The CMA predicts exchangeable, sorbed, and complexed lead concentrations of 19.3, 21.7, and 117 mg kg^{-1}, respectively. Both modeling approaches accurately predict zinc partitioning in this soil, although the NCMA is a slightly better predictor than the CMA.

99-1-7-12 Zinc (Tables 47 and 48)

The total zinc concentration reported for sample 99-1-7-12 is 1,822 mg kg^{-1}. The soluble, exchangeable, and sorbed/complexed zinc concentrations are 32.1, 6.40, and 10.7 mg kg^{-1}, respectively. The NCMA predicts exchangeable, sorbed, and complexed zinc concentrations of 11.0, 0.081, and 46.5 mg kg^{-1}, respectively, while the CMA predicts exchangeable, sorbed, and complexed zinc concentrations of 10.4, 0.081, and 25.7 mg kg^{-1}, respectively. Although the NCMA and CMA can predict zinc partitioning in this soil, the CMA is a better predictor than the NCMA.

98-3-5-10 Zinc (Tables 49 and 50)

The total zinc concentration reported for sample 98-3-5-10 is 18,020 mg kg^{-1}. The soluble, exchangeable, and sorbed/complexed zinc concentrations are 163, 0, and 631 mg kg^{-1}, respectively. The NCMA predicts exchangeable, sorbed, and complexed zinc concentrations of 74.2, 195, and 1,067 mg kg^{-1}, respectively. The CMA predicts exchangeable, sorbed, and complexed zinc concentrations of 48.9, 130, and 259 mg kg^{-1}, respectively.

Table 47. Comparison of modeling output data to experimental data for zinc in sample 99-1-7-12 [non-competitive modeling approach – zinc only]

Modeling Data: [99-1-7-12] [Input and Predicted Concentrations]	Input Soluble Zinc[1]	Predicted Exchangeable Zinc[2]	Predicted Sorbed and Complexed Zinc[2]	Total Predicted E, S, and C[3] Zinc
	mg L^{-1}	mg kg^{-1}	mg kg^{-1}	mg kg^{-1}
	0.803	11.0	0.081 [S]; 46.5 [C]	57.6
Experimental Data: [99-1-7-12] $[Zn^{+2}_{Total}]$ = 1,822 mg kg^{-1}	**Soluble Zinc[1]**	**Exchangeable Zinc[4]**	**Sorbed and Complexed Zinc[5]**	**Total E, S, and C[3] Zinc**
Vacuum Extraction Method	mg kg^{-1}	mg kg^{-1}	mg kg^{-1}	mg kg^{-1}
0.01M $Ca(NO_3)_2$ Extractable	32.1	-	-	-
0.03M $La(NO_3)_3$ Extractable	[32.1]	6.40	-	-
0.05M $Pb(NO_3)_2$ Extractable	[32.1]	[6.40]	10.7	17.1

1 Soluble zinc concentration based on extraction with 0.01M calcium nitrate.

2 Predicted value obtained from the sum of all component desorption curves at reported soluble zinc concentration.

3 [E] Exhangeable; [S] Sorbed; [C] Complexed.

4 Exchangeable zinc equals 0.03M lanthanum nitrate extractable zinc minus 0.01M calcium nitrate extractable zinc (i.e., 38.5-32.1).

5 Sorbed and complexed zinc equals 0.05M lead nitrate extractable zinc minus the sum of 0.03M lanthanum nitrate extractable zinc and 0.01M calcium nitrate extractable zinc (i.e., 49.2-(6.40+32.1)).

Table 48. Comparison of modeling output data to experimental data for zinc in sample 99-1-7-12 [competitive modeling approach – zinc with cadmium, copper, and lead]

Modeling Data: [99-1-7-12] [Input and Predicted Concentrations]	Input Soluble Zinc[1]	Predicted Exchangeable Zinc[2]	Predicted Sorbed and Complexed Zinc[2]	Total Predicted E, S, and C[3] Zinc
	mg L^{-1}	mg kg^{-1}	mg kg^{-1}	mg kg^{-1}
	0.803	10.4	0.080 [S]; 25.7 [C]	36.2
Experimental Data: [99-1-7-12] $[\text{Zn}^{+2}_{\text{Total}}]$ = 1,822 mg kg^{-1}	Soluble Zinc[1]	Exchangeable Zinc[4]	Sorbed and Complexed Zinc[5]	Total E, S, and C[3] Zinc
Vacuum Extraction Method	mg kg^{-1}	mg kg^{-1}	mg kg^{-1}	mg kg^{-1}
0.01M $Ca(NO_3)_2$ Extractable	32.1	-	-	-
0.03M $La(NO_3)_3$ Extractable	[32.1]	6.40	-	-
0.05M $Pb(NO_3)_2$ Extractable	[32.1]	[6.40]	10.7	17.1

1 Soluble zinc concentration based on extraction with 0.01M calcium nitrate.

2 Predicted value obtained from the sum of all component desorption curves at reported soluble zinc concentration.

3 [E] Exhangeable; [S] Sorbed; [C] Complexed.

4 Exchangeable zinc equals 0.03M lanthanum nitrate extractable zinc minus 0.01M calcium nitrate extractable zinc (i.e., 38.5-32.1).

5 Sorbed and complexed zinc equals 0.05M lead nitrate extractable zinc minus the sum of 0.03M lanthanum nitrate extractable zinc and 0.01M calcium nitrate extractable zinc (i.e., 49.2-(6.40+32.1)).

Table 49. Comparison of modeling output data to experimental data for zinc in sample 98-3-5-10 [non-competitive modeling approach – zinc only]

Modeling Data: [98-3-5-10] [Input and Predicted Concentrations]	Input Soluble Zinc[1]	Predicted Exchangeable Zinc[2]	Predicted Sorbed and Complexed Zinc[2]	Total Predicted E, S, and C[3] Zinc
	mg L^{-1}	mg kg^{-1}	mg kg^{-1}	mg kg^{-1}
	4.08	74.2	195 [S]; 1,067 [C]	1,336
Experimental Data: [98-3-5-10] [Zn$^{+2}_{\text{Total}}$] = 18,020 mg kg^{-1}	**Soluble Zinc[1]**	**Exchangeable Zinc[4]**	**Sorbed and Complexed Zinc[5]**	**Total E, S, and C[3] Zinc**
Vacuum Extraction Method	mg kg^{-1}	mg kg^{-1}	mg kg^{-1}	mg kg^{-1}
0.01M $Ca(NO_3)_2$ Extractable	163	-	-	-
0.03M $La(NO_3)_3$ Extractable	[163]	0	-	-
0.05M $Pb(NO_3)_2$ Extractable	[163]	[0]	631	631

[1] Soluble zinc concentration based on extraction with 0.01M calcium nitrate.

[2] Predicted value obtained from the sum of all component desorption curves at reported soluble zinc concentration.

[3] [E] Exhangeable; [S] Sorbed; [C] Complexed.

[4] Exchangeable zinc equals 0.03M lanthanum nitrate extractable zinc minus 0.01M calcium nitrate extractable zinc (i.e., 152-163).

[5] Sorbed and complexed zinc equals 0.05M lead nitrate extractable zinc minus the sum of 0.03M lanthanum nitrate extractable zinc and 0.01M calcium nitrate extractable zinc (i.e., 794-(0+163)).

Table 50. Comparison of modeling output data to experimental data for zinc in sample 98-3-5-10 [competitive modeling approach – zinc with cadmium, copper, and lead]

Modeling Data: [98-3-5-10] [Input and Predicted Concentrations]	Input Soluble Zinc[1]	Predicted Exchangeable Zinc[2]	Predicted Sorbed and Complexed Zinc[2]	Total Predicted E, S, and C[3] Zinc
	mg L^{-1}	mg kg^{-1}	mg kg^{-1}	mg kg^{-1}
	4.08	48.9	130 [S]; 259 [C]	438
Experimental Data: [98-3-5-10] [Zn^{+2}_{Total}] = 18,020 mg kg^{-1}	Soluble Zinc[1]	Exchangeable Zinc[4]	Sorbed and Complexed Zinc[5]	Total E, S, and C[3] Zinc
Vacuum Extraction Method	mg kg^{-1}	mg kg^{-1}	mg kg^{-1}	mg kg^{-1}
0.01M $Ca(NO_3)_2$ Extractable	163	-	-	-
0.03M $La(NO_3)_3$ Extractable	[163]	0	-	-
0.05M $Pb(NO_3)_2$ Extractable	[163]	[0]	631	631

[1] Soluble zinc concentration based on extraction with 0.01M calcium nitrate.

[2] Predicted value obtained from the sum of all component desorption curves at reported soluble zinc concentration.

[3] [E] Exhangeable; [S] Sorbed; [C] Complexed.

[4] Exchangeable zinc equals 0.03M lanthanum nitrate extractable zinc minus 0.01M calcium nitrate extractable zinc (i.e., 152-163).

[5] Sorbed and complexed zinc equals 0.05M lead nitrate extractable zinc minus the sum of 0.03M lanthanum nitrate extractable zinc and 0.01M calcium nitrate extractable zinc (i.e., 794-(0+163)).

No exchangeable zinc is reported for this soil because the concentration of soluble zinc is greater than the concentration of exchangeable zinc. Both modeling approaches predict an exchangeable zinc concentration in the range of values reported for both soluble and exchangeable zinc. The CMA is a better predictor of sorbed/complexed zinc than the NCMA.

98-3-20-25 Zinc (Tables 51 and 52)

The total zinc concentration reported for sample 98-3-20-25 is 14,120 mg kg^{-1}. The soluble, exchangeable, and sorbed/complexed zinc concentrations are 133, 0, and 310 mg kg^{-1}, respectively. The NCMA predicts exchangeable, sorbed, and complexed zinc concentrations of 51.0, 341, and 504 mg kg^{-1}, respectively. The CMA predicts exchangeable, sorbed, and complexed zinc concentrations of 39.2, 216, and 140 mg kg^{-1}.

No exchangeable zinc is reported for this soil because the concentration of soluble zinc is greater than the concentration of exchangeable zinc. Both modeling approaches predict an exchangeable zinc concentration in the range of values reported for both soluble and exchangeable zinc. The CMA is a better predictor of sorbed/complexed zinc than the NCMA.

Summary of Zinc Modeling

At the lower pHs and concentrations of total and soluble zinc, both modeling approaches can predict zinc partitioning. In sample 99-1-0-7, the NCMA is a better predictor of zinc partitioning than the CMA, while the opposite is indicated in sample 99-

Table 51. Comparison of modeling output data to experimental data for zinc in sample 98-3-20-25 [non-competitive modeling approach – zinc only]

Modeling Data: [98-3-20-25] [Input and Predicted Concentrations]	Input Soluble Zinc[1]	Predicted Exchangeable Zinc[2]	Predicted Sorbed and Complexed Zinc[2]	Total Predicted E, S, and C[3] Zinc
	mg L^{-1}	mg kg^{-1}	mg kg^{-1}	mg kg^{-1}
	3.33	51.0	341 [S]; 504 [C]	896
Experimental Data: [98-3-20-25] [Zn^{+2}_{Total}] = 14,120 mg kg^{-1}	**Soluble Zinc[1]**	**Exchangeable Zinc[4]**	**Sorbed and Complexed Zinc[5]**	**Total E, S, and C[3] Zinc**
Vacuum Extraction Method	mg kg^{-1}	mg kg^{-1}	mg kg^{-1}	mg kg^{-1}
0.01M $Ca(NO_3)_2$ Extractable	133	-	-	-
0.03M $La(NO_3)_3$ Extractable	[133]	0	-	-
0.05M $Pb(NO_3)_2$ Extractable	[133]	[0]	310	310

1 Soluble zinc concentration based on extraction with 0.01M calcium nitrate.

2 Predicted value obtained from the sum of all component desorption curves at reported soluble zinc concentration.

3 [E] Exhangeable; [S] Sorbed; [C] Complexed.

4 Exchangeable zinc equals 0.03M lanthanum nitrate extractable zinc minus 0.01M calcium nitrate extractable zinc (i.e., 131-133).

5 Sorbed and complexed zinc equals 0.05M lead nitrate extractable zinc minus the sum of 0.03M lanthanum nitrate extractable zinc and 0.01M calcium nitrate extractable zinc (i.e., 443-(0+133)).

Table 52. Comparison of modeling output data to experimental data for zinc in sample 98-3-20-25 [competitive modeling approach – zinc with cadmium, copper, and lead]

Modeling Data: [98-3-20-25] [Input and Predicted Concentrations]	Input Soluble Zinc[1]	Predicted Exchangeable Zinc[2]	Predicted Sorbed and Complexed Zinc[2]	Total Predicted E, S, and C[3] Zinc
	mg L^{-1}	mg kg^{-1}	mg kg^{-1}	mg kg^{-1}
	3.33	39.2	216 [S]; 140 [C]	395
Experimental Data: [98-3-20-25] $[Zn^{+2}_{Total}]$ = 14,120 mg kg^{-1}	**Soluble Zinc[1]**	**Exchangeable Zinc[4]**	**Sorbed and Complexed Zinc[5]**	**Total E, S, and C[3] Zinc**
Vacuum Extraction Method	mg kg^{-1}	mg kg^{-1}	mg kg^{-1}	mg kg^{-1}
0.01M $Ca(NO_3)_2$ Extractable	133	-	-	-
0.03M $La(NO_3)_3$ Extractable	[133]	0	-	-
0.05M $Pb(NO_3)_2$ Extractable	[133]	[0]	310	310

1 Soluble zinc concentration based on extraction with 0.01M calcium nitrate.

2 Predicted value obtained from the sum of all component desorption curves at reported soluble zinc concentration.

3 [E] Exhangeable; [S] Sorbed; [C] Complexed.

4 Exchangeable zinc equals 0.03M lanthanum nitrate extractable zinc minus 0.01M calcium nitrate extractable zinc (i.e., 131-133).

5 Sorbed and complexed zinc equals 0.05M lead nitrate extractable zinc minus the sum of 0.03M lanthanum nitrate extractable zinc and 0.01M calcium nitrate extractable zinc (i.e., 443-(0+133)).

1-7-12. At higher pHs and concentrations of total and soluble zinc, the CMA is a better predictor of sorbed/complexed zinc than the NCMA. Predicted zinc partitioning in the CMA is within reasonable variation of the experimental zinc data. Because the soluble zinc concentrations reported for the 98-1 soil profile are greater than the reported exchangeable zinc concentrations, no exchangeable zinc is reported for this location. However, the similar zinc concentrations reported for 0.01M $Ca(NO_3)_2$ and 0.03M $La(NO_3)_3$ are within a reasonable range of the predicted exchangeable zinc concentrations.

6.0 THE IMPACT ON METAL PARTITIONING PREDICTION DUE TO UNCERTAINTY IN CLAY, FEOOH AND SOM WEIGHTING FACTORS

A key step in the modeling approach developed in this research is the calculation of weighting factors that proportion the different specimen materials into a mixture approximating an actual soil. The uncertainty in these weighting factors, which are based on clay composition estimates and assumptions regarding what percent of the reported total Al^{3+}, Fe^{3+}, and soil organic carbon (SOC) concentrations are involved in metals binding, may significantly impact metal partitioning predictions. The evaluation of the impacts on predicted concentrations of exchangeable, sorbed, and complexed metals due to the uncertainty in these key components could provide information on which weighting factor has the most significant impact on a surrogate soil.

Because this modeling effort included such a large number of variables (i.e. four metals, three pH values, four textures, and a range of total Al^{3+}, Fe^{3+}, and SOC concentrations), this evaluation is limited in scope to five basic cases. Case $^{\#}1$ (the base case) represents surrogate soils constructed as described in Section 4.0 (Materials and Methods) and the modeling results reported in Section 5.0 (Results and Discussion). Case $^{\#}2$ represents surrogate soils where montmorillonite replaces illite as the dominant clay mineral (i.e. the estimated illite and montmorillonite percentages are switched), while the estimated percentage of kaolinite remains the same. Case $^{\#}2$ increases the concentrations of exchangeable and specific sorption binding sites associated with clay minerals by 97% and 2.7% respectively, in surrogate soil 99-1-7-12 and 39% and 10% respectively, in surrogate soil 98-3-20-25. Case #3, which represents surrogate soils where the total Al^{3+} concentration is reduced by 50% (the estimated clay composition remains unchanged), causes a 50% decrease in the concentrations of exchangeable and specific sorption binding sites associated with kaolinite, illite, and montmorillonite. Case #4 represents surrogate soils where the FeOOH/total Fe^{3+} ratio is increased from 0.5 (case #1) to 1.0, which doubles the concentration of specific sorption binding sites associated with FeOOH. Case #5, which represents surrogate soils where the SOM/SOC ratio is decreased from 1.0 (case #1) to 0.5, causes a 50% decrease in the concentration of complexation binding sites associated with SOM.

Total Al^{3+}, Fe^{3+}, and SOC data reported for three soils (99-1-0-7, 98-3-5-10, 98-3-20-25) are used in this evaluation. Sample 99-1-0-7 contains the lowest total Al^{3+}, Fe^{3+}, and SOC concentrations of the four Leadville soils used in this research. As a result, the surrogate soil constructed from 99-1-0-7 data contains the lowest estimated concentrations of exchangeable, specific sorption, and complexation binding sites. The surrogate soil constructed from 98-3-20-25 data (which has the highest concentrations of total Al^{3+} and Fe^{3+} of the four Leadville soils) contains the highest estimated concentrations of exchangeable and specific sorption binding sites associated with the three clay minerals and FeOOH. The surrogate soil constructed from sample 98-3-5-10 data (which has the highest concentration of SOC of the four Leadville soils) contains the highest estimated concentration of complexation binding sites. In addition, the lowest predicted concentrations of exchangeable, sorbed, and complexed metals are reported for surrogate soil 99-1-7-12. Surrogate soil 98-3-20-25 contains the highest predicted concentrations of exchangeable and sorbed metals, while surrogate soil 98-3-5-10 contains the highest predicted concentration of complexed metals.

The impacts of cases #2-#5 on predicted concentrations of exchangeable, sorbed, or complexed metals associated with the five specimen materials are linear in all cases (Appendix D, Tables D-1 to D-11). Using case #2 in surrogate soil 98-3-20-25 as an example (Appendix D, Tables D-6 and D-7), the estimated percent of illite decreases from 77% to 7%, while the estimated percent of montmorillonite increases from 7% to 77%, an 11-fold decrease and increase respectively, in the two clay minerals. The recalculated illite and montmorillonite weighting factors also decrease and increase approximately 11-fold (i.e. the illite weighting factor decreases from 0.297 to 0.028 and the montmorillonite weighting factor increases from 0.033 to 0.356). As a result, the predicted concentrations of exchangeable metals bound to illite decrease approximately 11-fold, while the predicted concentrations of exchangeable and sorbed metals bound to montmorillonite increase approximately 11-fold. The same effect is noted for case #3 in both surrogate soils where a 50% decrease in the total Al^{3+} concentration results in a 50% decrease in predicted concentrations of exchangeable and sorbed metals bound to kaolinite, illite, and montmorillonite (Appendix D, Tables D-1, D-3, D-6, and D-8). In case #4, the increase in the $FeOOH/Fe^{3+}$ ratio from 0.5 to 1.0 doubles the predicted concentrations of sorbed metals bound to FeOOH in both surrogate soils (Appendix D, Tables D-1, D-4, D-6, and D-9). In case #5, the decrease in the SOM/SOC ratio from 1.0 to 0.5 in both surrogate soils results in a 50% decrease in the predicted concentrations of complexed metals bound to SOM (Appendix D, Tables D-1, D-5, D-10, and D-11). The 1:1 response to changes in the various weighting factors is due to the fact that cases $^{\#}2$-$^{\#}5$ have no impact on the soluble metals concentrations used as model inputs nor the sorption curves used to calculate predicted concentrations of exchangeable, sorbed, and complexed metals. Cases $^{\#}2$-$^{\#}5$ impact only the final calculation step in the modeling process, the calculation of weighting factors.

Table 53 shows the changes in total predicted concentrations of exchangeable and sorbed metals bound to clay minerals do not reflect a 1:1 response to changes in the clay weighting factors (e.g. the impacts of cases $^{\#}2$ and $^{\#}3$ on surrogate soil 98-3-20-25). The changes in total predicted concentrations of sorbed and complexed metals bound to FeOOH and SOM show an approximate 1:1 response to changes in the FeOOH and SOM weighting factors (e.g. the impacts of cases $^{\#}4$ and $^{\#}5$ on surrogate soils 99-1-7-12, 98-3-20-25, and 98-3-5-10). The variation in response of the different specimen materials to changes in the weighting factors is primarily due to a combination of three factors; 1. the number and types of specimen materials making up a class of binding sites (i.e. exchangeable, sorbed, or complexed binding sites), 2. the affinities of the four metals for the different specimen materials, and 3. the predicted concentrations of metals bound to the different specimen materials in a particular class of binding sites. First, as previously described in Section 4.0, Materials and Methods, the total predicted concentrations of exchangeable and sorbed metals are the sum of concentrations of metals bound to two or more specimen materials. For example, the total predicted concentration of exchangeable metals is the sum of concentrations of metals bound to cation exchange sites on kaolinite,

Table 53. The impact of clay, FeOOH, and SOM weighting factors on predicted concentrations of total exchangeable, total sorbed, and total complexed metals (CMA).

99-1-7-12	Case #1	Case #2			Case #1	Case #2		98-3-20-25	Case #1	Case #2			Case #1	Case #2	
Exchangeable	mg kg^{-1}	mg kg^{-1}	%*	**Sorbed**	mg kg^{-1}	mg kg^{-1}	%*	**Exchangeable**	mg kg^{-1}	mg kg^{-1}	%*	**Sorbed**	mg kg^{-1}	mg kg^{-1}	%*
Cd	0.557	0.900	62	Cd	0.001	0.001	0	Cd	10.7	20.5	92	Cd	36.3	38.3	6
Cu	0.876	1.11	27	Cu	0.222	0.229	3	Cu	3.18	3.31	4	Cu	3.14	5.15	64
Pb	1.87	2.61	40	Pb	19.0	19.0	0	Pb	2.29	2.94	28	Pb	25.7	30.5	19
Zn	10.4	15.7	51	Zn	0.080	0.091	14	Zn	39.2	89.1	127	Zn	216	260	20

99-1-7-12	Case #1	Case #3			Case #1	Case #3		98-3-20-25	Case #1	Case #3			Case #1	Case #3	
Exchangeable	mg kg^{-1}	mg kg^{-1}	%*	**Sorbed**	mg kg^{-1}	mg kg^{-1}	%*	**Exchangeable**	mg kg^{-1}	mg kg^{-1}	%*	**Sorbed**	mg kg^{-1}	mg kg^{-1}	%*
Cd	0.557	0.301	-46	Cd	0.001	0.001	0	Cd	10.7	8.40	-22	Cd	36.3	36.3	0
Cu	0.876	0.658	-25	Cu	0.222	0.219	-1	Cu	3.18	3.14	-1	Cu	3.14	3.04	-3
Pb	1.87	1.16	-38	Pb	19.0	18.9	-1	Pb	2.29	2.08	-9	Pb	25.7	25.4	-1
Zn	10.4	5.63	-46	Zn	0.080	0.075	-6	Zn	39.2	22.5	-43	Zn	216	214	-1

99-1-7-12	Case #1	Case #4		98-3-20-25	Case #1	Case #4		99-1-7-12	Case #1	Case #5		98-3-5-10	Case #1	Case #5	
Sorbed	mg kg^{-1}	mg kg^{-1}	%*	**Sorbed**	mg kg^{-1}	mg kg^{-1}	%*	**Complexed**	mg kg^{-1}	mg kg^{-1}	%*	**Complexed**	mg kg^{-1}	mg kg^{-1}	%*
Cd	0.001	0.002	100	Cd	36.3	72.1	99	Cd	1.71	0.854	-50	Cd	228	114	-50
Cu	0.222	0.435	96	Cu	3.14	6.04	92	Cu	15.6	7.80	-50	Cu	237	119	-50
Pb	19.0	37.6	98	Pb	25.7	50.6	97	Pb	22.6	11.3	-50	Pb	261	130	-50
Zn	0.080	0.150	88	Zn	216	426	97	Zn	25.7	12.9	-50	Zn	259	129	-50

* represents the percent increase/decrease in predicted concentrations between case 1 and cases 2, 3, 4, or 5.

Case #1 represents surrogate soils as described in Sections 4.0 and 5.0.

Case #2 represents surrogate soils where montmorillonite replaces illite as the dominant clay mineral.

Case #3 represents surrogate soils where the estimated clay composition remains the same, but total Al^{3+} is reduced by 50%.

Case #4 represents surrogate soils where the FeOOH/total Fe^{3+} ratio increases from 0.5 to 1.0.

Case #5 represents surrogate soils where the SOM/SOC ratio decreases from 1.0 to 0.5.

illite, montmorillonite, dissolved SOM, plus (D) and (G) metal complexes associated with solid SOM. The total predicted concentration of sorbed metals is the sum of concentrations of metals bound to specific sorption sites on kaolinite, montmorillonite, and the strong and weak specific sorption sites associated with FeOOH. The total predicted concentration of complexed metals is solely the concentration of metals bound to solid SOM. Thus, any change in an individual weighting factor will have a direct 1:1 impact only on the predicted concentrations of metals bound to the affected specimen material. Predicted concentrations of metals bound to specimen materials unaffected by a particular test case will not be impacted. Second, the predicted concentrations of metals reflect the affinities of the different metals for a particular binding site on a specimen material. The approximate affinity sequence for kaolinite, illite, montmorillonite, and FeOOH is Pb>Cu>Zn>Cd, while the approximate affinity sequence for SOM is Cu>Pb>Zn>Cd. Third, the predicted concentrations of metals bound to each specimen material in a class of binding sites can significantly influence the response when one or more of the specimen materials in that class of binding sites is changed. For example, in surrogate soil 99-1-7-12 (Table 53) where a large concentration of sorbed lead is bound to the strong and weak binding sites associated with FeOOH and a small concentration of sorbed lead is bound to the three clay minerals, changing the clay fraction (i.e. cases $^{\#}2$ and $^{\#}3$) will have a small impact on the total predicted concentration of sorbed lead. However, in the case of zinc in surrogate soil 98-3-20-25 (Table 53), a large concentration of exchangeable zinc is bound to illite and montmorillonite, thus any change in the clay fraction (cases $^{\#}2$ and $^{\#}3$) will have a great impact on the total predicted concentration of exchangeable zinc. As Table 53 shows, sorting out the influence of each factor on the change in predicted concentrations of metals caused by one of the test cases is difficult and as a consequence, only generalizations can be made.

Generally speaking, in surrogate soils 99-1-7-12 and 98-3-20-25, cases #2 and #3 impact predicted concentrations of exchangeable cadmium and zinc more than exchangeable copper and lead. The results suggest the majority of exchangeable cadmium and zinc is bound to the clay fraction, while the majority of exchangeable copper and lead is bound to the FeOOH and SOM fractions. Overall, the impact of cases #2 and #3 on the predicted concentrations of exchangeable metals is greater in surrogate soil 99-1-7-12 than in surrogate soil 98-3-20-25. This result is due to the significantly lower predicted concentrations of exchangeable metals bound to the clay and SOM fractions in surrogate soil 99-1-7-12 versus 98-3-20-25. Thus, the change in the predicted concentrations of exchangeable metals bound to the clay fraction in surrogate soil 99-1-7-12 is not buffered by any significant concentrations of exchangeable metals bound to SOM. The impact of case #2 on the predicted concentrations of sorbed metals is greatest in surrogate soil 98-3-20-25 and is due to the high concentrations of metals plus the significant increase in specific sorption binding sites associated with montmorillonite.

The changes in predicted concentrations of sorbed metals reported for case #4 (Table 53) show an approximate two-fold increase in both surrogate soils. The two-fold increase corresponds to the doubling of specific sorption binding sites associated with FeOOH. The result is due to the fact that the majority of specific sorption sites available in these two surrogate soils is associated with FeOOH. Thus, a change in the FeOOH content results in an approximate 1:1 change in the predicted concentrations of sorbed metals. The changes in predicted concentrations of complexed metals reported for case #5 (Table 53) show a two-fold decrease in both surrogate soils. The identical changes are due to the fact that the SOM fraction consists only of metals bound to solid SOM. Thus, a decrease in the concentration of SOM also decreases the predicted concentrations of complexed metals by approximately the same amount.

Table 54 summarizes for each test case, the increase or decrease in the sum of predicted concentrations of metals (i.e. total exchangeable metals + total sorbed metals + total complexed metals). The percent changes reported in Table 54 for each test case are generally less than the percent changes reported in Table 53 for individual classes of binding sites. The smaller changes reported in Table 54 reflect the varying influence of each class of binding sites on the overall predicted concentrations of metals. In both surrogate soils, the impacts of cases #2 and #3 on the predicted concentrations of cadmium, copper, lead, and zinc are greater for cadmium and zinc than copper and lead. As discussed previously, the results are due to the fact that a high proportion of the cadmium and zinc are associated with the clay fraction. Thus, any change in the clay fraction due to cases #2 and #3 will impact cadmium and zinc more than copper or lead. For case #4, the results suggest that a significant fraction of the cadmium, lead, and zinc present in surrogate soil 98-3-20-25 is bound to FeOOH and that any change in the FeOOH weighting factor will cause a larger change in the predicted concentrations of metals than a similar change in the clay fraction. The small change in the predicted concentration of copper in surrogate soil 98-3-20-25 may reflect the fact that the majority

Table 54. The impact of clay, FeOOH, and SOM weighting factors on total predicted (exchangeable, sorbed, and complexed) metals concentrations (CMA).

99-1-7-12	Case #1 mg kg^{-1*}	Case #2 mg kg^{-1*}	Case #3 mg kg^{-1*}	Case #4 mg kg^{-1*}	Case #5 mg kg^{-1*}
Cd	2.27	2.61	2.01	2.27	1.39
Cu	16.7	16.9	16.5	16.9	8.68
Pb	43.5	44.2	42.7	62.1	31.9
Zn	36.2	41.5	31.4	36.3	23.0

99-1-7-12	Case #1 mg kg^{-1*}	Case #2 %	Case #3 %	Case #4 %	Case #5 %
Cd	2.27	15	-11	0	-39
Cu	16.7	1	-1	1	-48
Pb	43.5	2	-2	43	-27
Zn	36.2	15	-13	0	-37

98-3-20-25	Case #1 mg kg^{-1*}	Case #2 mg kg^{-1*}	Case #3 mg kg^{-1*}	Case #4 mg kg^{-1*}
Cd	173	185	171	209
Cu	135	137	135	138
Pb	160	165	159	185
Zn	395	489	376	605

98-3-20-25	Case #1 mg kg^{-1*}	Case #2 %	Case #3 %	Case #4 %
Cd	173	7	-1	21
Cu	135	2	0	2
Pb	160	3	0	16
Zn	395	24	-5	53

98-3-5-10	Case #1 mg kg^{-1*}	Case #5 mg kg^{-1*}
Cd	261	142
Cu	264	143
Pb	417	284
Zn	438	302

98-3-5-10	Case #1 mg kg^{-1*}	Case #5 %
Cd	261	-46
Cu	264	-46
Pb	417	-32
Zn	438	-31

* Sum of predicted total exchangeable, total sorbed, and total complexed metals concentrations.

Case #1 represents surrogate soils as described in Sections 4.0 and 5.0.

Case #2 represents surrogate soils where montmorillonite replaces illite as the dominant clay mineral.

Case #3 represents surrogate soils where the estimated clay composition remains the same, but total Al^{3+} is reduced by 50%.

Case #4 represents surrogate soils where the FeOOH/total Fe^{3+} ratio increases from 0.5 to 1.0.

Case #5 represents surrogate soils where the SOM/SOC ratio decreases from 1.0 to 0.5.

of all copper present in this surrogate soil is bound to SOM. In surrogate soil 99-1-7-12, case $^{\#}4$ causes a large increase in lead sorption and a <1% increase in bound cadmium, copper, and zinc. The results reflect the combination of lead's much stronger affinity for FeOOH than the other three metals and the limited availability of specific sorption binding sites in surrogate soil 99-1-7-12.

The 50% decrease in SOM causes the greatest change in predicted concentrations of metals in both surrogate soils. The results indicate that in surrogate soil 98-3-5-10, significant fractions of each metal are bound to the SOM fraction. However, the changes reported in surrogate soil 99-1-7-12 indicate that the low concentrations of metals bound to the different specimen materials do not buffer the impact of case $^{\#}5$ on this system. The less than 1:1 response to case $^{\#}5$ as reported for complexed metals in Table 53 is the influence of metals bound to FeOOH and clay minerals, which are not affected by case $^{\#}5$.

Based on the results of this evaluation, uncertainty in SOM weighting factors cause the greatest changes in predicted concentrations of metals. Uncertainty in FeOOH weighting factors can have significant impacts on predicted concentrations of metals particularly in soils at higher pHs and concentrations of total Fe^{3+}. Overall, uncertainty in clay weighting factors are expected to have the least impact on the sum of predicted concentrations of metals due to the fact that the concentrations of exchangeable and specific sorption binding sites associated with clay minerals constitute a small fraction of the total concentration of available binding sites. However, in certain situations such as high clay soils with high concentrations of metals, uncertainty in clay weighting factors will have a significant impact on predicted concentrations of exchangeable metals, particularly cadmium and zinc. Any changes in the predicted concentrations of exchangeable metals is of significant interest because of the direct influence of exchangeable metals concentrations on the prediction of potentially bioavailable (i.e. soluble) metals.

7.0 SUMMARY AND CONCLUSIONS

Competitive and non-competitive modeling approaches were developed to predict cadmium, copper, lead, and zinc partitioning in contaminated pasture soils near Leadville, CO. Both modeling approaches included surrogate soils comprised of five specimen materials [i.e. kaolinite, illite, montmorillonite, iron oxide (FeOOH), and soil organic matter (SOM)]. The physical and chemical properties of the specimen materials, which were described with data obtained primarily from the literature, represent individual soil components in four contaminated soils. To approximate natural soils, the compositions of the surrogate soils were adjusted using a unique set of weighting factors calculated from XRD and total aluminum, iron, and soil organic carbon (SOC) data. The sorption of cadmium, copper, lead, and zinc was modeled using soluble metals data and two chemical equilibrium/speciation software programs; MINEQL$^+$, Version 4.5 and Visual MINTEQ, Version 2.30. MINEQL$^+$ was selected to model the clay and oxide fractions, while Visual MINTEQ was used for SOM modeling. Within these two software programs, the Vanselow selectivity coefficient and four surface complexation models (i.e. Constant Capacitance Model, Generalized Two-Layer Model, Stockholm Humic Model, and a non-electrostatic surface complexation model) were selected to describe the sorption processes of these four metals to individual specimen materials.

Predicted concentrations of exchangeable, sorbed, and complexed metals were compared to experimental data generated from the selective extraction of four contaminated soils. The non-competitive modeling approach (NCMA) and competitive modeling approach (CMA) were tested across a range of pHs, soil textures, SOC levels, and concentrations of soluble cadmium, copper, lead, and zinc, and total aluminum and iron. Summaries of the comparison of experimental data to predicted concentrations of metals in the NCMA and CMA are provided in Tables 55 and 56, respectively.

The comparisons of experimental data to predicted concentrations of exchangeable, sorbed, and complexed metals are largely qualitative because the selectivities and efficiencies of the various extractant solutions used in the selective extraction procedure could not be quantified. The lack of quantitation is due to the uncertainty of an extractant solution's ability to recover 100% of a metal bound to one type of reactive site (e.g. sorbed) or individual soil component (e.g. FeOOH). The problem of quantifying the selectivities and efficiencies of extractant solutions is common to all sequential or selective extraction procedures.

As a first approximation, the concentrations of exchangeable, sorbed, and complexed metals predicted by the two modeling approaches should be similar to the concentrations of metals recovered from soils during the selective extraction process. As the data show in Tables 55 and 56, similar concentrations of metals are reported by the selective extraction procedure and the two modeling approaches. To provide a more precise description of the predictive capabilities of both modeling approaches, it is assumed that predicted concentrations of metals within one order of magnitude (i.e. ±10X) of the experimental data are acceptable modeling results. The percent of one order of magnitude that predicted concentrations of metals are over or under the

Table 55. Comparison of experimental metals data to predicted concentrations of exchangeable and sorbed/complexed cadmium, copper, lead, and zinc [non-competitive modeling approach]

	Experimental Total Metals	Experimental Soluble Metals	Experimental Exchangeable Metals	Predicted[1] Exchangeable Metals	Experimental Sorbed/ Complexed Metals	Predicted[1] Sorbed/ Complexed Metals
	mg kg^{-1}	mg L^{-1}	mg kg^{-1}	mg kg^{-1}	mg kg^{-1}	mg kg^{-1}
Cadmium						
99-1-0-7	43.2	0.227	6.52	4.71	13.4	119
99-1-7-12	11.2	0.080	1.56	0.563	0.590	2.06
98-3-5-10	98.0	0.835	12.2	35.0	60.4	767
98-3-20-25	146	0.940	34.9	23.0	24.8	512
Copper						
99-1-0-7	633	0.008	0.276	1.65	102	81.6
99-1-7-12	336	0.026	9.06	0.976	44.0	21.2
98-3-5-10	435	0.018	0.520	6.30	66.2	306
98-3-20-25	213	0.006	0.104	1.55	2.76	93.1
Lead						
99-1-0-7	4,430	0.008	11.8	2.42	NA[2]	315
99-1-7-12	3,230	0.087	117	2.32	NA[2]	74.7
98-3-5-10	18,600	0.235	81.8	41.8	NA[2]	3,410
98-3-20-25	14,400	0.031	30.5	16.8	NA[2]	1,790
Zinc						
99-1-0-7	7,760	1.63	26.4	21.4	204	218
99-1-7-12	1,820	0.803	6.40	11.0	10.7	46.6
98-3-5-10	18,000	4.08	<0.00[3]	74.2	631	1,260
98-3-20-25	14,100	3.33	<0.00[4]	51.0	310	845

[1] Non-competitive modeling approach.

[2] Not analyzed because sorbed and complexed metals were extracted with 0.05M $Pb(NO_3)_2$.

[3] Exchangeable zinc calculated by subtracting total soluble zinc (163 mg kg^{-1}) from total exchangeable zinc (152 mg kg^{-1}).

[4] Exchangeable zinc calculated by subtracting total soluble zinc (133 mg kg^{-1}) from total exchangeable zinc (131 mg kg^{-1}).

Table 56. Comparison of experimental metals data to predicted concentrations of exchangeable and sorbed/complexed cadmium, copper, lead, and zinc [competitive modeling approach]

	Experimental Total Metals	Experimental Soluble Metals	Experimental Exchangeable Metals	Predicted[1] Exchangeable Metals	Experimental Sorbed/ Complexed Metals	Predicted[1] Sorbed/ Complexed Metals
	mg kg^{-1}	mg L^{-1}	mg kg^{-1}	mg kg^{-1}	mg kg^{-1}	mg kg^{-1}
Cadmium						
99-1-0-7	43.2	0.227	6.52	3.12	13.4	59.0
99-1-7-12	11.2	0.080	1.56	0.557	0.590	1.71
98-3-5-10	98.0	0.835	12.2	15.0	60.4	246
98-3-20-25	146	0.940	34.9	10.7	24.8	162
Copper						
99-1-0-7	633	0.008	0.276	2.12	102	92.6
99-1-7-12	336	0.026	9.06	0.876	44.0	15.8
98-3-5-10	435	0.018	0.520	5.93	66.2	258
98-3-20-25	213	0.006	0.104	3.18	2.76	132
Lead						
99-1-0-7	4,430	0.008	11.8	1.04	NA[2]	171
99-1-7-12	3,230	0.087	117	1.87	NA[2]	41.6
98-3-5-10	18,600	0.235	81.8	7.24	NA[2]	410
98-3-20-25	14,400	0.031	30.5	2.29	NA[2]	158
Zinc						
99-1-0-7	7,760	1.63	26.4	19.3	204	139
99-1-7-12	1,820	0.803	6.40	10.4	10.7	25.8
98-3-5-10	18,000	4.08	<0.00[3]	48.9	631	389
98-3-20-25	14,100	3.33	<0.00[4]	39.2	310	356

[1] Competitive modeling approach.

[2] Not analyzed because sorbed and complexed metals were extracted with 0.05M $Pb(NO_3)_2$.

[3] Exchangeable zinc calculated by subtracting total soluble zinc (163 mg kg^{-1}) from total exchangeable zinc (152 mg kg^{-1}).

[4] Exchangeable zinc calculated by subtracting total soluble zinc (133 mg kg^{-1}) from total exchangeable zinc (131 mg kg^{-1}).

experimental data was calculated for each metal in the four soils (Table 55). The calculated percent values provide a common reference point for discussing the performance of the two modeling approaches. Small percent values indicate a closer fit of the experimental data than large percent values. However, predicted concentrations of metals can easily exceed the one order of magnitude criteria in cases where very low concentrations of metals are extracted from soils (e.g. exchangeable copper for the 98-3 soil profile range from 0.104 to 0.520 mg kg^{-1}). The accuracy of both modeling approaches at very low concentrations is not precise enough to consistently predict trace levels of metals within one order of magnitude. Thus, exceeding the one order of magnitude criteria at very low concentrations of metals does not necessarily indicate poor model performance.

Table 57 shows the NCMA and CMA can predict within one order of magnitude, exchangeable cadmium concentrations in all four soils, exchangeable copper and zinc in the 99-1 soil profile, and exchangeable lead concentrations in three out of four soils. Both modeling approaches exceed the one order of magnitude criteria for exchangeable copper in the 98-3 soil profile and exchangeable lead in sample 99-1-7-12.

The copper results are likely the combination of very low exchangeable copper concentrations (i.e. 0.104-0.520 mg kg^{-1}) reported for the 98-3 soil profile and the inability of the two modeling approaches to consistently predict within one order of magnitude at low concentrations of metals. The reason both modeling approaches exceed the criteria limits in predicting exchangeable lead in sample 99-1-7-12 is probably due to the unexpectedly high quantity of exchangeable lead (i.e. 117 mg kg^{-1}) recovered. Based

Table 57. Performance comparison of the non-competitive and competitive modeling approaches based on percent of one order of magnitude

	NCMA[1] Exchangeable Metals	CMA[2] Exchangeable Metals	NCMA Sorbed and Complexed Metals	CMA Sorbed and Complexed Metals
	% OM[3]	% OM	% OM	% OM
Cadmium				
99-1-0-7	31	58	88	38
99-1-7-12	71	71	28	21
98-3-5-10	21	2.6	**130**	34
98-3-20-25	38	77	**220**	62
Copper				
99-1-0-7	54	66	22	10
99-1-7-12	99	100	58	71
98-3-5-10	**120**	**120**	40	32
98-3-20-25	**160**	**340**	**360**	**520**
Lead				
99-1-0-7	88	100	NC[5]	NC
99-1-7-12	**110**	**110**	NC	NC
98-3-5-10	54	100	NC	NC
98-3-20-25	50	100	NC	NC
Zinc				
99-1-0-7	21	30	0.76	35
99-1-7-12	8.0	6.9	37	16
98-3-5-10	51[3]	68[3]	11	43
98-3-20-25	61[4]	70[4]	19	1.6

[1] Non-competitive modeling approach.

[2] Competitive modeling approach.

[3] Percent of one order of magnitude.

[3] For comparison purposes only, the total exchangeable zinc concentration reported for 98-3-5-10 (152 mg kg-1) was assumed to be correct.

[4] For comparison purposes only, the total exchangeable zinc concentration reported for 98-3-20-25 (131 mg kg-1) was assumed to be correct.

[5] Not calculated because 0.05M Pb(NO3)2 was used to extract sorbed and complexed metals.

Bold - One order of magnitude exceeded.

on the calculated percent values, the NCMA is a better predictor of exchangeable lead than the CMA.

No evaluation of predicted exchangeable zinc in the 98-3 soil profile can be made because slightly more total soluble zinc (i.e. 98-3-5-10, 163 mg kg^{-1}; 98-3-20-25, 133 mg kg^{-1}) was recovered than total exchangeable zinc (i.e. 98-3-5-10, 152 mg kg^{-1}; 98-3-20-25, 131 mg kg^{-1}). As described in Section 4.0, the exchangeable zinc concentration is calculated by subtracting the concentration of total soluble zinc from the concentration of total exchangeable zinc. In the case of the 98-3 soil profile, a value of <0 mg kg^{-1} of exchangeable zinc is reported. The results are unexpected and the data suggest that a significant fraction of the zinc in these two soils is associated primarily with the soluble fraction rather than the exchangeable fraction. However, if the assumption is made that the concentrations of total exchangeable zinc reported for these two soils are correct, both modeling approaches predict exchangeable zinc concentrations within one order of magnitude of the experimental data (Table 57).

The NCMA and CMA can also predict within one order of magnitude; sorbed and complexed cadmium, copper, and zinc in the 99-1 soil profile, sorbed and complexed zinc in the 98-3 soil profile, and sorbed and complexed copper in sample 98-3-5-10. Although, both modeling approaches overpredict sorbed and complexed cadmium concentrations in three out of four soils (Tables 55 and 56), the CMA is a better predictor of sorbed and complexed cadmium than the NCMA. Based on a review of the performance of both modeling approaches with regards to cadmium and the other three metals, the source of cadmium overprediction may be associated with the cadmium binding constants selected from the literature to model the FeOOH and SOM fractions.

In sample 98-3-20-25, the NCMA and CMA exceed one order of magnitude in predicting sorbed and complexed copper. The failure to predict sorbed and complexed copper in this particular soil may be associated with the unexpectedly low concentrations of sorbed and complexed copper (i.e. 2.76 mg kg^{-1}) recovered rather than a problem with either modeling approach.

Since 0.05M $Pb(NO_3)_2$ was used to extract sorbed and complexed metals from these soils, no evaluation of model performance can be made for sorbed and complexed lead. However, the predicted concentrations of sorbed and complexed lead reported for these soils (Tables 55 and 56) appear to be reasonable estimates of potential lead partitioning. The conclusion is based on a comparison of total lead and zinc concentrations, metal cation affinity sequences reported for clay minerals (Farrah et al, 1980), FeOOH (Dzombak and Morel, 1990), and humic substances (Gustafsson, 2004), binding constants for lead and zinc, and predicted zinc partitioning.

Based on the evaluation of data listed in Tables 55-57, both modeling approaches with few exceptions, are able to provide reasonable estimates of the experimental data across a range of pHs and soil compositions. Qualitatively, the CMA is a better predictor of sorbed and complexed metals than the NCMA, while the NCMA is a slightly better predictor of exchangeable metals. Of interest, is the finding that the two modeling approaches which were developed with data obtained primarily from the literature and supplemented with XRD and total aluminum, iron, and SOC data, can provide reasonable estimates of metal partitioning independently of metal partitioning data derived from the selective extraction process. The results support the conclusion that a qualitative determination of metal partitioning can be achieved by either the selective extraction and analyses of contaminated soils or the application of modeling systems consisting of surrogate soils supplemented with data from the literature.

Based on a review of the eight metal partitioning tables in Appendix C, both modeling approaches can be simplified. In this study, the exchangeable fraction consists of metals from cation exchange sites associated with kaolinite, illite, and montmorillonite, dissolved SOM metal complexes, and diffuse layer and charge screening metal complexes associated with solid SOM. The sorbed metals fraction consists of specific sorption sites associated with kaolinite, montmorillonite, and FeOOH. Based simply on the percent of the total predicted exchangeable and sorbed metals contributed by each specimen material and the percent changes in predicted concentrations of metals due to changes in clay weighting factors (Section 6.0), the exchangeable and sorbed fractions can be reduced without the introduction of much predictive error to illite and FeOOH, respectively. Thus, the modeling of these contaminated soils can be accomplished with surrogate soils consisting of three specimen materials; illite for exchangeable metals, FeOOH for sorbed metals, and SOM for complexed metals. A study by Dijkstra et al (2004) reported a similar conclusion in which FeOOH/AlOOH, SOM, and illite clay were considered the three primary soil components necessary to model metals contaminated soils in the Netherlands.

The weighting factors used in this study can be modified to adjust the surrogate soils for use with other contaminated soils of similar composition. Total aluminum, iron, SOC, and XRD data are the primary requirements for adjusting the weighting factors. One possible modification to the calculation of FeOOH weighting factors is to combine the concentrations of total iron and total manganese. Metal binding constants for manganese oxides are in the same general range of metal binding constants listed for FeOOH. The 'new' oxide (FeOOH and MnO/MnOOH) weighting factor would represent a more generalized oxide fraction. In cases where XRD data indicate the significant presence of AlOOH minerals, a portion of the total aluminum can be combined with total iron and total manganese to generate an oxide weighting factor representing FeOOH, AlOOH, and MnO/MnOOH. In that event, the calculation of clay weighting factors will require adjustment to compensate for the reduced amount of aluminum available. In soils that contain peat, the SOM weighting factor can be converted to a peat weighting factor using the conversion factors and multipliers listed in Section 4.0, Materials and Methods.

As previously discussed in Section 6.0, the inherent uncertainty in the clay, FeOOH, and SOM weighting factors can have significant impacts on the prediction of metal partitioning in these contaminated soils. The uncertainty in the weighting factors is due to the method used to estimate the clay composition and the assumptions regarding what percent of the reported total Al^{3+}, Fe^{3+} and SOC concentrations are involved in metals binding. Errors in the values of SOM weighting factors have the greatest impact on the prediction of metal partitioning in the four contaminated soils. Errors in the values of FeOOH weighting factors can have significant impacts on predicted metal partitioning in slightly acid soils containing high concentrations of metals, specific sorption binding sites, and Fe^{3+}. Errors in the values of SOM and FeOOH weighting factors have less impact on the prediction of metal partitioning in strongly acid soils with low concentrations of Fe^{3+}, SOC, and metals. Errors in the values of clay weighting factors, which have the least impact on the overall prediction of metal partitioning, can significantly impact the predicted partitioning of metals associated with the clay fraction in soils containing high concentrations of illites and smectites.

To verify the performance of both modeling approaches, quantification of the selectivities and efficiencies of the extractant solutions used in the selective extraction procedure is highly recommended. Additional research into the impacts of the horizontal shaker system (HSS) and the vacuum extraction system (VES) on the recovery of metals is also recommended. Table 20 data show the HSS recovered 2-36X more lead and 4-23X more zinc than the VES. The greater recovery of these two metals by the HSS correlated poorly with the predicted partitioning of lead and zinc (e.g. zinc, Table 1, Appendix E). The smaller quantities of metals recovered by the VES provided a better fit of predicted lead and zinc partitioning (e.g. zinc, Table 1, Appendix C). As described previously in section 5.1.4, the goal of this research is to develop a general modeling approach that can predict metal partitioning in relatively undisturbed soils and not the partitioning of metals in soil suspensions subjected to agitation similar to that provided by the HSS. Therefore, the larger quantities of metals recovered with a selective extraction procedure using the HSS is not necessarily a good result for the purpose of this research.

The data listed in Tables 55 and 56 also show that compared to the very high concentrations of total lead and zinc reported for these soils, low concentrations of exchangeable, sorbed, and complexed lead and zinc were recovered by the selective extraction process or predicted by the two modeling approaches. The results suggest that the conclusions of environmental risk studies based primarily on total metals data may not describe the true potential a contaminated site poses to the environment. Estimates of metals associated with the exchangeable, sorbed, and complexed fractions in soils can provide important data regarding the long-term potential of these fractions to supply metals to the most bioavailable fraction, soluble metals.

The application of the NCMA and CMA to additional contaminated soils on the Bernie Smith Ranch or contaminated soils from other locations can provide opportunities to test the validity of the general modeling approach and determine the impacts on the prediction of metal partitioning due to uncertainty in the clay, FeOOH, and SOM weighting factors. The additional data can lead to further refinements in the modeling approach. One benefit in using the NCMA and CMA in studies of metals contaminated soils is the reduction in the amount of data required to apply the general modeling approach. Estimates of metal partitioning in contaminated soils can be generated using appropriate specimen material(s) modeling parameters and a small dataset consisting of soluble metals, total aluminum, total iron, SOC, pH, and XRD data.

8.0 LITERATURE CITED

Al-Farraj, A. 2002. Association of Heavy Metals with Secondary Iron Oxide Minerals. Ph.D. Dissertation, Department of Crop and Soil Sciences, Colorado State University, Fort Collins, CO 80523.

Alloway, B.J. 1993. Heavy Metals in Soils. John Wiley and Sons, Inc., Somerset, NJ, 08873.

Altin, O., H.O. Ozbelge, and T. Dogu. 1998. Use of general purpose adsorption isotherms for heavy metal-clay mineral interactions. J. Colloid Interf. Sci. 198: 130-140.

Andersson, A. 1977. The distribution of heavy metals in soils and soil material as influenced by the ionic radius. Swed. J. Agr. Res. 7: 79-83.

Arnfalk, P., S.A. Wasay, and S. Tokunaga. 1996. A comparative study of Cd, Cr(III), Cr(VI), Hg, and Pb uptake by minerals and soil materials. Water Air Soil Poll. 87: 131-148.

Atkinson, R. J., A. M. Posner, and J. P. Quirk. 1968. Crystal nucleation in Fe(III) solutions and hydroxide gels. J. Inorg. Nucl. Chem. 30: 2371-2381.

Auboiroux, M., F. Melou, F. Bergaya, and J.C. Touray. 1998. Hard and soft acid-base model applied to bivalent cation selectivity on a 2:1 clay mineral. Clay Clay Miner. 46(5): 546-555.

Backes, C.A., R.G. McLaren, A.W. Rate, and R.S. Swift. 1995. Kinetics of cadmium and cobalt desorption from iron and manganese oxides. Soil Sci. Soc. Am. J. 59: 778-785.

Barbier, F., G. Duc, and M. Petit-Ramel. 2000. Adsorption of lead and cadmium ions from aqueous solution to the montmorillonite/water interface. Colloids and Surfaces A: Physicochemical and Engineering Aspects 166: 153-159.

Basta, N. T., D. J. Pantone, and M. A. Tabatabi. 1993. Path analysis of heavy metal adsorption by soil. Agron. J. 85: 1054-1057.

Benedetti, M. F., C. J. Milne, D. G. Kinniburgh, W. H. van Riemsdijk, and L. K. Koopal. 1995. Metal ion binding to humic substances: application of the non-ideal competitive adsorption model. Environ. Sci. Technol. 29: 446-657.

Benjamin, M. M. and J. O. Leckie. 1981. Multiple-site adsorption of Cd, Cu, Zn and Pb on amorphous iron oxyhydroxide. J. Colloid Interf. Sci., 79: 209-221.

Benyahya, L. and J. Garnier. 1999. Effect of salicylic acid upon trace-metal sorption (Cd^{II}, Zn^{II}, Co^{II}, and Mn^{II}) onto alumina, silica, and kaolinite as a function of pH. Environ. Sci. Technol. 33: 1398-1407.

Bereket, G., A.Z. Aroguz, and M.Z. Ozel. 1997. Removal of Pb(II), Cu(II), and Zn(II) from aqueous solutions by adsorption on bentonite. J. Colloid Interf. Sci. 187: 338-343.

Bingham, F.T., A.L. Page, and J.R. Sims. 1964. Retention of Cu and Zn by H-montmorillonite. Soil Sci. Soc. Proc. :351-354.

Bittell, J.E. and R.J. Miller. 1974. Lead, cadmium, and calcium selectivity coefficients on a montmorillonite, illite, and kaolinite. J. Environ. Qual. 3: 250-253.

Bloom, P.R. and M.B. McBride. 1979. Metal ion binding and exchange with hydrogen ions in acid-washed peat. Soil Sci. Soc. Am. J. 43: 687-692.

Bradbury, M.H. and B. Baeyens. 1997a. A mechanistic description of Ni and Zn sorption on Na-montmorillonite. Part I: Titration and sorption measurements. J. Contam. Hydrol. 27: 199-222.

Bradbury, M.H. and B. Baeyens. 1997b. A mechanistic description of Ni and Zn sorption on Na-montmorillonite. Part II: Modelling. J. Contam. Hydrol. 27: 223-248.

Broadbent, F.E. 1953. The soil organic fraction. Adv. Agron. 5: 153-183.

Brookins, D.G. 1989. Chapter 8. Aqueous Geochemistry of Rare Earth Elements. Reviews in Mineralogy. Volume 21: Geochemistry and Mineralogy of Rare Earth Elements. Mineralogical Society of America., Washington, DC, 20006.

Brunauer, S., P. H. Emmett, and E. Teller. 1938. Adsorption of gases in multimolecular layers. J. Amer. Chem. Soc. 60: 309-319.

Buchter, B., B. Davidoff, M. C. Amacher, C. Hinz, I. K. Iskandar, and H. M. Selim. 1989. Correlation of Freundlich Kd and n retention parameters with soils and elements. Soil Sci. 148: 370-379.

Bunzl, K. 1974a. Kinetics of ion exchange in soil organic matter. II. Ion exchange during continuous addition of Pb^{2+}-ions to humic acid and peat. J. Soil Sci. 25: 343-356.

Bunzl, K. 1974b. Kinetics of ion exchange in soil organic matter. III. Differential ion exchange reactions of Pb^{2+}-ions in humic acid and peat. J. Soil Sci. 25: 517-532.

Bunzl, K., W. Schmidt, and B. Sansoni. 1976. Kinetics of ion exchange in soil organic matter. IV. Adsorption and desorption of Pb^{2+}, Cu^{2+}, Cd^{2+}, Zn^{2+}, and Ca^{2+} by peat. J. Soil Sci. 27: 32-41.

Clementz, D.M., T.J. Pinnavaia, and M.M. Mortland. 1973. Stereochemistry of hydrated copper (II) ions on the interlamellar surfaces of layer silicates. An electron spin resonance study. J. Phys. Chem. 77: 196-200.

Cowan, C.E., J.M. Zachara, and C.T. Resch. 1991. Cadmium adsorption on iron oxides in the presence of alkaline-earth elements. Environ. Sci. Technol. 25: 437-446.

Cowan, C.E., J.M. Zachara, S.C. Smith, and C.T. Resch. 1992. Individual sorbent contributions to cadmium sorption on ultisols of mixed mineralogy. Soil Sci. Soc. Am. J. 56: 1084-1094.

Crist, R.H., J.R. Martin, and J. Chonko. 1996. Uptake of metals on peat moss: An ion exchange process. Environ. Sci. Technol. 30: 2456-2461.

Davis J.A. 1984. Complexation of trace metals by adsorbed natural organic matter. Geochim. et Cosmochim. Acta 48: 679-691.

Davis, J.A. and J.O. Leckie. 1978. Surface ionization and complexation at the oxide/water interface. II. Surface properties of amorphous iron oxyhydroxide and adsorption of metal ions. J. Colloid Interf. Sci. 67: 90-107.

Davis, J. A. and D. B. Kent. 1990. Chapter 5. Surface Complexation Modeling in Aqueous Geochemistry. *In* Mineral-Water Interface Geochemistry, Reviews in Mineralogy Vol. 23., M. F. Hochella and A. F. White, eds., Mineralogical Society of America, Washington, D. C.

Dijkstra, J.J., J.C.L. Meeussen, and R.N.J. Comans. 2004. Leaching of heavy metals from contaminated soils: An experimental and modeling study. Environ. Sci. Technol. 38: 4390-4395.

Dugger, D.L., J.H. Stanton, B.N. Irby, B.L. McConnell, W.W. Cummings, and R.W. Maatman. 1964. The exchange of twenty metal ions with the weakly acidic silanol group of silica gel. J. Phys. Chem. 68: 757-760.

Dwayne, G. C. and E. Tipping. 1998. Testing a humic speciation model by titration of copper-amended natural waters. Environ. Int. 24: 609-616.

Dzombak, D. A. and F. M. M. Morel. 1986. Sorption of cadmium on hydrous ferric oxide at high sorbate/sorbent ratios: equilibrium, kinetics, and modeling. J. Colloid Interf. Sci. 112: 588-598.

Dzombak, D.A., A.M. ASCE, and F.M.M. Morel. 1987. Adsorption of inorganic pollutants in aquatic systems. J. Hydraul. Eng.-ASCE 113: 430-475.

Dzombak, D. A. and F. M. M. Morel. 1990. Surface complexation modeling: hydrous ferric oxide. John Wiley & Sons, Inc. New York, N. Y.

Echeverria, J.C., E. Churio, and J.J. Garrido. 2002. Retention mechanisms of Cd on illite. Clay Clay Miner. 50: 614-623.

El-Sayed, M.H., R.G. Burau, and K.L. Babcock. 1970. Thermodynamics of copper (II) – calcium exchange on bentonite clay. Soil Sci. Soc. Amer. Proc. 34: 397-400.

Elzinga, E.J., J.J.M. Van Grinsven, and F.A. Swartjes. 1999. General purpose Freundlich isotherms for cadmium, copper, and zinc in soils. Eur. J. Soil Sci. 50: 139-149.

Evangelou, V.P., M. Marsi, and M.M. Vandiviere. 1999. Stability of Ca^{2+}-, Cd^{2+}-, Cu^{2+}-[illite-humic] complexes and pH influence. Plant and Soil 213: 63-74.

Farley, K.J., D.A. Dzombak, and F.M.M. Morel. 1985. A surface precipitation model for the sorption of cations on metal oxides. J. Colloid Interf. Sci. 106: 226-242.

Farrah, H. and W.F. Pickering. 1978. Extraction of heavy metal ions sorbed on clays. Water Air Soil Poll. 9: 491-498.

Farrah, H., D. Hatton, and W.F. Pickering. 1980. The affinity of metal ions for clay surfaces. Chem. Geol. 28: 55-68.

Fic, M. and M. Isenbeck-Schroter. 1989. Batch studies for the investigation of the mobility of the heavy metals Cd, Cr, Cu and Zn. J. Contam. Hydrol. 4: 69-78.

Ford, R.G., P.M. Bertsch, and K.J. Farley. 1997. Change in transition and heavy metal partitioning during hydrous iron oxide aging. Environ. Sci. Technol. 31: 2028-2033.

Gao, Y., A.T. Kan, and M.B. Tomson. 2003. Critical evaluation of desorption phenomena of heavy metals from natural sediments. Environ. Sci. Technol. 37: 5566-5573.

Garcia-Miragaya, J., R. Cardenas, and A.L. Page. 1983. Sorption of Cd and Zn on kaolinite and montmorillonite. P. 1244-1248. *In* Heavy Metals in the Environment.

Garcia-Miragaya, J., R. Cardenas, and A.L. Page. 1986. Surface loading on Cd and Zn sorption by kaolinite and montmorillonite from low concentration solutions. Water Air Soil Poll. 27: 181-190.

Gee, G.W. and J.W. Bauder. 1986. Chapter 15, Particle Size Analysis. pp. 383-411. *In* Methods of Soil Analysis: Physical and Mineralogical Methods. Part 1. Second Edition. Agronomy Monograph No. 9. American Society of Agronomy, Madison, WI, 53711.

Gerritse, R.G. and W. van Driel. 1984. The relationship between adsorption of trace metals, organic matter, and pH in temperate soils. J. Environ. Qual. 13: 197-204.

Gier, S. and W.D. Johns. 2000. Heavy metal-adsorption on micas and clay minerals studied by X-ray photoelectron spectroscopy. Appl. Clay Sci. 16: 289-299.

Glover, L.J., M.J. Eick, and P.V. Brady. 2002. Desorption kinetics of cadmium^{2+} and lead^{2+} from goethite: Influence of time and organic acids. Soil Sci. Soc. Am. J 66: 797-804.

Goldberg, S. 1995. Adsorption models incorporated into chemical equilibrium models. Ch. 5. *In* Chemical Equilibrium and Reaction Models. SSSA Special Publication Number 42. Soil Science Society of America, Inc. and American Society of Agronomy, Inc., Madison, WI.

Gomes, P.C., M.P.F. Fontes, A.G. da Silva, E. de S. Mendonca, and A.R. Netto. 2001. Selectivity sequence and competitive adsorption of heavy metals by Brazilian soils. Soil Sci. Soc. Am. J. 65: 1115-1151.

Gough, L.P., H.T. Shacklette, and A.A. Case. 1979. Element concentrations toxic to plants, animals, and man. Geological Survey Bulletin 1466, United States Department of Interior, Geological Survey, U. S. Government Printing Office, Washington, DC, 20402.

Gray, C.W., R.G. McLaren, A.H.C. Roberts, and L.M. Condron. 1999. Solubility, sorption and desorption of native and added cadmium in relation to properties of soils in New Zealand. Eur. J. Soil Sci. 50: 127-137.

Gustafsson, J.P. 2001. Modeling the acid-base properties and metal complexation of humic substances with the Stockholm Humic Model. J. Colloid Interf. Sci. 244: 102-112.

Gustafsson, J.P. 2004. Visual MINTEQ, Version 2.31. KTH, Department of Land and Water Resources Engineering, Stockholm, Sweden.

Gustafsson, J.P. and J.W.J. van Schaik. 2003a. Cation binding in a mor layer: batch experiments and modelling. Eur. J. Soil Sci. 54: 295-310.

Gustafsson, J.P., P. Pechova, and D. Berggren. 2003b. Modeling metal binding to soils: The role of natural organic matter. Environ. Sci. Technol. 37: 2767-2774.

Harter and Baker. 1977. Applications and misapplications of the Langmuir equation to soil adsorption phenomena. Soil Sci. Soc. Am. J. 41: 1077-1080.

Hartman, T. 2004. Mines Are Deep Trouble. Report: Abandoned sites slowly polluting state's water supplies. August 19, 2004. Rocky Mountain News, Denver, CO.

Hatton, D. and W.F. Pickering. 1980. The effect of pH on the retention of Cu, Pb, Zn and Cd by clay-humic acid mixtures. Water Air Soil Poll. 14: 13-21.

Hayes, K.F. and J.O. Leckie. 1987. Modeling ionic strengths on cation adsorption at hydrous oxide/solution interfaces. J. Colloid Interf. Sci. 115: 564-572.

Helios-Rybicka, E. 1983. Zn, Cd and Mn sorption on some clay minerals. Mineralogia Polonica 14: 57-63.

Helios-Rybicka, E., W. Calmano, and A. Breeger. 1995. Heavy metals sorption/desorption on competing clay minerals; an experimental study. Appl. Clay Sci. 9: 369-381.

Heydemann, A. 1959. Adsorption from very dilute copper solutions on clay minerals. Geochim. et Cosmochim. Acta 15: 305-329.

Hickey, M.G. and J.A. Kittrick. 1984. Chemical partitioning of cadmium, copper, nickel and zinc in soils and sediments containing high levels of heavy metals. J. Environ. Qual. 13: 372-376.

Hildebrand, E.E. and W.E. Blum. 1974. Lead fixation by clay minerals. Naturwissenschaften 61: 169-170.

Holm, T.R. and X.F. Zhu. 1994. Sorption by kaolinite of Cd^{2+}, Pb^{2+}, and Cu^{2+} from landfill leachate-contaminated groundwater. J. Contam. Hydrol. 16: 271-287.

Hossner, L.R. 1996. Chapter 3. Dissolution for Total Elemental Analysis. *In* Methods of Soil Analysis: Chemical Methods. Part 3. SSSA Book Series No. 5. Soil Science Society of America, Inc. and American Society of Agronomy, Inc., Madison, WI, 53711.

Huang C.P. and W. Stumm. 1973. Specific adsorption of cations on hydrous -Al_2O_3. J. Colloid Interf. Sci. 43: 409-420.

HydroGeoLogic, Inc.; Allison Geoscience Consultants, Inc. 1999. MINTEQA2/ PRODEFA2, a geochemical assessment model for environmental systems: user manual supplement for version 4.0; U. S. Environmental Protection Agency; Athens, GA.

Hyun, S.P., Y.H. Cho, S.J. Kim, and P.S. Hahn. 2000. Cu(II) sorption mechanism on montmorillonite: An electron paramagnetic resonance study. J. Colloid Interf. Sci. 222: 254-261.

Ikshan, J., B.B. Johnson, and J.D. Wells. 1999. A comparative study of the adsorption of transition metals on kaolinite. J. Colloid Interf. Sci. 217: 403-410.

Janssen, R.P.T., M.G.M. Bruggenwert, and W.H. van Riemsdijk. 2003a. Effect of Al hydroxide polymers on cation exchange of montmorillonite. Eur. J. Soil Sci. 54: 335-345.

Janssen, R.P.T., M.G.M. Bruggenwert, and W.H. van Riemsdijk. 2003b. Zinc ion adsorption on montmorillonite-Al hydroxide polymer systems. Eur. J. Soil Sci. 54: 347-355.

Jarvis, S.C. 1986. Forms of Al in some acid permanent grassland soils. J. Soil Sci. 37: 211-222.

Jopony, M. and S.D. Young. 1994. The solid-solution equilibria of lead and cadmium in polluted soils. Eur. J. Soil Sci. 45:59-70.

Jung, J., Y. Cho, and P. Hahn. 1998. Comparative study of Cu^{2+} adsorption on goethite, hematite and kaolinite: Mechanistic modeling approach. Bull. Korean Chem. Soc. 19: 324-327.

Kalbitz, K. and R. Wennrich. 1998. Mobilization of heavy metals and arsenic in polluted wetland soils and its dependence on dissolved organic matter. Sci. Total Environ. 209: 27-39.

Keizer, P. and M.G.M. Bruggenwert. 1991. Adsorption of heavy metals by clay-aluminum hydroxide complexes. p. 177-203. Interactions at the Soil Colloid-Soil Solution Interface. G.H. Bolt et al (eds.). Kluwer Academic Publishers. Printed in the Netherlands.

Kent, D.B., V.S. Tripathi, N.B. Ball, J.O. Leckie, and M.D. Siegel. 1988. Surface-complexation modeling of radionuclide adsorption in subsurface environments. *Prepared for* U. S. Nuclear Regulatory Commission, NUREG/CR-4807, SAND 86-7175.

Kerndorff, H. and M. Schnitzer. 1980. Sorption of metals on humic acid. Geochim. et Cosmochim. Acta 44: 1701-1708.

Khan, S. and N.N. Khan. 1985. Thermodynamics of Pb^{2+} exchange with Na^{+}, Ca^{2+} and Mg^{2+} on illite surfaces. Clay Res. 4: 75-80.

Kinniburgh, D.G. 1986. General purpose adsorption isotherms. Environ. Sci. Technol. 20: 895-904.

Kinniburgh, D.G., M.L. Jackson, and J.K. Sayers. 1976. Adsorption of alkaline earth, transition, and heavy metal cations by hydrous ferric oxide gels of iron and aluminum. Soil Sci. Soc. Am. J. 40: 796-799.

Kinniburgh, D.G., C.J. Milne, M.F. Benedetti, J.P. Pinheiro, J. Filius, L.K. Koopal, and W.H. van Riemsdijk. 1996. Metal ion binding by humic acid: Application of the NICA-Donnan model. Environ. Sci. Technol. 30: 1687-1698.

Klages, M.G. and R.W. Hopper. 1980. Clay minerals in northern plains coal overburden as measured by X-ray diffraction. Soil Sci. Soc. Am. J. 46: 415-419.

Kou, S., P.E. Heilman, and A.S. Baker. 1983. Distribution and forms of copper, zinc, cadmium, iron, and manganese in soils near a copper smelter. Soil Sci. 135: 101-109.

Krishnamoorthy, C. and R. Overstreet. 1950. An experimental evaluation of ion-exchange relationships. Soil Sci. 69: 41-53.

Krishnamurti, G.S.R., P.M. Huang, K.C.J. van Rees, L.M. Kozak, and H.P.W. Rostad. 1995. Speciation of particulate-bound cadmium in soils and its bioavailability. Analyst 120: 656-665.

Krishnamurti, G.S.R., P.M. Huang, L.M. Kozak, H.P.W. Rostad, and K.C.J. van Rees. 1997. Distribution of cadmium in selected soil profiles of Saskatchewan, Canada: Speciation and availability. Can. J. Soil Sci. 77: 613-619.

Le Riche, H.H. and A.H. Weir. 1963. A method of studying trace elements in soil fractions. J Soil Sci. 14: 225-235.

Levy, D.B. 1990. Heavy Metal Contamination in Soils and Plant Species of the Arkansas Valley near Leadville, Colorado. Master Thesis, Department of Soil and Crop Sciences, Colorado State University, Fort Collins, CO.

Li, Z. and L.M. Shuman. 1996. Heavy metal movement in metal-contaminated soil profiles. Soil Sci. 161: 656-666.

Lindsay, W.L. 2001. Chemical Equilibria in Soils. The Blackburn Press, Caldwell, NJ.

Loeppert, R.H. and D.L. Saurez. 1996. Chapter 15, carbonate and gypsum. pp. 444-448. *In* Methods of Soil Analysis: Chemical Methods. Part 3. SSSA Book Series No. 5. Soil Science Society of America, Inc. and American Society of Agronomy, Inc., Madison, WI, 53711.

Lofts, S., D.J. Spurgeon, C. Svendsen, and E. Tipping. 2004. Deriving soil critical limits for Cu, Zn, Cd, and Pb: A method based on free ion concentrations. Environ. Sci. Technol. 38: 3623-3631.

Lothenbach, B., G. Furrer, and R. Schulin. 1997. Immobilization of heavy metals by polynuclear aluminum and montmorillonite compounds. Environ. Sci. Technol. 31: 1452-1462.

Loux, N. T., D. S. Brown, C. R. Chafin, J. D. Allison, and S. M. Hassan. 1989. Chemical speciation and competitive cationic partitioning on sandy aquifer material. Chem. Spec. Bioavailab. 1: 111-125.

Lutzenkirchen, J. and P. Behra. 1997. A new approach for modelling potential effects in cation adsorption onto binary (hydr)oxides. J. Contam. Hydrol. 26: 257-268.

Lyon, J.S., T.J. Hilliard, and T.N. Bethell. 1993. Burden of Gilt. Mineral Policy Center, Washington, DC. 68p.

Manceau, A., N. Tamura, R.S. Celestre, A.A. MacDowell, N. Geoffroy, G. Sposito, and H.A. Padmore. 2003. Molecular-scale speciation of Zn and Ni in soil ferromanganese nodules from loess soils of the Mississippi Basin. Environ. Sci. Technol. 37:75-80.

Marinsky, J.A., A. Wolf, and K. Bunzl. 1980. The binding of trace amounts of lead(II), copper(II), cadmium(II), zinc(II), and calcium(II) to soil organic matter. Talanta 27: 461-468.

Matocha, C.J., E.J. Elzinga, and D.L. Sparks. 2002. Reactivity of Pb(II) at the Mn(III,IV) (oxyhydr)oxide-water interface. Environ. Sci. Technol. 35: 2967-2972.

McBride, M.B. 1976. Origin and position of exchange sites in kaolinite: An ESR study. Clay Clay Miner. 24: 88-92.

McBride, M.B. 1978. Transition metal bonding in humic acid: An ESR study. Soil Sci. 126: 200-209.

McBride, M.B. 1979. An interpretation of cation selectivity variations in M^+-M^+ exchange on clays. Clay Clay Miner. 27: 417-422.

McBride, M.B. 1980. Interpretation of the variability of selectivity coefficients for exchange between ions of unequal charge on smectites. Clay Clay Miner. 28: 255-261.

McBride, M.B. and M.M. Mortland. 1974. Copper(II) interactions with montmorillonite: evidence from physical methods. Soil Sci. Soc. Am. Proc. 38: 408-415.

McBride, M., S. Sauve, and W. Hendershot. 1997. Solubility control of Cu, Zn, Cd, and Pb in contaminated soils. Eur. J. Soil Sci. 48: 337-346.

McBride, M.B., C.E. Martinez, and S. Sauve. 1998. Copper(II) activity in aged suspensions of goethite and organic matter. Soil Sci. Soc. Am. J. 62: 1542-1548.

McLaren, R.G. and D.V. Crawford. 1973a. Studies on soil copper. I. The fractionation of copper in soils. J. Soil Sci. 24: 172-181.

McLaren, R.G. and D.V. Crawford. 1973b. Studies on soil copper. II. The specific adsorption of copper by soils. J. Soil Sci. 24: 443-452.

McLaren, R.G., J.G. Williams, and R.S. Swift. 1983. Some observations on the desorption and distribution of copper with soil components. J. Soil Sci. 34: 325-331.

Merrington, G. and B.J. Alloway. 1994. The flux of Cd, Cu, Pb, and Zn in mining polluted soils. Water Air Soil Poll. 73: 333-344.

Miller, W.P. and W.W. McFee. 1983. Distribution of cadmium, zinc, copper, and lead in soils of industrial northwestern Indiana. J. Environ. Qual. 12: 29-33.

Miller, W.P., D.C. Martens, and L.W. Zelazny. 1986. Effect of sequence in extraction of trace metals from soils. Soil Sci. Soc. Am. J. 50: 598-601.

Moore, D. M. and R. C. Reynolds. 1997. X-Ray Diffraction and the Identification and Analysis of Clay Minerals, Second Edition. Oxford University Press, Inc., New York, NY, 10016

Morley, G.F. and G.M. Gadd. 1995. Sorption of toxic metals by fungi and clay minerals. Mycol. Res. 99: 1429-1438.

Morton, J.D., J.D. Semrau, and K.F. Hayes. 2003. An X-ray absorption spectroscopy study of the structure and reversibility of copper adsorbed to montmorillonite clay. Geochim. et Cosmochim. Acta 65: 2709-2722.

Nakhone, L.N. 1997. Cadmium adsorption and desorption on humic acid, montmorillonite, goethite, kaolinite, and calcareous clay. Discov. Innovat. 9: 53-71.

Nelson, D.W. and L.E. Sommers. 1996. Chapter 34, total carbon, organic carbon, and organic matter. pp. 963-977, 985, and 1001. *In* Methods of Soil Analysis: Chemical Methods. Part 3. SSSA Book Series No. 5. Soil Science Society of America, Inc. and American Society of Agronomy, Inc., Madison, WI, 53711.

O'Day, P.A., S.A. Carroll, and G.A. Waychunas. 1998. Rock-water interactions controlling zinc, cadmium, and lead concentrations in surface waters and sediments, U.S. Tri-State Mining District. 1. Molecular identification using X-ray absorption spectroscopy. Environ. Sci. Technol. 32: 943-955.

Ostergren, J.D., G.E. Brown, G.A. Parks, and T.N. Tingle. 1999. Quantitative speciation of lead in selected mine tailings from Leadville, CO. Environ. Sci. Technol. 33: 1627-1636.

Otto, W.H., W.R. Carper, and C.K. Larive. 2001a. Measurement of cadmium(II) and calcium(II) complexation by fulvic acids using ^{113}Cd NMR. Environ. Sci. Technol. 35: 1463-1468.

Otto, W.H., W.R. Carper, and C.K. Larive. 2001b. Examination of cadmium(II) complexation by the Suwannee River fulvic acid using ^{113}Cd NMR relaxation measurements. Environ. Sci. Technol. 35: 4900-4904.

Pais, I. And J.B. Jones. 1997. The Handbook of Trace Elements. St. Lucie Press, Boca Raton, FL, 33431.

Paulson, A.J. and L. Balistrieri. 1999. Modeling removal of Cd, Cu, Pb, and Zn in acidic groundwater during neutralization by ambient surface waters and groundwaters. Environ. Sci. Technol. 33: 3850-3856.

Puls, R.W., R.M. Powell, D. Clark, and C.J. Eldred. 1991. Effects of pH, solid/solution ratio, ionic strength, and organic acids on Pb and Cd sorption on kaolinite. Water Air Soil Poll. 57/58: 423-430.

Radovanovic, H. and A. Koelmans. 1998. Prediction of *in situ* trace metal distribution coefficients for suspended solids in natural waters. Environ. Sci. Technol. 32: 753-759.

Rida, A. M. M. A. and M.B. Bouche. 1997. Heavy metal linkages with mineral, organic and living soil compartments. Soil Biochem. 29: 649-655.

Robertson, A.P. and J.O. Leckie. 1998. Acid/base, copper binding, and Cu^{2+}/H^+ exchange properties of goethite, an experimental and modeling study. Environ. Sci. Technol. 32: 2519-2530.

Ronngren, L., S. Sjoberg, Z. Sun, W. Forsling, and P.W. Schindler. 1991. Surface reactions in aqueous metal sulfide systems. 2. Ion exchange and acid/base reactions at the ZnS-H_2O interface. J. Colloid Interf. Sci. 145: 396-404.

Sanders, J.R. and S.P. McGrath. 1988. Experimental measurements and computer predictions of copper complex formation by soluble soil organic matter. Environ. Pollut. 49: 63-76.

Sarrett, G., J. Balesdent, L. Bouziri, J. Garnier, M.A. Marcus, N. Geoffroy, F. Panfill, and A. Manceau. 2004. Zn speciation in the organic horizon of a contaminated soil by micro-X-ray fluorescence, micro- and powder-EXAFS spectroscopy, and isotopic dilution. Environ. Sci. Technol. 38: 2792-2801.

Sauve, S.F. 1999. Chemical Speciation, Solubility and Bioavailability of Lead, Copper, and Cadmium in Contaminated Soils. Ph.D. Dissertation, Cornell University, Cornell, NY.

Sauve, S., M.B. McBride, and W.H. Hendershot. 1997. Speciation of lead in contaminated soils. Environ. Pollut. 98: 149-155.

Sauve, S., A. Dumestre, M. McBride, and W. Hendershot. 1998a. Derivation of soil quality criteria using predicted chemical speciation of Pb^{2+} and Cu^{2+}. Environ. Toxicol. Chem. 17: 1481-1489.

Sauve, S., M. McBride, and W. Hendershot. 1998b. Lead phosphate solubility in water and soil suspensions. Environ. Sci. Technol. 32: 388-393.

Sauve, S., M. McBride, and W. Hendershot. 1998c. Soil solution speciation of lead(II): Effects of organic matter and pH. Soil Sci. Soc. Am. J. 62: 618-621.

Sauve, S., W.A. Norvell, M. McBride, and W. Hendershot. 2000a. Speciation and complexation of cadmium in extracted soil solutions. Environ. Sci. Technol. 34: 291-296.

Sauve, S., W. Hendershot, and H.E. Allen. 2000b. Solid-solution partitioning of metals in contaminated soils: Dependence on pH, total metal burden, and organic matter. Environ. Sci. Technol. 34: 1125-1131.

Sauve, S., S. Manna, M. Turmel, A.G. Roy, and F. Courchesne. 2003. Solid-solution partitioning of Cd, Cu, Ni, Pb, and Zn in the organic horizons of a forest soil. Environ. Sci. Technol. 37: 5191-5196.

Schecher, W.D. and D.C. McAvoy. 1994. MINEQL$^+$: A Chemical Equilibrium Program for Personal Computers, Version 3.0, User's Manual. Environmental Research Software, Hallowell, ME.

Schecher, W.D. and D.C. McAvoy. 2001. MINEQL$^+$: A Chemical Equilibrium Modeling System, Version 4.5 for Windows, User's Manual. Environmental Research Software, Hallowell, ME.

Schindler, P.W., B. Furst, R. Dick, and P.U. Wolf. 1976. Ligand properties of surface silanol groups. I. Surface complex formation with Fe^{3+}, Cu^{2+}, Cd^{2+}, and Pb^{2+}. J. Colloid Interf. Sci. 55: 469-475.

Schindler, P.W., P. Liechti, and J.C. Westall. 1987. Adsorption of copper, cadmium, and lead from aqueous solution to the kaolinite/water interface. Neth. J. Agr. Sci. 35: 219-230.

Schnitzer, R. and R. Roberts. 2004. Settled, Mined & Left Behind. The legacy of abandoned hardrock mines for the rivers and fish of the American west, and solution for cleaning them up. A report produced by Trout Unlimited's Public Lands Initiative, Boulder, CO.

Selim, H.M., B. Buchter, and L. Ma. 1992. Modeling the transport and retention of cadmium in soils: Multireaction and multicomponent approaches. Soil Sci. Soc. Am. J. 56: 1004-1015.

Shukla, L.M., D. Gowrisankar, and R. Prasad. 1998. Sorption and desorption of cadmium in soils. Ann. Agr. Res. 19: 393-397.

Shukla, L.M. 2000. Sorption of zinc and cadmium on soil clays. Agrochimica 44: 101-106.

Shuman, L.M. 1977. Adsorption of Zn by Fe and Al hydrous oxides as influenced by aging and pH. Soil Sci. Soc. Am. J. 41:703-706.

Shuman, L.M. 1979. Zinc, manganese, and copper in soil fractions. Soil Sci. 127: 10-17.

Slavek, J. and W.F. Pickering. 1981. The effect of pH on the retention of Cu, Pb, Cd, and Zn by clay-fulvic acid mixture. Water Air Soil Poll. 16: 209-221.

Soon, Y.K. and T.E. Bates. 1982. Chemical pools of cadmium, nickel and zinc in polluted soils and some preliminary indications of their availability to plants. J. Soil Sci. 33: 477-488.

Sparks, D.L. 1995. Environmental Soil Chemistry. Academic Press, San Diego, CA, 92101.

Sposito, G. 1989. The Chemistry of Soils. Oxford University Press, Inc., New York, NY, 10016.

Sposito, G. and S.V. Mattigod. 1979. Ideal behavior in Na^+-trace metal cation exchange on Camp Berteau montmorillonite. Clay Clay Miner. 27: 125-128.

Sposito, G., K.M. Holtzclaw, C.T. Johnston, and C.S. LeVesque-Madore. 1981. Thermodynamics of sodium-copper exchange on Wyoming bentonite at 298^0K. Soil Sci. Soc. Am. J. 45:1079-1084.

Sposito, G., L.J. Lund, and A.C. Chang. 1982. Trace metal chemistry in arid-zone field soils amended with sewage sludge: I. Fractionation of Ni, Cu, Zn, Cd, and Pb in solid phases. Soil Sci. Soc. Am. J. 46: 260-264.

Stadler, M. and P.W. Schindler. 1993. Modeling of H^+ and Cu^{2+} adsorption on calcium-montmorillonite. Clay Clay Miner. 41: 288-296.

Stahl, R.S. and B.R. James. 1991a. Zinc sorption by iron-oxide-coated sand as a function of pH. Soil Sci. Soc. Am. J. 55:1287-1290.

Stahl, R.S. and B.R. James. 1991b. Zinc sorption by manganese-oxide-coated sand as a function of pH. Soil Sci. Soc. Am. J. 55:1291-1294.

Stevenson, F.J. 1995. Humus Chemistry. Genesis, Composition, Reactions. Second Edition. John Wiley and Sons, Inc., New York, NY.

Stover, R.C., L.E. Sommers, and D.J. Silviera. 1976. Evaluation of metals in waste-water sludge. J. Water Pollut. Control Fed. 48: 2165-2175.

Strawn, D.G. and D.L. Sparks. 1999. The use of XAFS to distinguish between inner- and outer-sphere lead adsorption complexes on montmorillonite. J. Colloid Interf. Sci. 216: 257-269.

Stuanes, A. 1976. Adsorption of Mn^{2+}, Zn^{2+}, Cd^{2+} and Hg^{2+} from binary solutions by mineral material. Acta Agr. Scand. 26: 243-250.

Stumm, W. and J.J. Morgan. 1996. Aquatic Chemistry: Chemical Equilibria and Rates in Natural Waters (3rd Ed). John Wiley and Sons, New York, NY.

Sumner, M.E. and W.P. Miller. 1996. Chapter 40. Cation exchange capacity and exchange coefficients. pp. 1218-1222. *In* Methods of Soil Analysis: Chemical Methods. Part 3. SSSA Book Series No. 5. Soil Science Society of America, Inc. and American Society of Agronomy, Inc., Madison, WI, 53711.

Swallow, K.C., D.N. Hume, and F.M.M. Morel. 1980. Sorption of copper and lead by hydrous ferric oxide. Environ. Sci. Technol. 14: 1326-1331.

Tessier, A. 1992. Chapter 11. Sorption of trace elements on natural particles in oxic environments. *In* Environmental Particles, Volume 1., J. Buffle and H.P. van Leeuwen (eds.), Lewis Publishers, Boca Raton, FL.

Tessier, A., P.G.C. Campbell, and M. Bisson. 1979. Sequential extraction procedure for the speciation of particulate trace metals. Anal. Chem. 51: 844-850.

Tingle, T.N., R.S. Borch, M.F. Hochella, C.H. Becker, and W.J. Walker. 1993. Characterization of lead on mineral surfaces in soils contaminated by mining and smelting. Appl. Surf. Sci. 72: 301-306.

Tipping, E. 1993. Modeling the competition between alkaline earth cations and trace metal species for binding by humic substances. Environ. Sci. Technol. 27: 520-529.

Tipping, E. 1994. WHAM – A chemical equilibrium model and computer code for waters, sediments, and soils incorporating a discrete/electrostatic model of ion-binding by humic substances. Comput. Geosci. 20: 973-1023.

Tipping, E. 1998. Humic ion-binding model VI: An improved description of the interactions of protons and metal ions with humic substances. Aquat. Geochem. 4: 3-48.

Tipping, E. and M.A. Hurley. 1992. A unifying model of cation binding by humic substances. Geochim. et Cosmochim. Acta 56: 3627-3641.

Tonkin, J.W., L.S. Balistrieri, and J.W. Murray. 2004. Modeling sorption of divalent cations on hydrous manganese oxide using the diffuse double layer model. Appl. Geochem. 19: 29-53.

Tyler, L.D. and M.B. McBride. 1982. Mobility and extractability of cadmium, copper, nickel, and zinc in organic and mineral soil columns. Soil Sci. 134(3): 198-205.

U.S. Geological Survey. 1997. A Plan for the USGS Abandoned Mine Lands Initiative, 1997-2001. *Prepared by* the USGS Initiative Implementation Team and Colorado and Montana Watershed Team.

Van Benschoten, J.E., W.H. Young, M.R. Matsumoto, and B.E. Reed. 1998. A nonelectrostatic surface complexation model for lead sorption on soils and mineral surfaces. J. Environ. Qual. 27: 24-30.

Van Bladel, R., H. Halen, and P. Cloos. 1993. Calcium-zinc and calcium-cadmium exchange in suspensions of various types of clays. Clay Miner. 28: 33-38.

Van Olphen, H. and J.J. Fripiat. 1979. Data Handbook for Clay Materials and other Non-Metallic Minerals. Pergamon Press, Elmsford, NY, 10523.

Verburg, K. and P. Baveye. 1994. Hysteresis in the binary exchange of cations on 2:1 clay minerals: A critical review. Clay Clay Miner. 42(2): 207-220.

Voegelin, A., V. Vulava, and R. Kretzschmar. 2001. Reaction-based model describing competitive sorption and transport of Cd, Zn, and Ni in an acidic soil. Environ. Sci. Technol. 35: 1651-1657.

Voegelin, A. and R. Kretzschmar. 2003. Modelling sorption and mobility of cadmium and zinc in soils with scaled exchange coefficients. Eur. J. Soil Sci. 54: 387-400.

Wold, J. and W.F. Pickering. 1981. Influence of electrolytes on metal ion sorption by clays. Chem. Geol. 33: 91-99.

Wu, Q., W.H. Hendershot, W.D. Marshall, and Y. Ge. 2000. Speciation of cadmium, copper, lead, and zinc in contaminated soils. Commun. Soil Sci. Plant Anal. 31: 1129-1140.

Zachara, J.M., S.C. Smith, C.T. Resch, and C.E. Cowan. 1992. Cadmium sorption to soil separates containing layer silicates and iron and aluminum oxides. Soil Sci. Soc. Am. J. 56: 1074-1084.

Zachara, J.M., S.C. Smith, J.P. McKinley, and C.T. Resch. 1993. Cadmium sorption on specimen and soil smectites in sodium and calcium electrolytes. Soil Sci. Soc. Am. J. 57: 1491-1501.

Ziper, C., S. Komarneni, and D.E. Baker. 1988. Specific cadmium sorption in relation to the crystal chemistry of clay minerals. Soil Sci. Soc. Am. J. 52:49-53.

APPENDIX A

References for Montmorillonite Cation Exchange Capacity And Surface Area Calculations

Cation Exchange References (Median of 37 Values)

Auboiroux et al. 1998. Clay Clay Miner. 46: 546-555.

Banin. 1968. Israel J. Chem. 6: 27-36.

Barbier et al. 2000. Colloids and Surfaces A: Physicochemical and Engineering Aspects 166: 153-159.

Bittell and Miller. 1974. J. Environ. Qual. 3: 250-253.

Bradbury and Baeyens. 1997a,b. J. Contam. Hydrol. 27: 199-248.

Clay Minerals Society datasheet.

Cowan et al. 1992. Soil Sci. Soc. Am. J. 56: 1084-1094.

Fawzy et al. 1973. Plant and Soil 39: 497-505.

Helios-Rybicka. 1983. Mineralogia Polonica 14: 57-63.

Hirsh et al. 1989. Soil Sci. Soc. Am. J. 53: 716-721.

Janssen et al. 2003a,b. Eur. J. Soil Sci. 54: 335-355.

Kraepiel et al. 1999. J. Colloid Interf. Sci. 210: 43-54.

Krishnamoorthy and Overstreet. 1950. Soil Sci. 69: 41-53.

Levy and Shainberg. 1972. Clay Clay Miner. 20: 37-46.

Lothenbach et al. 1997. Environ. Sci. Technol. 31: 1452-1462.

Maes and Cremers. 1986. Chapter 13. Clay Minerals and Zeolites. Geochemical Processes at Mineral Surfaces. American Chemical Society, Washington, DC.

Shainberg et al. 1980. Soil Sci. Soc. Am. J. 44: 960-964.

Shainberg et al. 1987. Clay Clay Miner. 35: 68-73.

Sposito et al. 1983. Soil Sci. Soc. Am. J. 47: 51-56.

Stadler and Schindler. 1993. Clay Clay Miner. 41: 288-296.

Stuanes. 1976. Acta Agr. Scand. 26: 243-250.

Suarez and Zahow. 1989. Soil Sci. Soc. Am. J. 53: 52-57.

Upson. 2004. Calculated from structural formula provided by Clay Minerals Society datasheet.

Van Bladel et al. 1993. Clay Miner. 28: 33-38.

Van Olphen and Fripiat. 1979. Data Handbook for Clay Materials and other Non-Metallic Minerals. Pergamon Press, Elmsford, NY.

Zachara et al. 1992. Soil Sci. Soc. Am. J. 56: 1074-1084.

Zachara and McKinley. 1993. Aquat. Sci. 55: 250-261.

Zhang and Sparks. 1996. Soil Sci. Soc. Am. J. 60: 1750-1757.

Ziper et al. 1988. Soil Sci. Soc. Am. J. 52: 49-53.

Surface Area (BET) References (Median of 7 Values)

Barbier et al. 2000. Colloids and Surfaces A: Physicochemical and Engineering Aspects 166: 153-159.

Clay Minerals Society datasheet.

Lothenbach et al. 1997. Environ. Sci. Technol. 31: 1452-1462.

Stadler and Schindler. 1993. Clay Clay Miner. 41: 288-296.

Van Olphen and Fripiat. 1979. Data Handbook for Clay Materials and other Non-Metallic Minerals. Pergamon Press, Elmsford, NY.

Surface Area (EGME) References (Median of 3 Values)

Shainberg et al. 1987. Clay Clay Miner. 35: 68-73.

Stadler and Schindler. 1993. Clay Clay Miner. 41: 288-296.

Van Olphen and Fripiat. 1979. Data Handbook for Clay Materials and other Non-Metallic Minerals. Pergamon Press, Elmsford, NY.

APPENDIX B

Total Metal and Major Cation Concentrations, Carbon Speciation, and Texture Data for All 1998 and 1999 Soils

Table B-1. Concentrations of total metal and major cations for soil profile 98-1

Samples	98-1-0-5	98-1-0-5 (Duplicate)	98-1-5-10	98-1-10-15	98-1-15-20
Cations	mg kg^{-1}	mg kg^{-1}	mg kg^{-1}	mg kg^{-1}	mg kg^{-1}
Ca	6226	6767	5546	6519	4978
Mg	5040	5376	4291	7432	6966
Na	5601	5098	5522	3389	6883
K	23435	19145	22675	20865	24125
P	1850	1993	990	2029	1372
Al	47188	44478	39618	55198	60028
Fe	52971	57088	33128	85413	54327
Mn	4893	5204	2671	3631	941
Ti	2679	2723	2084	2891	3732
Cu	856	864	349	1160	691
Zn	10516	11606	5523	21036	10026
Ni	12.1	12.7	7.52	10.4	13.3
Mo	10.5	9.42	3.58	8.14	3.79
Cd	46.4	51.5	24.7	52.6	35.1
Cr	23.0	25.1	14.5	42.1	39.3
Sr	134	143	139	245	165
B	125	126	77.1	220	135
Ba	510	535	697	4.01	763
Pb	5994	6263	5563	36215	22785
Si	9.60	0.000	2.20	2.80	28.4
V	54.1	59.5	40.3	92.2	86.0

Table B-2. Concentrations of total metal and major cations for soil profile 98-2

Samples	98-2-0-5	98-2-5-10	98-2-10-15	98-2-15-20
Cations	mg kg^{-1}	mg kg^{-1}	mg kg^{-1}	mg kg^{-1}
Ca	11075	10445	5174	3791
Mg	6403	9613	5509	6605
Na	4518	3249	10920	5283
K	16045	20175	26915	24355
P	2897	2208	944	1328
Al	42538	54848	54808	55888
Fe	42121	74100	25662	76269
Mn	3060	2605	554	3332
Ti	2809	2986	4627	3153
Cu	583	735	64.7	334
Zn	12866	21226	2788	11466
Ni	12.2	11.7	8.83	10.4
Mo	9.64	2.52	0.758	0.000
Cd	106	81.4	36.9	70.2
Cr	26.5	42.1	31.8	24.5
Sr	125	184	155	129
B	91.1	247	85.1	242
Ba	418	211	765	938
Pb	7833	49315	404	12915
Si	0.000	210	98.4	161
V	55.5	98.6	62.1	107

Table B-3. Concentrations of total metal and major cations for soil profile 98-3

Samples	98-3-0-5	98-3-5-10	98-3-10-15	98-3-15-20	98-3-20-25	98-3-25-30
Cations	mg kg^{-1}	mg kg^{-1}	mg kg^{-1}	mg kg^{-1}	mg kg^{-1}	mg kg^{-1}
Ca	10735	8654	6212	5794	2877	3908
Mg	6543	7905	7842	8002	6217	5792
Na	5723	5412	3224	3004	3706	7499
K	17915	20045	21225	23165	21975	22745
P	1543	1366	1963	1414	1163	1035
Al	46238	45838	52408	49528	50858	51908
Fe	62378	61849	86857	82598	117493	50803
Mn	3994	3375	4054	2951	8741	3114
Ti	2849	2919	4255	3001	3243	3475
Cu	535	435	1132	608	212	105
Zn	20866	18016	24516	17936	14116	6632
Ni	10.8	8.03	12.7	10.8	10.8	11.2
Mo	13.7	0.000	0.000	0.000	0.000	0.634
Cd	120	97.7	103	88.6	145	106
Cr	24.9	25.1	45.3	36.8	35.9	29.2
Sr	159	183	272	170	115	157
B	146	171	185	304	325	150
Ba	95.2	215	41.1	374	626	1154
Pb	10895	18635	34545	27555	14435	2173
Si	0.000	56.0	186	283	51.3	107
V	64.0	73.2	99.3	113	126	72.6

Table B-4. Concentrations of total metal and major cations for soil profile 99-1

Samples	99-1-0-7	99-1-0-7 (Duplicate)	99-1-7-12	99-1-12-21	99-1-12-21 (Duplicate)	99-1-21-40
Cations	mg kg^{-1}	mg kg^{-1}	mg kg^{-1}	mg kg^{-1}	mg kg^{-1}	mg kg^{-1}
Ca	4411	4289	2284	2860	2891	3804
Mg	4817	4820	4051	6835	7511	5439
Na	4629	5795	4422	4084	5005	6656
K	18705	22905	19825	22145	24425	21945
P	904	1012	861	1551	1586	1113
Al	43928	41748	38848	55968	61628	42478
Fe	59117	62727	54999	69098	71580	307033
Mn	3683	3857	1410	6936	7021	1012
Ti	2797	2828	2997	3433	3686	3604
Cu	599	667	335	576	607	89.5
Zn	7533	7979	1818	4476	4436	2966
Ni	7.81	9.06	5.87	13.5	13.6	12.6
Mo	10.3	12.2	3.70	5.25	7.72	0.259
Cd	40.7	45.2	11.0	26.6	26.3	42.4
Cr	19.7	21.2	22.9	40.1	39.5	31.4
Sr	120	122	102	130	141	118
B	139	148	120	207	167	164
Ba	127	171	694	775	847	726
Pb	4299	4560	3228	12515	12935	519
Si	3.30	41.8	0.000	117	67.6	289
V	55.6	59.7	58.1	104	106	65.9

Table B-5. Concentrations of total metal and major cations for soil profile 99-2

Samples	99-2-0-7	99-2-7-11	99-2-11-15
Cations	mg kg^{-1}	mg kg^{-1}	mg kg^{-1}
Ca	5763	3853	3019
Mg	7496	5964	4285
Na	3686	3951	7844
K	22185	19425	26365
P	1490	1021	700
Al	60848	47088	43388
Fe	66922	61133	29904
Mn	4213	5087	2383
Ti	3162	2829	2808
Cu	777	274	110
Zn	11396	7397	3214
Ni	14.4	11.7	7.69
Mo	16.1	2.75	1.40
Cd	57.7	46.8	30.0
Cr	35.3	27.2	12.5
Sr	136	139	188
B	153	137	66.8
Ba	332	763	1068
Pb	8915	9127	1114
Si	0.000	0.000	8.00
V	83.5	79.5	48.8

Figure B-1: Location 98-1 Soil Texture Profile

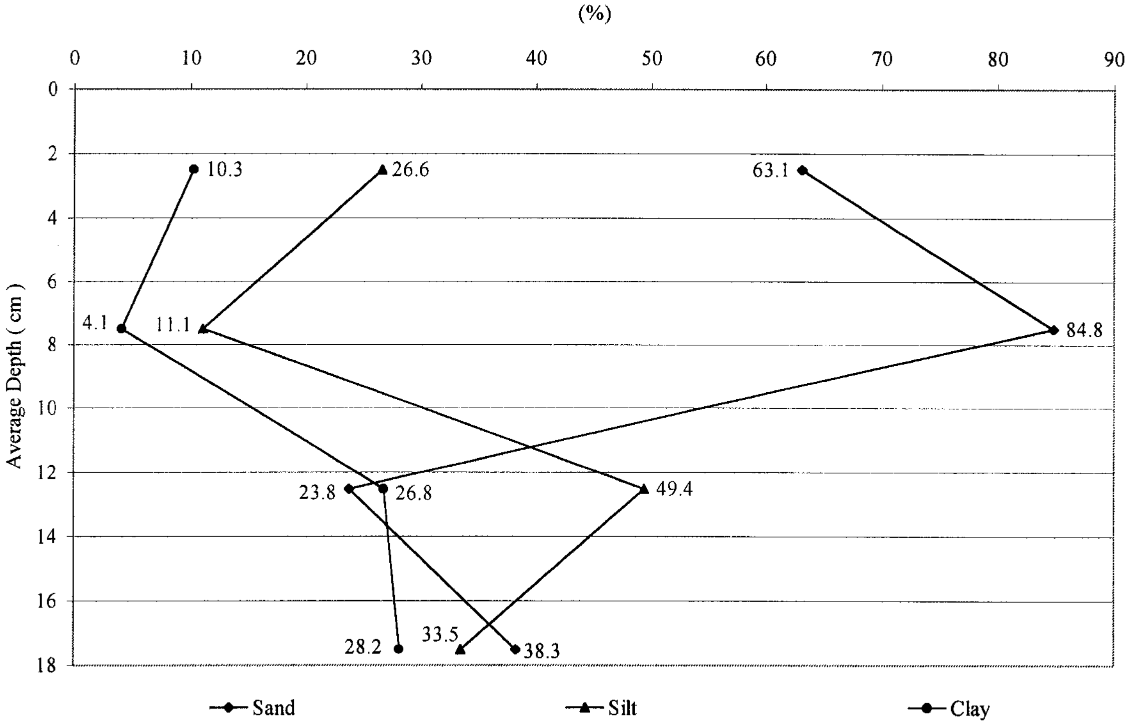

Figure B-2: Location 98-1 Soil Carbon Profile

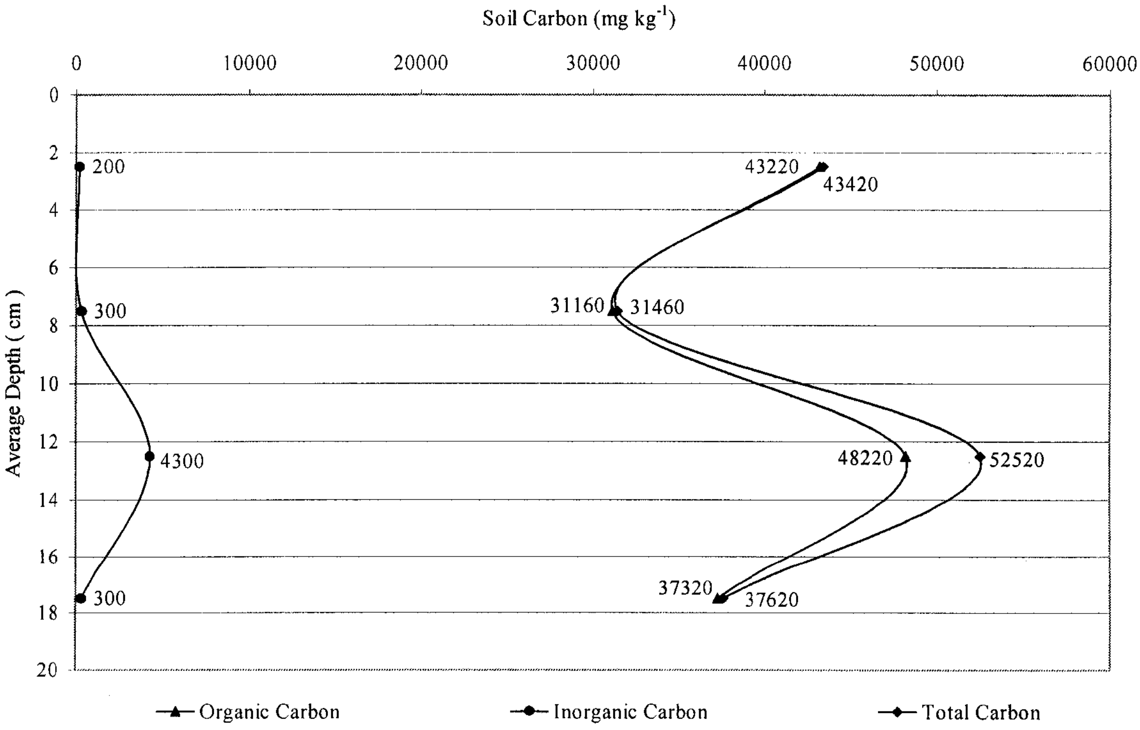

Figure B-3: Location 98-2 Soil Texture Profile

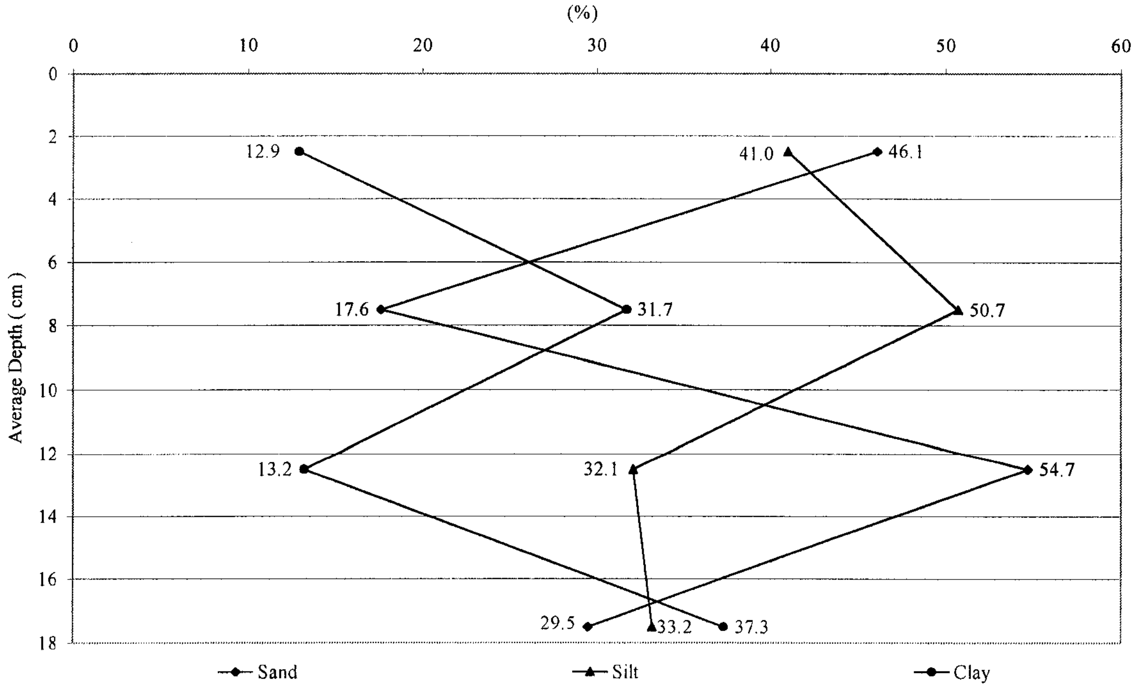

Figure B-4: Location 98-2 Soil Carbon Profile

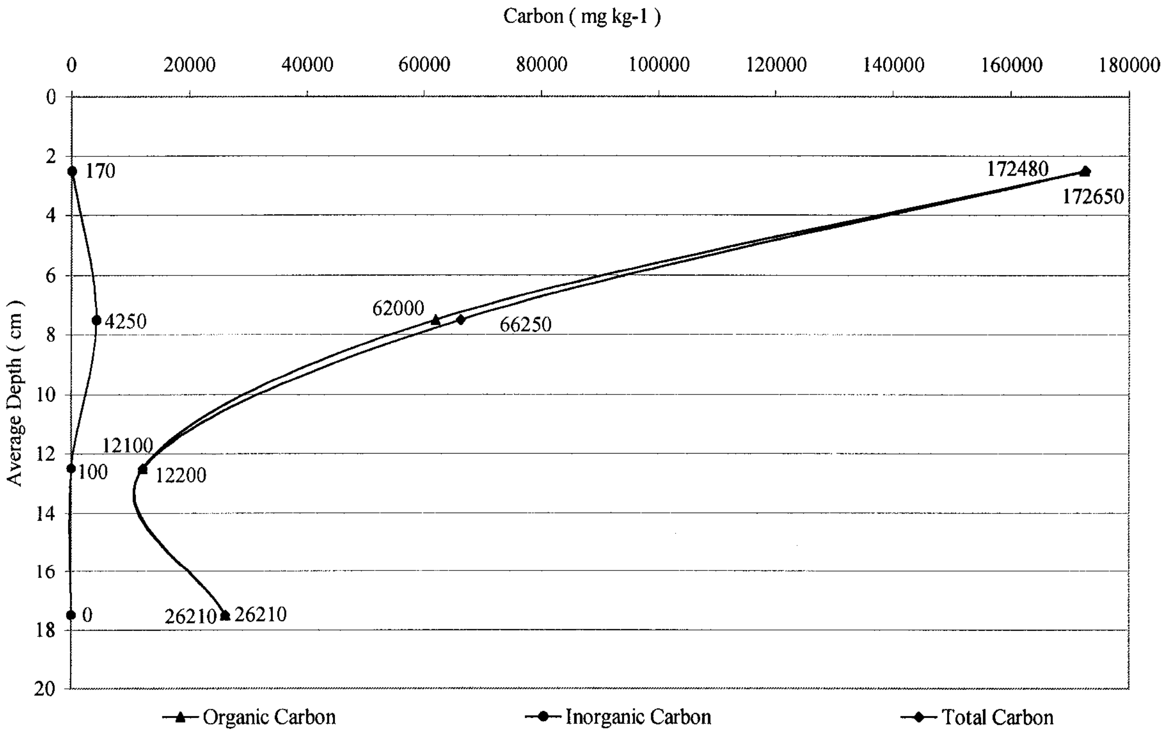

Figure B-5: Location 98-3 Soil Texture Profile

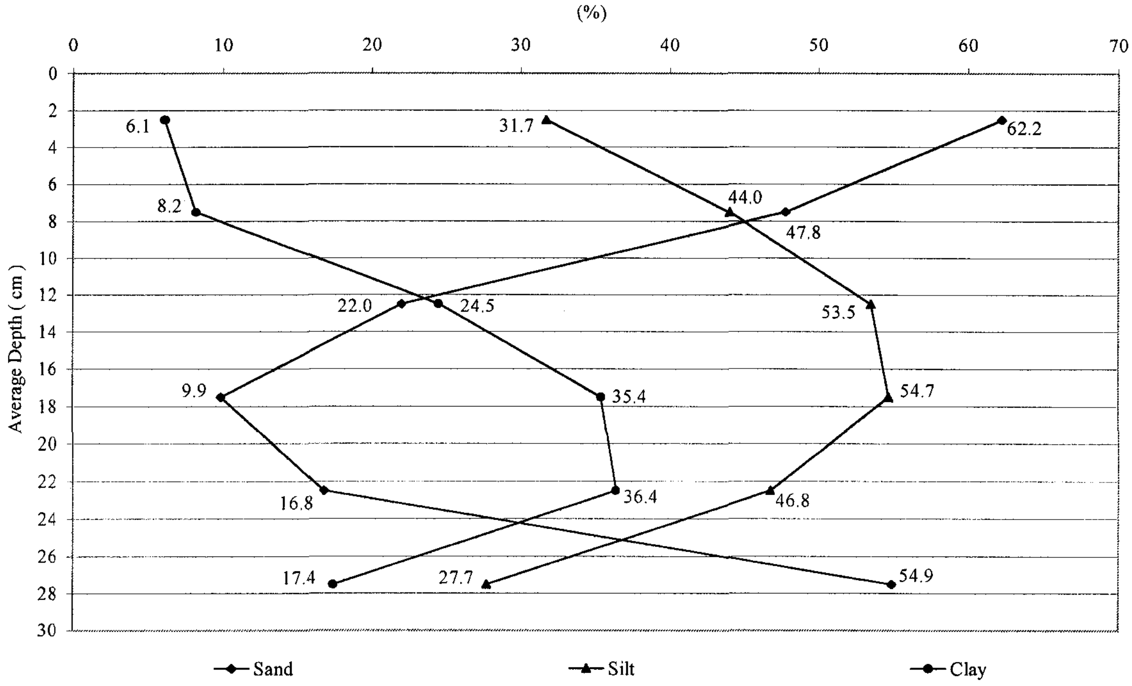

Figure B-6: Location 98-3 Soil Carbon Profile

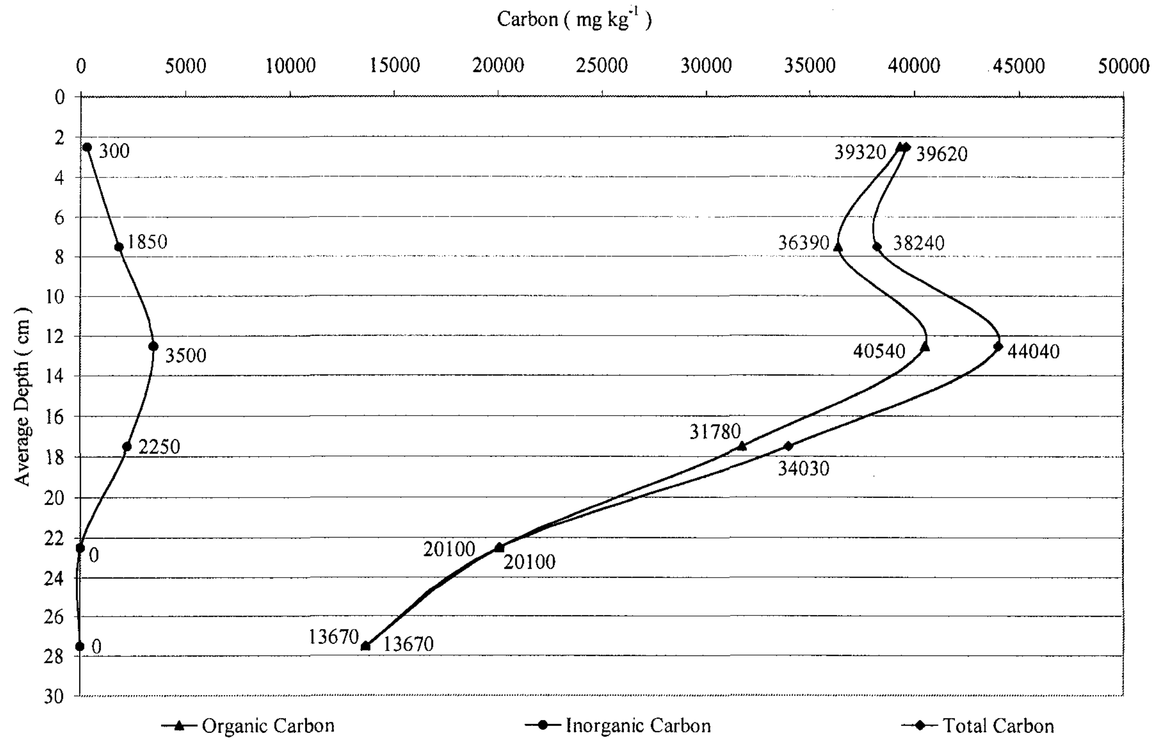

Figure B-7: Location 99-1 Soil Texture Profile

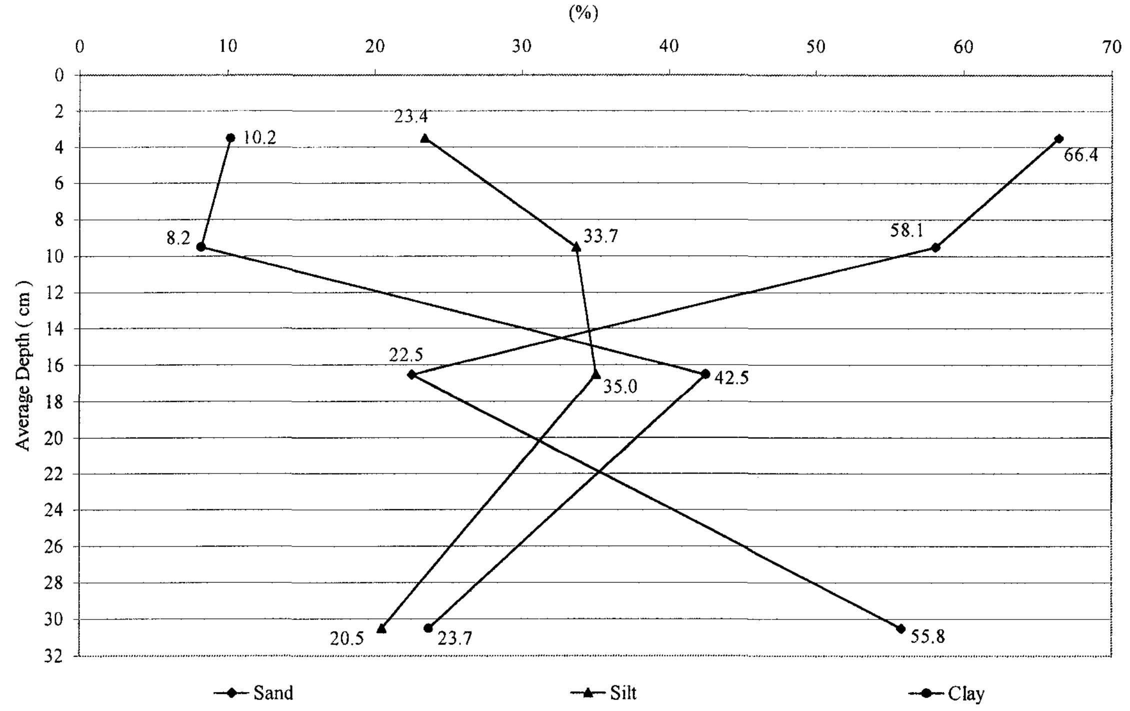

Figure B-8: Location 99-1 Soil Carbon profile

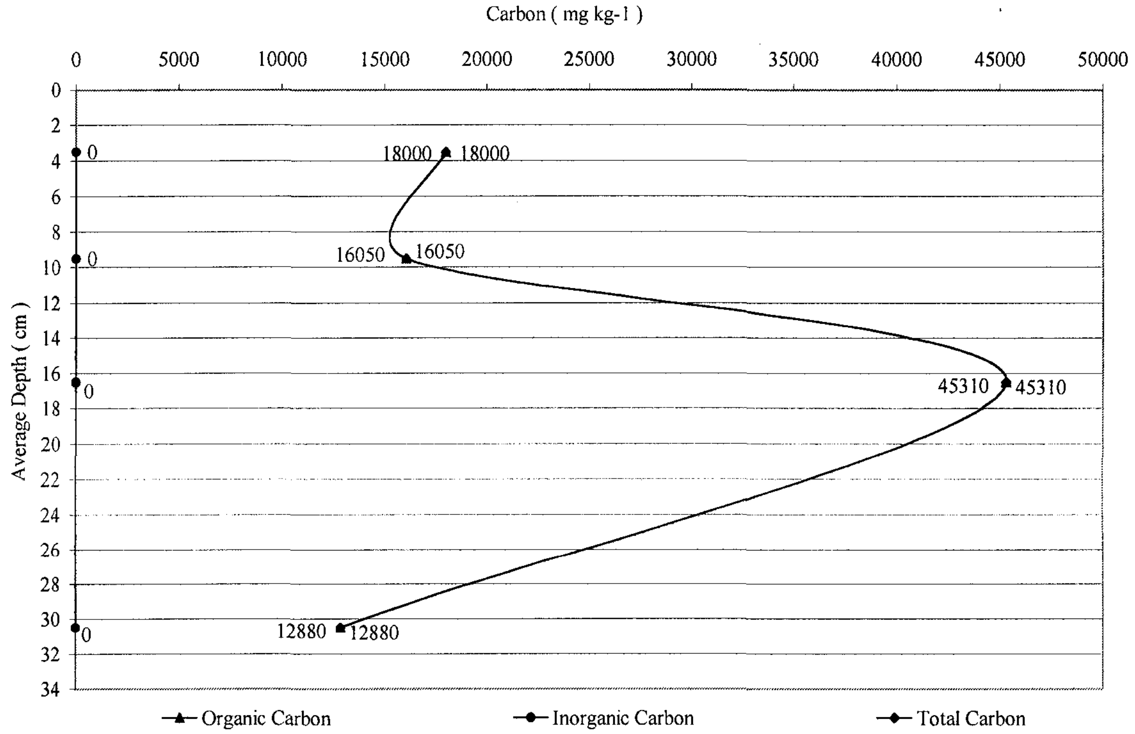

Figure B-9: Location 99-2 Soil Texture Profile

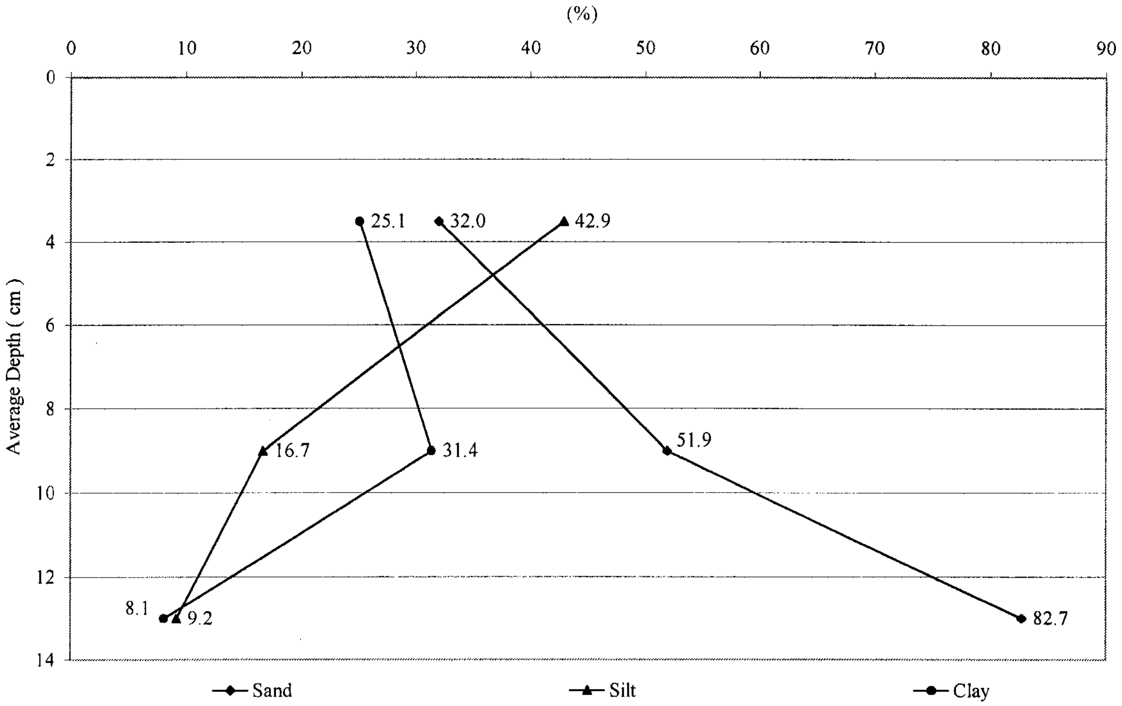

Figure B-10: Location 99-2 Soil Carbon profile

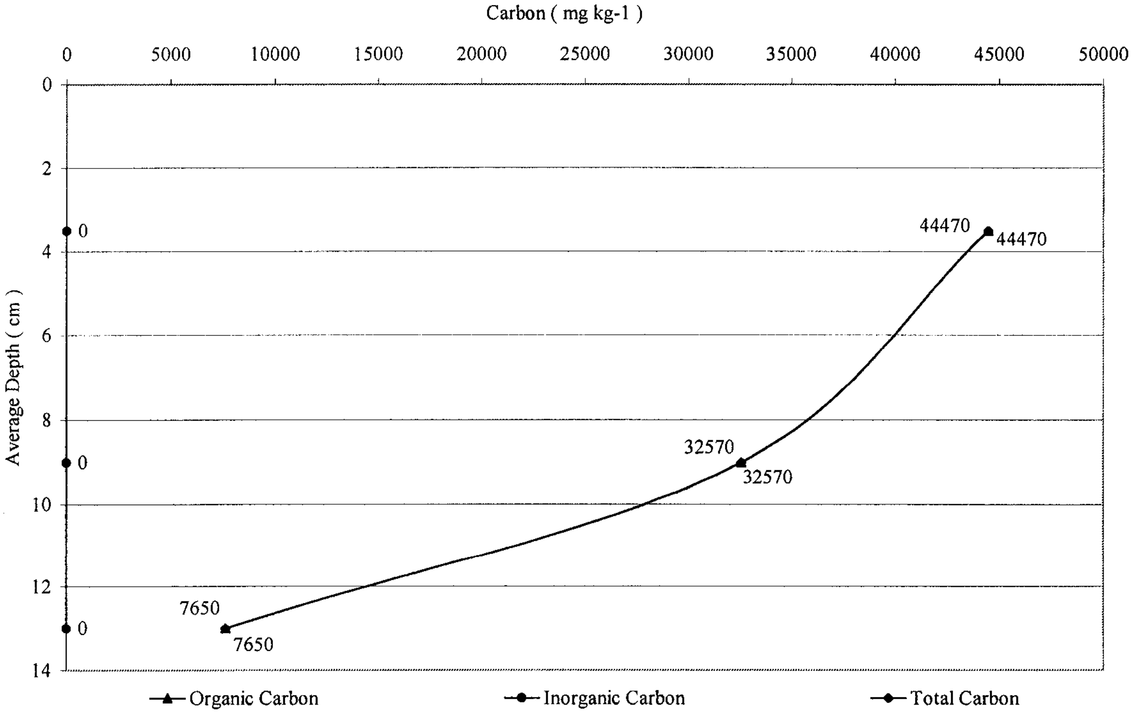

APPENDIX C

Sample 99-1-0-7 Zinc Master Table
and
Metal Partitioning Summary Tables
for
Samples 99-1-0-7, 99-1-7-12,
98-3-5-10, and 98-3-20-25
Using 2003-2004
Selective Extraction Data

Table C-1. Sample 99-1-0-7 zinc master table

99-1-0-7 Zinc

Kaolinite	**Kaolinite**	**Kaolinite**	**Kaolinite**	**Illite**	**Illite**
Input	Output	Output	Output	Input	Output
Total Zinc	Total Zinc (all species) in Solution [Input Zn - Total Exchangeable and Sorbed Zn]	Total Exchangeable Zinc (K)*	Total Sorbed Zinc (K)*	Total Zinc	Total Zinc (all Species) in Solution [Input Zn - Total Exchangeable Zn]
(mg/l)	(mg/l)	(mg/kg)	(mg/kg)	(mg/l)	(mg/l)
1,000	980	15.1	4.08	1,000	772
500	485	11.5	2.45	500	341
100	95.4	3.80	0.573	100	57.2
50	47.5	2.06	0.293	50	27.6
10	9.47	0.442	0.060	10	5.33
5	4.73	0.223	0.030	5	2.65
	1.63**	**0.077**	**0.010**		**1.63****
1	0.946	0.045	0.006	1	0.529
0.5	0.473	0.022	0.003	0.5	0.265
0.1	0.095	0.004	0.001	0.1	0.053
0.05	0.047	0.002	0.000	0.05	0.026
0.01	0.009	0.000	0.000	0.01	0.005
* Weighting Factor Applied					
** Experimental Data					
Predicted Exchangeable		0.077			
Predicted Sorbed			0.010		
Predicted Complexed					

Table C-1. Sample 99-1-0-7 zinc master table (cont.)

Illite	**Montmorillonite**	**Montmorillonite**	**Montmorillonite**	**Montmorillonite**	**FeOOH**
Output	Input	Output	Output	Output	Input
X2-Zn (I)*	Total Zinc	Total Zinc (all species) in Solution [Input Zn - Total Exchangeable and Sorbed Zn]	X2-Zn (M)*	SO-Zn+ (M)*	Total Zinc
(mg/kg)	(mg/l)	(mg/l)	(mg/kg)	(mg/kg)	(mg/l)
1615	1,000	499	579	117	1,000
1125	500	197	354	67.0	500
303	100	29.2	84.7	13.7	100
159	50	13.9	43.4	6.79	50
33.0	10	2.66	8.86	1.35	
16.6		**1.63****	**5.42**	**0.825**	10
10.2	5	1.33	4.44	0.670	5
3.33	1	0.264	0.890	0.134	1
1.67	0.5	0.132	0.445	0.067	0.5
0.334	0.1	0.026	0.089	0.013	0.1
0.167	0.05	0.013	0.045	0.007	0.05
0.033	0.01	0.003	0.009	0.001	0.01
10.2			5.42		
				0.825	

Table C-1. Sample 99-1-0-7 zinc master table (cont.)

FeOOH Output Total Zinc (all species) in Solution [Input Zn - Total Sorbed Zn] (mg/l)	**FeOOH** Output S(st)O-Zn+ (Fe)* (mg/kg)	**FeOOH** Output S(wk)O-Zn+ (Fe)* (mg/kg)	**SOM** Input Total Zinc (mg/l	**SOM** Output Total Zinc (all species) in Solution [Input Zn - Total Exchangeable and Complexed Zn] (mg/l)	**SOM** Output Total Exchangeable Zinc (D) (Solid HA and FA)(SOM)* (mg/kg)
529	177	512	1000	120	0.449
220	174	235	500	10.3	4.04
12.1	115	13.8		**1.63****	**2.25**
3.55	63.6	4.23	100	0.056	1.93
1.63**	**32.0**	**1.96**	50	0.014	0.985
0.490	13.3	0.614	10	0.001	0.160
0.246	6.65	0.296	5	0.001	0.074
0.045	1.34	0.058	1	0.000	0.014
0.024	0.667	0.029	0.5	0.000	0.007
0.005	0.134	0.006	0.1	0.000	0.001
0.002	0.067	0.003	0.05	0.000	0.001
0.000	0.013	0.001	0.01	0.000	0.000
					2.25
	32.0	1.96			

Table C-1. Sample 99-1-0-7 zinc master table (cont.)

SOM Output Total Complexed Zinc (Solid HA and FA)(SOM)* (mg/kg)	**SOM** Output Total Exchangeable Zinc (Dissolved FA)(SOM)* (mg/kg)		Total Soluble Zinc (mg/kg)[mg/l]	"Predicted" Total Exchangeable Zinc (mg/kg)	"Predicted" Total Sorbed and Complexed Zinc (mg/kg)	"Predicted" Total Zinc (mg/kg)
1007	33.3					
559	15.1					
183	**3.49**					
115	1.40					
57.5	0.590					
11.6	0.104					
5.78	0.051					
1.16	0.010					
0.579	0.005					
0.116	0.001					
0.058	0.000					
0.012	0.000					
	3.49			**"21.4"**		
					"34.8"	
183					**"183"**	**"239"**
		Experimental Data				
		0.01M $Ca(NO_3)_2$ Extractable	**(65.2)[1.63]**			
		0.03M $La(NO_3)_3$ Extractable		**26.4 [91.6-65.2]**		
		0.05M $Pb(NO_3)_2$ Extractable			**204 [296-91.6]**	
		HNO_3-$HClO_4$-HF Extractable				**7,760**

Summary Table Definitions

TX [kaolinite] - total exchangeable metals

TS [kaolinite] – total sorbed metals

X2 [illite, montmorillonite] – total exchangeable metals

SO [montmorillonite] – total sorbed metals

st [FeOOH] – total sorbed metals associated with strong affinity sites

wk [FeOOH] – total sorbed metals associated with weak affinity sites

(D) [SOM] – total exchangeable metals associated with diffuse layer

TC(S) [SOM] – total complexed metals associated with solid HA and FA

TC(D) [SOM] – total exchangeable metals associated with dissolved HA and FA

Table C-2. Modeling output for sample 99-1-0-7 [non-competitive modeling approach]

99-1-0-7						
	Predicted Value	Weighting Factor	Adjusted Predicted Value		Metal	Total Exchangeable
						[TX,X2,(D),TC(D)]
	(mg kg^{-1})		(mg kg^{-1})			(mg kg^{-1})
Kaolinite					Cadmium	4.71
TX-Cd	0.240	0.031663081	0.008		Copper	1.65
TS-Cd	0.022	0.031663081	0.001		Lead	2.42
TX-Cu	0.041	0.031663081	0.001		Zinc	21.4
TS-Cu	0.022	0.031663081	0.001			
TX-Pb	0.041	0.031663081	0.001			**Total Sorbed**
TS-Pb	0.047	0.031663081	0.001			**[TS,SO, st,wk]**
TX-Zn	2.43	0.031663081	0.077			**(mg kg^{-1})**
TS-Zn	0.326	0.031663081	0.010		Cadmium	0.992
					Copper	8.40
Illite					Lead	149
X2-Cd	2.72	0.235924818	0.642		Zinc	34.8
X2-Cu	0.292	0.235924818	0.069			
X2-Pb	0.290	0.235924818	0.068			**Total Complexed**
X2-Zn	43.3	0.235924818	10.2			**[TC(S)]**
						(mg kg^{-1})
Montmorillonite					Cadmium	118
X2-Cd	9.65	0.046366727	0.447		Copper	73.2
SO-Cd+	0.314	0.046366727	0.015		Lead	166
X2-Cu	0.806	0.046366727	0.037		Zinc	183
SO-Cu+	1.76	0.046366727	0.082			
X2-Pb	0.750	0.046366727	0.035			
SO-Pb+	0.802	0.046366727	0.037			
X2-Zn	117	0.046366727	5.42			
SO-Zn+	17.8	0.046366727	0.825			
FeOOH						
st-Cd	19.7	0.04868162	0.959			
wk-Cd	0.348	0.04868162	0.017			
st-Cu	140	0.04868162	6.82			
wk-Cu	30.8	0.04868162	1.50			
st-Pb	3040	0.04868162	148			
wk-Pb	27.4	0.04868162	1.33			
st-Zn	657	0.04868162	32.0			
wk-Zn	40.3	0.04868162	1.96			
SOM						
Cd(D)	66.3	0.034201026	2.27			
TC(S)Cd	3441	0.034201026	118			
TC(D)Cd	39.1	0.034201026	1.34			
Cu(D)	2.70	0.034201026	0.092			
TC(S)Cu	2139	0.034201026	73.2			
TC(D)Cu	42.3	0.034201026	1.45			
Pb(D)	6.74	0.034201026	0.231			
TC(S)Pb	4841	0.034201026	166			
TC(D)Pb	60.8	0.034201026	2.08			
Zn(D)	65.8	0.034201026	2.25			
TC(S)Zn	5347	0.034201026	183			
TC(D)Zn	102	0.034201026	3.49			

Table C-3. Modeling output for sample 99-1-0-7 [competitive modeling approach]

99-1-0-7 CCPZ					
	Predicted Value (mg kg^{-1})	**Weighting Factor**	**Adjusted Predicted Value (mg kg^{-1})**	**Metal**	**Total Exchangeable [TX,X2,(D),TC(D)] (mg kg^{-1})**
Kaolinite				Cadmium	3.12
TX-Cd	0.228	0.031663081	0.007	Copper	2.12
TS-Cd	0.019	0.031663081	0.001	Lead	1.04
TX-Cu	0.018	0.031663081	0.001	Zinc	19.3
TS-Cu	0.019	0.031663081	0.001		
TX-Pb	0.035	0.031663081	0.001		**Total Sorbed**
TS-Pb	0.043	0.031663081	0.001		**[TS,SO,st,wk]**
TX-Zn	2.85	0.031663081	0.090		**(mg kg^{-1})**
TS-Zn	0.098	0.031663081	0.003	Cadmium	0.977
				Copper	16.2
Illite				Lead	107
X2-Cd	2.72	0.235924818	0.642	Zinc	21.7
X2-Cu	0.292	0.235924818	0.069		
X2-Pb	0.290	0.235924818	0.068		**Total Complexed**
X2-Zn	42.5	0.235924818	10.0		**[TC(S)]**
					(mg kg^{-1})
Montmorillonite				Cadmium	57.8
X2-Cd	9.65	0.046366727	0.447	Copper	76.4
SO-Cd+	0.314	0.046366727	0.015	Lead	63.9
X2-Cu	0.807	0.046366727	0.037	Zinc	117
SO-Cu+	1.77	0.046366727	0.082		
X2-Pb	0.750	0.046366727	0.035		
SO-Pb+	0.802	0.046366727	0.037		
X2-Zn	116	0.046366727	5.38		
SO-Zn+	17.2	0.046366727	0.798		
FeOOH					
st-Cd	19.4	0.04868162	0.944		
wk-Cd	0.347	0.04868162	0.017		
st-Cu	253	0.04868162	12.3		
wk-Cu	78.0	0.04868162	3.80		
st-Pb	2154	0.04868162	105		
wk-Pb	36.9	0.04868162	1.80		
st-Zn	390	0.04868162	19.0		
wk-Zn	39.5	0.04868162	1.92		
SOM					
Cd(D)	37.9	0.034201026	1.30		
TC(S)Cd	1689	0.034201026	57.8		
TC(D)Cd	21.0	0.034201026	0.718		
Cu(D)	1.72	0.034201026	0.059		
TC(S)Cu	2233	0.034201026	76.4		
TC(D)Cu	57.1	0.034201026	1.95		
Pb(D)	2.72	0.034201026	0.093		
TC(S)Pb	1867	0.034201026	63.9		
TC(D)Pb	24.5	0.034201026	0.838		
Zn(D)	48.2	0.034201026	1.65		
TC(S)Zn	3429	0.034201026	117		
TC(D)Zn	63.7	0.034201026	2.18		

Table C-4. Modeling output for sample 99-1-7-12 [non-competitive modeling approach]

99-1-7-12	Predicted Value (mg kg^{-1})	Weighting Factor	Adjusted Predicted Value (mg kg^{-1})	Metal	Total Exchangeable [TX,X2,(D),TC(D)] (mg kg^{-1})
Kaolinite					
TX-Cd	0.085	0.014934263	0.001	Cadmium	0.563
TS-Cd	0.000	0.014934263	0.000	Copper	0.976
TX-Cu	0.132	0.014934263	0.002	Lead	2.32
TS-Cu	0.001	0.014934263	0.000	Zinc	11.0
TX-Pb	0.446	0.014934263	0.007		
TS-Pb	0.004	0.014934263	0.000		**Total Sorbed**
TX-Zn	1.20	0.014934263	0.018		**[TS,SO,st,wk]**
TS-Zn	0.006	0.014934263	0.000		**(mg kg^{-1})**
				Cadmium	0.001
Illite				Copper	0.222
X2-Cd	0.955	0.190197977	0.182	Lead	26.6
X2-Cu	0.955	0.190197977	0.182	Zinc	0.081
X2-Pb	3.18	0.190197977	0.605		
X2-Zn	21.4	0.190197977	4.07		**Total Complexed**
					[TC(S)]
Montmorillonite					**(mg kg^{-1})**
X2-Cd	3.41	0.096750964	0.330	Cadmium	2.06
SO-Cd+	0.001	0.096750964	0.000	Copper	21.0
X2-Cu	2.58	0.096750964	0.250	Lead	48.1
SO-Cu+	0.057	0.096750964	0.006	Zinc	46.5
X2-Pb	8.28	0.096750964	0.801		
SO-Pb+	0.090	0.096750964	0.009		
X2-Zn	58.1	0.096750964	5.62		
SO-Zn+	0.089	0.096750964	0.009		
FeOOH					
st-Cd	0.024	0.043950759	0.001		
wk-Cd	0.000	0.043950759	0.000		
st-Cu	4.07	0.043950759	0.179		
wk-Cu	0.838	0.043950759	0.037		
st-Pb	604	0.043950759	26.5		
wk-Pb	1.19	0.043950759	0.052		
st-Zn	1.56	0.043950759	0.069		
wk-Zn	0.065	0.043950759	0.003		
SOM					
Cd(D)	0.505	0.030495915	0.015		
TC(S)Cd	67.4	0.030495915	2.06		
TC(D)Cd	1.16	0.030495915	0.035		
Cu(D)	0.458	0.030495915	0.014		
TC(S)Cu	689	0.030495915	21.0		
TC(D)Cu	17.3	0.030495915	0.528		
Pb(D)	1.21	0.030495915	0.037		
TC(S)Pb	1578	0.030495915	48.1		
TC(D)Pb	28.7	0.030495915	0.875		
Zn(D)	13.0	0.030495915	0.396		
TC(S)Zn	1525	0.030495915	46.5		
TC(D)Zn	29.6	0.030495915	0.903		

Table C-5. Modeling output for sample 99-1-7-12 [competitive modeling approach]

99-1-7-12 CCPZ	Predicted Value (mg kg^{-1})	Weighting Factor	Adjusted Predicted Value (mg kg^{-1})	Metal	Total Exchangeable [TX,X2,(D),TC(D)] (mg kg^{-1})
Kaolinite					
TX-Cd	0.081	0.014934263	0.001	Cadmium	0.557
TS-Cd	0.000	0.014934263	0.000	Copper	0.876
TX-Cu	0.059	0.014934263	0.001	Lead	1.87
TS-Cu	0.000	0.014934263	0.000	Zinc	10.4
TX-Pb	0.387	0.014934263	0.006		
TS-Pb	0.004	0.014934263	0.000		**Total Sorbed**
TX-Zn	1.42	0.014934263	0.021		**[TS,SO,st,wk]**
TS-Zn	0.000	0.014934263	0.000		**(mg kg^{-1})**
				Cadmium	0.001
Illite				Copper	0.222
X2-Cd	0.955	0.190197977	0.182	Lead	19.0
X2-Cu	0.955	0.190197977	0.182	Zinc	0.080
X2-Pb	3.16	0.190197977	0.601		
X2-Zn	21.2	0.190197977	4.03		**Total Complexed**
					[TC(S)]
Montmorillonite					**(mg kg^{-1})**
X2-Cd	3.41	0.096750964	0.330	Cadmium	1.71
SO-Cd+	0.001	0.096750964	0.000	Copper	15.6
X2-Cu	2.60	0.096750964	0.252	Lead	22.6
SO-Cu+	0.058	0.096750964	0.006	Zinc	25.7
X2-Pb	8.28	0.096750964	0.801		
SO-Pb+	0.090	0.096750964	0.009		
X2-Zn	57.3	0.096750964	5.54		
SO-Zn+	0.089	0.096750964	0.009		
FeOOH					
st-Cd	0.023	0.043950759	0.001		
wk-Cd	0.000	0.043950759	0.000		
st-Cu	4.07	0.043950759	0.179		
wk-Cu	0.838	0.043950759	0.037		
st-Pb	429	0.043950759	18.9		
wk-Pb	1.00	0.043950759	0.044		
st-Zn	1.54	0.043950759	0.068		
wk-Zn	0.065	0.043950759	0.003		
SOM					
Cd(D)	0.494	0.030495915	0.015		
TC(S)Cd	56.0	0.030495915	1.71		
TC(D)Cd	0.941	0.030495915	0.029		
Cu(D)	0.345	0.030495915	0.011		
TC(S)Cu	511	0.030495915	15.6		
TC(D)Cu	14.1	0.030495915	0.430		
Pb(D)	0.840	0.030495915	0.026		
TC(S)Pb	740	0.030495915	22.6		
TC(D)Pb	14.1	0.030495915	0.430		
Zn(D)	10.1	0.030495915	0.308		
TC(S)Zn	844	0.030495915	25.7		
TC(D)Zn	17.0	0.030495915	0.518		

Table C-6. Modeling output for sample 98-3-5-10 [non-competitive modeling approach]

98-3-5-10	**Predicted Value** (mg kg^{-1})	**Weighting Factor**	**Adjusted Predicted Value** (mg kg^{-1})	**Metal**	**Total Exchangeable [TX,X2,(D),TC(D)]** (mg kg^{-1})
Kaolinite				Cadmium	35.0
TX-Cd	0.883	0.039035856	0.034	Copper	6.30
TS-Cd	0.506	0.039035856	0.020	Lead	41.8
TX-Cu	0.089	0.039035856	0.003	Zinc	74.2
TS-Cu	0.301	0.039035856	0.012		
TX-Pb	1.18	0.039035856	0.046		**Total Sorbed**
TS-Pb	8.86	0.039035856	0.346		**[TS,SO, st,wk]**
TX-Zn	6.06	0.039035856	0.237		**(mg kg^{-1})**
TS-Zn	3.28	0.039035856	0.128	Cadmium	34.1
				Copper	13.2
Illite				Lead	1,052
X2-Cd	9.96	0.250353909	2.49	Zinc	195
X2-Cu	0.641	0.250353909	0.160		
X2-Pb	8.37	0.250353909	2.10		**Total Complexed**
X2-Zn	107	0.250353909	26.8		**[TC(S)]**
					(mg kg^{-1})
Montmorillonite				Cadmium	733
X2-Cd	35.3	0.042316273	1.49	Copper	293
SO-Cd+	5.55	0.042316273	0.235	Lead	2,355
X2-Cu	1.18	0.042316273	0.050	Zinc	1,067
SO-Cu+	12.4	0.042316273	0.525		
X2-Pb	22.1	0.042316273	0.935		
SO-Pb+	113	0.042316273	4.78		
X2-Zn	283	0.042316273	12.0		
SO-Zn+	199	0.042316273	8.42		
FeOOH					
st-Cd	668	0.04942204	33.0		
wk-Cd	16.8	0.04942204	0.830		
st-Cu	202	0.04942204	9.98		
wk-Cu	53.4	0.04942204	2.64		
st-Pb	11587	0.04942204	573		
wk-Pb	9582	0.04942204	474		
st-Zn	2630	0.04942204	130		
wk-Zn	1151	0.04942204	56.9		
SOM					
Cd(D)	298	0.069143074	20.6		
TC(S)Cd	10603	0.069143074	733		
TC(D)Cd	150	0.069143074	10.4		
Cu(D)	15.3	0.069143074	1.06		
TC(S)Cu	4244	0.069143074	293		
TC(D)Cu	72.7	0.069143074	5.03		
Pb(D)	55.9	0.069143074	3.87		
TC(S)Pb	34056	0.069143074	2355		
TC(D)Pb	503	0.069143074	34.8		
Zn(D)	133	0.069143074	9.20		
TC(S)Zn	15433	0.069143074	1067		
TC(D)Zn	376	0.069143074	26.0		

Table C-7. Modeling output for sample 98-3-5-10 [competitive modeling approach]

98-3-5-10 CCPZ						
	Predicted Value (mg kg^{-1})	**Weighting Factor**	**Adjusted Predicted Value (mg kg^{-1})**		**Metal**	**Total Exchangeable [TX,X2,(D),TC(D)] (mg kg^{-1})**
Kaolinite					Cadmium	15.0
TX-Cd	0.837	0.039035856	0.033		Copper	5.93
TS-Cd	0.462	0.039035856	0.018		Lead	7.24
TX-Cu	0.041	0.039035856	0.002		Zinc	48.9
TS-Cu	0.290	0.039035856	0.011			
TX-Pb	1.04	0.039035856	0.041			**Total Sorbed**
TS-Pb	8.03	0.039035856	0.313			**[TS,SO, st,wk]**
TX-Zn	7.07	0.039035856	0.276			**(mg kg^{-1})**
TS-Zn	1.43	0.039035856	0.056		Cadmium	18.4
					Copper	20.6
Illite					Lead	149
X2-Cd	9.87	0.250353909	2.47		Zinc	130
X2-Cu	0.641	0.250353909	0.160			
X2-Pb	8.37	0.250353909	2.10			**Total Complexed**
X2-Zn	104	0.250353909	26.0			**[TC(S)]**
						(mg kg^{-1})
Montmorillonite					Cadmium	228
X2-Cd	35.1	0.042316273	1.49		Copper	237
SO-Cd+	5.38	0.042316273	0.228		Lead	261
X2-Cu	1.80	0.042316273	0.076		Zinc	259
SO-Cu+	18.9	0.042316273	0.800			
X2-Pb	22.0	0.042316273	0.931			
SO-Pb+	110	0.042316273	4.65			
X2-Zn	273	0.042316273	11.6			
SO-Zn+	159	0.042316273	6.73			
FeOOH						
st-Cd	351	0.04942204	17.3			
wk-Cd	16.6	0.04942204	0.820			
st-Cu	264	0.04942204	13.0			
wk-Cu	137	0.04942204	6.77			
st-Pb	2769	0.04942204	137			
wk-Pb	128	0.04942204	6.33			
st-Zn	1302	0.04942204	64.3			
wk-Zn	1201	0.04942204	59.4			
SOM						
Cd(D)	119	0.069143074	8.23			
TC(S)Cd	3303	0.069143074	228			
TC(D)Cd	40.1	0.069143074	2.77			
Cu(D)	4.35	0.069143074	0.301			
TC(S)Cu	3426	0.069143074	237			
TC(D)Cu	77.9	0.069143074	5.39			
Pb(D)	7.04	0.069143074	0.487			
TC(S)Pb	3769	0.069143074	261			
TC(D)Pb	53.2	0.069143074	3.68			
Zn(D)	104	0.069143074	7.19			
TC(S)Zn	3742	0.069143074	259			
TC(D)Zn	54.7	0.069143074	3.78			

Table C-8. Modeling output for sample 98-3-20-25 [non-competitive modeling approach]

98-3-20-25	**Predicted Value (mg kg^{-1})**	**Weighting Factor**	**Adjusted Predicted Value (mg kg^{-1})**		**Metal**	**Total Exchangeable [TX,X2,(D),TC(D)] (mg kg^{-1})**
Kaolinite					Cadmium	23.0
TX-Cd	0.994	0.038610373	0.038		Copper	1.55
TS-Cd	0.569	0.038610373	0.022		Lead	16.8
TX-Cu	0.030	0.038610373	0.001		Zinc	51.0
TS-Cu	0.100	0.038610373	0.004			
TX-Pb	0.155	0.038610373	0.006			**Total Sorbed**
TS-Pb	1.19	0.038610373	0.046			**[TS,SO, st,wk]**
TX-Zn	4.95	0.038610373	0.191			**(mg kg^{-1})**
TS-Zn	2.68	0.038610373	0.103		Cadmium	71.6
					Copper	14.7
Illite					Lead	739
X2-Cd	11.2	0.296722909	3.32		Zinc	341
X2-Cu	0.214	0.296722909	0.063			
X2-Pb	1.10	0.296722909	0.326			**Total Complexed**
X2-Zn	87.7	0.296722909	26.0			**[TC(S)]**
						(mg kg^{-1})
Montmorillonite					Cadmium	440
X2-Cd	39.7	0.033118255	1.31		Copper	78
SO-Cd+	6.23	0.033118255	0.206		Lead	1,050
X2-Cu	0.460	0.033118255	0.015		Zinc	504
SO-Cu+	4.84	0.033118255	0.160			
X2-Pb	2.86	0.033118255	0.095			
SO-Pb+	14.8	0.033118255	0.490			
X2-Zn	233	0.033118255	7.72			
SO-Zn+	165	0.033118255	5.46			
FeOOH						
st-Cd	741	0.093866412	69.6			
wk-Cd	18.9	0.093866412	1.77			
st-Cu	124	0.093866412	11.6			
wk-Cu	31.8	0.093866412	2.98			
st-Pb	6466	0.093866412	607			
wk-Pb	1399	0.093866412	131			
st-Zn	2610	0.093866412	245			
wk-Zn	964	0.093866412	90.5			
SOM						
Cd(D)	314	0.038191146	12.0			
TC(S)Cd	11530	0.038191146	440			
TC(D)Cd	166	0.038191146	6.34			
Cu(D)	6.25	0.038191146	0.239			
TC(S)Cu	2054	0.038191146	78.4			
TC(D)Cu	32.3	0.038191146	1.23			
Pb(D)	55.8	0.038191146	2.13			
TC(S)Pb	27495	0.038191146	1050			
TC(D)Pb	371	0.038191146	14.2			
Zn(D)	136	0.038191146	5.19			
TC(S)Zn	13197	0.038191146	504			
TC(D)Zn	311	0.038191146	11.9			

Table C-9. Modeling output for sample 98-3-20-25 [competitive modeling approach]

98-3-20-25	Predicted Value (mg kg^{-1})	Weighting Factor	Adjusted Predicted Value (mg kg^{-1})
Kaolinite			
TX-Cd	0.940	0.038610373	0.036
TS-Cd	0.518	0.038610373	0.020
TX-Cu	0.013	0.038610373	0.001
TS-Cu	0.097	0.038610373	0.004
TX-Pb	0.138	0.038610373	0.005
TS-Pb	1.08	0.038610373	0.042
TX-Zn	5.78	0.038610373	0.223
TS-Zn	1.18	0.038610373	0.046
Illite			
X2-Cd	11.1	0.296722909	3.29
X2-Cu	0.214	0.296722909	0.063
X2-Pb	1.10	0.296722909	0.326
X2-Zn	85.8	0.296722909	25.5
Montmorillonite			
X2-Cd	39.5	0.033118255	1.31
SO-Cd+	6.04	0.033118255	0.200
X2-Cu	0.591	0.033118255	0.020
SO-Cu+	6.22	0.033118255	0.206
X2-Pb	2.91	0.033118255	0.096
SO-Pb+	15.0	0.033118255	0.497
X2-Zn	226	0.033118255	7.48
SO-Zn+	137	0.033118255	4.54
FeOOH			
st-Cd	366	0.093866412	34.4
wk-Cd	18.7	0.093866412	1.76
st-Cu	24.9	0.093866412	2.34
wk-Cu	6.33	0.093866412	0.594
st-Pb	267	0.093866412	25.1
wk-Pb	0.716	0.093866412	0.067
st-Zn	1268	0.093866412	119
wk-Zn	987	0.093866412	92.6
SOM			
Cd(D)	119	0.038191146	4.54
TC(S)Cd	3305	0.038191146	126
TC(D)Cd	40.2	0.038191146	1.54
Cu(D)	4.36	0.038191146	0.167
TC(S)Cu	3388	0.038191146	129
TC(D)Cu	76.7	0.038191146	2.93
Pb(D)	7.19	0.038191146	0.275
TC(S)Pb	3449	0.038191146	132
TC(D)Pb	41.7	0.038191146	1.59
Zn(D)	105	0.038191146	4.01
TC(S)Zn	3662	0.038191146	140
TC(D)Zn	51.3	0.038191146	1.96

Metal	Total Exchangeable [TX,X2,(D),TC(D)] (mg kg^{-1})
Cadmium	10.7
Copper	3.18
Lead	2.29
Zinc	39.2
	Total Sorbed [TS,SO, st,wk] (mg kg^{-1})
Cadmium	36.3
Copper	3.14
Lead	25.7
Zinc	216
	Total Complexed [TC(S)] (mg kg^{-1})
Cadmium	126
Copper	129
Lead	132
Zinc	140

APPENDIX D

Metal Partitioning Summary Tables
for
The Evaluation of Uncertainty in
Clay, FeOOH, and SOM
Weighting Factors
[Surrogate Soils 99-1-7-12, 98-3-5-10, 98-3-20-25]

Table D-1. Case $^{\#}$1 modeling output for sample 99-1-7-12 [CMA].

99-1-7-12 Case #1	**Predicted Value (mg kg^{-1})**	**Weighting Factor**	**Adjusted Predicted Value (mg kg^{-1})**	**Metal**	**Total Exchangeable [TX,X2,(D),TC(D)] (mg kg^{-1})**
Kaolinite					
TX-Cd	0.081	0.015	0.001	Cadmium	0.557
TS-Cd	0.000	0.015	0.000	Copper	0.876
TX-Cu	0.059	0.015	0.001	Lead	1.87
TS-Cu	0.000	0.015	0.000	Zinc	10.4
TX-Pb	0.387	0.015	0.006		
TS-Pb	0.004	0.015	0.000		**Total Sorbed [TS,SO,st,wk] (mg kg^{-1})**
TX-Zn	1.42	0.015	0.021		
TS-Zn	0.000	0.015	0.000		
Illite				Cadmium	0.001
X2-Cd	0.955	0.190	0.182	Copper	0.222
X2-Cu	0.955	0.190	0.182	Lead	19.0
X2-Pb	3.16	0.190	0.601	Zinc	0.080
X2-Zn	21.2	0.190	4.03		
					Total Complexed [TC(S)] (mg kg^{-1})
Montmorillonite					
X2-Cd	3.41	0.097	0.330		
SO-Cd+	0.001	0.097	0.000		
X2-Cu	2.60	0.097	0.252	Cadmium	1.71
SO-Cu+	0.058	0.097	0.006	Copper	15.6
X2-Pb	8.28	0.097	0.801	Lead	22.6
SO-Pb+	0.090	0.097	0.009	Zinc	25.7
X2-Zn	57.3	0.097	5.54		
SO-Zn+	0.089	0.097	0.009		**Total Exchangeable, Sorbed, and Complexed (mg kg^{-1})**
FeOOH					
st-Cd	0.023	0.044	0.001		
wk-Cd	0.000	0.044	0.000		
st-Cu	4.07	0.044	0.179	Cadmium	2.27
wk-Cu	0.838	0.044	0.037	Copper	16.7
st-Pb	429	0.044	18.9	Lead	43.5
wk-Pb	1.00	0.044	0.044	Zinc	36.2
st-Zn	1.54	0.044	0.068		
wk-Zn	0.065	0.044	0.003		**Case #1**
SOM					Kaolinite 8%
Cd(D)	0.494	0.030	0.015		Illite 64%
TC(S)Cd	56.0	0.030	1.71		Montmorillonite 28%
TC(D)Cd	0.941	0.030	0.029		
Cu(D)	0.345	0.030	0.011		
TC(S)Cu	511	0.030	15.6		
TC(D)Cu	14.1	0.030	0.430		
Pb(D)	0.840	0.030	0.026		
TC(S)Pb	740	0.030	22.6		
TC(D)Pb	14.1	0.030	0.430		
Zn(D)	10.1	0.030	0.308		
TC(S)Zn	844	0.030	25.7		
TC(D)Zn	17.0	0.030	0.518		

Table D-2. Case $^{\#}2$ modeling output for sample 99-1-7-12 [CMA].

99-1-7-12 Case #2	Predicted Value (mg kg^{-1})	Weighting Factor	Adjusted Predicted Value (mg kg^{-1})
Kaolinite			
TX-Cd	0.081	0.015	0.001
TS-Cd	0.000	0.015	0.000
TX-Cu	0.059	0.015	0.001
TS-Cu	0.000	0.015	0.000
TX-Pb	0.387	0.015	0.006
TS-Pb	0.004	0.015	0.000
TX-Zn	1.42	0.015	0.021
TS-Zn	0.000	0.015	0.000
Illite			
X2-Cd	0.955	0.081	0.077
X2-Cu	0.955	0.081	0.077
X2-Pb	3.16	0.081	0.255
X2-Zn	21.2	0.081	1.71
Montmorillonite			
X2-Cd	3.41	0.228	0.778
SO-Cd+	0.001	0.228	0.000
X2-Cu	2.60	0.228	0.593
SO-Cu+	0.058	0.228	0.013
X2-Pb	8.28	0.228	1.89
SO-Pb+	0.090	0.228	0.021
X2-Zn	57.3	0.228	13.1
SO-Zn+	0.089	0.228	0.020
FeOOH			
st-Cd	0.023	0.044	0.001
wk-Cd	0.000	0.044	0.000
st-Cu	4.07	0.044	0.179
wk-Cu	0.838	0.044	0.037
st-Pb	429	0.044	18.9
wk-Pb	1.00	0.044	0.044
st-Zn	1.54	0.044	0.068
wk-Zn	0.065	0.044	0.003
SOM			
Cd(D)	0.494	0.030	0.015
TC(S)Cd	56.0	0.030	1.71
TC(D)Cd	0.941	0.030	0.029
Cu(D)	0.345	0.030	0.011
TC(S)Cu	511	0.030	15.6
TC(D)Cu	14.1	0.030	0.430
Pb(D)	0.840	0.030	0.026
TC(S)Pb	740	0.030	22.6
TC(D)Pb	14.1	0.030	0.430
Zn(D)	10.1	0.030	0.308
TC(S)Zn	844	0.030	25.7
TC(D)Zn	17.0	0.030	0.518

Metal	Total Exchangeable [TX,X2,(D),TC(D)] (mg kg^{-1})
Cadmium	0.900
Copper	1.11
Lead	2.61
Zinc	15.7

Metal	Total Sorbed [TS,SO,st,wk] (mg kg^{-1})
Cadmium	0.001
Copper	0.229
Lead	19.0
Zinc	0.091

Metal	Total Complexed [TC(S)] (mg kg^{-1})
Cadmium	1.71
Copper	15.6
Lead	22.6
Zinc	25.7

Metal	Total Exchangeable, Sorbed, and Complexed (mg kg^{-1})
Cadmium	2.61
Copper	16.9
Lead	44.2
Zinc	41.6

Case #2

Kaolinite 8%
Illite 28%
Montmorillonite 64%

Table D-3. Case #3 modeling output for sample 99-1-7-12 [CMA].

99-1-7-12 Case #3	Predicted Value (mg kg^{-1})	Weighting Factor	Adjusted Predicted Value (mg kg^{-1})
Kaolinite			
TX-Cd	0.081	0.007	0.001
TS-Cd	0.000	0.007	0.000
TX-Cu	0.059	0.007	0.000
TS-Cu	0.000	0.007	0.000
TX-Pb	0.387	0.007	0.003
TS-Pb	0.004	0.007	0.000
TX-Zn	1.42	0.007	0.011
TS-Zn	0.000	0.007	0.000
Illite			
X2-Cd	0.955	0.095	0.091
X2-Cu	0.955	0.095	0.091
X2-Pb	3.16	0.095	0.301
X2-Zn	21.2	0.095	2.02
Montmorillonite			
X2-Cd	3.41	0.048	0.165
SO-Cd+	0.001	0.048	0.000
X2-Cu	2.60	0.048	0.126
SO-Cu+	0.058	0.048	0.003
X2-Pb	8.28	0.048	0.401
SO-Pb+	0.090	0.048	0.004
X2-Zn	57.3	0.048	2.77
SO-Zn+	0.089	0.048	0.004
FeOOH			
st-Cd	0.023	0.044	0.001
wk-Cd	0.000	0.044	0.000
st-Cu	4.07	0.044	0.179
wk-Cu	0.838	0.044	0.037
st-Pb	429	0.044	18.9
wk-Pb	1.00	0.044	0.044
st-Zn	1.54	0.044	0.068
wk-Zn	0.065	0.044	0.003
SOM			
Cd(D)	0.494	0.030	0.015
TC(S)Cd	56.0	0.030	1.71
TC(D)Cd	0.941	0.030	0.029
Cu(D)	0.345	0.030	0.011
TC(S)Cu	511	0.030	15.6
TC(D)Cu	14.1	0.030	0.430
Pb(D)	0.840	0.030	0.026
TC(S)Pb	740	0.030	22.6
TC(D)Pb	14.1	0.030	0.430
Zn(D)	10.1	0.030	0.308
TC(S)Zn	844	0.030	25.7
TC(D)Zn	17.0	0.030	0.518

Metal	Total Exchangeable [TX,X2,(D),TC(D)] (mg kg^{-1})
Cadmium	0.301
Copper	0.658
Lead	1.16
Zinc	5.63

	Total Sorbed [TS,SO,st,wk] (mg kg^{-1})
Cadmium	0.001
Copper	0.219
Lead	18.9
Zinc	0.075

	Total Complexed [TC(S)] (mg kg^{-1})
Cadmium	1.71
Copper	15.6
Lead	22.6
Zinc	25.7

	Total Exchangeable, Sorbed, and Complexed (mg kg^{-1})
Cadmium	2.01
Copper	16.5
Lead	42.7
Zinc	31.4

Case #3

0.5 x [Al^{3+}]

Table D-4. Case $^{\#}$4 modeling output for sample 99-1-7-12 [CMA].

99-1-7-12 Case #4	Predicted Value (mg kg^{-1})	Weighting Factor	Adjusted Predicted Value (mg kg^{-1})	Metal	Total Exchangeable [TX,X2,(D),TC(D)] (mg kg^{-1})
Kaolinite					
TX-Cd	0.081	0.015	0.001	Cadmium	0.557
TS-Cd	0.000	0.015	0.000	Copper	0.876
TX-Cu	0.059	0.015	0.001	Lead	1.87
TS-Cu	0.000	0.015	0.000	Zinc	10.4
TX-Pb	0.387	0.015	0.006		
TS-Pb	0.004	0.015	0.000		**Total Sorbed**
TX-Zn	1.42	0.015	0.021		**[TS,SO,st,wk]**
TS-Zn	0.000	0.015	0.000		**(mg kg^{-1})**
Illite				Cadmium	0.002
X2-Cd	0.955	0.190	0.182	Copper	0.435
X2-Cu	0.955	0.190	0.182	Lead	37.6
X2-Pb	3.16	0.190	0.601	Zinc	0.150
X2-Zn	21.2	0.190	4.03		
					Total Complexed
Montmorillonite					**[TC(S)]**
X2-Cd	3.41	0.097	0.330		**(mg kg^{-1})**
SO-Cd+	0.001	0.097	0.000		
X2-Cu	2.60	0.097	0.252	Cadmium	1.71
SO-Cu+	0.058	0.097	0.006	Copper	15.6
X2-Pb	8.28	0.097	0.801	Lead	22.6
SO-Pb+	0.090	0.097	0.009	Zinc	25.7
X2-Zn	57.3	0.097	5.54		
SO-Zn+	0.089	0.097	0.009		**Total Exchangeable,**
					Sorbed, and
FeOOH					**Complexed**
st-Cd	0.023	0.087	0.002		**(mg kg^{-1})**
wk-Cd	0.000	0.087	0.000		
st-Cu	4.07	0.087	0.356	Cadmium	2.27
wk-Cu	0.838	0.087	0.073	Copper	16.9
st-Pb	429	0.087	37.5	Lead	62.1
wk-Pb	1.00	0.087	0.087	Zinc	36.4
st-Zn	1.54	0.087	0.135		
wk-Zn	0.065	0.087	0.006		**Case #4**
SOM					2.0 x [FeOOH]
Cd(D)	0.494	0.030	0.015		
TC(S)Cd	56.0	0.030	1.71		
TC(D)Cd	0.941	0.030	0.029		
Cu(D)	0.345	0.030	0.011		
TC(S)Cu	511	0.030	15.6		
TC(D)Cu	14.1	0.030	0.430		
Pb(D)	0.840	0.030	0.026		
TC(S)Pb	740	0.030	22.6		
TC(D)Pb	14.1	0.030	0.430		
Zn(D)	10.1	0.030	0.308		
TC(S)Zn	844	0.030	25.7		
TC(D)Zn	17.0	0.030	0.518		

Table D-5. Case #5 modeling output for sample 99-1-7-12 [CMA].

99-1-7-12 Case #5	**Predicted Value (mg kg^{-1})**	**Weighting Factor**	**Adjusted Predicted Value (mg kg^{-1})**
Kaolinite			
TX-Cd	0.081	0.015	0.001
TS-Cd	0.000	0.015	0.000
TX-Cu	0.059	0.015	0.001
TS-Cu	0.000	0.015	0.000
TX-Pb	0.387	0.015	0.006
TS-Pb	0.004	0.015	0.000
TX-Zn	1.42	0.015	0.021
TS-Zn	0.000	0.015	0.000
Illite			
X2-Cd	0.955	0.190	0.182
X2-Cu	0.955	0.190	0.182
X2-Pb	3.16	0.190	0.601
X2-Zn	21.2	0.190	4.03
Montmorillonite			
X2-Cd	3.41	0.097	0.330
SO-Cd+	0.001	0.097	0.000
X2-Cu	2.60	0.097	0.252
SO-Cu+	0.058	0.097	0.006
X2-Pb	8.28	0.097	0.801
SO-Pb+	0.090	0.097	0.009
X2-Zn	57.3	0.097	5.54
SO-Zn+	0.089	0.097	0.009
FeOOH			
st-Cd	0.023	0.044	0.001
wk-Cd	0.000	0.044	0.000
st-Cu	4.07	0.044	0.179
wk-Cu	0.838	0.044	0.037
st-Pb	429	0.044	18.9
wk-Pb	1.00	0.044	0.044
st-Zn	1.54	0.044	0.068
wk-Zn	0.065	0.044	0.003
SOM			
Cd(D)	0.494	0.015	0.008
TC(S)Cd	56.0	0.015	0.854
TC(D)Cd	0.941	0.015	0.014
Cu(D)	0.345	0.015	0.005
TC(S)Cu	511	0.015	7.80
TC(D)Cu	14.1	0.015	0.215
Pb(D)	0.840	0.015	0.013
TC(S)Pb	740	0.015	11.3
TC(D)Pb	14.1	0.015	0.215
Zn(D)	10.1	0.015	0.154
TC(S)Zn	844	0.015	12.9
TC(D)Zn	17.0	0.015	0.259

Metal	**Total Exchangeable [TX,X2,(D),TC(D)] (mg kg^{-1})**
Cadmium	0.535
Copper	0.655
Lead	1.64
Zinc	10.0

	Total Sorbed [TS,SO,st,wk] (mg kg^{-1})
Cadmium	0.001
Copper	0.222
Lead	19.0
Zinc	0.080

	Total Complexed [TC(S)] (mg kg^{-1})
Cadmium	0.854
Copper	7.80
Lead	11.3
Zinc	12.9

	Total Exchangeable, Sorbed, and Complexed (mg kg^{-1})
Cadmium	1.39
Copper	8.68
Lead	31.9
Zinc	23.0

Case #5

0.5 x [SOM]

Table D-6. Case #1 modeling output for sample 98-3-20-25 [CMA].

98-3-20-25 Case #1	Predicted Value (mg kg^{-1})	Weighting Factor	Adjusted Predicted Value (mg kg^{-1})
Kaolinite			
TX-Cd	0.940	0.039	0.036
TS-Cd	0.518	0.039	0.020
TX-Cu	0.013	0.039	0.001
TS-Cu	0.097	0.039	0.004
TX-Pb	0.138	0.039	0.005
TS-Pb	1.08	0.039	0.042
TX-Zn	5.78	0.039	0.223
TS-Zn	1.18	0.039	0.046
Illite			
X2-Cd	11.1	0.297	3.29
X2-Cu	0.214	0.297	0.063
X2-Pb	1.10	0.297	0.326
X2-Zn	85.8	0.297	25.5
Montmorillonite			
X2-Cd	39.5	0.033	1.31
SO-Cd+	6.04	0.033	0.200
X2-Cu	0.591	0.033	0.020
SO-Cu+	6.22	0.033	0.206
X2-Pb	2.91	0.033	0.096
SO-Pb+	15.0	0.033	0.497
X2-Zn	226	0.033	7.48
SO-Zn+	137	0.033	4.54
FeOOH			
st-Cd	366	0.094	34.4
wk-Cd	18.7	0.094	1.76
st-Cu	24.9	0.094	2.34
wk-Cu	6.33	0.094	0.594
st-Pb	267	0.094	25.1
wk-Pb	0.716	0.094	0.067
st-Zn	1268	0.094	119
wk-Zn	987	0.094	92.6
SOM			
Cd(D)	119	0.038	4.54
TC(S)Cd	3305	0.038	126
TC(D)Cd	40.2	0.038	1.54
Cu(D)	4.36	0.038	0.167
TC(S)Cu	3388	0.038	129
TC(D)Cu	76.7	0.038	2.93
Pb(D)	7.19	0.038	0.275
TC(S)Pb	3449	0.038	132
TC(D)Pb	41.7	0.038	1.59
Zn(D)	105	0.038	4.01
TC(S)Zn	3662	0.038	140
TC(D)Zn	51.3	0.038	1.96

Metal	Total Exchangeable [TX,X2,(D),TC(D)] (mg kg^{-1})
Cadmium	10.7
Copper	3.18
Lead	2.29
Zinc	39.2

	Total Sorbed [TS,SO, st,wk] (mg kg^{-1})
Cadmium	36.3
Copper	3.14
Lead	25.7
Zinc	216

	Total Complexed [TC(S)] (mg kg^{-1})
Cadmium	126
Copper	129
Lead	132
Zinc	140

	Total Exchangeable, Sorbed, and Complexed (mg kg^{-1})
Cadmium	173
Copper	135
Lead	160
Zinc	395

Case #1

Kaolinite 16%
Illite 77%
Montmorillonite 7%

Table D-7. Case $^{\#}$2 modeling output for sample 98-3-20-25 [CMA].

98-3-20-25 Case #2	Predicted Value (mg kg^{-1})	Weighting Factor	Adjusted Predicted Value (mg kg^{-1})
Kaolinite			
TX-Cd	0.940	0.039	0.036
TS-Cd	0.518	0.039	0.020
TX-Cu	0.013	0.039	0.001
TS-Cu	0.097	0.039	0.004
TX-Pb	0.138	0.039	0.005
TS-Pb	1.08	0.039	0.042
TX-Zn	5.78	0.039	0.223
TS-Zn	1.18	0.039	0.046
Illite			
X2-Cd	11.1	0.028	0.306
X2-Cu	0.214	0.028	0.006
X2-Pb	1.10	0.028	0.030
X2-Zn	85.8	0.028	2.37
Montmorillonite			
X2-Cd	39.5	0.356	14.1
SO-Cd+	6.04	0.356	2.15
X2-Cu	0.591	0.356	0.210
SO-Cu+	6.22	0.356	2.21
X2-Pb	2.91	0.356	1.04
SO-Pb+	15.0	0.356	5.34
X2-Zn	226	0.356	80.5
SO-Zn+	137	0.356	48.8
FeOOH			
st-Cd	366	0.094	34.4
wk-Cd	18.7	0.094	1.76
st-Cu	24.9	0.094	2.34
wk-Cu	6.33	0.094	0.594
st-Pb	267	0.094	25.1
wk-Pb	0.716	0.094	0.067
st-Zn	1268	0.094	119
wk-Zn	987	0.094	92.6
SOM			
Cd(D)	119	0.038	4.54
TC(S)Cd	3305	0.038	126
TC(D)Cd	40.2	0.038	1.54
Cu(D)	4.36	0.038	0.167
TC(S)Cu	3388	0.038	129
TC(D)Cu	76.7	0.038	2.93
Pb(D)	7.19	0.038	0.275
TC(S)Pb	3449	0.038	132
TC(D)Pb	41.7	0.038	1.59
Zn(D)	105	0.038	4.01
TC(S)Zn	3662	0.038	140
TC(D)Zn	51.3	0.038	1.96

Metal	Total Exchangeable [TX,X2,(D),TC(D)] (mg kg^{-1})
Cadmium	20.5
Copper	3.31
Lead	2.94
Zinc	89.1

Metal	Total Sorbed [TS,SO, st,wk] (mg kg^{-1})
Cadmium	38.3
Copper	5.15
Lead	30.5
Zinc	260

Metal	Total Complexed [TC(S)] (mg kg^{-1})
Cadmium	126
Copper	129
Lead	132
Zinc	140

Metal	Total Exchangeable, Sorbed, and Complexed (mg kg^{-1})
Cadmium	185
Copper	137
Lead	165
Zinc	489

Case #2

Kaolinite 16%
Illite 7%
Montmorillonite 77%

Table D-8. Case #3 modeling output for sample 98-3-20-25 [CMA].

98-3-20-25 Case #3	**Predicted Value (mg kg^{-1})**	**Weighting Factor**	**Adjusted Predicted Value (mg kg^{-1})**
Kaolinite			
TX-Cd	0.940	0.019	0.018
TS-Cd	0.518	0.019	0.010
TX-Cu	0.013	0.019	0.000
TS-Cu	0.097	0.019	0.002
TX-Pb	0.138	0.019	0.003
TS-Pb	1.08	0.019	0.021
TX-Zn	5.78	0.019	0.112
TS-Zn	1.18	0.019	0.023
Illite			
X2-Cd	11.1	0.148	1.65
X2-Cu	0.214	0.148	0.032
X2-Pb	1.10	0.148	0.163
X2-Zn	85.8	0.148	12.7
Montmorillonite			
X2-Cd	39.5	0.017	0.65
SO-Cd+	6.04	0.017	0.100
X2-Cu	0.591	0.017	0.010
SO-Cu+	6.22	0.017	0.103
X2-Pb	2.91	0.017	0.048
SO-Pb+	15.0	0.017	0.248
X2-Zn	226	0.017	3.74
SO-Zn+	137	0.017	2.27
FeOOH			
st-Cd	366	0.094	34.4
wk-Cd	18.7	0.094	1.76
st-Cu	24.9	0.094	2.34
wk-Cu	6.33	0.094	0.594
st-Pb	267	0.094	25.1
wk-Pb	0.716	0.094	0.067
st-Zn	1268	0.094	119
wk-Zn	987	0.094	92.6
SOM			
Cd(D)	119	0.038	4.54
TC(S)Cd	3305	0.038	126
TC(D)Cd	40.2	0.038	1.54
Cu(D)	4.36	0.038	0.167
TC(S)Cu	3388	0.038	129
TC(D)Cu	76.7	0.038	2.93
Pb(D)	7.19	0.038	0.275
TC(S)Pb	3449	0.038	132
TC(D)Pb	41.7	0.038	1.59
Zn(D)	105	0.038	4.01
TC(S)Zn	3662	0.038	140
TC(D)Zn	51.3	0.038	1.96

Metal	**Total Exchangeable [TX,X2,(D),TC(D)] (mg kg^{-1})**
Cadmium	8.40
Copper	3.14
Lead	2.08
Zinc	22.5

	Total Sorbed [TS,SO, st,wk] (mg kg^{-1})
Cadmium	36.3
Copper	3.04
Lead	25.4
Zinc	214

	Total Complexed [TC(S)] (mg kg^{-1})
Cadmium	126
Copper	129
Lead	132
Zinc	140

	Total Exchangeable, Sorbed, and Complexed (mg kg^{-1})
Cadmium	171
Copper	135
Lead	160
Zinc	377

Case #3

0.5 X [Al^{3+}]

Table D-9. Case #4 modeling output for sample 98-3-20-25 [CMA].

98-3-20-25 Case #4	Predicted Value (mg kg^{-1})	Weighting Factor	Adjusted Predicted Value (mg kg^{-1})
Kaolinite			
TX-Cd	0.940	0.039	0.036
TS-Cd	0.518	0.039	0.020
TX-Cu	0.013	0.039	0.001
TS-Cu	0.097	0.039	0.004
TX-Pb	0.138	0.039	0.005
TS-Pb	1.08	0.039	0.042
TX-Zn	5.78	0.039	0.223
TS-Zn	1.18	0.039	0.046
Illite			
X2-Cd	11.1	0.297	3.29
X2-Cu	0.214	0.297	0.063
X2-Pb	1.10	0.297	0.326
X2-Zn	85.8	0.297	25.5
Montmorillonite			
X2-Cd	39.5	0.033	1.31
SO-Cd+	6.04	0.033	0.200
X2-Cu	0.591	0.033	0.020
SO-Cu+	6.22	0.033	0.206
X2-Pb	2.91	0.033	0.096
SO-Pb+	15.0	0.033	0.497
X2-Zn	226	0.033	7.48
SO-Zn+	137	0.033	4.54
FeOOH			
st-Cd	366	0.187	68.4
wk-Cd	18.7	0.187	3.49
st-Cu	24.9	0.187	4.65
wk-Cu	6.33	0.187	1.18
st-Pb	267	0.187	49.9
wk-Pb	0.716	0.187	0.134
st-Zn	1268	0.187	237
wk-Zn	987	0.187	184
SOM			
Cd(D)	119	0.038	4.54
TC(S)Cd	3305	0.038	126
TC(D)Cd	40.2	0.038	1.54
Cu(D)	4.36	0.038	0.167
TC(S)Cu	3388	0.038	129
TC(D)Cu	76.7	0.038	2.93
Pb(D)	7.19	0.038	0.275
TC(S)Pb	3449	0.038	132
TC(D)Pb	41.7	0.038	1.59
Zn(D)	105	0.038	4.01
TC(S)Zn	3662	0.038	140
TC(D)Zn	51.3	0.038	1.96

Metal	Total Exchangeable [TX,X2,(D),TC(D)] (mg kg^{-1})
Cadmium	10.7
Copper	3.18
Lead	2.29
Zinc	39.2
	Total Sorbed [TS,SO, st,wk] (mg kg^{-1})
Cadmium	72.1
Copper	6.04
Lead	50.6
Zinc	426
	Total Complexed [TC(S)] (mg kg^{-1})
Cadmium	126
Copper	129
Lead	132
Zinc	140
	Total Exchangeable, Sorbed, and Complexed (mg kg^{-1})
Cadmium	209
Copper	138
Lead	185
Zinc	605
	Case #4
	2.0 x [FeOOH]

Table D-10. Case #1 modeling output for sample 98-3-5-10 [CMA].

98-3-5-10 Case #1	**Predicted Value (mg kg^{-1})**	**Weighting Factor**	**Adjusted Predicted Value (mg kg^{-1})**
Kaolinite			
TX-Cd	0.837	0.039	0.033
TS-Cd	0.462	0.039	0.018
TX-Cu	0.041	0.039	0.002
TS-Cu	0.290	0.039	0.011
TX-Pb	1.04	0.039	0.041
TS-Pb	8.03	0.039	0.313
TX-Zn	7.07	0.039	0.276
TS-Zn	1.43	0.039	0.056
Illite			
X2-Cd	9.87	0.250	2.47
X2-Cu	0.641	0.250	0.160
X2-Pb	8.37	0.250	2.10
X2-Zn	104	0.250	26.0
Montmorillonite			
X2-Cd	35.1	0.042	1.49
SO-Cd+	5.38	0.042	0.228
X2-Cu	1.80	0.042	0.076
SO-Cu+	18.9	0.042	0.800
X2-Pb	22.0	0.042	0.931
SO-Pb+	110	0.042	4.65
X2-Zn	273	0.042	11.6
SO-Zn+	159	0.042	6.73
FeOOH			
st-Cd	351	0.049	17.3
wk-Cd	16.6	0.049	0.820
st-Cu	264	0.049	13.0
wk-Cu	137	0.049	6.77
st-Pb	2769	0.049	137
wk-Pb	128	0.049	6.33
st-Zn	1302	0.049	64.3
wk-Zn	1201	0.049	59.4
SOM			
Cd(D)	119	0.069	8.23
TC(S)Cd	3303	0.069	228
TC(D)Cd	40.1	0.069	2.77
Cu(D)	4.35	0.069	0.301
TC(S)Cu	3426	0.069	237
TC(D)Cu	77.9	0.069	5.39
Pb(D)	7.04	0.069	0.487
TC(S)Pb	3769	0.069	261
TC(D)Pb	53.2	0.069	3.68
Zn(D)	104	0.069	7.19
TC(S)Zn	3742	0.069	259
TC(D)Zn	54.7	0.069	3.78

Metal	**Total Exchangeable [TX,X2,(D),TC(D)] (mg kg^{-1})**
Cadmium	15.0
Copper	5.93
Lead	7.24
Zinc	48.9

	Total Sorbed [TS,SO, st,wk] (mg kg^{-1})
Cadmium	18.4
Copper	20.6
Lead	149
Zinc	130

	Total Complexed [TC(S)] (mg kg^{-1})
Cadmium	228
Copper	237
Lead	261
Zinc	259

	Total Exchangeable, Sorbed, and Complexed (mg kg^{-1})
Cadmium	261
Copper	264
Lead	417
Zinc	428

Case #1

Kaolinite 20%
Illite 70%
Montmorillonite 10%

Table D-11. Case #5 modeling output for sample 98-3-5-10 [CMA].

98-3-5-10 Case #5	**Predicted Value (mg kg^{-1})**	**Weighting Factor**	**Adjusted Predicted Value (mg kg^{-1})**
Kaolinite			
TX-Cd	0.837	0.039	0.033
TS-Cd	0.462	0.039	0.018
TX-Cu	0.041	0.039	0.002
TS-Cu	0.290	0.039	0.011
TX-Pb	1.04	0.039	0.041
TS-Pb	8.03	0.039	0.313
TX-Zn	7.07	0.039	0.276
TS-Zn	1.43	0.039	0.056
Illite			
X2-Cd	9.87	0.250	2.47
X2-Cu	0.641	0.250	0.160
X2-Pb	8.37	0.250	2.10
X2-Zn	104	0.250	26.0
Montmorillonite			
X2-Cd	35.1	0.042	1.49
SO-Cd+	5.38	0.042	0.228
X2-Cu	1.80	0.042	0.076
SO-Cu+	18.9	0.042	0.800
X2-Pb	22.0	0.042	0.931
SO-Pb+	110	0.042	4.65
X2-Zn	273	0.042	11.6
SO-Zn+	159	0.042	6.73
FeOOH			
st-Cd	351	0.049	17.3
wk-Cd	16.6	0.049	0.820
st-Cu	264	0.049	13.0
wk-Cu	137	0.049	6.77
st-Pb	2769	0.049	137
wk-Pb	128	0.049	6.33
st-Zn	1302	0.049	64.3
wk-Zn	1201	0.049	59.4
SOM			
Cd(D)	119	0.035	4.12
TC(S)Cd	3303	0.035	114
TC(D)Cd	40.1	0.035	1.39
Cu(D)	4.35	0.035	0.150
TC(S)Cu	3426	0.035	119
TC(D)Cu	77.9	0.035	2.69
Pb(D)	7.04	0.035	0.244
TC(S)Pb	3769	0.035	130
TC(D)Pb	53.2	0.035	1.84
Zn(D)	104	0.035	3.60
TC(S)Zn	3742	0.035	129
TC(D)Zn	54.7	0.035	1.89

Metal	**Total Exchangeable [TX,X2,(D),TC(D)] (mg kg^{-1})**
Cadmium	9.50
Copper	3.08
Lead	5.16
Zinc	43.4

	Total Sorbed [TS,SO, st,wk] (mg kg^{-1})
Cadmium	18.4
Copper	20.6
Lead	149
Zinc	130

	Total Complexed [TC(S)] (mg kg^{-1})
Cadmium	114
Copper	119
Lead	130
Zinc	129

	Total Exchangeable, Sorbed, and Complexed (mg kg^{-1})
Cadmium	142
Copper	143
Lead	284
Zinc	302

Case #5

0.5 x [SOM]

APPENDIX E

Sample 99-1-0-7 Zinc
Master Table
Using 2000
Selective Extraction Data

Table E-1. Sample 99-1-0-7 zinc master table

99-1-0-7 Zinc

Kaolinite Input Total Zinc (mg/l)	**Kaolinite** Output Total Zinc (all species) in Solution [Input Zn - Total Exchangeable and Sorbed Zn] (mg/l)	**Kaolinite** Output Total Exchangeable Zinc (K)* (mg/kg)	**Kaolinite** Output Total Sorbed Zinc (K)* (mg/kg)	**Illite** Input Total Zinc (mg/l)	**Illite** Output Total Zinc (all Species) in Solution [Input Zn - Total Exchangeable Zn] (mg/l)
1,000	980	15.1	4.08	1,000	772
500	485	11.5	2.45	500	341
100	95.4	3.80	0.573	100	57.2
50	47.5	2.06	0.293	50	27.6
	16.5**	**0.741**	**0.103**		**16.5****
10	9.47	0.442	0.060	10	5.33
5	4.73	0.223	0.030	5	2.65
1	0.946	0.045	0.006	1	0.529
0.5	0.473	0.022	0.003	0.5	0.265
0.1	0.095	0.004	0.001	0.1	0.053
0.05	0.047	0.002	0.000	0.05	0.026
0.01	0.009	0.000	0.000	0.01	0.005
* Weighting Factor Applied					
** Experimental Data					
Predicted Exchangeable		0.741			
Predicted Sorbed			0.103		
Predicted Complexed					

Table E-1. Sample 99-1-0-7 zinc master table (cont.)

Illite	**Montmorillonite**	**Montmorillonite**	**Montmorillonite**	**Montmorillonite**	**FeOOH**
Output	Input	Output	Output	Output	Input
X2-Zn (I)*	Total Zinc	Total Zinc (all species) in Solution [Input Zn - Total Exchangeable and Sorbed Zn]	X2-Zn (M)*	SO-Zn+ (M)*	Total Zinc
(mg/kg)	(mg/l)	(mg/l)	(mg/kg)	(mg/kg)	(mg/l)
1615	1,000	499	579	117	1,000
1125	500	197	354	67.0	500
303	100	29.2	84.7	13.7	
159		**16.5****	**50.3**	**7.96**	100
96.2	50	13.9	43.4	6.79	50
33.0	10	2.66	8.86	1.35	10
16.6	5	1.33	4.44	0.670	5
3.33	1	0.264	0.890	0.134	1
1.67	0.5	0.132	0.445	0.067	0.5
0.334	0.1	0.026	0.089	0.013	0.1
0.167	0.05	0.013	0.045	0.007	0.05
0.033	0.01	0.003	0.009	0.001	0.01
96.2			50.3		
				7.96	

Table E-1. Sample 99-1-0-7 zinc master table (cont.)

FeOOH	**FeOOH**	**FeOOH**	**SOM**	**SOM**	**SOM**
Output	Output	Output	Input	Output	Output
Total Zinc (all species) in Solution [Input Zn - Total Sorbed Zn]	S(st)O-Zn+ (Fe)*	S(wk)O-Zn+ (Fe)*	Total Zinc	Total Zinc (all species) in Solution [Input Zn - Total Exchangeable and Complexed Zn]	Total Exchangeable Zinc (D) (Solid HA and FA)(SOM)*
(mg/l)	(mg/kg)	(mg/kg)	(mg/l	(mg/l)	(mg/kg)
529	177	512	1000	120	0.449
220	174	235		**16.5****	**3.95**
16.5**	**116**	**18.4**	500	13.7	4.04
12.1	115	13.8	100	1.68	1.93
3.55	63.6	4.23	50	0.848	0.985
0.490	13.3	0.614	10	0.137	0.160
0.246	6.65	0.296	5	0.063	0.074
0.045	1.34	0.058	1	0.012	0.014
0.024	0.667	0.029	0.5	0.006	0.007
0.005	0.134	0.006	0.1	0.001	0.001
0.002	0.067	0.003	0.05	0.001	0.001
0.000	0.013	0.001	0.01	0.000	0.000
					3.95
	116	18.4			

Table E-1. Sample 99-1-0-7 zinc master table (cont.)

SOM Output Total Complexed Zinc (Solid HA and FA)(SOM)*	**SOM** Output Total Exchangeable Zinc (Dissolved FA)(SOM)*		Total Soluble Zinc	"Predicted" Total Exchangeable Zinc	"Predicted" Total Sorbed and Complexed Zinc	"Predicted" Total Zinc
(mg/kg)	(mg/kg)		(mg/kg)[mg/l]	(mg/kg)	(mg/kg)	(mg/kg)
1007	33.3					
571	**15.6**					
559	15.1					
115	1.40					
57.5	0.590					
11.6	0.104					
5.78	0.051					
1.16	0.010					
0.579	0.005					
0.116	0.001					
0.058	0.000					
0.012	0.000					
	15.6			**"167"**		
					"143"	
571					**"571"**	**"881"**
		Experimental Data				
		DIW Extractable	**(660)[16.5]**			
		0.05M $Ca(NO_3)_2$ Extractable		**566 [1,226-660]**		
		0.03M $La(NO_3)_3$ Extractable		**1,006 [1,666-660]**		
		0.05M $Pb(NO_3)_2$ Extractable			**1,333 [2,999-1,666]**	
		HNO_3-$HClO_4$-HF Extractable				**7,760**